Analyse mathématique et numérique de modèles quantiques pour les semiconducteurs

Jihène Kéfi

THÈSE EN CO-TUTELLE PRÉSENTÉE À L'UNIVERSITÉ TOULOUSE III - PAUL SABATIER

pour obtenir le grade de

DOCTEUR DE L'UNIVERSITÉ TOULOUSE III

et de

DOCTEUR DE L'ÉCOLE NATIONALE D'INGÉNIEURS DE TUNIS

Spécialité : Mathématiques Appliquées

par

Jihène Kefi

Titre : Analyse mathématique et numérique de modèles quantiques pour les semiconducteurs.

Soutenue le 19 Décembre 2003 devant le jury composé de MM :

N. Ben Abdallah	Professeur à l'Université Toulouse 3	Directeur de thèse
J. Carrillo	Professeur à l'Université de Barcelone	Rapporteur
P. Degond	Directeur de recherche, CNRS	Invité
L. El Asmi	Maître de Conférence à l'École Polytechnique de Tunisie	Examinateur
T. Goudon	Professeur à l'Université de Lille 1	Rapporteur
T. Hadhri	Professeur à l'École Polytechnique de Tunisie	Directeur de thèse
M. Jaoua	Professeur à l'École Nationale d'Ingénieurs de Tunis	Examinateur

Mathématiques pour l'Industrie et la Physique

Equations aux Dérivées Partielles, Modélisation, Optimisation et Calcul Scientifique

Unité Mixte de Recherches 5640 CNRS - Univ. Paul Sabatier Toulouse 3 - INSA Toulouse - Université Toulouse 1

UFR MIG, Univ. Paul Sabatier Toulouse 3, 118 route de Narbonne, 31062 TOULOUSE cédex 4, France

Tel : (33) 05 61 55 83 14, Fax : (33) 05 61 55 83 85, Mail : umrmip@mip.ups-tlse.fr

La patience est la clé de la persévérance .

A mes parents,

Remerciements

Ce travail n'aurait pas été possible sans l'aide de nombreuses personnes.

Je tiens à remercier, tout particulièrement, Monsieur le Professeur Naoufel Ben Abdallah, un de mes Directeurs de thèse, qui, à la fin de mon D.E.A (Diplôme d'étude Approfondi) m'a fait confiance en me proposant ce projet. Sa disponibilité, ses qualités d'enseignant et son côté humain, ont permis mon apprentissage à la recherche.

Je remercie Monsieur le Professeur Taïeb Hadhri, mon autre Directeur de thèse, également pour la confiance qu'il m'a témoignée au début de ce projet, pour sa disponibilité et ses qualités humaines.

J'adresse mes remerciements à Messieurs les Professeurs José Carrillo et Thierry Goudon de l'honneur qu'ils me font en acceptant de juger cette thèse et d'en être les rapporteurs. Leurs commentaires pertinents et l'intérêt qu'ils ont accordé à ce travail m'ont permis d'en améliorer la rédaction.

Je tiens à remercier très spécialement Monsieur le Professeur Pierre Degond, Directeur de recherche au CNRS, qui m'a chaleureusement accueilli au MIP depuis mon stage de DEA et m'a donné l'opportunité de m'investir dans un travail très intéressant. Je le remercie de sa bienveillance à mon égard. C'est pour moi un réel plaisir de pouvoir le compter aujourd'hui parmi les membres du jury.

Je voudrais aussi exprimer ma gratitude à Monsieur le Professeur Lassaad El Asmi qui a accepté de faire partie du jury. Je voudrais plus particulièrement remercier Monsieur le Professeur Mohamed Jaoua sans qui cette belle aventure n'aurait pas vu le jour.

Je tiens également à exprimer ma reconnaissance à Mademoiselle Hédia Chaker pour les conseils qu'elle m'a prodigués et les divers discussions qui m'ont enrichies.

Tout au long de ce travail, j'ai eu l'occasion de discuter avec de nombreuses personnes. Je voudrais les remercier du temps qu'elles m'ont accordé, particulièrement Fabrice Deluzet, Miloslav Grundmann, Claudia Negulescu, Eric Polizzi, Olivier Pinaud, Olivier Saut pour leurs remarques judicieuses et leurs aides très précieuses.

Cette thèse a été effectuée en co-tutelle entre l'École Nationale d'Ingénieurs de Tunis et l'Université Paul Sabatier de Toulouse.

Merci au personnel administratif et technique des deux institutions pour leur disponibilité et leur dévouement.

Un grand merci aux secrétaires Christine Marty, Marie Louize Perez et Danièle Ricardou qui se sont occupées efficacement de nombre de détails pratiques.

Et Maintenant, je voudrais adresser mes plus grands remerciements à mes parents ici présents qui m'ont donné l'amour des sciences. Puisque, déjà, dans les années 60, mon père avait travaillé sur les transistors au CEA à Sacaly et au CENG de Grenoble. Ma mère qui m'a toujours pousser à persévérer et donner le goût du travail bien fait. Un grand merci à tout les deux sans oublier toute ma grande famille.

Je remercie mon fiancé, Nourredine, pour son réconfort et sa patience. Sa présence et sa compréhension ont été pour moi d'un grand soutien moral.

Je ne voudrais pas oublié tous mes amis, mathématiciens ou non, sans qui cette thèse ne se serait jamais aussi bien passée.

Table des matières

Table des figures

Introduction générale

Au début du troisième millénaire, on est déjà à l'ère de la nanotechnologie où il est possible de créer, observer, déplacer, agencer des objets de la taille d'un atome, nanoagrégat ou nanocristal. On commence à savoir fabriquer des nano-objets, plus complexes, possédant des formes et des fonctions bien définies, comme des nanocircuits ou des nanomachines. On s'oriente là vers une miniaturisation extrême des dispositifs électroniques. L'exemple le plus connu est probablement celui des circuits intégrés : alors que la dimension d'un transistor était de quelques micromètres en 1970, elle est aujourd'hui de 130 nanomètres.

Deux approches existent. Une approche ascendante appelée "bottom-up" car elle utilise les plus petits éléments accessibles de la matière pour concevoir des nanocomposants puis des nanomachines. La seconde descendante appelée "top-down" consiste à réduire la taille des composants constituant les machines nées de la microélectronique. Les nanocircuits posent cependant des problèmes de fonctionnement qui sont loin d'être résolus. À cette échelle, la mécanique quantique ([5], [22], [36], [84], [85], [86]...) s'impose, avec des lois de comportement complètement différentes de celles des objets macroscopiques. Les électrons qui circulent dans ces composants acquièrent un caractère ondulatoire qui les rends plus difficilement prévisibles. Pour cela, on a eu besoin de modélisation et simulation numérique.

D'autre part, suite à l'émergence des semi-conducteurs à petite bande interdite, de nouveaux dispositifs ont fait leur apparition ces dernières années. Parmi les différents dispositifs semi-conducteurs de taille nanométrique répondant à ce critère, on s'intéresse aux composants à effet tunnel résonnant dont deux catégories existent l'une intrabande et l'autre interbande (nous détaillerons plus loin leur signification). Pour définir le transport interbande, il faut avoir recours à l'approximation dite $k.P$ de l'équation de Schrödinger ([60], [61],...) que nous rappellerons succinctement ci dessous.

Les physiciens et les électroniciens ont déjà travaillé sur ces types de dispositifs où un certain nombre de résultats expérimentaux a été obtenu ([100], [104], [105], [109]...). Pour mieux comprendre les phénomènes qui interagissent dans les semiconducteurs, des études mathématiques de l'équation de Schrödinger décrivant le transport dans ce type de dispositifs ont aussi été effectuées ([11], [12], [13], [14], [15], [17], [18], [19], [38], [39], [40], [89], [90], [93], [94], [95], [101], [111]...).

1 Structure cristalline

À l'échelle quantique, un semi-conducteur est un matériau à l'état solide cristallisé avec une conductivité électronique intrinsèque. Dans l'espace $\mathbb{R}^3$, un cristal est un arrangement d'atomes selon un réseau cristallin L (voir figure 1).

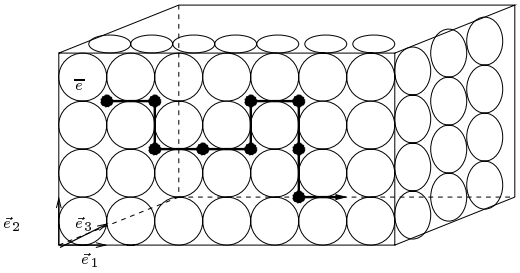

FIG. 1: Le réseau L.

Soient $(\vec{e_i})_{(i=1..3)}$ une base de vecteurs de L tel que

$$L = \{a_1\vec{e_1} + a_2\vec{e_2} + a_3\vec{e_3} | a_1, a_2, a_3 \in \mathbb{Z}\}.$$

La base duale $(\vec{e_i^*})_{(i=1..3)}$ est déterminée par l'équation

$$\vec{e_i}.\vec{e_j^*} = 2\pi\delta_{ij}, \quad \forall i, j = 1, 2, 3$$

et le réseau dual L^* (" réseau réciproque ") s'écrit

$$L^* = \{a_1\vec{e_1^*} + a_2\vec{e_2^*} + a_3\vec{e_3^*} | a_1, a_2, a_3 \in \mathbb{Z}\}.$$

La cellule élémentaire du réseau L est défini par

$$C = \left\{ \sum_{i=1}^{3} t_i\vec{e_i} \mid 0 \leq t_1, t_2, t_3 < 1 \right\}$$

et la zone de Brillouin B est la cellule élémentaire du réseau dual L^*. Elle est le petit volume de l'espace réciproque ; contenant l'origine ; qui est entièrement compris entre les plans médians des vecteurs du réseau réciproque partant de l'origine.

$$B = \left\{ k \in \mathbb{R}^3, |k| \leq \min_{K \in L^* - 0} |k + K| \right\}.$$

On note par conséquent,

$$|C||B| = (2\pi)^3$$

où $|.|$ représente le volume.

Le réseau d'atomes ou d'ions génère une distribution périodique de charge électrique, qui induit un potentiel périodique $V_c(x)$ ayant la propriété suivante

$$V_c(x + l) = V_c(x), \quad \text{sur} \quad \mathbb{R}^3, \quad \forall \ l \in L. \tag{1.1}$$

L'état d'un électron libre se déplaçant dans un potentiel périodique est donné par la fonction d'onde Ψ solution de l'équation de Schrödinger dépendante du temps

$$i\hbar\frac{\partial\Psi}{\partial t} = -\frac{\hbar^2}{2m}\Delta\Psi + V_c(x)\Psi + V(x)\Psi \tag{1.2}$$

où $m, \hbar$ sont respectivement la masse élémentaire de l'électron et la constante de Planck réduite. Le potentiel V est un potentiel macroscopique qui prend en compte les potentiels appliqués et ceux générés par les charges distribuées (dopage, électrons, etc..). V varie à une échelle spatiale beaucoup plus grande que le potentiel cristallin V_c. Dans une première approximation, on peut considérer qu'il est localement constant. On regarde alors l'équation

$$i\hbar\frac{\partial\Psi}{\partial t} = -\frac{\hbar^2}{2m}\Delta\Psi + V_c(x)\Psi. \tag{1.3}$$

On note par l'opérateur H

$$H\Psi = -\frac{\hbar^2}{2m}\Delta\Psi + V_c(x)\Psi.$$

L'équation (1.3) devient

$$i\hbar\frac{\partial\Psi}{\partial t} = H\Psi. \tag{1.4}$$

Lorsque l'Hamiltonien H ne dépend pas explicitement du temps, c'est le cas des systèmes conservatifs, qui correspond aux systèmes classiques dont l'énergie est une constante du mouvement. On peut chercher les solutions Ψ sous la forme

$$\Psi = \psi\, e^{\frac{-iEt}{\hbar}} \tag{1.5}$$

où ψ dépend des coordonnées de l'espace mais ne dépend pas du temps. Cette solution représente un état d'énergie E. Substituant cette expression dans l'équation (1.4), on obtient

$$H\psi = E\psi \tag{1.6}$$

qui porte le nom d'équation de Schrödinger indépendante du temps.

Lorsque le système se trouve dans un état représenté par une onde telle que celle de l'expression (1.5), on dit qu'il est dans un état stationnaire d'énergie E, et la fonction d'onde ψ indépendante du temps est couramment désignée sous le nom de fonction d'onde de l'état stationnaire, bien que la fonction d'onde véritable en diffère par le facteur de phase $e^{\frac{-iEt}{\hbar}}$.

Afin d'acquérir une certaine pratique de l'équation de Schrödinger avant d'aborder les problèmes d'interprétation des phénomènes quantiques, nous allons tout au

long de cette étude nous ramener à une équation de Schrödinger à une dimension. Nous avons vu qu'il est possible de séparer dans l'équation de Schrödinger (1.4) les variables de temps et d'espace, ce qui a conduit à l'équation aux valeurs propres (1.6). Nous nous proposons alors de séparer aussi les variables d'espaces.
Le problème à une dimension est intéressant non seulement comme modèle simple permettant de mettre en évidence un certain nombre de propriétés que l'on trouve dans des situations plus complexes, mais aussi parce que dans bien des problèmes il est possible de se ramener après quelques manipulations adéquates à la résolution d'équation de même type que l'équation de Schrödinger à une dimension.

L'opérateur H a un spectre avec une structure de bande. D'après le théorème de Bloch l'un des théorèmes de base les plus importants concernant la structure de bande, si le potentiel V_c vérifie (1.1), alors il existe une famille de base complète $b_{n,k}$ telle que

$$b_{n,k}(x) = e^{ik.x} u_{n,k}(x), \tag{1.7}$$

où n est l'indice de bande correspondant aux différentes solutions d'un même vecteur d'onde k et $u_{n,k}(x)$ est la fonction de Bloch. Elle est aussi périodique de la périodicité du réseau. On remarque alors que toute fonction $\psi \in L^2(\mathbb{R})$ solution de l'équation de Schrödinger (1.6) vérifie

$$\psi(x) = \frac{1}{|B|} \sum_n \int_B \varphi_n(k) b_{n,k}(x) dk \text{ où } \varphi_n(k) = \int_{\mathbb{R}} \psi(x) \overline{b_{n,k}(x)} dx.$$

D'autre part, en insérant (1.7) dans l'équation de Schrödinger (1.6), $u_{n,k}$ satisfait l'équation suivante

$$(\frac{p^2}{2m} + \frac{h}{m} k.p + \frac{h^2 k^2}{2m} + V_c(x)) u_{n,k}(x) = E_n(k) u_{n,k}(x), \tag{1.8}$$

où p est l'opérateur moment donné par $p = -i\hbar \frac{d}{dx}$.

Lorsque $k = 0$, l'équation (1.8) prend une forme particulièrement simple

$$(\frac{-\hbar^2}{2m} \frac{d^2}{d^2 x} + V_c(x)) u_{n,0}(x) = E_n(0) u_{n,0}(x), \tag{1.9}$$

où $E_n(0)$ est l'énergie de la énième bande au niveau de $k = 0$. Elle est associée à la fonction de Bloch $u_{n,0}$.

L'opérateur $\frac{\hbar k.p}{m}$ dans (1.8) est alors traité comme une perturbation dans l'Hamiltonien de Schrödinger. Il permet de déterminer les fonctions d'ondes $u_{n,k}(x)$ et les valeurs d'énergie $E_n(k)$ pour des petites valeurs de k voisines de $k = 0$ en fonction de $u_{n,0}(x)$ et $E_n(0)$. D'après Kohn-Luttinger [77], on peut utiliser $e^{ikx} u_{n,0}$ comme base complète adaptée à l'étude autour de $k = 0$. Ainsi, ψ s'écrit

$$\psi = \sum_n F_n(x) u_{n,0}(x),$$

où

$$F_n(x) = \frac{1}{|B|}\int_B \varphi_n(k^{'})e^{ik^{'}x}dk^{'}.$$

Lorsqu'on projette l'équation de Schrödinger (1.6) sur cette nouvelle base, on obtient le système $k.P$ sur les fonctions F_n appelées fonctions enveloppes.

$$(-\frac{h^2}{2m}\frac{d^2}{d^2x} + E_n(0))F_n(x) + i\hbar\sum_{n^{'}}\frac{P_{n,n^{'}}}{m}\frac{dF_{n^{'}}}{dx}(x) = EF_n(x), \tag{1.10}$$

où

$$P_{n,n^{'}} = -i\hbar\int u_{n^{'},0}\frac{du_{n,0}}{dx}dx \text{ et } P_{n,n^{'}} = P_{n^{'},n}.$$

L'équation (1.10) s'écrit aussi sous forme matricielle

$$\begin{pmatrix} -\frac{h^2}{2m}\frac{d^2}{d^2x} + E_1(0) & & -i\hbar\frac{P_{n,n^{'}}}{m}\frac{d}{dx} \\ & \ddots & \\ -i\hbar\frac{P_{n,n^{'}}}{m}\frac{d}{dx} & & -\frac{h^2}{2m}\frac{d^2}{d^2x} + E_n(0) \end{pmatrix}\begin{pmatrix} F_1(x) \\ \vdots \\ F_n(x) \end{pmatrix} = E\begin{pmatrix} F_1(x) \\ \vdots \\ F_n(x) \end{pmatrix}. \tag{1.11}$$

Si on considère F_n comme une onde plane s'écrivant $F_n(x) = a_n e^{ikx}$, on a alors

$$\begin{pmatrix} \frac{h^2k^2}{2m} + E_1(0) & & \hbar\frac{P_{n,n^{'}}}{m}k \\ & \ddots & \\ \hbar\frac{P_{n,n^{'}}}{m}k & & \frac{h^2k^2}{2m} + E_n(0) \end{pmatrix}\begin{pmatrix} a_1 \\ \vdots \\ a_n \end{pmatrix} = E\begin{pmatrix} a_1 \\ \vdots \\ a_n \end{pmatrix}. \tag{1.12}$$

En résolvant cette équation par rapport à E, on obtient une relation de dispersion dont les solutions sont les bandes d'énergie $(E_i)_{i=1,..,n}(k)$. Ces énergies sont discrètes, elles existent entre les bandes d'énergies interdites aux électrons (appelées gap). D'autre part, les électrons sont des fermions et obéissent au principe d'exclusion de Pauli. Ils ne peuvent donc pas être dans le même état quantique. Les électrons remplissent les états d'énergie distribués en bande, par énergie croissante. Parmi ces bandes, on cite la bande conduction, la bande de valence et la bande spin-orbite (voir figure 2).

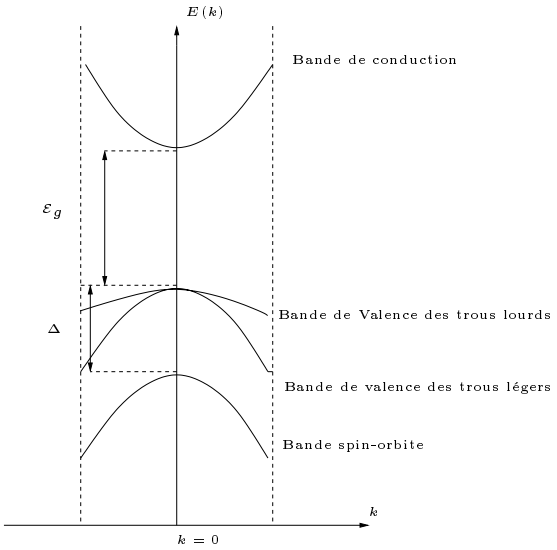

FIG. 2: Les bandes d'énergies .

Au voisinage de $k = 0$ qui correspond au minimum de la bande de conduction, c'est à dire dans la région du diagramme énergétique où sont localisés les électrons de conduction, on peut développer la fonction $E_n(k)$ en série de Taylor. Dans la mesure où il s'agit d'un minimum, la dérivée première est nulle, de sorte qu'en limitant le développement au deuxième ordre, l'énergie s'écrit

$$E_n(k) = E_n(0) + \frac{k^2}{2}\frac{d^2E_n(0)}{d^2k}.$$

On peut aussi l'écrire sous la forme suivante

$$E_n(k) = E_n(0) + \frac{\hbar^2 k^2}{2m^*},$$

où m^* est la masse effective donnée par

$$m^* = \frac{\hbar^2}{\frac{d^2E_n(0)}{d^2k}}. \tag{1.13}$$

De plus, il faut noter que dans cette vision semi-classique, un électron de la n-ième bande est décrit par une particule ponctuelle se déplaçant à la vitesse $v_n(k)$ donnée par la vitesse de groupe du paquet d'onde associé à l'électron dans une vision quantique :

$$v_n(k) = \frac{1}{\hbar}\frac{dE_n(k)}{dk}.$$

Par conséquent, l'équation (1.11) devient

$$-\frac{\hbar^2}{2m^*}\frac{d^2F_n}{d^2x} + V(x)F_n = E_n(k)F_n, \tag{1.14}$$

où V est un potentiel extérieur.

Les effets de la structure de bande sont incorporés dans les paramètres du matériau tel que E_n et m^*. Ainsi, l'électron au voisinage du minimum de la bande de conduction se comporte comme un électron libre de masse m^*. Dans la mesure où la courbure de la bande de conduction varie peu au voisinage du minimum, la masse effective m^* est *constante* et par suite l'énergie $E_n(k)$ varie quadratiquement avec le vecteur d'onde k. Cette loi de variation constitue ce que l'on appelle *l'approximation des bandes paraboliques.*
Lorsque l'énergie cinétique des électrons devient très importante l'électron s'éloigne de $E_n(0)$ dans l'espace des énergies, sa masse effective *varie* et l'approximation parabolique n'est plus justifiée.

Plusieurs résultats expérimentaux, théoriques et numériques sur cette équation (1.14) ont été réalisés [11], [12], [13], [14], [15], [17], [18], [19], [89], [90], [93], [94], [95], [101] et [111]. Or ce modèle (1.14) découle de l'approximation la plus générale de la masse effective

$$-\frac{\hbar^2}{2}\frac{d}{dx}(\frac{1}{m^*(x)}\frac{d\psi}{dx}) + V(x)\psi = \frac{q^2}{2m}\psi, \tag{1.15}$$

où $q = \hbar k$ est le moment.

Cette équation (1.15) a été étudiée par [3], [4], [9], [16], [20], [40], [43], [44], [47] et [48]. Dans le chapitre 1 de ce mémoire (voir [62]), on a fait une analyse mathématique rigoureuse de ce modèle couplé avec Poisson. On a aussi effectué une analyse asymptotique minutieuse type limite semi-classique de ce modèle vers le modèle cinétique associé. Pour cela, on a utilisé la transformée de Wigner ([42], [52], [53], [55], [74], [81], [82], [118], [122]...).

Ces deux modèles précédents (1.14) et (1.15) semblent être insuffisants. Ils sont encore au stade simplificateurs de point de vue électronique pour décrire les phénomènes physiques qui puissent interagir entre les différentes bandes d'énergie qui constituent le semi-conducteur.

Si on restreint la projection de l'équation (1.14) aux quatres premières bandes tel que la bande de conduction, ensuite la bande de valence qui est considérée dégénérée d'où une bande de valence associée aux trous lourds et une autre associée aux trous légers et la dernière bande celle associée au spin orbite (voir figure 2) , on obtient l'Hamiltonien de Kane [60] et [61]. Il est donné par une matrice 8×8

$$\begin{pmatrix} \mathbb{H}_1 & 0 \\ 0 & \mathbb{H}_1 \end{pmatrix} \tag{1.16}$$

avec

$$\mathbb{H}_1 = \begin{pmatrix} -\frac{\hbar^2}{2m}\frac{d^2}{dx^2} + V(x) & i\sqrt{\frac{2}{3}}\hbar P\frac{d}{dx} & -i\sqrt{\frac{1}{3}}\hbar P\frac{d}{dx} & 0 \\ i\sqrt{\frac{2}{3}}\hbar P\frac{d}{dx} & -\frac{\hbar^2}{2m}\frac{d^2}{dx^2} - \mathcal{E}_g + V(x) & 0 & 0 \\ -i\sqrt{\frac{1}{3}}\hbar P\frac{d}{dx} & 0 & -\frac{\hbar^2}{2m}\frac{d^2}{dx^2} - \mathcal{E}_g - \Delta + V(x) & 0 \\ 0 & 0 & 0 & -\frac{\hbar^2}{2m}\frac{d^2}{dx^2} - \mathcal{E}_g + V(x) \end{pmatrix}$$

où m est la masse de l'électron, $\mathcal{E}_g$ est l'énergie du gap, P est le coefficient de couplage entre la bande de conduction et la bande de valence et Δ est le gap entre la bande de valence et la bande spin-orbite.

Dans notre mémoire, on a étudié le modèle de Kane à deux bandes comme dans ([6], [23], [43], [107] et [115]) où on a découplé la bande de valence des trous lourds et on a négligé le couplage spin-orbite. Dans notre étude, on lui a donné le nom de Schrödinger à deux bandes. Il s'écrit alors

$$\begin{pmatrix} -\frac{\hbar^2}{2m}\frac{d^2}{dx^2} + V(x) & i\hbar P\frac{d}{dx} \\ i\hbar P\frac{d}{dx} & -\frac{\hbar^2}{2m}\frac{d^2}{dx^2} - \mathcal{E}_g + V(x) \end{pmatrix} \psi = E\psi. \tag{1.17}$$

Dans la résolution du modèle à quatre bande, Kane a déjà noté la non-parabolicité de ces différentes bandes la bande de conduction, la bande de valence associée aux trous légers, la bande de valence associée aux trous lourds et la bande associée au spin orbite. Suite à ça plusieurs études prenant en compte la non-parabolicité dans la structure de bande ont été effectuées ([7], [8], [41], [43], [69], [92] et [115]). En résolvant l'équation (1.16), l'énergie cinétique d'un électron sur la bande de conduction E_c, la bande de valence associée aux trous légers E_v et celle associée au spin orbite E_{spin} peut s'écrire comme suit

$$E_{c,v} = \frac{\hbar^2 k^2}{2m} + \frac{\mathcal{E}_g}{2}\left(1 \pm (1 + \frac{8P^2}{\mathcal{E}_g^2}k^2)^{\frac{1}{2}}\right), \tag{1.18}$$

$$E_{spin} = \frac{\hbar^2 k^2}{2m} - \Delta - \frac{P^2 k^2}{3(\mathcal{E}_g + \Delta)} - \frac{(2\mathcal{E}_g + \Delta)P^4 k^4}{3(\mathcal{E}_g + \Delta)^2 \Delta}. \tag{1.19}$$

L'énergie cinétique d'un électron sur la bande de valence associée aux trous lourds $E_{v,lourd}$ est par contre considérée parabolique et s'écrit comme suit

$$E_{v,lourd} = \frac{\hbar^2 k^2}{2m}. \tag{1.20}$$

Les équations (1.18) et (1.19) peuvent être développées comme suit pour l'énergie cinétique de la bande de conduction

$$E_c = \mathcal{E}_g + \frac{\hbar^2}{2m_c^*}k^2 - \frac{1}{\mathcal{E}_g}\left(\frac{\hbar^2}{2m_c^*} - \frac{\hbar^2}{2m}\right)^2 k^4, \tag{1.21}$$

pour la bande de valence

$$E_v = -\frac{\hbar^2}{2m_v^*}k^2 - \frac{1}{\mathcal{E}_g}\left(\frac{\hbar^2}{2m_v^*} - \frac{\hbar^2}{2m}\right)^2 k^4 \tag{1.22}$$

et pour la bande spin orbite

$$E_{spin} = -\Delta - \frac{\hbar^2 k^2}{2m_{spin}^*} - \frac{3(2\mathcal{E}_g + \Delta)P}{\Delta}\left(\frac{\hbar^2}{2m_{spin}^*} - \frac{\hbar^2}{2m}\right)^2 k^4 \tag{1.23}$$

où

$$1/m_c^* \equiv 1/m + 4P^2/(3\hbar^2\mathcal{E}_g), \quad 1/m_v^* \equiv 4P^2/(3\hbar^2\mathcal{E}_g) - 1/m$$

avec $m_{c,v}^*$ est la masse effective selon la bande d'énergie de conduction ou de valence et

$$1/m_{spin}^* \equiv P^2/(3\hbar^2(\mathcal{E}_g + \Delta)) - 1/m$$

avec m_{spin}^* est la masse effective selon la bande spin orbite. Ici, les termes d'ordre élevés, proportionnels à k^6 sont négligés. Alternativement, on écrit les équations précédentes (1.21)-(1.22)-(1.23) comme suit

$$E_c = \mathcal{E}_g + \frac{q^2}{2m_c^*} - \alpha_c\frac{q^4}{4m_c^{*2}}, \tag{1.24}$$

$$E_v = -\frac{q^2}{2m_v^*} + \alpha_v\frac{q^4}{4m_v^{*2}}, \tag{1.25}$$

$$E_{spin} = -\Delta - \frac{q^2}{2m_{spin}^*} - \alpha_{spin}\frac{q^4}{4m_{spin}^{*2}} \tag{1.26}$$

où

$$\alpha_c = \frac{1}{\mathcal{E}_g}\left(1 - \frac{m_c^*}{m}\right)^2, \quad \alpha_v = \frac{1}{\mathcal{E}_g}\left(\frac{m_v^*}{m} - 1\right)^2 \text{ et } \alpha_{spin} = \frac{3(2\mathcal{E}_g + \Delta)P}{\Delta}\left(1 - \frac{m_{spin}^*}{m}\right)^2.$$

Dans (1.24) et (1.25) le terme en q^4 est de signe contraire à celui de q^2 tandis que les deux signes sont identiques pour (1.26). Ainsi, au signe prés, on a l'énergie cinétique E qui s'écrit comme suit

$$E(q) = \frac{q^2}{2m^*} + \alpha\frac{q^4}{4m^{*2}} \tag{1.27}$$

où m^* la masse effective et le coefficient α peut être positif ou négatif selon la bande d'énergie. Lorsque α est positif, l'énergie $E(q)$ est croissante en fonction de q^2 alors que ce n'est pas le cas lorsque $\alpha < 0$ pour lequel l'énergie $E(q)$ n'est monotone que pour k trés petit.

Dans le chapitre 2 on s'est restreint au cas où α est positif ce qui correspond à l'énergie cinétique de la bande spin orbite (1.26) et pour lequel le problème couplé

avec l'équation de Poisson est bien posé. En restant dans le cadre d'une étude unidimensionnelle et en se basant sur la théorie de la masse effective, on définit l'opérateur $\mathbb{K}$ d'ordre 4 de Kohn-Luttinger (voir [77]) comme suit

$$\mathbb{K} = -\frac{\hbar^2}{2m}\frac{d^2}{dx^2} + \alpha\frac{\hbar^4}{4m^2}\frac{d^4}{dx^4}. \tag{1.28}$$

Dans les simulations numériques présentées dans le chapitre 3, le cas $\alpha < 0$ est également testé.

Dans les deux derniers chapitres 4 et 5, on a consacré notre étude au modèle Schrödinger à deux bandes définit dans (1.17). On s'est intéressé à l'étude mathématique de ce modèle dans le cas linéaire ensuite dans le cas non-linéaire lorsqu'on couple avec Poisson. En dernier lieu, on a analysé numériquement ce modèle et on a représenté les caractéristiques physiques tel que la courbe courant-tension, la transmission et la densité électronique.

2 Plan d'étude

La présente thèse est consacrée à l'étude d'un modèle de transport quantique et se décompose essentiellement en deux parties. On y étudie un modèle quantique appelé modèle de Schrödinger où deux approches sont définies. L'une monobande et la seconde multibande. Dans tous les cas, la démarche est la même. En effet, du point de vue mathématique elle consiste à définir un opérateur H de la façon suivante

$$H\Psi = E\Psi. \tag{2.29}$$

Ensuite, on dérive les conditions aux bords transparentes qui permettent dans le cas linéaire de démontrer l'existence et unicité de solution. Dans le cas non-linéaire où le potentiel est self-consistant, on montre l'existence de solution.
Du point de vue numérique, le principe est encore le même dans les deux approches. Il est basé sur un schéma itératif. Il consiste à résoudre un grand nombre de fois cette équation (2.29) suivant la valeur de l'énergie E au cours de chaque itération où le potentiel est donné au départ. On obtient la fonction d'onde Ψ pour chaque énergie E. Ensuite, on calcule la densité électronique associée à ces fonctions d'ondes. En injectant dans l'équation unidimensionnelle standard de Poisson

$$-\frac{d}{dx}(\epsilon_r(x)\frac{dV}{dx}) \quad = \quad e(N_D - n(x)), \tag{2.30}$$

on détermine le nouveau potentiel. Le test d'arrêt du schéma itératif consiste à comparer le nouveau potentiel avec le potentiel précédent en norme L^∞ par exemple. Il est à noter que pour plus de diversité, on a utilisé dans notre étude pour le modèle Kohn-Luttinger de la première partie une méthode d'éléments finis alors que dans la seconde partie, on a utilisé la méthode de différence finie pour le modèle Schrödinger à deux bandes.

2.1 Description de la première partie : Monoband transport

La première partie de la présente thèse concerne une approche monobande du modèle Schrödinger. En premier lieu, elle comporte l'étude mathématique du modèle Schrödinger avec masse variable couplé avec Poisson ainsi que la limite semi-classique de ce modèle. En second lieu, elle concerne l'étude mathématique du modèle Kohn-Luttinger, qui provient d'une approche non-parabolique de l'énergie, couplé avec Poisson. Et en dernier lieu, on termine cette première partie par une étude numérique du modèle Kohn-Luttinger.

2.1.1 Chapitre 1 : The Schrödinger with variable mass model (en collaboration avec N. Ben Abdallah [16] et [62])

On étudie le modèle quantique Schrödinger avec masse variable unidimensionnel dans le cas stationnaire lors d'injection d'électron simultanée de part et d'autre d'une zone quantique notée Q. Le modèle est décrit par l'équation suivante

$$-\frac{\hbar^2}{2}\frac{d}{dx}(\frac{1}{m(x)}\frac{d\psi_q^{\pm}}{dx}) - eV(x)\psi_q^{\pm} = [\frac{q^2}{2m_{\pm}} - eV_{\pm} + \frac{i\hbar\nu}{2}]\psi_q^{\pm}, \qquad q \geq 0, \quad x \in [0,1], \quad (2.31)$$

où $\psi_q^{\pm}$ est la fonction d'onde associée à un électron qui arrive par la gauche $(+)$ (resp. par la droite $(-)$). e est la charge électrique élémentaire et (x,q) sont les variables position et moment. Le paramètre de régularisation $\nu \geq 0$ est un coefficient d'absorption. La limite semi-classique est effectuée uniquement dans le cas $\nu > 0$ (voir Théorème 2.2). Tandis que ν peut être pris égal à zéro dans l'étude du modèle linéaire ou non-linéaire de Schrödinger avec masse variable (voir Théorème 2.1).

La zone quantique est soumise à une différence de potentiel $V_- - V_+$ où $V_+ = V(0)$ et $V_- = V(1)$. On considère le cas où $V_+ > V_-$, le cas contraire se traite de la même manière. De plus, on suppose que la masse effective m est dépendante de la position x à l'intérieur de la zone Q et qu'elle est constante ailleurs et $m_+ = m(0),\ m_- = m(1)$.

D'autre part, connaissant l'expression du potentiel de part et d'autre de la zone quantique, on peut résoudre explicitement l'équation de Schrödinger avec masse variable et on obtient

$$\psi_q^-(x) = e^{i\frac{q}{\hbar}x} + r_q^- e^{-i\frac{q}{\hbar}x},\ \psi_q^+(x) = t_q^+ e^{-\frac{i}{\hbar}\sqrt[+]{q^2\frac{m_-}{m_+}+2em_-(V_- - V_+)}x} \text{ pour } x < 0, \quad (2.32)$$

$$\psi_q^-(x) = t_q^- e^{\frac{i}{\hbar}\sqrt[+]{q^2\frac{m_+}{m_-}+2em_+(V_+ - V_-)}(x-1)},\psi_q^+(x) = e^{-i\frac{q}{\hbar}(x-1)} + r_q^+ e^{i\frac{q}{\hbar}(x-1)} \text{ pour } x > 1, \quad (2.33)$$

où $r_q^{\pm}$ et $t_q^{\pm}$ sont respectivement les coefficients de réflection et de transmission. $\sqrt[+]{a}$ $(a \in \mathbb{R})$ représente la racine carrée complexe dont la partie imaginaire est positive. On peut ensuite se ramener à l'intervalle $[0,1]$, en éliminant les coefficients $r_q^{\pm}$ et $t_q^{\pm}$. On obtient alors les conditions aux bords type Fourier suivantes

$$\hbar\psi_q^{-'}(0) + iq\psi_q^-(0) = 2iq, \quad \hbar\psi_q^{+'}(0) = -i\sqrt[+]{\frac{m_-}{m_+}q^2 + 2em_-(V_- - V_+)}\psi_q^+(0), \quad (2.34)$$

$$\hbar\psi_q^{-'}(1) = i\sqrt{\frac{m_+}{m_-}q^2 + 2em_+(V_+ - V_-)}\psi_q^-(1), \quad \hbar\psi_q^{+'}(1) - iq\psi_q^+(1) = -2iq. \tag{2.35}$$

Pour déterminer l'expression de la densité de charge, on suppose qu'il existe deux sources placées en $-\infty$ et $+\infty$ selon des profils de distributions $G^-(q)$ et $G^+(q)$. Par conséquent, la densité de charge vaut

$$n(x) = \int_0^{+\infty} G^-(q)|\psi_q^-(x)|^2 dq + \int_0^{+\infty} G^+(q)|\psi_q^+(x)|^2 dq.$$

Une fois que la densité est déterminée, le potentiel V résout l'équation de Poisson

$$\frac{d^2V}{dx^2} = n(x), \tag{2.36}$$

avec comme conditions aux bords

$$V(0) = V_-, \qquad V(1) = V_+. \tag{2.37}$$

On énonce tout d'abord les hypothèses suivantes

Hypothèses 2.1

$(H-1)$ *Il existe* c *et* $C > 0$ *tel que* $c \leq m(x) \leq C$.
$(H-2)$ G^- *et* G^+ *sont deux fonctions à support compact et vérifient*

$$G^\pm \geq 0 \text{ et } \int_0^{+\infty} G^\pm(q)dq < \infty.$$

Dans la suite, on suppose que $supp\, G^\pm \subset [0, q_0]$ avec $q_0 > 0$.

Dans [62], sous les hypothèses précédentes et en utilisant le théorème de point fixe Leray-Schauder (voir ref.[54]), on montre l'existence de solution du modèle stationnaire Schrödinger avec masse variable couplé avec Poisson.

Théorème 2.1 *Sous les hypothèses (H-1)-(H-2) et lorsque* $\nu = 0$*, le système (2.31)-(2.37) admet une solution* $(\psi_q^\pm, V)$ *tel que*

$$\psi_q^\pm \in H^1(0,1) \quad et \quad V \in W^{2,+\infty}(0,1).$$

Avant d'énoncer le théorème principal de ce chapitre, on définit d'abord la transformée de Wigner, associée à une fonction d'onde ψ, par

$$W^\hbar[\psi](x,p) = \frac{1}{2\pi}\int_{\mathbb{R}} e^{i\eta p}\overline{\psi}\left(x + \frac{\hbar}{2}\eta\right)\psi\left(x - \frac{\hbar}{2}\eta\right)d\eta, \tag{2.38}$$

où $\overline{\psi}$ désigne le conjugué de ψ. Ensuite, on introduit l'espace des fonctions tests

$$\mathcal{A} = \left\{ \varphi = \varphi(x,p) \,/\, \mathcal{F}_p(\varphi)(x,\eta) \in L^1\left(\mathbb{R}_\eta; C([0,1]_x)\right) \right\} \text{ (voir [74])},$$

où $\mathcal{F}_p$ est la transformée de Fourier par rapport à p. On définit par $\mathcal{A}'$ l'espace dual de $\mathcal{A}$.

On suppose aussi que le potentiel électrostatique vérifie les hypothèses suivantes

Hypothèses(H)

- Si $V_- > V_+$, on suppose alors que $V'(x) \leq 0$ au voisinage de $x = 1$.
- Si $V_- < V_+$, on suppose alors que $V'(x) \geq 0$ au voisinage de $x = 0$.

Théorème 2.2 *Soit $V \in C^2(0,1)$ fixé et vérifie les hypothèses (H) . Soit $\nu > 0$ et $(\psi_q^{\pm})_{q\in\mathbb{R}^+}$ la solution du problème (2.31)-(2.35). Supposons également que $m \in C^2(0,1)$ et que $G^{\pm}$ satisfait $\int_0^{+\infty}(1+q)G^{\pm}(q)dq < \infty$. On définit par $\mathcal{O}$ une fonction C^∞ à support compact identiquement égale à 1 au voisinage de $[0,1]$. Alors la fonction de Wigner défini pour $(x,p) \in [0,1]\times\mathbb{R}$*

$$\omega_\hbar(x,p) = \int_0^{+\infty} G^+(q)W^\hbar[\mathcal{O}\psi_q^+](x,p)dq + \int_0^{+\infty} G^-(q)W^\hbar[\mathcal{O}\psi_q^-](x,p)dq, \quad (2.39)$$

converge, quand $\hbar$ tend vers zéro, dans $\mathcal{A}'$ faible vers l'unique solution f du problème suivant*

$$(\mathcal{P}_{Lim}) \begin{cases} \dfrac{d\mathcal{E}}{dp}\dfrac{df}{dx} - \dfrac{d\mathcal{E}}{dx}\dfrac{df}{dp} + \nu f = 0 & sur\ \ [0,1], \\ f(0,p) = G^-(p), \quad f(1,-p) = G^+(p), & p > 0, \end{cases}$$

où $\mathcal{E} = \frac{p^2}{2m(x)} - eV(x)$ est l'énergie totale.

Finalement, l'objectif de notre étude est atteint. Il s'agit d'analyser des conditions aux limites sur l'équation de Schrödinger avec masse variable se réduisant dans la limite semi-classique à des conditions aux bords rentrantes pour le modèle cinétique. Notons de plus que la différence entre la limite semi-classique du problème Schrödinger avec masse variable qu'on aborde ici et celle étudiée lorsque m est constante (voir [11] et [15]) se situe au niveau du problème vérifié par la limite de la transformée de Wigner associée à $\psi_q^{\pm}$. Ce dernier est un problème dépendant de q, q étant l'implusion de l'électron en $x = 0$. Pour cela et afin de retrouver le problème cinétique limite, on a été amené à une étude rigoureuse du support de la limite de la transformée de Wigner sur la courbe caractéristique issue de $(x = 0, p = q)$.

2.1.2 Chapitre 2 : Mathematical analysis of the Kohn-Luttinger model

Dans ce chapitre, on s'intéresse au cas où la masse m est considérée constante et la structure de la bande d'énergie est donnée par l'approximation non-parabolique (1.25). Dans le cas unidimensionnel, l'opérateur associé à cette énergie est l'opérateur de Kohn-Luttinger $\mathbb{K}$ donnée par (1.28).

On étudie alors l'équation de Kohn-Luttinger (qu'on notera KL)

$$\mathbb{K}\psi_q - eV(x)\psi_q = E(q)\psi_q \tag{2.40}$$

avec les conditions aux bords mixtes types Fourier suivantes

$$\hbar^2\psi_q''(0) = \hbar(q_- - iq)\psi_q'(0) + iqq_-\psi_q(0) - 2iq(q_- - iq) \tag{2.41}$$
$$\hbar^3\psi_q'''(0) = \hbar(q_-^2 - iq(q_- - iq))\psi_q'(0) + iqq_-(q_- - iq)\psi_q(0) - 2iqq_-(q_- - iq) \tag{2.42}$$
$$\hbar^2\psi_q''(1) = -\hbar(p_- - ip_+)\psi_q'(1) + ip_+p_-\psi_q(1) \tag{2.43}$$
$$\hbar^3\psi_q'''(1) = \hbar(p_-^2 - ip_+(p_- - ip_+))\psi_q'(1) - ip_+p_-(p_- - ip_+)\psi_q(1). \tag{2.44}$$

Le potentiel est self-consistant. Il vérifie l'équation de Poisson suivante

$$\frac{d^2V}{d^2x} = n(x) \tag{2.45}$$
$$V(0) = V_1, \quad V(1) = V_2. \tag{2.46}$$

La densité de charge $n(x)$ est donnée par

$$n(x) = \int_0^{+\infty} G(q)|\psi_q(x)|^2 dq.$$

On suppose que la distribution G est une fonction positive bornée et à support compact de façon que

$$\int_0^{+\infty} q^n G(q) dq < \infty, \quad \forall n \in \mathbb{N}.$$

Pour la résolution de ce type de problème couplé (2.40)-(2.46), on étudie tout d'abord le cas linéaire. Ensuite, une fois que l'existence et unicité de solution est assurée, on passe à l'étude complète du problème couplé. Dans cette étude on est affronté à un sérieux problème (similaire au problème rencontré dans la résolution du problème couplé Schrödinger-Poisson dans le cas multi-dimensionnel (voir [12])), il réside en fait dans l'existence de modes propres $E_j = E(q_j)$ et $j \geq 0$ pour lesquels les résultats d'existence et d'unicité de solution du problème Kohn-Luttinger linéaire ne sont pas vérifiés.

Cependant, comme dans [12], la densité électronique associée au problème couplé est égale à la somme de la densité associée à ces états propres et de celle associée aux états de scattering

$$n(x) = \int_0^{+\infty} G(q)|\psi_q(x)|^2 dq + \sum_{j\in\mathbb{N}^*}\sum_{l=1}^{d_j} \lambda_j^l |\phi_j^l(x)|^2. \tag{2.47}$$

$G(q)$ représente le profil de la source placée en $-\infty$ associé à l'état de scattering ψ_q. $\lambda_j^l \geq 0$ sont les coefficients d'occupation et ϕ_j^l sont les états propres de l'opérateur $\mathbb{K} - eV$ (voir section 1 du chapitre 2).

On se rend compte assez facilement que la définition de $\mathbf{n}(\mathbf{x})$ dans (2.47) pose bien un problème. En effet, les fonctions ψ_q sont les états de scattering du problème Kohn-Luttinger. Si le principe d'absorption limite peut assurer la construction de ces états alors il n'est pas facile d'en déduire leur comportement au voisinage d'une valeur propre plongée dans le spectre continu. Ainsi au voisinage d'une valeur propre E_j, on dispose uniquement de l'estimation

$$||\psi_q||_{L^2(0,1)} \leq \frac{C}{|E(q) - E_j|}$$

qui donne lieu à une singularité non-intégrable.

Pour résoudre ce problème, on adopte une procédure d'absorption limite non-linéaire (utilisée aussi dans [12] et [78]). On commence par ajouter un terme d'absorption $\frac{i\hbar\nu}{4}$ à l'énergie, dans l'équation de Kohn-Luttinger pour assurer l'unicité

$$\mathbb{K}\psi_q^\nu = [E(q) + i\frac{\hbar\nu}{4}]\psi_q^\nu$$

où $\mathbb{K}$ est l'opérateur de Kohn-Luttinger et $\nu > 0$. Ce qui, en vue des conditions aux limites, rend le problème bien posé. La densité électronique est calculée par la formule

$$n^\nu(x) = \int_0^{+\infty} G(q)|\psi_q^\nu(x)|^2 dq.$$

La deuxième étape est de construire une solution du problème couplé avec l'équation de Poisson

$$\frac{d^2V^\nu}{d^2x} = n^\nu(x).$$

On montre l'existence de solution du problème couplé modifié pour $\nu > 0$ par le théorème de point fixe Leray-Schauder [54]. Ensuite, on passe à la limite $\nu \to 0$ dans le problème non-linéaire. On obtient une densité électronique somme de la densité des états de scattering et de la densité des états propres.

Ce modèle sera utilisé dans la pratique pour la simulation des composants du type diode à effet tunnel résonnant intrabande (qu'on notera RTD, Resonant Tunneling Diode), d'où le chapitre 3 suivant.

2.1.3 Chapitre 3 : Numerical analysis of the KL model : Application to the intraband device

On a résolu numériquement le problème couplé (Kohn-Luttinger)-Poisson par une méthode itérative de Gummel linéaire. On a choisi une méthode d'éléments finis. Conformément au cadre fonctionnel du problème Kohn-Luttinger, on a donc utilisé des éléments finis Hermitiens. Le but de cette étude numérique est la simulation numérique d'une RTD (voir figure 3) en utilisant une relation de dispersion non-parabolique.

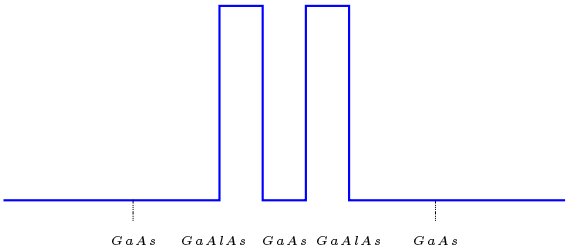

FIG. 3: Diode à effet tunnel résonnant intrabande (RTD).

Il s'agit de déterminer les caractéristiques type courbe courant-tension donnée par l'expression de la densité de courant suivante

$$J(V) = \frac{e\hbar}{2m}\left(\int_0^{+\infty} G(k)\left(-\alpha\frac{\hbar^2}{m}\Im m(\overline{\psi}.\frac{d^3\psi}{dx^3} - \frac{d\overline{\psi}}{dx}.\frac{d^2\psi}{dx^2}) + 2\Im m(\overline{\psi}.\frac{d\psi}{dx})\right)dk, \quad (2.48)$$

la densité de charge

$$n(x) = \int_0^{+\infty} G(k)|\psi(x)|^2 dk, \quad (2.49)$$

et le coefficient de transmission donné par

$$T(q) = \frac{p_+}{q(q_-^2 + q^2)}|\hbar\psi'(1) + p_-\psi(1)|^2 \quad (2.50)$$

où $\Im m$ partie imaginaire.

Les résultats obtenus sont présentés dans les figures suivantes pour le cas parabolique et non-parabolique. Les phénomènes observés sont d'une nature similaire à celle trouvée dans [18], [19], [40], [47], [48], [84], [94] pour le cas parabolique lorsque $\alpha = 0$; dans [69] pour le cas non-parabolique lorsque $\alpha < 0$.

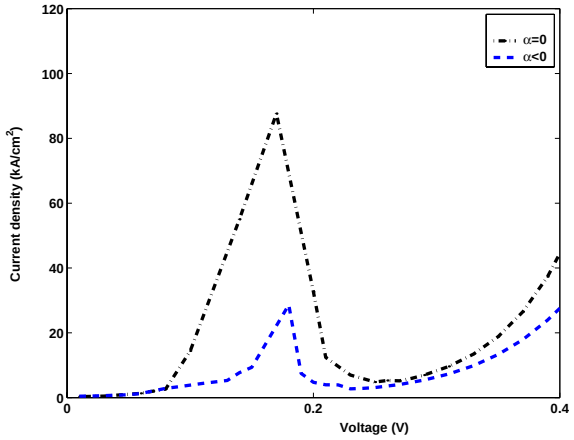

FIG. 4: Les courbes caractéristiques courant-tension pour une RTD.

Dans la figure 4, on a présenté les courbes caractéristiques courant-tension respectivement pour le cas parabolique lorsque $\alpha = 0$ et non-parabolique lorsque α non

nul. Les courbes sont en accord très satisfaisant avec les mesures expérimentales qui prévoient de plus petites densités de courant dans le cas non-parabolique.

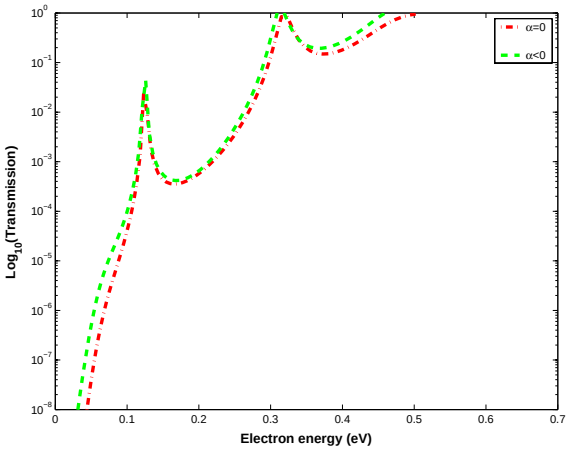

FIG. 5: Les coefficients de transmission pour une RTD.

L'effet de résonance apparaît clairement dans la figure 5, où le graphique du logarithme de la probabilité T (2.50) de transmission pour la diode à effet tunnel résonnant est tracé en fonction de l'énergie en eV. On a comparé la transmission pour l'approximation parabolique et non-parabolique. Notons que l'effet est légèrement plus prononcé pour l'approximation non-parabolique quand $\alpha < 0$. Le résultat principal est que la différence dans la transmission est tout à fait petite dans toute la gamme d'énergie considérée.

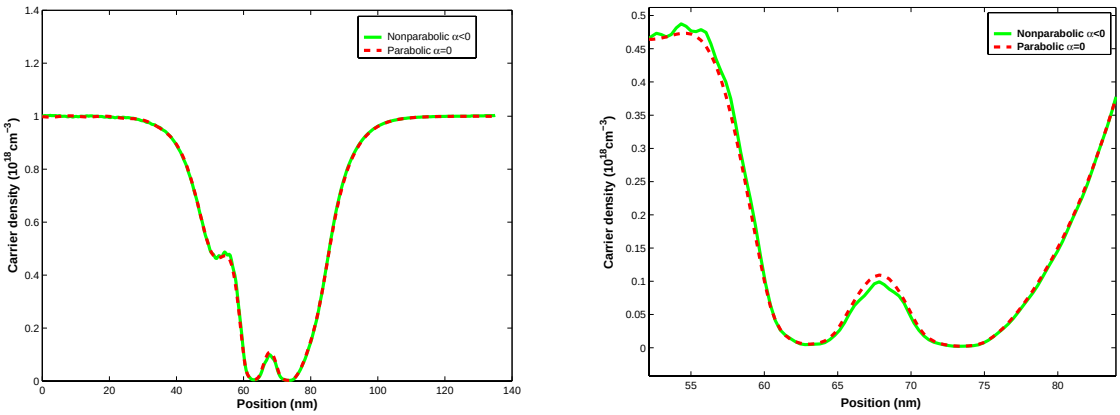

FIG. 6: La densité électronique lorsque $\alpha = 0$ et $\alpha < 0$.

De même dans la figure 6, on note une légère réduction de la densité électronique dans la zone du puits de la diode à effet tunnel résonnant (voir fig3) due à l'effet de non-parabolicité.

2.2 Description de la deuxième partie : Multiband transport

La deuxième partie est consacrée à l'approche Multibande plus précisément à l'approche bibande du modèle Schrödinger où une étude mathématique est effectuée ainsi qu'une étude numérique.

2.2.1 Chapitre 4 : The two-band Schrödinger model

Dans ce chapitre, on a évoqué la question du couplage entre la bande de conduction et la bande de valence. Pour cela, on s'est intéressé au modèle Schrödinger à deux bandes. Il provient du modèle Kane. Le modèle à deux bandes modélise les phénomènes interbandes dans les diodes à effet tunnel résonnant. Dans le cas adimensionné, il est défini par

$$\begin{pmatrix} -\frac{d^2}{dx^2} + V(x) & iP\frac{d}{dx} \\ iP\frac{d}{dx} & -\frac{d^2}{dx^2} - 2\delta + V(x) \end{pmatrix} \mathbf{\Psi}(x) = E\mathbf{\Psi}(x). \tag{2.51}$$

Une première étape vers l'analyse de ce modèle est d'établir les conditions aux limites quantiques qui tiennent compte d'un courant électronique non nul. En effet, on a dérivé les conditions aux bords suivantes

$$\frac{d\Psi}{dx}(0) - iK_-(E)\Psi(0) = i(k_c(E)I_2 - K_-(E))\vec{e_c}^+(E) \tag{2.52}$$

$$\frac{d\Psi}{dx}(1) - iK_+(E - V_1)\Psi(1) = 0, \tag{2.53}$$

pour lesquels on a montré l'existence de solutions dans le cas linéaire lorsque V est fixé.
Avant d'énoncer le théorème principal de ce chapitre, on a défini tout d'abord les quantités macroscopiques issues du modèle Schrödinger à deux bandes. En notant par $f_0(E)$ la statistique de distribution selon laquelle on a injecté les électrons, on a défini la densité de charge par

$$n(x) = \int_0^{+\infty} f_0(E)|\Psi(x)|^2 \frac{dE}{V_c(E)} \tag{2.54}$$

et la densité de courant

$$J(x) = \int_0^{+\infty} f_0(E)\left(\Im m(\mathbb{D}\,\Psi \bullet \Psi)\right)\frac{dE}{V_c(E)}, \tag{2.55}$$

où $V_c(E)$ est la vitesse de groupe et $\mathbb{D}$ est la matrice suivante

$$\mathbb{D} = \begin{pmatrix} \frac{d}{dx} & -iP \\ -iP & \frac{d}{dx} \end{pmatrix}. \tag{2.56}$$

Pour le cas non-linéaire, le potentiel V est self-consistant, il est soumis à l'équation de Poisson

$$\frac{d^2V}{dx^2} = n(x), \tag{2.57}$$

avec les conditions aux bords suivantes

$$V(0) = 0, \qquad V(1) = V_1 > 0. \tag{2.58}$$

On a énoncé ici le résultat principal qu'on a démontré dans ce chapitre. Avant cela, on a supposé en plus que la distribution $f_0(E)$ est une fonction C^∞ à support compact tel que *supp* $f_0(E) \subset [0, E_0]$ avec $E_0 > 0$ et vérifie

$$f_0(E) \geq 0 \text{ et } \int_0^{+\infty} f_0(E)dE < \infty. \tag{2.59}$$

Théorème 2.3 *Sous l'hypothèse (2.59), le système (2.51)-(2.58) admet une solution* $(\mathbf{\Psi}, V)$ *tel que*

$$\mathbf{\Psi} \in H^1(0,1) \times H^1(0,1), \quad V \in W^{2,+\infty}(0,1).$$

La preuve de ce théorème est aussi basée sur un argument de point fixe. Le principe reste le même que celui utilisé dans l'étude du modèle Schrödinger à une bande que ce soit Schrödinger avec masse variable ou Kohn-Luttinger.

Le modèle bibande qu'on vient de présenter peut être utilisé pour modéliser le transport électronique dans une diode à effet tunnel résonnant interbande (qu'on notera RITD, Resonant Interband Tunneling Diode). D'où le but du dernier chapitre 5.

2.2.2 Chapitre 5 : Numerical analysis : Application to InAs/AlSb/GaSb/AlSb/InAs Interband device

Dans ce chapitre, on a considéré une diode à effet tunnel résonnant interbande unidimensionnelle représentée dans la figure 7.

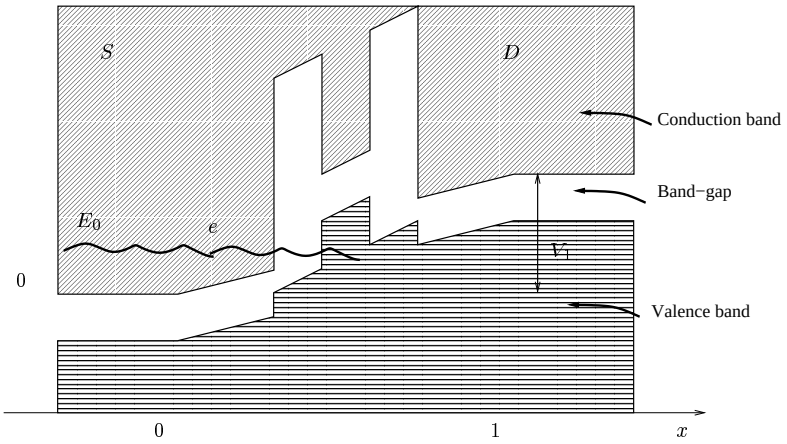

FIG. 7: Représentation schématique du diagramme de bandes d'énergie d'une diode à effet tunnel résonnant interbande unidimensionnelle sous l'effet d'une différence de potentiel V_1.

Elle est basée sur la juxtaposition de matériaux provoquant la présence d'un gap brisé avec un recouvrement local des bandes de conduction et de valence. Les électrons, dans ce type de structure, se déplacent de la bande conduction vers la bande de valence à travers le puits quantique. L'électrode émettrice S est placée en $x = 0$ alors que l'électrode collectrice D est placée en $x = 1$. On applique une différence de potentielle positive entre les deux électrodes. On suppose que $V(0) = 0$ et $V(1) = V_1 > 0$.

On a effectué la résolution de l'équation de Schrödinger à deux bandes comme une équation différentielle ordinaire en utilisant la méthode de Runge-Kutta d'ordre 4 à pas adaptatif. Pour le problème couplé, on a utilisé une procédure itérative type Gummel linéaire.

Le code numérique, qu'on a implémenté, se décompose en deux parties. Pour une énergie E et un potentiel V données, on a commencé par calculer la fonction d'onde Ψ à partir de l'équation de Schrödinger à deux bandes. On en déduit le coefficient de transmission. En répétant cette procédure pour un nombre fini d'énergie, les coefficients de transmission obtenus sont ensuite utilisés pour calculer la densité de courant associé au potentiel donné. On a calculé aussi la densité de charge. On a utilisé sa valeur pour calculer une nouvelle valeur du champs V en résolvant l'équation de Poisson.

Les résultats numériques obtenus sont les suivants. Pour la courbe caractéristique courant-tension, on obtient

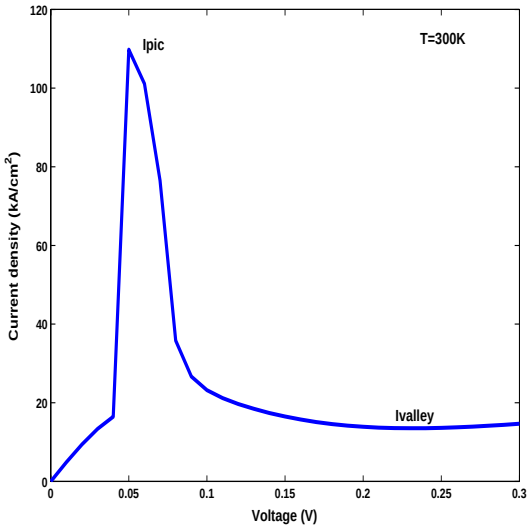

FIG. 8: La courbe caractéristique courant-tension de la diode InAs/AlSb/GaSb/AlSb/InAs à effet tunnel résonnant interbande lorsque $T = 300K$ avec une largeur des barrières AlSb est de $10Ang$ et celle du puits GaSb de $30Ang$.

Le pic du courant est de l'ordre de 110 kA/cm^2. Il est atteint pour une polarisation de 0.05 Volt. On explique ceci par le fait qu'il y a eu un effet tunnel à travers

la bande de valence. Le rapport entre la valeur au pic du courant et celle du courant à la vallée est de 8.3. Ces valeurs sont bonnes à premier à bord. Par exemple, le pic du courant, atteint pour un voltage de 0.05 Volt, est comparable à ce qu' a été obtenu expérimentalement dans l'étude faite par Söderström et al dans [106]. Le rapport pic-vallée est aussi satisfaisant. La valeur simulée du pic du courant est 10 fois plus grande que celle obtenue expérimentalement (voir par exemple dans [64]). La première explication possible et courante [21] est que la simulation numérique d'une diode est trop idéale par rapport au détail d'une mesure expérimentale d'une telle structure. De plus, une largeur de barrière ou du puits inexacte peut changer la valeur du pic du courant ainsi que celle de la vallée. En effet, des études expérimentales montrant l'influence de paramètres géométriques (largeur du puits et des barrières) sur la caractéristique courant-tension d'une RITD ont été réalisées dans [63] et [64].

Le second résultat de simulation est montré dans la figure 9, qui compare le coefficient de transmission en fonction de l'énergie pour deux valeurs de potentiel. L'une obtenue lorsque le courant a atteint le pic et l'autre lorsqu'il a atteint la vallée dans la figure 8.

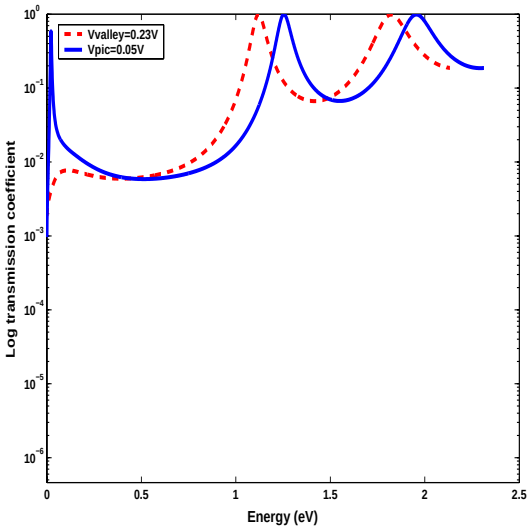

FIG. 9: Spectre de transmission de la diode double barrière RITD sous deux polarisations $Vpic = 0.05\,Volt$ et $Vvallee = 0.23\,Volt$.

L'effet de résonnance apparaît clairement dans la figure 9, où le graphique du coefficient de transmission est tracé en fonction de l'énergie en eV. On note que l'effet est plus prononcé pour la tension appliquée correspondante au pic du courant (courbe pleine) plutôt que celle correspondante au courant de la vallée. Le premier pic est atteint pour une basse énergie $0.02\,eV$ dans la région du $0.15\,eV$ correspondant à la bande de valence. Les deux pics suivants sont atteints pour des énergies plus élevées correspondants aux énergies de résonance dans la bande conduction. Ces constatations sont similaires aux résultats obtenus par Vanbésien, Duez et son équipe

(voir [43] et [115]).

Première partie

Monoband transport

Chapitre 1

The Schrödinger with variable mass model

Sommaire

This chapter has been a subject of paper [62] to appear on Quarterly of Applied Mathematics, under the title

"The Schrödinger with variable mass model : mathematical analysis and semi-classical limit"

It makes even a subject of a note [16] on collaboration with Naoufel Ben Abdallah on Comptes Rendus de l'Académie des Sciences de Paris (C. R. Acad. Sci. Paris, tome. 331, Série I, pp 165-170, 2000).

Abstract.
In this paper, we propose and analyze a one-dimensional stationary quantum-transport model : the Schrödinger with variable mass. In the first part, we prove the existence of a solution for this model, with a self-consistent potential determined by the Poisson problem, whereas, in the second part, we rigorously study its semi-classical limit which gives us the kinetic model limit. The rigorous limit was based on the analysis of the support of the Wigner transform.

Key words. Schrödinger with variable mass ; semi-classical limit ; Wigner transform.

1 Introduction

Electronic devices based on heterostructures are dominated by quantum-interference effects, such as tunneling effect or wave interference. These phenomena usually take place on active regions of the devices. One of the most representative devices in describing such physical phenomena is the Resonant Tunneling Diode (RTD). In general, semiconductor devices are three-dimensional structures. Here, the RTD is represented in one dimension because of its geometry and doping profiles. We assume that the quantum zone (Q) occupies an interval $[0, 1]$. In addition, when the length of the quantum zone (Q) is of the order of some nanometers, an electron submitted to the microscopic periodic potential, behaves like an electron of an effective mass m depending on material. Therefore, we have to consider an effective mass approximation in studying such devices. The more appropriate approach to effective-mass theory, is the use of the Daniel Ben Duke approach which more conveniently includes the mass variation effects [20]. In one dimension, the associated Hamiltonian is written as

$$H = -\frac{\hbar^2}{2}\frac{d}{dx}(\frac{1}{m(x)}\frac{d}{dx}).$$

It corresponds to the Schrödinger Hamiltonian when the mass is constant. We know that the Schrödinger model has first been extensively analyzed in different contexts and settings (see refs [28], [29], [42], [89] and [90]...). There is a solution when the potential is either prescribed or computed self-consistently. Its semi-classical limit has been analyzed in order to derive the interface conditions and to define the kinetic model limit (see refs [12], [52], [53], [74], [81], [82], [96]...).
The mathematical analysis for the quantum and kinetic models developed up to now do not take into account the variation of mass. The purpose of the present paper is to study the quantum model Schrödinger with variable mass and to derive the associated kinetic model .
The paper is organized as follows : in section 2, we set the problem and define the model. In section 3, we prove the existence of a solution when the model is coupled to Poisson. Finally, in the section 4, the semi-classical limit is investigated when analyzing the support of Wigner transform and we conclude in section 5.

2 Setting of the problem

As mentioned above and as treated in ref [12], the quantum region (Q) is represented by an interval $[0, 1]$. We suppose that the electrons, with charge $-e$, are emitted at both sides of the region (Q). An external potential V is applied at the edges of the device. We suppose that each edge is connected with the same material, so for $x < 0$, $V(x) = V_-$ and for $x > 1$, $V(x) = V_+$. Furthermore, the effective mass depends on the variable x inside the Q zone and is constant outside. We denote by m_- its value for $x \leq 0$ and m_+ its value for $x > 1$. Then, let $\psi_q^{\pm}$ be the wave function associated to electrons injected at the left side $(-)$ and the right side $(+)$ of the Q

zone according to the momentum q. It describes the transport of electron by the following equation

$$-\frac{\hbar^2}{2}\frac{d}{dx}(\frac{1}{m(x)}\frac{d\psi_q^{\pm}}{dx}) - eV(x)\psi_q^{\pm} = [\frac{q^2}{2m_{\pm}} - eV_{\pm} + i\frac{\hbar\nu}{2}]\psi_q^{\pm}, \qquad q \geq 0, \quad x \in [0,1].$$

We have added an absorption term $i\frac{\hbar\nu}{2}$ in the second term of the left hand side of the previous equation. The coefficient ν is non-negative and $\hbar$ is the reduced Planck constant. The absorption term is not needed in the analysis of the Schrödinger with variable mass-Poisson for a fixed $\hbar$. However, when passing to the limit $\hbar \to 0$, it will provide independent a priori estimates.
For the boundary conditions at $x = 0$ and $x = 1$, we assume that $\psi_q^{\pm}$ is a wave coming from $\pm\infty$ with an amplitude equals to 1. A part of it is reflected by the potential and goes back to $\pm\infty$, whereas the other part is transmitted and travels to $\mp\infty$.
Since V is defined on the intervals $]-\infty, 0]$ and $[1, +\infty[$, the Schrödinger with variable mass can be solved explicitly and is given by

$$\psi_q^-(x) = e^{i\frac{q}{\hbar}x} + r_q^- e^{-i\frac{q}{\hbar}x},\ \psi_q^+(x) = t_q^+ e^{-\frac{i}{\hbar}\sqrt[+]{q^2\frac{m_-}{m_+}+2em_-(V_- - V_+)}x} \text{ for } x < 0 \tag{2.1}$$

$$\psi_q^-(x) = t_q^- e^{\frac{i}{\hbar}\sqrt[+]{q^2\frac{m_+}{m_-}+2em_+(V_+ - V_-)}(x-1)},\ \psi_q^+(x) = e^{-i\frac{q}{\hbar}(x-1)} + r_q^+ e^{i\frac{q}{\hbar}(x-1)} \text{ for } x > 1 \tag{2.2}$$

where $r_q^{\pm}$ and $t_q^{\pm}$ are respectively the reflection and the transmission coefficients and $\sqrt[+]{a}$ ($a \in \mathbb{R}$) the complex square root with non-negative imaginary part.
The Schrödinger with variable mass can be reduced to the interval $[0,1]$. We eliminate the coefficients $r_q^{\pm}$ and $t_q^{\pm}$. Then, we obtain Fourier type boundary conditions

$$\hbar\psi_q^{-'}(0) + iq\psi_q^-(0) = 2iq, \quad \hbar\psi_q^{+'}(0) = -i\sqrt[+]{\frac{m_-}{m_+}q^2 + 2em_-(V_- - V_+)}\psi_q^+(0)$$

$$\hbar\psi_q^{-'}(1) = i\sqrt[+]{\frac{m_+}{m_-}q^2 + 2em_+(V_+ - V_-)}\psi_q^-(1), \quad \hbar\psi_q^{+'}(1) - iq\psi_q^+(1) = -2iq.$$

In order to define the charge density, we assume that there exist sources at $-\infty$ and $+\infty$ sending the electrons according to a profile $G^-(q)$ and $G^+(q)$. Hence, the charge density is equal to

$$n(x) = \int_0^{+\infty} G^-(q)|\psi_q^-(x)|^2 dq + \int_0^{+\infty} G^+(q)|\psi_q^+(x)|^2 dq.$$

Once the charge density is defined, the potential V solves the Poisson equation

$$\frac{d^2V}{dx^2} = n(x),$$

with the following boundary conditions

$$V(0) = V_-, \qquad V(1) = V_+.$$

3 Existence of solutions

In this section, we use the Leray-Schauder fixed point Theorem (see ref.[54]) to prove the existence of a solution for the stationary Schrödinger with variable mass-Poisson problem. We follow the method given in ref.[15]. Before stating the main Theorem of this section, let's first recall the system

$$-\frac{\hbar^2}{2}\frac{d}{dx}(\frac{1}{m(x)}\frac{d\psi_q^{\pm}}{dx}) - eV(x)\psi_q^{\pm} = [\frac{q^2}{2m_{\pm}} - eV_{\pm} + i\frac{\hbar\nu}{2}]\psi_q^{\pm},\ q \geq 0,\ x \in [0,1]. \quad (3.3)$$

$$\hbar\psi_q^{-'}(0) + iq\psi_q^{-}(0) = 2iq, \hbar\psi_q^{+'}(0) = -i\sqrt{\frac{m_-}{m_+}q^2 + 2em_-(V_- - V_+)}\psi_q^{+}(0) \quad (3.4)$$

$$\hbar\psi_q^{-'}(1) = i\sqrt{\frac{m_+}{m_-}q^2 + 2em_+(V_+ - V_-)}\psi_q^{-}(1), \hbar\psi_q^{+'}(1) - iq\psi_q^{+}(1) = -2iq \quad (3.5)$$

coupled with the Poisson problem

$$\frac{d^2V}{dx^2} = n(x), \quad (3.6)$$

$$V(0) = V_-, \qquad V(1) = V_+. \quad (3.7)$$

The charge density n is given by

$$n(x) = \int_0^{+\infty} G^-(q)|\psi_q^-(x)|^2dq + \int_0^{+\infty} G^+(q)|\psi_q^+(x)|^2dq. \quad (3.8)$$

For the sake of clarity in the sequel, we will note

$$n(x) = n^-(x) + n^+(x), \quad \text{where } n^{\pm}(x) = \int_0^{+\infty} G^{\pm}(q)|\psi_q^{\pm}(x)|^2dq. \quad (3.9)$$

Second, we assume the following

Hypotheses 3.1

$(H-1)$ *There exist* c *and* $C > 0$ *such that* $c \leq m(x) \leq C$.
$(H-2)$ G^- *and* G^+ *are compactly supported functions and verify*

$$G^{\pm} \geq 0 \text{ and } \int_0^{+\infty} G^{\pm}(q)dq < \infty.$$

In the sequel, we assume that *supp* $G^{\pm} \subset [0, q_0]$ with $q_0 > 0$.

Theorem 3.2 *Under hypotheses* $(H-1)-(H-2)$ *and when* $\nu \geq 0$, *the system (3.3)-(3.7) admits a solution* $(\psi_q^{\pm}, V)$ *such that*

$$\psi_q^{\pm} \in H^1(0,1) \quad \text{and} \quad V \in W^{2,+\infty}(0,1).$$

In order to prove this Theorem, we will construct the solution $(\psi_q^{\pm}, V)$ with a fixed point procedure. Starting with a potential $V \in L^\infty(0,1)$, we solve (3.3)-(3.5). We find a solution which we note by $\psi_q^{\pm}(V)$. Then, we define the charge density $n(V)$ associated to $\psi_q^{\pm}(V)$ to which we propose a new potential noted by V^*. It is computed by solving the Poisson equation

$$\frac{d^2V^*}{d^2x} = n(V)$$

and satisfies the boundary conditions

$$V^*(0) = V_-, \qquad V^*(1) = V_+.$$

In the sequel, we will denote by T, the operator transforming V into V^*

$$\begin{array}{ccc} T : L^\infty(0,1) & \longrightarrow & L^\infty(0,1) \\ V & \longmapsto & V^* \end{array} \tag{3.10}$$

To prove that $(V, \psi_q^{\pm}(V))$ is a solution of the Schrödinger with variable mass-Poisson system, we need to prove that V is a fixed point of T. For this, we apply the Leray-Schauder fixed point Theorem (see ref.[54]).

The proof of Theorem 3.2 is organized in several steps. At first, we prove the following Theorem.

Theorem 3.3 *Let V in $L^\infty(0,1)$, m satisfies $(H-1)$ and $\nu \geq 0$, then the Schrödinger with variable mass problem (3.3)-(3.5) admits a unique solution $\psi_q^{\pm} \in H^1(0,1)$.*

Proof. Let $\varphi \in H^1(0,1)$ as a test function. Then, we integrate from 0 to 1. This gives the following formulation

$$\int_0^1 \left\{ \left[-\frac{\hbar^2}{2}\frac{d}{dx}\left(\frac{1}{m(x)}\frac{d}{dx}\right) - e(V(x) - V_{\pm}) - \frac{q^2}{2m_{\pm}} - i\frac{\hbar\nu}{2} \right] \psi_q^{\pm}(x) \right\} \overline{\varphi}(x)dx = 0. \tag{3.11}$$

Afterthat, we integrate by parts and use the boundary conditions (3.4)-(3.5). We obtain for $\psi = \psi_q^-$

$$\frac{\hbar^2}{2}\int_0^1 \frac{1}{m(x)}{\psi_q^-}'\overline{\varphi}'dx - \int_0^1 [e(V - V_-) + \frac{q^2}{2m_-} + i\frac{\hbar\nu}{2}]\psi_q^-\overline{\varphi}dx -$$
$$\frac{i\hbar}{2m_+}\sqrt{\frac{m_+}{m_-}q^2 + 2em_+(V_+ - V_-)}\psi_q^-(1)\overline{\varphi}(1) - \frac{i\hbar}{2m_-}q\psi_q^-(0)\overline{\varphi}(0) = -\frac{i\hbar}{m_-}q\overline{\varphi}(0). \tag{3.12}$$

For $\psi = \psi_q^+$, we get

$$\frac{\hbar^2}{2}\int_0^1 \frac{1}{m(x)}{\psi_q^+}'\overline{\varphi}'dx - \int_0^1 [e(V - V_+) + \frac{q^2}{2m_+} + i\frac{\hbar\nu}{2}]\psi_q^+\overline{\varphi}dx -$$
$$\frac{i\hbar q}{2m_+}\psi_q^+(1)\overline{\varphi}(1) - \frac{i\hbar}{2m_-}\sqrt{\frac{m_-}{m_+}q^2 + 2em_-(V_- - V_+)}\psi_q^+(0)\overline{\varphi}(0) = \frac{i\hbar}{m_+}q\overline{\varphi}(1). \tag{3.13}$$

The variational problem (3.12) and (3.13) can be written as

$$\left\{ \begin{array}{l} \text{search } \psi_q{}^{\pm} \in H^1(0,1), \text{such that} \\ \forall \varphi \in H^1(0,1), \quad Q^{\pm}(\psi_q{}^{\pm}, \varphi) + C^{\pm}(\psi_q{}^{\pm}, \varphi) = L^{\pm}(\varphi), \end{array} \right. \tag{3.14}$$

with

$$Q^{\pm}(\psi_q{}^{\pm}, \varphi) = \frac{1}{m(x)} \psi_q^{\pm\,'} \overline{\varphi}' dx + \int_0^1 \psi_q^{\pm} \overline{\varphi} dx, \tag{3.15}$$

$$\begin{aligned} C^{+}(\psi_q{}^{+}, \varphi) &= -\int_0^1 [e(V - V_+) + \frac{q^2}{2m_+} + i\frac{\hbar\nu}{2}] \psi_q^{+} \overline{\varphi} dx - \int_0^1 \psi_q^{+} \overline{\varphi} dx \\ &\quad - \frac{i\hbar q}{2m_+} \psi_q^{+}(1)\overline{\varphi}(1) - \frac{i\hbar}{2m_-} \sqrt{\frac{m_-}{m_+} q^2 + 2em_-(V_- - V_+)} \psi_q^{+}(0)\overline{\varphi}(0), \end{aligned} \tag{3.16}$$

$$\begin{aligned} C^{-}(\psi_q{}^{-}, \varphi) &= \int_0^1 [e(V - V_-) + \frac{q^2}{2m_-} + i\frac{\hbar\nu}{2}] \psi_q^{-} \overline{\varphi} dx - \int_0^1 \psi_q^{-} \overline{\varphi} dx \\ &\quad - \frac{i\hbar}{2m_+} \sqrt{\frac{m_+}{m_-} q^2 + 2em_+(V_+ - V_-)} \psi_q^{-}(1)\overline{\varphi}(1) - \frac{i\hbar}{2m_-} q \psi_q^{-}(0)\overline{\varphi}(0), \end{aligned} \tag{3.17}$$

$$L^{+}(\varphi) = -\frac{i\hbar}{m_-} q \overline{\varphi}(0), \quad L^{-}(\varphi) = \frac{i\hbar}{m_+} q \overline{\varphi}(1). \tag{3.18}$$

We can easily prove the following estimates

$$Q^{\pm}(\psi, \psi) \geq C ||\psi||^2_{H^1(0,1)} \tag{3.19}$$

$$\begin{aligned} C^{\pm}(\psi, \varphi) &\leq C ||\psi||_{L^2(0,1)} ||\varphi||_{L^2(0,1)} + C ||\psi||_{C^0(0,1)} ||\varphi||_{C^0(0,1)} \\ &\leq C ||\psi||_{H^1(0,1)} ||\varphi||_{H^1(0,1)}. \end{aligned} \tag{3.20}$$

According to the Riesz representation, there exist $A_{Q^{\pm}}\psi$, $A_{C^{\pm}}\psi$ and $f_{L^{\pm}} \in H^1(0,1)$ such that

$$Q^{\pm}(\psi, \varphi) = < A_{Q^{\pm}}\psi, \varphi >_{H^1(0,1)}, \quad C^{\pm}(\psi, \varphi) = < A_{C^{\pm}}\psi, \varphi >_{H^1(0,1)} \text{ and } L^{\pm}(\varphi) = < f_{L^{\pm}}, \varphi >_{H^1(0,1)}.$$

Then, the variational problem (3.14) reads

$$A_{Q^{\pm}}\psi + A_{C^{\pm}}\psi = f_{L^{\pm}}.$$

We notice that $A_{Q^{\pm}}$ is inversible whereas$A_{C^{\pm}}$ is a compact operator from $H^1(0,1)$ to $H^1(0,1)$. Therefore the Fredhlom alternative insures that the variational problem (3.14) is uniquely solvable if $A_{Q^{\pm}} + A_{C^{\pm}}$ is injective. But this is equivalent to prove that the variational problem (3.14) with vanishing right hand side has no solution but the identically vanishing one.

We thus consider a solution ψ of where the right hand side is set equal to zero, choose the test function $\varphi = \psi^{\pm}$ and take the imaginary part of (3.14). We get for ψ^{+}

$$\frac{q}{m_+} |\psi_q^{+}(1)|^2 + \frac{1}{m_-} \sqrt{[\frac{m_-}{m_+} q^2 + 2em_-(V_- - V_+)]^{+}} |\psi_q^{+}(0)|^2 + \nu \int_0^1 |\psi_q^{+}(x)|^2 dx = 0 \tag{3.21}$$

and for ψ^-

$$\frac{1}{m_+}\sqrt{[\frac{m_+}{m_-}q^2+2em_+(V_+-V_-)]^+}|\psi_q^-(1)|^2+\frac{q}{m_-}|\psi_q^-(0)|^2++\nu\int_0^1|\psi_q^-(x)|^2dx=0, \quad (3.22)$$

where, for a real number a, the relation $\sqrt{(a)^+}=\Re e(\sqrt[+]{a})$ holds with $(a)^+=max(a,0)$.

Then, we can deduce that

$$\psi_q^-(1)=0 \quad \text{and } \psi_q^+(0)=0.$$

Using the homogenous version of the boundary conditions (3.4)-(3.5), we also have

$$\psi_q^{-'}(1)=0 \quad \text{and } \psi_q^{+'}(0)=0.$$

In this case, we cannot use the Cauchy Lipschitz Theorem due to the fact that the Schrödinger with variable mass equation is a second-order ordinary differential equation with variable coefficients. For this, integrating equation (3.3) two times from 0 to x, using that V is bounded in $L^\infty(0,1)$ and that m satisfies $(H-1)$, we get the following estimate

$$|\psi_q^\pm(x)| \leq C\int_0^x(x-t)|\psi_q^\pm(t)|dt.$$

Then, as a consequence of the Gronwall Lemma, we get that

$$|\psi_q^\pm(x)| \leq 0 \qquad \forall x\in[0,1]$$

which implies that $\psi_q^\pm=0$.

Now, we give the following a priori estimates.

3.1 A priori estimates

First, let us give some bounds on $\psi_q^\pm$. Choosing $\psi_q^\pm$ as a test function in (3.14) and taking the imaginary part, we obtain

$$R_{q,\pm}^\nu+T_{q,\pm}^\nu+\frac{\nu m_\pm}{q}\int_0^1|\psi_q^\pm(x)|^2dx=1 \quad (3.23)$$

with

$$R_{q,-}^\nu = |\psi_q^-(0)-1|^2,\ T_{q,-}^\nu=\frac{m_-}{qm_+}\sqrt{[\frac{m_+}{m_-}q^2+2em_+(V_+-V_-)]^+}|\psi_q^-(1)|^2 \quad (3.24)$$

$$R_{q,+}^\nu = |\psi_q^+(1)-1|^2,\ T_{q,+}^\nu=\frac{m_+}{qm_-}\sqrt{[\frac{m_-}{m_+}q^2+2em_-(V_--V_+)]^+}|\psi_q^+(0)|^2. \quad (3.25)$$

Equation (3.23) with the boundary conditions (3.4)-(3.5) implies

$$|\psi_q^-(0)| \leq 2, \quad |\hbar\psi_q^{-'}(0)| \leq 2q \tag{3.26}$$

$$|\psi_q^+(1)| \leq 2, \quad |\hbar\psi_q^{+'}(1)| \leq 2q. \tag{3.27}$$

Lemma 3.4 *Let $V \in L^\infty(0,1)$, $\psi_q^\pm$ solution of ((3.3)-(3.5)) and let $q_0 > 0$ be given. Then, there exists $C > 0$ depending on q_0 such that $\forall q \in [0, q_0]$*

$$||\psi_q^\pm||_{L^\infty(0,1)} \leq Ce^{C\sqrt{||V||_{L^\infty}}}. \tag{3.28}$$

For the proof we need the subsequent Lemma.

Lemma 3.5 *Let Y continuous and satisfy*

$$|Y(t)| \leq a\int_0^t \int_0^s |Y(u)|dudt + b$$

where a and b are constants. If Y_0 is a solution of the equation

$$Y_0(t) = a\int_0^t \int_0^s Y_0(u)dudt + b$$

then

$$|Y(t)| \leq Y_0(t).$$

Proof Lemma 3.5 . Let consider Y_0 the limit of Y_0^ϵ such that

$$Y_0^\epsilon(t) = a\int_0^t \int_0^s Y_0^\epsilon(u)dudt + b + \epsilon.$$

We have

$$Y_0^\epsilon(0) = b + \epsilon > b \geq |Y(0)|.$$

Then, there exists t_0^ϵ such that $\forall t \in [0, t_0^\epsilon]$, we have $Y(t) \leq Y_0^\epsilon(t)$.

Moreover, we can prove easily that

$$I = \{t \in [0,1] \text{ such that } Y(s) \leq Y_0^\epsilon(s), \quad \forall s \in [0,t]\}$$

is an open and closed set. Then, $I = [0,1]$ and $|Y(t)| \leq Y_0^\epsilon(t), \quad \forall t \in [0,1]$. Consequently, when ϵ goes to zero, we obtain $|Y(t)| \leq Y_0(t), \quad \forall t \in [0,1]$.

Furthermore, Y_0 satisfy the following system

$$\begin{cases} Y_0^{''}(t) = aY_0(t) \\ Y_0(0) = b, \quad Y_0^{'}(0) = 0, \end{cases}$$

where the solution is $Y_0(t) = b\sinh(\sqrt{a}t)$. Afterthat, we get

$$|Y_0(t)| \leq be^{\sqrt{a}}.$$

This ends the proof of Lemma.

Proof Lemma 3.4. We treat the case with ψ_q^-. Integrating equation (3.3) between 0 and x two times, we get

$$\psi_q^-(x) = \int_0^x m(s) \int_0^s a(t)\psi_q^-(t)dtds + \int_0^x \frac{m(s)}{m^-}\psi_q^{-'}(0)ds + \psi_q^-(0) \tag{3.29}$$

where

$$a(t) = -\frac{2}{\hbar^2}(\frac{q^2}{2m_-} + e(V(x) - V_-))$$

and

$$||a(t)||_{L^\infty} \leq C(q^2 + ||V||_{L^\infty}).$$

Using the above estimates (3.26) and denoting by $C_1 = C(q^2 + ||V||_{L^\infty})$, there exists C_2 depending on q such that equation (3.29) is bounded by

$$|\psi_q^-(x)| \leq C_1 \int_0^x \int_0^s |\psi_q^-(x)|dtds + C_2.$$

From Lemma 3.5, we deduce that

$$||\psi_q^-||_{L^\infty(0,1)} \leq C_2 e^{C_1\sqrt{||V||_{L^\infty}}}.$$

C_1 and C_2 depend on q but $q \in [0, q_0]$. Then, for all q in this intervall, the corresponding constant are bounded by an independent constant C of q such that

$$||\psi_q^-||_{L^\infty(0,1)} \leq C e^{C\sqrt{||V||_{L^\infty}}}.$$

In order to apply the Leray-Schauder fixed point Theorem (see ref.[54]), we need to prove that T, defined by (3.10), is compact, continuous and to have a uniform bound on fixed points of σT for $\sigma \in [0, 1]$. Let us begin by the last step.

Lemma 3.6 *:*
There exists a constant $M > 0$, such that $\forall \sigma \in [0, 1]$ and for all $V \in L^\infty(0, 1)$ such that $V = \sigma TV$ and where T is defined by (3.10), we have

$$||V||_{W^{2,\infty}(0,1)} \leq M. \tag{3.30}$$

Proof. The proof of this Lemma 3.6 follows in analogy with that of Theorem V.1 in ref. [12]. We again use $\psi_q^\pm$ as a test function in (3.14), but now we take the real part. This leads to

$$\frac{\hbar^2}{2}\int_0^1 \frac{1}{m(x)}|\psi_q^{\pm\prime}(x)|^2dx - \int_0^1 [e(V(x) - V_\pm) + \frac{q^2}{2m_\pm}]|\psi_q^\pm(x)|^2dx \quad \leq \quad C_1 q$$

where C_1 depends on $\hbar$. Multiplying this inequality by $G^{\pm}(q)$ and integrating with respect to q, we obtain

$$\frac{\hbar^2}{2}\int_0^{+\infty}\int_0^1 \frac{1}{m(x)} G^{\pm}(q)|\psi_q^{\pm\prime}(x)|^2 dxdq - e\int_0^1 V(x).n^{\pm}(x)dx$$
$$+eV_{\pm}\int_0^1 n^{\pm}(x)dx - \int_0^1\int_0^{+\infty} \frac{q^2}{2m_{\pm}} G^{\pm}(q)|\psi_q^{\pm}(x)|^2 dxdq \leq C_2, \qquad (3.31)$$

where, $n^{\pm}(x)$ is given by (3.9) and $C_2(= C_1\int_0^{+\infty} qG^{\pm}(q)dq) > 0$. Since $G^{\pm}$ is a compactly supported function, we have

$$\int_0^1\int_0^{+\infty} \frac{q^2}{2m_{\pm}} G^{\pm}(q)|\psi_q^{\pm}(x)|^2 dxdq \leq C_3\int_0^1 n^{\pm}(x)dx.$$

Therefore, inequality (3.31) becomes

$$\frac{\hbar^2}{2}\int_0^{+\infty}\int_0^1 \frac{1}{m(x)} G^{\pm}(q)|\psi_q^{\pm\prime}(x)|^2 dxdq - e\int_0^1 V(x).n^{\pm}(x)dx \leq C_2 + C_4\int_0^1 n^{\pm}(x)dx, \quad (3.32)$$

with $C_4(= C_3 - eV_{\pm}) > 0$.

Introducing the kinetic energy density

$$K(x) \;=\; K^-(x) + K^+(x) \qquad (3.33)$$

where

$$K^{\pm}(x) \;=\; \frac{\hbar^2}{2}\int_0^{+\infty} \frac{1}{m(x)} G^{\pm}(q)|\psi_q^{\pm\prime}(x)|^2 dq.$$

Inequality (3.32) takes the following form

$$\int_0^1 K(x)dx - e\int_0^1 V(x).n(x)dx \leq C_2 + C_4\int_0^1 n(x)dx. \qquad (3.34)$$

Using the identities

$$\frac{d^2V_\sigma}{dx^2} = \sigma n(x), \quad V_\sigma(0) = \sigma V_-, \quad V_\sigma(1) = \sigma V_+, \qquad (3.35)$$

we have

$$\int_0^1 K(x)dx + e\int_0^1 \frac{1}{\sigma}|V_\sigma^{'}|^2 dx \leq C_2 + \frac{C_4}{\sigma}|V_\sigma^{'}(1) - V_\sigma^{'}(0)| \leq C_2 + \frac{2C_4}{\sigma}||V_\sigma^{'}||_{L^\infty(0,1)}. (3.36)$$

The compactness of the support of $G^{\pm}$ and the bound of $\frac{1}{m}$ (see hypothesis (H-1)) leads to the following estimate

$$\int_0^1 K^{\pm}(x)dx \geq C_5\int_0^{+\infty} G^{\pm}(q)||\psi_q^{\pm^{'}}(x)||^2_{L^2(0,1)}dq. \qquad (3.37)$$

Now, let us use estimates (3.26), (3.27) and the following relation between $\psi_q^{\pm}$ and $\psi_q^{\pm'}$

$$\psi_q^{-2}(x) = \psi_q^{-2}(0) + 2\int_0^x \psi_q^{-'}(u)\psi_q^{-}(u)du,\ \psi_q^{+2}(x) = \psi_q^{+2}(1) - 2\int_x^1 \psi_q^{+'}(u)\psi_q^{+}(u)du.$$

Then, we obtain

$$||\psi_q^{\pm'}||^2_{L^2(0,1)} \geq C_6||\psi_q^{\pm}||^2_{L^\infty(0,1)} - C_7,$$

for which inequality (3.37) becomes

$$\int_0^1 K^{\pm}(x)dx \geq C_5C_6\int_0^{+\infty} G^{\pm}(q)||\psi_q^{\pm}||^2_{L^\infty(0,1)}dq - C'\ (C' = C_7\int_0^{+\infty} G^{\pm}(q)dq). \quad (3.38)$$

Moreover, as the charge density $n^{\pm}$ satisfies

$$||n^{\pm}||_{L^\infty(0,1)} \leq \int_0^{+\infty} G^{\pm}(q)||\psi_q^{\pm}||^2_{L^\infty(0,1)}dq,$$

inequality (3.38) gives

$$\int_0^1 K^{\pm}(x)dx \quad \geq \quad C_8||n^{\pm}||_{L^\infty(0,1)} - C' \quad (C_8 \leq C_5C_6). \quad (3.39)$$

As V_σ is a solution of the Poisson problem (3.35), we have

$$\frac{1}{\sigma}||V_\sigma'||_{W^{1,\infty}(0,1)} \quad \leq \quad \frac{C_9}{\sigma}||V_\sigma||_{W^{2,\infty}(0,1)} \leq C_9||n||_{L^\infty(0,1)}.$$

Hence, for K, inequality (3.39) becomes

$$\int_0^1 K(x)dx \quad \geq \quad \frac{C_{10}}{\sigma}||V_\sigma'||_{W^{1,\infty}(0,1)} - C', \quad (C_{10} = \frac{C_8}{C_9}).$$

In view of (3.36), this leads to

$$\frac{C_{10}}{\sigma}||V_\sigma'||_{W^{1,\infty}(0,1)} + \frac{e}{\sigma}||V_\sigma'||^2_{L^2(0,1)} \quad \leq \quad C'' + \frac{2C_4}{\sigma}||V_\sigma'||_{L^\infty(0,1)}, \qquad (C'' = C_2 + C'). \quad (3.40)$$

In the above estimate, we notice non-homogeneity between the left and the right hand side. This is due to the nonlinear character of the system. Our purpose is to obtain a σ-independent bound. Indeed, a Gagliardo-Nirenberg interpolation result (see [27]) leads to

$$||f||_{L^\infty(0,1)} \quad \leq \quad C_{11}||f||^{\frac{2}{3}}_{L^2(0,1)}||f||^{\frac{1}{3}}_{W^{1,\infty}(0,1)}.$$

Applying this inequality to V_σ', we get

$$||V_\sigma'||_{L^\infty(0,1)} \quad \leq \quad C_{11}||V_\sigma'||^{\frac{2}{3}}_{L^2(0,1)}||V_\sigma'||^{\frac{1}{3}}_{W^{1,\infty}(0,1)}.$$

Then, applying Young inequality (see [27]), we have

$$C_{11}||V_\sigma^{'}||^{\frac{2}{3}}_{L^2(0,1)}||V_\sigma^{'}||^{\frac{1}{3}}_{W^{1,\infty}(0,1)} \leq \frac{C_{11}}{2}(||V_\sigma^{'}||^{\frac{4}{3}}_{L^2(0,1)} + ||V_\sigma^{'}||^{\frac{2}{3}}_{W^{1,\infty}(0,1)}).$$

Hence, under these previous manipulations, estimate (3.40) becomes

$$\frac{C_{10}}{\sigma}||V_\sigma^{'}||_{W^{1,\infty}(0,1)} + \frac{e}{\sigma}||V_\sigma^{'}||^2_{L^2(0,1)} \leq C^{''} + \frac{C_{12}}{\sigma}(||V_\sigma^{'}||^{4/3}_{L^2(0,1)} + ||V_\sigma^{'}||^{2/3}_{W^{1,\infty}(0,1)}), \quad (C_{12} = C_4 C_{11}).$$

Since the parameter σ is in $[0,1]$, we obtain a σ-independent bound

$$C_{10}||V^{'}||_{W^{1,\infty}(0,1)} - C_{12}||V^{'}||^{2/3}_{W^{1,\infty}(0,1)} + e||V^{'}||^2_{L^2(0,1)} - C_{12}||V^{'}||^{4/3}_{L^2(0,1)} \leq C^{''}.$$

Therefore, this estimate implies the bound of V in $W^{2,\infty}(0,1)$ by a constant C depending on C_{10}, e, C_{12} and $C^{''}$. Then, Lemma 3.6 is proved.

As a consequence of this result, even $V^*(= TV)$ solution of the Poisson problem is bounded in $W^{2,\infty}(0,1)$.

3.2 Compactness and continuity

Lemma 3.7 *The operator T, defined by (3.10), is a continuous and compact operator on $L^\infty(0,1)$.*

For the proof of this Lemma 3.7, we need the following subsequent Lemma.

Lemma 3.8 *The map defined by*

$$\begin{array}{rccc} S : \mathbb{R}^+_* \times L^\infty(0,1) & \longrightarrow & H^1(0,1) \\ (q, V) & \longmapsto & \psi_q^\pm(V) \end{array} \tag{3.41}$$

is continuous in $\mathbb{R}^+_* \times L^\infty(0,1)$.

Proof Lemma 3.8. Let q_j and V_j be a converging sequences respectively in $\mathbb{R}^+_*$ and $L^\infty(0,1)$. We denote by q and V their limits. We need to prove that $\psi_j = \psi^\pm_{q_j}(V_j(x))$ converges strongly in $H^1(0,1)$.
First of all, we prove easily that $\psi^\pm_q(x)$ is bounded in $L^2(0,1)$. This implies after a possible extraction of a sequence that ψ_j converges strongly in $L^2(0,1)$.
Then, passing to the limit in (3.3)-(3.5), we easily deduce that ψ_j converges strongly in $H^1(0,1)$ and that the limit $\psi^\pm_q$ of $(\psi)_j$ is nothing but $\psi^\pm_q(V)$ the unique solution of the problem (3.3)-(3.5) when $q \neq 0$. The uniqueness of the limit implies that all the sequence converges.

Proof Lemma 3.7. We first deduce from Lemma 3.4, regularities and proprieties of the Poisson equation that the image of a bounded set of $L^\infty(0,1)$ is a bounded set of $W^{2,\infty}(0,1)$. Since this space is compactly injected in $L^\infty(0,1)$, we conclude that

T is compact. To prove continuity, let V_j be a converging sequence in $L^\infty(0,1)$. Let V be its limit. Then, we denote by

$$(\psi_q^\pm)_j \quad = \quad \psi_q^\pm(V_j), \quad n_j = n((\psi_q^\pm)_j).$$

Since T is compact, we deduce after a possible extraction of a sequence that $V_j^*(= TV_j)$ converges strongly in $L^\infty(0,1)$ towards a limit V^*. Our purpose is to prove that $V^* = TV$. This incidentally will prove that there is no need to extract a subsequence. Since for any given q, $(\psi_q^\pm)_j$ and n_j are respectively bounded in $H^1(0,1)$ and $L^\infty(0,1)$, we have after a possible extraction that

$$(\psi_q^\pm)_j \quad \to \quad \psi_q^\pm \quad H^1(0,1) \text{ strong}, \quad n_j \rightharpoonup \tilde{n} \quad L^\infty(0,1) \text{ weak } *.$$

Passing to the limit in (3.3)-(3.5), we easily deduce that the limit $\psi_q^\pm$ of $(\psi_q^\pm)_j$ is nothing but $\psi_q^\pm(V)$. The uniqueness of the limit implies that all the sequence converges. In view of Lemma 3.8 and that $(\psi_q^\pm)_j$ converges strongly in $H^1(0,1)$, there exists $C > 0$ such that $\forall q \in [0, q_0]$ and $\forall j$, we have

$$||(\psi_q^\pm)_j||_{L^\infty(0,1)} \leq C.$$

Then, using the Lebesgue dominated convergence Theorem, we deduce the uniform convergence respect to x

$$\lim_{j \to +\infty} \int_0^{+\infty} G^\pm(q) |(\psi_q^\pm)_j(x)|^2 dq = \int_0^{+\infty} G^\pm(q) |\psi_q^\pm(x)|^2 dq.$$

We can now pass to the limit in

$$-{V_j^*}'' = n_j, \qquad \text{with } V_j(0) = V_- \qquad \text{and } V_j(1) = V_+$$

which leads to

$$-{V^*}'' = n, \qquad \text{with } V(0) = V_- \qquad \text{and } V(1) = V_+.$$

This leads to the end of the proof.

Finally, using Lemma 3.6 and Lemma 3.7, we can apply the Leray-Schauder Fixed Point Theorem (see ref.[54]) to T which implies the existence of a solution. This ends the proof of Theorem 3.2.

4 Semi-classical limit

Our purpose in this section is to pass to the limit $\hbar$ to zero in the Schrödinger with variable mass problem (3.3)-(3.5) and to obtain the kinetic model on the quantum region (Q). Due to the lack of estimates induced by turning points, here we shall prove the result only when the electric potential V is given and regular and when

the absorption ν is strictly positive and fixed. This semi-classical limit is introduced and is formally studied in ref [16].
Before we state with the main Theorem of this section, we define the Wigner transform (see ref [118]). In general case, for all $\psi \in L^2(\mathbb{R})$ and $\phi \in L^2(\mathbb{R})$, we denote by

$$W^\hbar[\psi,\phi] = \frac{1}{2\pi}\int_{\mathbb{R}} e^{i\eta p}\overline{\psi}(x+\frac{\hbar}{2}\eta)\phi(x-\frac{\hbar}{2}\eta)d\eta,\ \forall\ (x,p)\in\mathbb{R}^2, \tag{4.42}$$

where "$\bar{}$" denotes the complex conjugation. Moreover, when $\psi = \phi$, we note by $W^\hbar[\psi] = W^\hbar[\psi,\psi]$. Then, follow ref [74], we introduce the space of test-functions

$$\mathcal{A} = \left\{\ \varphi = \varphi(x,p)\ /\ \mathcal{F}_p(\varphi)(x,\eta) \in L^1\left(\mathbb{R}_\eta; C([0,1]_x)\right)\ \right\} \tag{4.43}$$

where $\mathcal{F}_p$ is the Fourier transform with respect to p

$$\mathcal{F}_p(\varphi(x,\eta)) = \frac{1}{2\pi}\int_{-\infty}^{+\infty} e^{i\eta p}\varphi(x,p)dp.$$

The norm on $\mathcal{A}$ is defined by

$$||\varphi||_{\mathcal{A}} = \int_{-\infty}^{+\infty} \underset{x\in(0,1)}{sup}\ |\mathcal{F}(\varphi(x,\eta))|d\eta$$

and in the sequel we will denote by $\mathcal{A}'$ the dual space of $\mathcal{A}$.

As treated in [11], we shall assume the following non resonance hypotheses on the electrostatic potential

Hypotheses(H)

- In case $V_- > V_+$, we suppose $V^{'}(x) \le 0$ in the vicinity of $x = 1$
- In case $V_- < V_+$, we suppose $V^{'}(x) \ge 0$ in the vicinity of $x = 0$

Theorem 4.1 *Let $V \in C^2(0,1)$ fixed and satisfies hypotheses (H). Let $\nu > 0$ and $\psi_q^\pm$ the solution of the problem (3.3)-(3.5) with $m \in C^2(0,1)$. We also assume that $G^\pm$ satisfies $\int_0^{+\infty}(1+q)G^\pm(q)dq < \infty$. We define $\mathcal{O}$ as a C^∞ compactly supported function identically equal to 1 in a neighborhood of $[0,1]$. Then, for $(x,p)\in[0,1]\times\mathbb{R}$, the Wigner function*

$$\omega_\hbar(x,p) = \int_0^{+\infty} G^+(q)W^\hbar[\mathcal{O}\psi_q^+](x,p)dq + \int_0^{+\infty} G^-(q)W^\hbar[\mathcal{O}\psi_q^-](x,p)dq \tag{4.44}$$

*converges in $\mathcal{A}'$ weakly *, when $\hbar$ goes to zero, toward the unique solution f of the problem*

$$(\mathcal{P}_{Lim})\begin{cases} \dfrac{d\mathcal{E}}{dp}\dfrac{df}{dx} - \dfrac{d\mathcal{E}}{dx}\dfrac{df}{dp} + \nu f = 0 & on\ \ [0,1], \\ f(0,p) = G^-(p), \quad f(1,-p) = G^+(p), & p > 0, \end{cases}$$

where $\mathcal{E} = \frac{p^2}{2m(x)} - eV(x)$ is the total energy.

Remark 4.2 *The total energy* $\mathcal{E}(x,p) = \frac{p^2}{2m(x)} - eV(x)$ *is conserved along the characteristic curves defined by*

$$\frac{dx}{dt} = \frac{p(t)}{m(x(t))}, \quad \frac{dp}{dt} = \frac{p^2}{2}\frac{m^{'}(x(t))}{m^2(x(t))} + eV^{'}(x(t)).$$

Before proving the Theorem, let us first begin by showing some technical estimates.

4.1 Estimates

Lemma 4.3 *Let* V *be in* $C^2(0,1)$ *then there exists a constant* $C > 0$ *independent of* V, q *and* $\hbar$ *such that*

$$\begin{aligned} ||\psi_q^{\pm}||_{L^2(0,1)} &\leq C\sqrt{q}, \quad ||\psi_q^{\pm^{'}}||_{L^2(0,1)} \leq C\frac{\sqrt{q(q+1)}}{\hbar}, \\ ||\psi_q^{\pm^{''}}||_{L^2(0,1)} &\leq C\frac{\sqrt{q}(q+1)}{\hbar^2}, \quad \forall q \in \mathbb{R}_+ . \end{aligned}$$

Proof. Since $\psi_q^{\pm}$ is a solution of the Schrödinger with variable mass problem (3.3)-(3.5), it verifies the weak formulations (3.12)-(3.13). Considering $\psi_q^{\pm}$ as a test function and taking the imaginary part given by (3.23), we obtain for $\nu > 0$

$$||\psi_q^{\pm}||^2_{L^2(0,1)} \leq Cq.$$

From the Schrödinger with variable mass and using the bound of m, we deduce that

$$||\psi_q^{\pm^{''}}||_{L^2(0,1)} \leq C\frac{\sqrt{q}(q+1)}{\hbar^2}.$$

Now, we take the real part of the formulation (3.12)-(3.13)

$$\frac{\hbar^2}{2}\int_0^1 \frac{1}{m(x)}|\psi_q^{-^{'}}(x)|^2dx - \int_0^1 [e(V-V_-) + \frac{q^2}{2m_-}]|\psi_q^-(x)|^2dx = -\frac{\hbar}{m_-}q\mathcal{I}m(\psi_q^-(0)), \quad (4.45)$$

$$\frac{\hbar^2}{2}\int_0^1 \frac{1}{m(x)}|\psi_q^{+^{'}}(x)|^2dx - \int_0^1 [e(V-V_+) + \frac{q^2}{2m_+}]|\psi_q^+(x)|^2dx = -\frac{\hbar}{m_+}q\mathcal{I}m(\psi_q^+(1)). \quad (4.46)$$

Then, using the estimates on $\psi_q^-(0)$ and $\psi_q^+(1)$ given by (3.26)-(3.27), we obtain

$$||\psi_q^{\pm^{'}}||_{L^2(0,1)} \leq C\frac{\sqrt{q(q+1)}}{\hbar}.$$

In the following, let us give some L^∞-bound on ψ_q^+ and ψ_q^-.

Lemma 4.4 *Let* V *be in* $C^2(0,1)$ *and satisfies Hypothesis (H). Then the following estimates hold*

$$\begin{aligned} |\psi_q^-(1)|^2 &\leq \frac{Cq}{\sqrt{|q^2 + 2em_-(V_+ - V_-)|}}, \quad \hbar^2||\psi_q^{-^{'}}||^2_{L^\infty} \leq Cq(1+q) \\ |\psi_q^+(0)|^2 &\leq \frac{Cq}{\sqrt{|q^2 + 2em_+(V_- - V_+)|}}, \quad \hbar^2||\psi_q^{+^{'}}||^2_{L^\infty} \leq Cq(1+q). \end{aligned}$$

Proof. For the sake of simplicity, we will only prove the estimate for ψ_q^-. We first recall that in view of the boundary condition (3.4) and the expression (3.23), we have

$$|\psi_q^-(0)| \leq 2, \quad |\hbar \psi_q^{-'}(0)| \leq 2q.$$

To look for the bound of ψ_q^- and $\psi_q^{-'}$ at $x = 1$, we distinguish two cases. This is illustrated in the following figure.

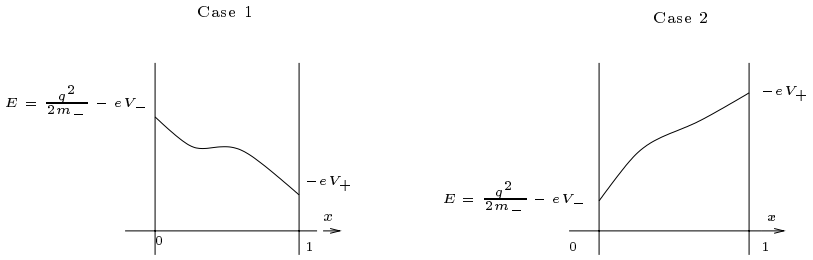

FIG. 1.1: The two cases.

Case 1 : The term $\sqrt[+]{q^2 + 2em_-(V_+ - V_-)} \in \mathbb{R}^+$. In view of the boundary condition (3.5) and the expressions (3.23), (3.24) and (3.25), we have

$$|\psi_q^-(1)|^2 \leq \frac{Cq}{\sqrt{q^2 + 2em_-(V_+ - V_-)}}, \quad \hbar^2 |\psi_q^{-'}(1)|^2 \leq Cq\sqrt{q^2 + 2em_-(V_+ - V_-)}.$$

Case 2 : The term $\sqrt[+]{q^2 + 2em_-(V_+ - V_-)} \in i\mathbb{R}^+$. We multiply (3.3) by $\overline{\psi_q^-}$ and we take the real part. After some algebra, we obtain the following equation on $|\psi_q^-|^2$

$$\frac{\hbar^2}{2}\frac{d}{dx}\left(\frac{1}{m(x)}\frac{d|\psi_q^-|^2}{dx}\right) = 2\left[-\frac{q^2}{2m_-} + e(V_- - V(x))\right]|\psi_q^-|^2 + \frac{\hbar^2}{m(x)}|\psi_q^{-'}|^2.$$

Due to the fact that the second term of the right hand side is non-negative and that $1/m(x)$ is bounded, we get the following inequality

$$C\hbar^2(|\psi_q^-|^2)'' \geq (eV_- - eV(x) - \frac{q^2}{2m_-})|\psi_q^-|^2. \tag{4.47}$$

Let us denote by

$$l = -q^2 + 2em_-(V_- - V_+) > 0.$$

Inequality (4.47) becomes

$$(|\psi_q^-|^2)'' \geq \frac{C}{\hbar^2}\left(l + 2em_-(V_+ - V(x))\right)|\psi_q^-|^2. \tag{4.48}$$

Besides, the boundary condition (3.4) at $x = 1$ yields to

$$(|\psi_q^-|^2)'(1) = -\frac{2}{\hbar}\sqrt{\frac{-m_+}{m_-}q^2 - 2em_+(V_+ - V_-)}|\psi_q^-|^2(1) \leq 0. \tag{4.49}$$

In order to solve (4.48)-(4.49), we have to bound the right hand side of inequality (4.48). Under Hypothesis (H), we distinguish the case where $V^{'}(1) < 0$ and the case where $V^{'}(1) = 0$. This can be illustrated in the following figure.

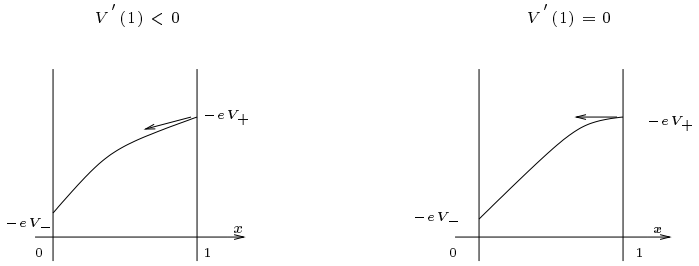

FIG. 1.2: Behavior of potential in neighborhood of $x = 1$

In case, where $V^{'}(1) < 0$, there exists $\delta_0 > 0$ such that $\forall x \in [1 - \delta_0]$, (4.48) verifies

$$(|\psi_q^-|^2)'' \geq C\frac{l}{\hbar^2}|\psi_q^-|^2. \tag{4.50}$$

Solving the above differential inequality with condition (4.49), we obtain

$$|\psi_q^-(x)|^2 \geq |\psi_q^-(1)|^2 e^{-C\frac{\sqrt{l}}{\hbar}(x-1)}, \quad \text{on } [1-\delta_0, 1].$$

Now, integrating with respect to x in $[1 - \delta_0, 1]$, we get

$$\delta_0|\psi_q^-(1)|^2 \leq |\psi_q^-(1)|^2 \int_{1-\delta_0}^{1} e^{-C\frac{\sqrt{l}}{\hbar}(x-1)}dx \leq \int_0^1 |\psi_q^-(x)|^2 dx \leq Cq.$$

Consequently, the estimate for $|\psi_q^-(1)|^2$ holds in this case.

In case $V^{'}(1) = 0$, as V is continuous, we have

$$\forall\, \epsilon > o,\ \exists\, \eta > 0 \ \text{ s.t } \ |x-1| < \eta \ \text{ and } \ |eV_+ - eV(x)| \leq \epsilon.$$

Using Taylor series expansion, we have the following estimate

$$|eV_+ - eV(x)| \leq \frac{e||V^{''}||_{L^\infty}}{2}(x-1)^2.$$

It suffices then that $\frac{e||V^{''}||_{L^\infty}}{2}|x-1|^2 \leq \frac{l}{2}$, to get $|x-1| \leq C\sqrt{l}$. Then, there exists an interval of length $\sqrt{l}$, for which the estimate holds.

We group the results and get the following estimate on $\psi_q^-(1)$, $\psi_q^{-'}(1)$

$$|\psi_q^-(1)|^2 \leq \frac{Cq}{\sqrt{|q^2 + 2em_-(V_+ - V_-)|}},\ \hbar^2|\psi_q^{-'}(1)|^2 \leq Cq\sqrt{|q^2 + 2em_-(V_+ - V_-)|}, \tag{4.51}$$

where C does not depend on q neither on $\hbar$. Then, the first estimate of the Lemma holds.

Let us now introduce the function

$$G(x) = \frac{\hbar^2}{2m(x)}|Re\,\psi_q^{-'}(x)|^2 + (\frac{q^2}{2m_-} - eV_- + eV(x))|Re\,\psi_q^-(x)|^2.$$

Using the Shrödinger with variable mass equation (3.3), we have

$$G^{'}(x) = eV^{'}(x)|Re\,\psi_q^-(x)|^2 + \frac{\hbar^2 m^{'}(x)}{2m^2(x)}|Re\,\psi_q^{-'}(x)|^2 + \hbar\nu Re\,\psi_q^{-'}(x)\mathcal{I}m\,\psi_q^-(x).$$

Since $||\psi_q^-||_{L^2(0,1)} \leq C\sqrt{q}$, $\hbar^2||\psi_q^{-'}||^2_{L^2(0,1)} \leq Cq(q+1)$ (see Lemma 4.3) and $m \in C^2(0,1)$, then

$$||G^{'}||_{L^1(0,1)} \leq Cq(q+1).$$

Moreover, (4.51) implies the estimate

$$|G(1)| \leq Cq(1+q).$$

Consequently, $G(x)(= -\int_x^1 G^{'}(t)dt + G(1))$ is bounded in L^∞ by $Cq(1+q)$.

Let now, a point $x_M \in [0,1]$ on which $|Re\,\psi_q^{-'}(x)|$ achieves its maximum. If $x_M = 0$ or $x_M = 1$ then

$$\hbar^2|Re\,\psi_q^{-'}(x_M)|^2 \leq Cq(1+q).$$

If $x_M \in [0,1]$ then $Re\,\psi_q^{-''}(x_M) = 0$. Using the Shrödinger with variable mass equation (3.3), we deduce that

$$(\frac{q^2}{2m_-} - eV_- + eV(x_M))|Re\,\psi_q^-(x_M)|^2 \leq Cq(1+q)$$

which implies in view of the bound on G, that

$$\hbar^2|Re\,\psi_q^{-'}(x_M)|^2 \leq Cq(1+q).$$

Hence in all cases we have

$$\sup_{x\in[0,1]} \hbar^2|Re\,\psi_q^{-'}(x)|^2 \leq Cq(1+q).$$

The same manipulation can be done by considering the imaginary part and finally yields

$$\hbar^2||\psi_q^{-'}||^2_{L^\infty} \leq Cq(1+q).$$

This ends the proof.

4.2 Property of Wigner transform

In the sequel, we shall denote the Wigner transform $W^\hbar$ associated to $\psi_q^\pm$ by different expressions

$$W_\hbar^\pm = W_\hbar^\pm(q,x,p) = W_q^{\hbar,\pm}(x,p) = W^\hbar[O\psi_q^\pm](x,p)$$

and its limit by

$$W^\pm = W^\pm(q,x,p) = W_q^\pm(x,p).$$

Lemma 4.5 *There exists $W^\pm \geq 0$, in $L^\infty_{Loc}\left(\mathbb{R}_q^+;\mathcal{A}'\right)$ such that $\frac{W^\pm}{(1+q)} \in L^\infty(\mathbb{R}_q^+;\mathcal{A}')$ and after a possible extraction, we have*

$$\frac{W_\hbar^\pm}{(1+q)} \underset{\hbar\to 0}{\rightharpoonup} \frac{W^\pm}{(1+q)} \quad \text{in} \quad L^\infty(\mathbb{R}_q^+;\mathcal{A}') \text{ weak } *.$$

Proof. Let Q be a test function in $\mathcal{A}$. We have

$$\begin{aligned}
&\left|\int_0^1\int_{-\infty}^{+\infty} Q(x,p)W_q^{\hbar,\pm}(x,p)dxdp\right| \\
&\quad\leq \int_0^1\int_{-\infty}^{+\infty} |\mathcal{F}_p(Q(x,\eta))O\overline{\psi_q^\pm}\left(x+\frac{\hbar}{2}\eta\right)O\psi_q^\pm\left(x-\frac{\hbar}{2}\eta\right)|dxd\eta \\
&\quad\leq ||Q||_{\mathcal{A}}||\psi_q^\pm||_{L^2}^2.
\end{aligned}$$

Besides, Lemma 4.3 implies that

$$||\frac{W_\hbar^\pm}{(1+q)}||_{\mathcal{A}'} \leq C$$

with C is independent of q and $\hbar$. A direct consequence is that there exists a subsequence (also denoted by $\hbar$) which converges to $\frac{W^\pm}{(1+q)}$ in $L^\infty(\mathbb{R}_q^+;\mathcal{A}')$ weak *.

Remark 4.6 *In order to lighten the already heavy notation, we note $\psi_q^\pm(\pm) = \psi_q^\pm\left(x \pm \frac{\hbar}{2}\eta\right)$ and analogously for $O(\pm)$ and $m(\pm)$.*

4.3 Proof of Theorem 4.1

To pass to the semi-classical limit in problem (3.3)-(3.4), we proceed analogously to ref. [11]. We shall see that new difficulties arise because the effective mass is not constant. A long but straightforward computation leads to the following identity

$$\begin{aligned}
\frac{p}{m(x)}\frac{dW_q^{\hbar,\pm}}{dx}(x,p) &= \sum_{i=1}^3 r_\hbar^i(x,p) + \left[p\frac{m'(x)}{m^2(x)} - \nu\right]W_q^{\hbar,\pm}(x,p) \\
&\quad -\frac{i}{2\pi m(x)}\left(\frac{q^2}{2m_\pm} - eV_\pm\right)\int_{-\infty}^{+\infty} e^{i\eta p}\delta_\hbar(m)O\overline{\psi_q^\pm}(+)O\psi_q^\pm(-)d\eta \\
&\quad +\frac{i}{2\pi m(x)}\int_{-\infty}^{+\infty} e^{i\eta p}\delta_\hbar(m\mathcal{V})O\overline{\psi_q^\pm}(+)O\psi_q^\pm(-)d\eta \qquad (4.52)
\end{aligned}$$

where

$$r^1_\hbar(x,p) = \frac{-\hbar}{m(x)}\mathcal{I}m(W^\hbar[O^{''}\psi^\pm_q, O\psi^\pm_q]), \quad r^2_\hbar(x,p) = \frac{-2\hbar}{m(x)}\mathcal{I}m(W^\hbar[O^{'}\psi^{\pm\prime}_q, O\psi^\pm_q])$$
$$r^3_\hbar(x,p) = -\hbar\frac{m^{'}(x)}{m^2(x)}\mathcal{I}m(W^\hbar[O^{'}\psi^\pm_q, O\psi^\pm_q])$$

and

$$\delta_\hbar(m\mathcal{V}) = \frac{m(+)\mathcal{V}(+) - m(-)\mathcal{V}(-)}{\hbar}, \quad \text{with} \quad \mathcal{V}(x) = -eV(x)$$
$$\delta_\hbar(m) = \frac{m(+) - m(-)}{\hbar}.$$

Let $Q(x,p)$ be a test function in $\mathcal{A}$. Multiplying (4.52) by Q and integrating with respect to (x,p) in $[0,1]\times\mathbb{R}$, we obtain

$$\begin{aligned}
&\int_0^1\int_{-\infty}^{+\infty} Q(x,p)\frac{p}{m(x)}\frac{dW^{\hbar,\pm}_q}{dx}(x,p)dxdp = \\
&\qquad \int_0^1\int_{-\infty}^{+\infty}\sum_{i=1}^5 r^i_\hbar(x,p)Q(x,p)dxdp \\
&+ \int_0^1\int_{-\infty}^{+\infty} Q(x,p)\left(p\frac{m^{'}(x)}{m(x)} - \nu\right)W^{\hbar,\pm}_q(x,p)\,d\eta dxdp \\
&- \frac{i}{2\pi}(\frac{q^2}{2m_\pm} - eV_\pm)\int_0^1\int_{-\infty}^{+\infty}\frac{Q(x,p)}{m(x)}\int_{-\infty}^{+\infty} e^{i\eta p}\eta\, m^{'}(x)O\overline{\psi^\pm_q}(+)O\psi^\pm_q(-)d\eta dxdp \\
&+ \frac{i}{2\pi}\int_0^1\int_{-\infty}^{+\infty}\frac{Q(x,p)}{m(x)}\int_{-\infty}^{+\infty} e^{i\eta p}\eta\,(m\mathcal{V})^{'}(x)O\overline{\psi^\pm_q}(+)O\psi^\pm_q(-)d\eta dxdp \qquad (4.53)
\end{aligned}$$

where

$$r^4_\hbar(x,p) = \frac{i}{2\pi m(x)}\int_{-\infty}^{+\infty} e^{i\eta p}\left[\delta_\hbar(m\mathcal{V}) - \eta(m\mathcal{V})^{'}\right]O\overline{\psi^\pm_q}(+)O\psi^\pm_q(-)d\eta$$
$$r^5_\hbar(x,p) = -\frac{i}{2\pi m(x)}(\frac{q^2}{2m_\pm} - eV_\pm)\int_{-\infty}^{+\infty} e^{i\eta p}\left[\delta_\hbar(m) - \eta\, m^{'}(x)\right]O\overline{\psi^\pm_q}(+)O\psi^\pm_q(-)d\eta.$$

After, we integrate by parts the first member of equation (4.53) and we multiply the resulting identity by a second test function $S(q)\in L^1(\mathbb{R}^+_q,(1+q)dq)$. Once more, we integrate with respect to q. This leads to the following identity

$$\begin{aligned}
&\int_0^{+\infty}\left(\left[\int_{-\infty}^{+\infty}\frac{p}{m(x)}Q(x,p)W^{\hbar,\pm}_q(x,p)dp\right]_0^1 - \int_0^1\int_{-\infty}^{+\infty} W^{\hbar,\pm}_q(x,p)\left(\frac{p}{m(x)}\frac{d}{dx}+\right.\right. \\
&\qquad \left.\left.\left((\frac{q^2}{2m_\pm} - eV_\pm + eV(x))\frac{m^{'}(x)}{m(x)} + eV^{'}(x)\right)\frac{d}{dp} - \nu\right)Q(x,p)dxdp\right)S(q)dq \\
&\qquad = \int_0^{+\infty}\left(\int_0^1\int_{-\infty}^{+\infty}\left(\sum_{i=1}^5 r^i_\hbar(x,p)\right)Q(x,p)dxdp\right)S(q)dq. \qquad (4.54)
\end{aligned}$$

Now, we pass to the limit in each member of (4.54). For the first term of the left-hand side of (4.54), we use the following Lemma.

Lemma 4.7 *Let $\psi_q^{\pm}$ solution of (3.1)-(3.3), then the following asymptotics hold in the strong L^∞ topology*

$$\begin{array}{lll} 1) & i) & \psi_q^-(\hbar\eta) = e^{iq\eta} + r_q^- e^{-iq\eta} + o(1), \\ & ii) & \psi_q^-(1+\hbar\eta) = t_q^-(e^{i\sqrt[+]{\frac{m_+}{m_-}q^2+2em_+(V_+-V_-)}\eta} + o(1)), \\ 2) & i) & \psi_q^+(\hbar\eta) = t_q^+(e^{-i\sqrt[+]{\frac{m_-}{m_+}q^2+2em_-(V_--V_+)}\eta} + o(1)), \\ & ii) & \psi_q^+(1+\hbar\eta) = e^{-iq\eta} + r_q^+ e^{+iq\eta} + o(1), \end{array}$$

where $o(1)$ is uniform when (q,η) lie in a bounded set.

Proof. We shall just give the details of 1-i). The others expansions follow in analogy. The proof relies on stability results for differential equations. First, we note

$$\phi_\hbar(\eta) = \psi_q^-(\hbar\eta),\ U_\hbar(\eta) = V(\hbar\eta) \text{ and } M_\hbar(\eta) = m(\hbar\eta).$$

Then, let

$$\delta_\hbar(\eta) = \psi_q^-(\hbar\eta) - e^{iq\eta} - r_q^- e^{-iq\eta}.$$

Using (3.4), it verifies

$$\delta_\hbar(0) = \delta_\hbar^{'}(0) = 0.$$

Straightforward algebra leads to

$$-\frac{1}{2m_1}\delta_\hbar^{''} = \frac{q^2}{2m_1}\delta_\hbar + (\frac{1}{2M_\hbar} - \frac{1}{2m_1})\phi_\hbar^{''} - \frac{M_\hbar^{'}}{2M_\hbar}\phi_\hbar^{'} + e(U_\hbar - V_1).$$

Since $U_\hbar$,(resp. $M_\hbar$) converges uniformly to V_1 (resp.m_1) on bounded intervals and since $M_\hbar^{'}(\eta) = \hbar m^{'}(\hbar\eta)$, then $\delta_\hbar$ converges in L^∞ weak* to the unique solution of

$$\left\{ \begin{array}{l} -\frac{1}{2m_1}\delta^{''} = \frac{q^2}{2m_1}\delta \\ \delta(0) = \delta^{'}(0) = 0 \end{array} \right.$$

$\delta = 0$. Moreover, $\delta_\hbar^{''}$ is bounded in L^∞ which proves that the convergence to zero of $\delta_\hbar$ holds in L^∞ strong. Then the proof ends.

Now, let's give the following result.

Lemma 4.8 *Let $S(q)$ be a test function in $L^1(\mathbb{R}_q^+, (1+q)dq)$. We assume that $Q(0,p)$ vanishes for non-positive p's and $Q(1,p)$ vanishes for positive p's. Then, when $\hbar$ tends to zero, we have*

$$i)\ \underset{\hbar\longrightarrow 0}{Lim} \int_0^{+\infty}\int_{\mathbb{R}} \frac{p}{m_-} Q(0,p) W_q^{\hbar,-}(0,p) S(q) dpdq \ = \ \int_0^{+\infty} \frac{q}{m_-} Q(0,q) S(q) dq,$$

$$
\begin{aligned}
ii)\ \underset{\hbar\longrightarrow 0}{Lim}\int_0^{+\infty}\int_{\mathbb{R}}\frac{p}{m_+}Q(1,p)W_q^{\hbar,-}(1,p)S(q)dpdq &= 0,\\
iii)\ \underset{\hbar\longrightarrow 0}{Lim}\int_0^{+\infty}\int_{\mathbb{R}}\frac{p}{m_-}Q(0,p)W_q^{\hbar,+}(0,p)S(q)dpdq &= 0,\\
iv)\ \underset{\hbar\longrightarrow 0}{Lim}\int_0^{+\infty}\int_{\mathbb{R}}\frac{p}{m_+}Q(1,p)W_q^{\hbar,+}(1,p)S(q)dpdq &= -\int_0^{+\infty}\frac{q}{m_+}Q(1,-q)S(q)dq.
\end{aligned}
$$

Proof. We use the same technique that is shown to prove Lemma B.1 in ref. [11]. We just prove i). The proof of the other terms is similar. We start from

$$
\begin{aligned}
&\int_0^{+\infty}\int_{-\infty}^{+\infty}\frac{p}{m_-}Q(0,p)W_q^{\hbar,-}(0,p)S(q)dpdq =\\
&\frac{1}{2\pi}\int_{-\infty}^{+\infty}\int_{-\infty}^{+\infty}\int_0^{+\infty}\frac{p}{m_-}Q(0,p)e^{i\eta p}\mathcal{O}\overline{\psi_q^-}\left(\frac{\hbar}{2}\eta\right)\mathcal{O}\psi_q^-\left(-\frac{\hbar}{2}\eta\right)S(q)d\eta dpdq,
\end{aligned}
$$

and replace $\psi_q^-(\frac{\hbar}{2}\eta)$ by its asymptotic expression $e^{i\frac{q}{2}\eta}+r_q^-e^{-i\frac{q}{2}\eta}+o(1)$ for $\eta<0$. This leads to

$$
\mathcal{O}\overline{\psi_q^-}\left(\frac{\hbar}{2}\eta\right)\mathcal{O}\psi_q^-\left(-\frac{\hbar}{2}\eta\right)=e^{-iq\eta}+2Re(r_q^-)+|r_q^-|^2e^{iq\eta}+o(1).
$$

Hence

$$
\begin{aligned}
&\underset{\hbar\longrightarrow 0}{Lim}\int_0^{+\infty}\int_{-\infty}^{+\infty}\frac{p}{m_-}Q(0,p)W_q^{\hbar,-}(0,p)S(q)dpdq =\\
&\underset{\hbar\longrightarrow 0}{Lim}\frac{1}{2\pi}\int_{-\infty}^{+\infty}\int_{-\infty}^{+\infty}\int_0^{+\infty}\frac{p}{m_-}Q(0,p)e^{i\eta p}\left[e^{-iq\eta}+2Re(r_q^-)+|r_q^-|^2e^{iq\eta}\right]S(q)d\eta dpdq. \quad (4.55)
\end{aligned}
$$

To prove rigorously this equality, we use the Lebesgue dominated convergence Theorem. Indeed, Lemma 4.4 implies that the integrand of the left hand side of (4.55) is bounded. Using the back Fourier transform with respect to η and noticing that $Q(0,p)$ vanishes for non-positive p's, we get

$$
\begin{aligned}
&\underset{\hbar\longrightarrow 0}{Lim}\int_0^{+\infty}\int_{-\infty}^{+\infty}\frac{p}{m_-}Q(0,p)W_q^{\hbar,-}(0,p)S(q)dpdq\\
&\quad=\underset{\hbar\longrightarrow 0}{Lim}\int_0^{+\infty}S(q)\frac{q}{m_-}\left[Q(0,q)-|r_q^-|^2Q(0,-q)\right]dq=\int_0^{+\infty}\frac{q}{m_-}Q(0,q)S(q)dq.
\end{aligned}
$$

This ends the proof of Lemma 4.8.

For the second integral term of the left-hand side of (4.54), we use Lemma 4.5, where $W_\hbar^\pm$ converges to $W^\pm$, $L^\infty_{Loc}(\mathbb{R}_q^+;\mathcal{A}')$ weak *. We obtain

$$
\begin{aligned}
&\underset{\hbar\longrightarrow 0}{Lim}\int_{\mathbb{R}^+}\int_{[0,1]\times\mathbb{R}}\left(W_q^{\hbar,\pm}(x,p)-W_q^{\pm}(x,p)\right)\left(\frac{p}{m(x)}\frac{d}{dx}+\right.\\
&\qquad\left.\left((\frac{q^2}{2m_\pm}-eV_\pm+eV(x))\frac{m'(x)}{m(x)}+eV'(x)\right)\frac{d}{dp}-\nu\right)Q(x,p)S(q)dxdpdq=0
\end{aligned}
$$

But for the right-hand side of (4.54), we use the following Lemma.

Lemma 4.9

$$\int_0^1 \int_{-\infty}^{+\infty} r_\hbar^i(x,p)Q(x,p)dxdp \underset{\hbar\longrightarrow O}{\longrightarrow} 0 \quad \textit{for all } i = 1,2,3,4,5.$$

Proof. Since $\|\psi_q^\pm\|^2_{L^2(0,1)} \leq Cq$, $\hbar^2\|\psi_q^{\pm'}\|^2_{L^2(0,1)} \leq Cq(q+1)$ and $\mathcal{O} \equiv 1$ sur $[0,1]$, we have

$$\int_0^1 \int_{\mathbb{R}} r_\hbar^i(x,p)Q(x,p)dxdp \underset{\hbar\longrightarrow 0}{\longrightarrow} 0 \qquad i = 1,3.$$

Then for $i = 4,5$, we write

$$\int_0^1 \int_{\mathbb{R}} r_\hbar^i(x,p)Q(x,p)dxdp = \int_0^1 \int_{\mathbb{R}} \mathcal{F}_p(Q(x,\eta))S_\hbar^i(x,\eta,q)dxdp$$

where we set by

$$\begin{aligned} S_\hbar^4(x,\eta,q) &= \frac{i}{m(x)}\left[\delta_\hbar(m\mathcal{V}) - \eta(m\mathcal{V})'\right] O\overline{\psi}_q^\pm(+)O\psi_q^\pm(-), \\ S_\hbar^5(x,\eta,q) &= -\frac{iE}{m(x)}\left[\delta_\hbar(m) - \eta m'(x)\right] O\overline{\psi}_q^\pm(+)O\psi_q^\pm(-). \end{aligned}$$

Using the bound of $\psi_q^\pm$ in $L^2(0,1)$ and that

$$\delta_\hbar(m\mathcal{V}) - \eta(m\mathcal{V})' \underset{\hbar\longrightarrow 0}{\longrightarrow} 0, \quad \delta_\hbar(m) - \eta m'(x) \underset{\hbar\longrightarrow 0}{\longrightarrow} 0,$$

we apply Lemma A.1 in ref. [11] to $r_\hbar^i$ (i=4,5). We obtain

$$\int_0^1 \int_{-\infty}^{+\infty} r_\hbar^i(x,p)Q(x,p)dxdp \underset{\hbar\longrightarrow 0}{\longrightarrow} 0, \quad \forall Q \in C_0^\infty(\mathbb{R},\mathbb{R}) \text{ for } i = 4,5.$$

Consequently, simultaneous for ψ_q^- and ψ_q^+, (4.54) converges to the following formulations

$$\begin{aligned} &\int_0^{+\infty} \frac{q}{m_-}Q(0,q)S(q)dq + \int_0^1 \int_{-\infty}^{+\infty} W_q^-(x,p)\left(\frac{p}{m(x)}\frac{d}{dx} + \right. \\ &\left.\left(\left(\frac{q^2}{2m_-} - eV_- + eV(x)\right)\frac{m'(x)}{m(x)} + eV'(x)\right)\frac{d}{dp} - \nu\right)Q(x,p)S(q)dxdpdq = 0, \end{aligned} \tag{4.56}$$

$$\begin{aligned} &\int_0^{+\infty} \frac{q}{m_+}Q(1,-q)S(q)dq + \int_0^1 \int_{-\infty}^{+\infty} W_q^+(x,p)\left(\frac{p}{m(x)}\frac{d}{dx} + \right. \\ &\left.\left(\left(\frac{q^2}{2m_+} - eV_+ + eV(x)\right)\frac{m'(x)}{m(x)} + eV'(x)\right)\frac{d}{dp} - \nu\right)Q(x,p)S(q)dxdpdq = 0. \end{aligned} \tag{4.57}$$

We remark that these formulations are nothing but the weak expression of the following problem

$$\frac{d}{dx}\left(\frac{p}{m(x)}W_q^\pm\right) + \left(\left(\frac{q^2}{2m_\pm} - e\left(V_\pm - V(x)\right)\right)\frac{m'(x)}{m(x)} + eV'(x)\right)\frac{dW_q^\pm}{dp} + \nu W_q^\pm = 0, \tag{4.58}$$

$$W_q^-(0,p) = \delta(p-q), \qquad W_q^-(1,-p) = 0, \qquad p > 0 \tag{4.59}$$

$$W_q^+(0,p) = 0, \qquad W_q^+(1,-p) = \delta(-p+q), \qquad p > 0. \tag{4.60}$$

The purpose is to get the problem $(\mathcal{P}_{Lim})$. So, first of all, we must remove dependence on q by analyzing the support of $W_q^{\pm}$. This will be done using the following Lemma.

Lemma 4.10 *The support of $W_q^{\pm}$ associated to $\psi_q^{\pm}$ is included in $\mathcal{C}^{\pm}$ where*

$$\mathcal{C}^{\pm} = \left\{ (x,p) \in]0,1[\times\mathbb{R} \ \ \textit{such that} \ \ \frac{p^2}{2m(x)} - eV(x) = \frac{q^2}{2m_{\pm}} - eV_{\pm} \right\}.$$

Before we state the proof, we define the operator $T^{*,\pm}$

$$T^{*,\pm} = T_0^{*,\pm} - \nu, \tag{4.61}$$

with

$$T_0^{*,\pm} \ = \ \frac{p}{m(x)}\frac{d}{dx} + \left((\frac{q^2}{2m_{\pm}} - eV_{\pm} + eV(x))\frac{m^{'}(x)}{m(x)} + eV^{'}(x) \right) \frac{d}{dp}.$$

Proof. As mentioned above, here we prove only the inclusion for W_q^-. Our purpose is to prove that supp $W_q^- \subset \mathcal{C}^-$, which is equivalent to show, for all $\Psi \in \mathcal{D}([0,1],\mathbb{R})$ such that $\Psi \equiv 0$ in the neighborhood of $\mathcal{C}^-$, we have

$$< W_q^-, \Psi >_{\mathcal{D}',\mathcal{D}} = 0.$$

For this, let us denote by φ the solution of the following equation

$$T^{*,-}(\varphi) = \Psi \tag{4.62}$$

with the boundary conditions

$$\varphi(0,p) = 0, \quad \text{for } p < 0, \quad \varphi(1,p) = 0, \quad \text{for } p > 0. \tag{4.63}$$

We recall that $T^{*,-}$ is defined by (4.61). But, as W_q^- is a solution of (4.58)-(4.59), then in the sense of duality, where φ is considered as a test function , we get

$$< W_q^-, T^{*,-}\varphi > -\frac{q}{m_-}\varphi(0,q) = 0. \tag{4.64}$$

In this formulation, it is readily seen that it suffices to prove $\varphi(0,p) = 0$ in the neighborhood of $p = q$. However, (4.64) cannot be used immediately because φ is not in $C^1([0,1]\times\mathbb{R})$. To overcome this difficulty, we regularize φ by a convolution procedure $\varphi_\epsilon = \varrho_\epsilon \star \varphi$ where ϱ_ϵ is a non-negative C^∞ approximation of the Dirac measure. For ϵ small, φ_ϵ satisfy (4.64) and

$$T^{*,-}\varphi_\epsilon \underset{\epsilon\to 0}{\to} \Psi, \ \ \text{in } C^0_{Loc}.$$

Now, we prove $\varphi(0,p) \equiv 0$ in neighborhood of the point $p = q$. Let

$$G(x,p) = g\left(m(x)\left(\frac{p^2}{2m(x)} - eV(x) - \frac{q^2}{2m_-} + eV_- \right) \right)$$

where g is a function in C^∞ such that $g(t) = 1$ in the neighborhood of the point $t = 0$ and $suppg \subset [-\alpha, \alpha]$, for a small $\alpha > 0$. The function G verifies $G\Psi = 0$. It satisfies $T_0^{*,-}G = 0$. Then $G\varphi$ is a solution of the following system

$$\left\{ \begin{array}{lcll} T^{*,-}(G\varphi) & = & 0 & \\ G\varphi(0,p) & = & 0, & p < 0 \\ G\varphi(1,p) & = & 0, & p > 0. \end{array} \right.$$

and the $G\varphi \equiv 0$. Using that $G(0,p) \equiv 1$ in the neighborhood of the point $p = q$, we have $\varphi(0,p) = 0$ in the neighborhood of the point $p = q$.

As a consequence of the previous Lemma, we replace the term

$$\left(\left(\frac{q^2}{2m_\pm} - e\left(V_\pm - V(x)\right) \right) \frac{m^{'}(x)}{m(x)} + eV^{'}(x) \right) \quad \text{by} \quad \left(\frac{p^2}{2m(x)} \frac{m^{'}(x)}{m(x)} + eV^{'}(x) \right).$$

Formulations (4.56) and (4.57) become

$$\int_0^{+\infty} \frac{q}{m_-} Q(0,q)S(q)dq + \int_0^1 \int_{-\infty}^{+\infty} W_q^-(x,p) \left(\frac{p}{m(x)} \frac{d}{dx} + \left(\frac{p^2}{2} \frac{m^{'}(x)}{m^2(x)} + eV^{'}(x) \right) \frac{d}{dp} - \nu \right) Q(x,p)S(q)dxdpdq = 0 \tag{4.65}$$

$$\int_0^{+\infty} \frac{q}{m_+} Q(1,-q)S(q)dq + \int_0^1 \int_{-\infty}^{+\infty} W_q^+(x,p) \left(\frac{p}{m(x)} \frac{d}{dx} + \left(\frac{p^2}{2} \frac{m^{'}(x)}{m^2(x)} + eV^{'}(x) \right) \frac{d}{dp} - \nu \right) Q(x,p)S(q)dxdpdq = 0. \tag{4.66}$$

Rewritten in terms of the energy $\mathcal{E} = \frac{p^2}{2m(x)} - eV(x)$ and removing the derivation on $W_q^\pm$, these formulations are nothing but the weak formulation of the following problem

$$\begin{array}{l} \dfrac{d\mathcal{E}}{dp}\dfrac{dW_q^\pm}{dx} - \dfrac{d\mathcal{E}}{dx}\dfrac{dW_q^\pm}{dp} + \nu W_q^\pm = 0, \\ W_q^-(0,p) = \delta(p-q), \qquad W_q^-(1,-p) = 0, \qquad\qquad p > 0 \\ W_q^+(0,p) = 0, \qquad W_q^+(1,-p) = \delta(-p+q), \qquad\qquad p > 0. \end{array}$$

Since $G^\pm(q)$ defined by (H-2) satisfies hypothesis of Lemma 4.8, we can take it as a test function in formulations (4.65) and (4.66), which implies, using the result of Lemma 4.5, that f defined by

$$f(x,p) = \int_0^{+\infty} G^+(q)\, W_q^+(x,p)\, dq + \int_0^{+\infty} G^-(q)\, W_q^-(x,p)\, dq$$

is nothing but the limit of the Wigner function $\omega_\hbar$ (defined by (4.44)) in $\mathcal{A}^{'}$ weak*. Moreover, it verifies

$$\frac{d\mathcal{E}}{dp}\frac{df}{dx} - \frac{d\mathcal{E}}{dx}\frac{df}{dp} + \nu f = 0$$

with the standard inflow boundary conditions

$$f(0,p) = \int_0^{+\infty} G^+(q)\, W_q^+(0,p)\, dq + \int_0^{+\infty} G^-(q)\, W_q^-(0,p)\, dq = G^-(p)$$

and

$$f(1,-p) = \int_0^{+\infty} G^+(q)\, W_q^+(1,p)\, dq + \int_0^{+\infty} G^-(q)\, W_q^-(1,-p)\, dq = G^+(p).$$

This completes the proof of the main Theorem of this paper.

5 Conclusion

The purpose of the present paper was to investigate the properties of an effective electron mass in a semiconductor device where quantum effects cannot be neglected. In a quantum region of such device, we require a more sophisticated model to take into account the variation of effective mass. For this, we have described such a suitable mathematical model the Schrödinger with variable mass. A natural work was a mathematical analysis of this model in the case where the electric potential is self-consistent. Finally, we have studied the semi-classical limit of this model which leads to its corresponding kinetic model. Both these models, the quantum and the kinetic one will probably constitute significant models to describe a far-from equilibrium transport in a resonant tunneling diode. More particularly, when we couple them under an appropriate interface conditions.

Acknowledgments. This work was supported by the T.M.R. project Asymptotic Methods in Applied kinetic Theory" # ERB FMRX CT97 0157, run by the European Community. I would also like to thank Professor N. Ben Abdallah for the valuable discussions and comments about this work.

Chapitre 2

Mathematical analysis of the Kohn-Luttinger model

Sommaire

1 Introduction

Since the pioneering work of Kohn and Luttinger [77] on the effective-mass approximation, much work has been done to improve the Schrödinger model. Kane ([60] and [61]) has derived the hamiltonian operator according to the first four bands via the $k.P$ approach. He deduced the non-parabolic nature of both the conduction and valence band [7], [8], [41], [43], [69], [92] and [115].

In the Kane's model, the kinetic energy of an electron in the conduction band E_c respectively in the valence band for light holes E_v and in the spin-orbit band E_{spin} can be written as

$$E_{c,v} = \frac{\hbar^2 k^2}{2m} + \frac{\mathcal{E}_g}{2}\left(1 \pm (1 + \frac{8P^2}{\mathcal{E}_g^2}k^2)^{\frac{1}{2}}\right), \tag{1.1}$$

$$E_{spin} = \frac{\hbar^2 k^2}{2m} - \Delta - \frac{P^2 k^2}{3(\mathcal{E}_g + \Delta)} - \frac{(2\mathcal{E}_g + \Delta)P^4 k^4}{3(\mathcal{E}_g + \Delta)^2 \Delta} \tag{1.2}$$

where m is the electron mass, $\mathcal{E}_g$ is the band gap energy of the material, the factor P is the coupling parameter between the two bands and the positive constant Δ is the spin-orbit splitting of the valence band.

Equation (1.1) and (1.2) can be expanded as follows for the kinetic energy of the conduction band

$$E_c = E_g + \frac{\hbar^2}{2m_c^*}k^2 - \frac{1}{E_g}\left(\frac{\hbar^2}{2m_c^*} - \frac{\hbar^2}{2m}\right)^2 k^4 + o(k^6), \tag{1.3}$$

for the valence band as

$$E_v = -\frac{\hbar^2}{2m_v^*}k^2 + \frac{1}{E_g}\left(\frac{\hbar^2}{2m} - \frac{\hbar^2}{2m_v^*}\right)^2 k^4 + o(k^6) \tag{1.4}$$

and for the spin-orbit band as

$$E_{spin} = -\Delta - \frac{\hbar^2}{2m_{spin}^*}k^2 - \frac{3(2\mathcal{E}_g + \Delta)P}{\Delta}\left(\frac{\hbar^2}{2m_{spin}^*} - \frac{\hbar^2}{2m}\right)^2 k^4 + o(k^6) \tag{1.5}$$

where

$$1/m_c^* \equiv 1/m + 4P^2/(\hbar^2\mathcal{E}_g), \quad 1/m_v^* \equiv 4P^2/(\hbar^2\mathcal{E}_g) - 1/m$$

and

$$1/m_{spin}^* \equiv P^2/(3\hbar^2(\mathcal{E}_g + \Delta)) - 1/m.$$

Here, higher order terms proportional to k^6 are neglected. Then, we may write the previous equations (1.3)-(1.4)-(1.5) as

$$E_c = \mathcal{E}_g + \frac{q^2}{2m_c^*} - \alpha_c \frac{q^4}{4m_c^{*2}} \tag{1.6}$$

$$E_v = -\frac{q^2}{2m_v^*} + \alpha_v \frac{q^4}{4{m_v^*}^2} \tag{1.7}$$

$$E_{spin} = -\Delta - \frac{q^2}{2m_{spin}^*} - \alpha_{spin} \frac{q^4}{4{m_{spin}^*}^2} \tag{1.8}$$

where $q = \hbar k$ is a momentum vector and where

$$\alpha_c = \frac{1}{\mathcal{E}_g}\left(1 - \frac{m_c^*}{m}\right)^2, \quad \alpha_v = \frac{1}{\mathcal{E}_g}\left(\frac{m_v^*}{m} - 1\right)^2 \text{ and } \alpha_{spin} = \frac{3(2\mathcal{E}_g + \Delta)P}{\Delta}\left(1 - \frac{m_{spin}^*}{m}\right)^2.$$

According to the effective mass theory, we have the following one dimensional Hamiltonian

$$\mathbb{K}_c = -\frac{\hbar^2}{2m_c^*}\frac{d^2}{dx^2} - \alpha_c \frac{\hbar^4}{4{m_c^*}^2}\frac{d^4}{dx^4}, \tag{1.9}$$

$$\mathbb{K}_v = \frac{\hbar^2}{2m_v^*}\frac{d^2}{dx^2} + \alpha_v \frac{\hbar^4}{4{m_v^*}^2}\frac{d^4}{dx^4}, \tag{1.10}$$

$$\mathbb{K}_{spin} = \frac{\hbar^2}{2m_{spin}^*}\frac{d^2}{dx^2} - \alpha_{spin} \frac{\hbar^4}{4{m_{spin}^*}^2}\frac{d^4}{dx^4}, \tag{1.11}$$

In point of view mathematic in order to get a uniform bound, the problem corresponding to the Hamiltonian $\mathbb{K}_{spin}$ coulped with the Poisson equation is well set whereas the problem corresponding to the Hamiltonian $\mathbb{K}_c$ or $\mathbb{K}_v$ is not. For this in the sequel, for clarity we omit $_{spin}$ and * in $\mathbb{K}_{spin}$ and multiply by $-$ which leads to the Kohn-Luttinger operator $\mathbb{K}$

$$\mathbb{K} = -\frac{\hbar^2}{2m}\frac{d^2}{dx^2} + \alpha \frac{\hbar^4}{4m^2}\frac{d^4}{dx^4} \tag{1.12}$$

with $\alpha > 0$.

It is a fourth order Hamiltonian which takes into account the effect of the band non-parabolicity of the energy in a simple way.

Remark 1.1 *When $\alpha = 0$, we obtain the classical parabolic approach of the Schrödinger equation*

$$-\frac{\hbar^2}{2m}\frac{d^2\psi_q}{dx^2} - eV(x)\psi_q = \frac{q^2}{2m}\psi_q.$$

We consider the following equation

$$\mathbb{K}\psi_q - eV(x)\psi_q = E(q)\psi_q. \tag{1.13}$$

The device occupies the interval $[0, 1]$. Particles are assumed to be injected at both sides of the device.

We propose in this chapter to study the quantum Kohn-Luttinger-Poisson model noted by (KLP) in the sequel. Then, the problem is stated as

$$\mathbb{K}\psi_q - eV(x)\psi_q = (E(q) - eV_1)\psi_q \tag{1.14}$$
$$\hbar^2 \psi_q''(0) = \hbar(q_- - iq)\psi_q'(0) + iqq_-\psi_q(0) - 2iq(q_- - iq) \tag{1.15}$$
$$\hbar^3 \psi_q'''(0) = \hbar(q_-^2 - iq(q_- - iq))\psi_q'(0) + iqq_-(q_- - iq)\psi_q(0) - 2iqq_-(q_- - iq) \tag{1.16}$$
$$\hbar^2 \psi_q''(1) = -\hbar(p_- - ip_+)\psi_q'(1) + ip_+p_-\psi_q(1) \tag{1.17}$$
$$\hbar^3 \psi_q'''(1) = \hbar(p_-^2 - ip_+(p_- - ip_+))\psi_q'(1) - ip_+p_-(p_- - ip_+)\psi_q(1). \tag{1.18}$$

The potential is self-consistent. It verifies the following Poisson equation

$$\frac{d^2V}{d^2x} = n(x), \tag{1.19}$$
$$V(0) = V_1, \quad V(1) = V_2. \tag{1.20}$$

Following [15], the electron density is given by

$$n(x) = \int_0^{+\infty} G(q)|\psi_q(x)|^2 dq,$$

where the distribution G is the statistic of the source at the reservoir. We assume that this function is bounded, non-negative, C^∞ with compact support and that it satisfies

$$\int_0^{+\infty} q^n G(q) dq < \infty, \quad \forall n \in \mathbb{N}.$$

For clarity, we focus our study on the left injection when $V_2 > V_1$. The other cases are treated exactly in the same manner. For the resolution of the coupled problem, we first show in section 2 how to derive the boundary condition and we define also some macroscopic quantities such as the charge and current density. Then, in section 3, we study the linear case. Once we prove the existence and uniqueness, we pass to the complete study of the coupled problem. But, in this study we meet a difficulty as in the case of the study of the multidimensional Schrödinger-Poisson model (see [12]). It consists of the existence of energies $E_j = E(q_j)$, with $j \geq 0$, for which the existence and uniqueness results are not proven.
Like in [12], the electron density associated to the coupled problem is equal to the sum of the density associated to the bound states and the density associated to the scattering states

$$n(x) = \int_0^{+\infty} G(q)|\psi_q(x)|^2 dq + \sum_{j\in\mathbb{N}^*} \sum_{l=1}^{d_j} \lambda_j^l |\phi_j^l(x)|^2 \tag{1.21}$$

where $G(q)$ is associated to the scattering state ψ_q and $\lambda_j^l \geq 0$ are the occupation coefficients of the bound states ϕ_j^l. The ϕ_j^l is an orthonormal basis of the subspace

$$S_j = ker(A_{E_j} - E_j) \tag{1.22}$$

with A_{E_j} is defined in (3.51)(3.52) (see section 3 of chapter 2) and

$$d_j = dim S_j. \tag{1.23}$$

We find difficulty in defining the particle density $\mathbf{n}(\mathbf{x})$. Indeed, in spite of the limiting absorption procedure, which ensures the existence of the scattering states, we can not deduce their behaviour in the neighborhood of an eigenvalue belonging to the continuous spectrum. Then, in the neighborhood of a bound state E_j, we have the following estimation

$$||\psi_q||_{L^2(0,1)} \leq \frac{C}{|E(q) - E_j|}$$

which gives rise to a non-integrable singularity in (1.21).

In order to overcome this difficulty, we use a nonlinear limiting absorption procedure (used even in [12] and [78]). We begin by adding the absorption term $\frac{i\hbar\nu}{4}$ to the energy of the Kohn-Luttinger equation

$$\mathbb{K}\psi_q^\nu = [E(q) + i\frac{\hbar\nu}{4}]\psi_q^\nu$$

for which we prove the uniqueness with $\nu > 0$. Considering the boundary conditions, this problem is well set. Then, the electron density is calculated by the following formula

$$n^\nu(x) = \int_0^{+\infty} G(q)|\psi_q^\nu(x)|^2 dq.$$

The second step is to construct the solution of the coupled problem with the Poisson equation

$$\frac{d^2V^\nu}{d^2x} = n^\nu(x).$$

In section 4, we prove the existence of a solution of the modified coupled problem for $\nu > 0$ using the Leray-Schauder fixed point Theorem [54]. Then, we prove the limit for ν going to zero of the non-linear problem. Finally, we obtain the electron density sum of both the scattering and bound states density.

2 The derivation of the boundary conditions

In this section, as V is constant on $]0,1[$, we can solve explicitly the equation (1.13) on $\mathbb{R}_{-]0,1[}$. It is a differential equation of order 4. As for the case of the Schrödinger model with variable mass in chapter 1, here we indicate that the device is also in a nonequilibruim state. For this, the scattering states can be represented by the wave functions transporting a non-zero current. They enable to determine the transparent boundary conditions. In this study, we discuss the different cases according to the side of electron injection and to the sign of the variation of the potential $V_2 - V_1$ (see figure 2.1).

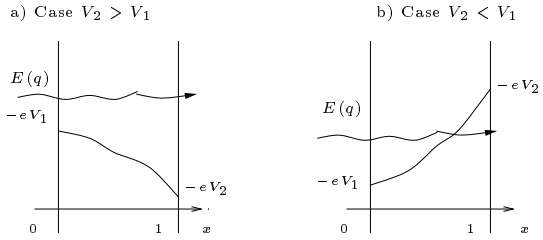

FIG. 2.1: Different cases of the potential variation.

2.1 The left injection

In this case, we denote by ψ_q^+ the wave function satisfying the Kohn-Luttinger equation

$$\mathbb{K}\psi_q^+ - eV(x)\psi_q^+ = (E(q) - eV_1)\psi_q^+. \tag{2.24}$$

First, we search ψ_q^+ respect to the scattering state when $x < 0$. The function ψ_q^+ is a plane wave. We can write it in the following way

$$\psi_q^+ = \sum_{j=1}^{4} a_j \psi_{k_j}, \qquad \text{such that } \psi_{k_j} = e^{ik_j x} \text{ and } a_j \in \mathbb{R}^+. \tag{2.25}$$

Then, inserting ψ_q^+ in equation (2.24) we obtain

$$\frac{\hbar^2 k^2}{2m} + \alpha \frac{\hbar^4 k^4}{4m^2} = E(q).$$

We set $\mathcal{Q} = \hbar^2 k^2$, the previous equation becomes

$$\alpha \mathcal{Q}^2 + 2m\mathcal{Q} - 4m^2 E(q) = 0 \tag{2.26}$$

where the discriminant is equal to

$$\Delta = (m + \alpha q^2)^2 \geq 0. \tag{2.27}$$

Consequently, we obtain two real solutions with different signs. We denote them respectively by $\mathcal{Q}_+$ and $\mathcal{Q}_-$,

$$\mathcal{Q}_+ = q^2, \quad \mathcal{Q}_- = -q^2 - \frac{2m}{\alpha}.$$

The corresponding wave vectors are k, satisfying (2.25) such that $k = \pm\frac{\sqrt{\mathcal{Q}}}{\hbar}$. For this, we set

$$q_+ = \sqrt{\mathcal{Q}_+} = q, \quad q_- = -i\sqrt{\mathcal{Q}_-} = \sqrt{q^2 + \frac{2m}{\alpha}}. \tag{2.28}$$

Then, we write

$$\psi_q^+(x) = a_1 e^{i\frac{q_+}{\hbar}x} + a_2 e^{-i\frac{q_+}{\hbar}x} + a_3 e^{\frac{q_-}{\hbar}x} + a_4 e^{-\frac{q_-}{\hbar}x}, \quad x < 0.$$

As we look for a wave ψ_q^+ coming from the left, with an amplitude equal to one and assuming that the wave does not explode on $-\infty$, we set $a_1 = 1$ and $a_4 = 0$. Then, ψ_q^+ can be expressed only in term of a_2 and a_3 in the following way

$$\psi_q^+(x) = e^{i\frac{q_+}{\hbar}x} + a_2 e^{-i\frac{q_+}{\hbar}x} + a_3 e^{\frac{q_-}{\hbar}x}, \quad x < 0.$$

By eliminating a_2 and a_3, we obtain the boundary conditions for the wave function. More precisely, we have

$$\begin{aligned}
\psi_q^+(0) &= 1 + a_2 + a_3, \\
\psi_q^{+'}(0) &= iq_+ - iq_+a_2 + q_-a_3, \\
\psi_q^{+''}(0) &= -q_+^2 - q_+^2a_2 + q_-^2a_3, \\
\psi_q^{+'''}(0) &= -iq_+^3 + iq_+^3a_2 + q_-^3a_3.
\end{aligned}$$

An easy computation leads to

$$\hbar^2\psi_q^{+''}(0) = \hbar(q_- - iq_+)\psi_q^{+'}(0) + iq_+q_-\psi_q^+(0) - 2iq_+(q_- - iq_+), \tag{2.29}$$

$$\hbar^3\psi_q^{+'''}(0) = \hbar(q_-^2 - iq_+(q_- - iq_+))\psi_q^{+'}(0) + iq_+q_-(q_- - iq_+)\psi_q^+(0) - 2iq_+q_-(q_- - iq_+). \tag{2.30}$$

Let us now determine ψ_q^+ for $x > 1$. In this case, the associated characteristic equation of the Kohn-Luttinger differential equation of order 4 is the following

$$\alpha Q^2 + 2mQ - 4m^2(E(q) + e(V_2 - V_1)) = 0. \tag{2.31}$$

After simplification, the discriminant is equal to

$$\Delta' = (m + \alpha q^2)^2 + 4\alpha m^2 e(V_2 - V_1). \tag{2.32}$$

We remark that the discriminant's sign depends on the sign of $V_2 - V_1$ (see figure 2.1 and 2.2).

$x = 0$	$x = 1$			
	$V_2 > V_1$	$V_2 < V_1$		
		$A > 0$		$A < 0$
		$q^2 < A$	$q^2 > A$	
	$\Delta' > 0$	$\Delta' < 0$	$\Delta' > 0$	$\Delta' > 0$
q_+, q_-	p_+, p_-	p_+^c, p_-^c	p_+, p_-	p_+, p_-

FIG. 2.2: Computing the momentum vectors according to the discriminant in the case of the left injection.

First, we treat the case where $V_2 > V_1$ (see figure 2.1.a). The discriminant is non-negative. We get two real roots of (2.31) with different signs, denoted by P_+ and P_- . They are equal to

$$\begin{aligned} P_+ &= \frac{-m + \sqrt{(m+\alpha q^2)^2 + 4\alpha m^2 e(V_2 - V_1)}}{\alpha} > 0, \\ P_- &= \frac{-m - \sqrt{(m+\alpha q^2)^2 + 4\alpha m^2 e(V_2 - V_1)}}{\alpha} < 0. \end{aligned}$$

For the same reasons, we search k verifying (2.25), such that $k = \pm\frac{\sqrt{Q}}{\hbar}$. We set then by

$$p_+ = \sqrt{P_+} = \sqrt{\frac{-m + \sqrt{(m+\alpha q^2)^2 + 4\alpha m^2 e(V_2 - V_1)}}{\alpha}}, \tag{2.33}$$

$$p_- = -i\sqrt{P_-} = \sqrt{\frac{m + \sqrt{(m+\alpha q^2)^2 + 4\alpha m^2 e(V_2 - V_1)}}{\alpha}}. \tag{2.34}$$

The wave function ψ_q^+ can be written as

$$\psi_q^+(x) = b_1 e^{i\frac{p_+}{\hbar}(x-1)} + b_2 e^{-i\frac{p_+}{\hbar}(x-1)} + b_3 e^{\frac{p_-}{\hbar}(x-1)} + b_4 e^{-\frac{p_-}{\hbar}(x-1)}, \quad x > 1,$$

where b_1, b_2, b_3 and b_4 are non-negative constants. In this case, the wave arrives at $x = 1$. It is transmitted and assuming that it does not explode at $+\infty$, the coefficients b_2 and b_3 are equal to zero. Thus,

$$\psi_q^+(x) = b_1 e^{i\frac{p_+}{\hbar}(x-1)} + b_4 e^{-\frac{p_-}{\hbar}(x-1)}, \quad x > 1.$$

Eliminating the remaining coefficients, we obtain at $x = 1$ with $V_2 - V_1 > 0$ the following boundary conditions

$$\begin{aligned} \hbar^2 {\psi_q^+}''(1) &= -\hbar(p_- - ip_+){\psi_q^+}'(1) + ip_+p_-\psi_q^+(1), \\ \hbar^3 {\psi_q^+}'''(1) &= \hbar(p_-^2 - ip_+(p_- - ip_+)){\psi_q^+}'(1) - ip_+p_-(p_- - ip_+)\psi_q^+(1). \end{aligned}$$

Let us now deal with the case $V_2 - V_1 < 0$ (see figure 2.1.b). We notice once again, that the sign of the discriminant (2.32) can change when q is small or great (see figure 2.1.b). For this purpose, we denote by

$$A = 2\frac{\sqrt{\alpha}}{\alpha}\sqrt{m^2 e(V_1 - V_2))} - \frac{m}{\alpha}. \tag{2.35}$$

If A is non-negative, we have two cases. Indeed, the term Δ' in (2.32) is negative when q^2 is less than or equal to A and positive when q^2 is greater than or equal to A. Finally, when A is negative, Δ' is always non-negative.

Hence, in the case of positive $\Delta^{'}$, we obtain the same boundary conditions as in the case of Δ in (2.27) which is positive when $V_2 > V_1$.

More particularly, we study the case when $\Delta^{'}$ is negative. We get $\sqrt{\Delta^{'}} = i\sqrt{-\Delta^{'}}$ and obtain consequently two conjugate complex roots of equation (2.31). We denote them by P_+^c and P_-^c.

$$\begin{aligned} P_+^c &= \frac{-m + i\sqrt{-(m+\alpha q^2)^2 - 4\alpha m^2 e(V_2 - V_1)}}{\alpha}, \\ P_-^c &= \frac{-m - i\sqrt{-(m+\alpha q^2)^2 - 4\alpha m^2 e(V_2 - V_1)}}{\alpha}. \end{aligned}$$

Once again, we search k such that $k = \pm\frac{\sqrt{\mathcal{Q}}}{\hbar}$. We calculate the square root of the two complex numbers P_+^c and P_-^c. For this, we first recall that for a complex number z, the square root is

$$\sqrt{z} = \pm\sqrt{|z|}e^{\frac{iarg(z)}{2}},$$

where $|z|$ is the modulus and $arg(z)$ is the argument.

The modulus of P_+^c and P_-^c are equal and satisfy

$$|P_+^c| = |P_-^c| = \frac{1}{\sqrt{\alpha}}\sqrt{(-q^2\,(2m + \alpha q^2) + 4m^2 e\,(V_2 - V_1))}.$$

Their arguments are of opposite signs and will be denoted by θ_+ and θ_-. They belong to the interval $]-\frac{\pi}{2}, \frac{\pi}{2}[$ and verify

$$\begin{aligned} \theta_+ &= arctg(-\frac{\sqrt{(-q^2\,(2m + \alpha q^2) + 4m^2 e\,(V_2 - V_1))}}{m}) \leq 0, \\ \theta_- &= arctg(\frac{\sqrt{(-q^2\,(2m + \alpha q^2) + 4m^2 e\,(V_2 - V_1))}}{m}) \geq 0. \end{aligned}$$

Now, we look for the square roots of the complex numbers P_+^c and P_-^c. They are conjugates and defined by

$$p_+^c = \sqrt{P_+^c} = \sqrt{|P_+^c|}e^{i\frac{\theta_+}{2}}, p_-^c = \sqrt{P_-^c} = \sqrt{|P_-^c|}e^{i\frac{\theta_-}{2}}. \tag{2.36}$$

Consequently in this case the wave function is written as

$$\psi_q^+(x) = c_1 e^{i\frac{p_+^c}{\hbar}(x-1)} + c_2 e^{-i\frac{p_+^c}{\hbar}(x-1)} + c_3 e^{\frac{ip_-^c}{\hbar}(x-1)} + c_4 e^{-\frac{ip_-^c}{\hbar}(x-1)}, \quad x > 1,$$

where c_1, c_2, c_3 and c_4 are non-negative constants. The wave is outgoing at $x = 1$ and we assume that it does not explode at $+\infty$. Then, the coefficients c_1 and c_4 are equal to zero and ψ_q^+ becomes

$$\psi_q^+(x) = c_2 e^{-i\frac{p_+^c}{\hbar}(x-1)} + c_4 e^{-\frac{ip_-^c}{\hbar}(x-1)}, \quad x > 1.$$

Eliminating the coefficients c_2 and c_4 on the previous equation, we get the following boundary conditions

$$\begin{aligned}\hbar^2\psi_q^{+''}(1) &= -i\hbar(p_-^c - p_+^c)\psi_q^{+'}(1) - p_+^c p_-^c \psi_q^+(1),\\ \hbar^3\psi_q^{+'''}(1) &= \hbar(-p_-^{c\,2} + p_+^c(p_-^c - p_+^c))\psi_q^{+'}(1) - ip_+^c p_-^c(p_-^c - p_+^c)\psi_q^+(1).\end{aligned}$$

Summary

When $V_2 > V_1$ and $V_2 < V_1$ with q such that (ie $q^2 \geq A$ (2.35)) we obtain the following system

$$\begin{aligned}&\mathbb{K}\psi_q^+ - eV(x)\psi_q^+ = (E(q) - eV_1)\psi_q^+,\\ &\hbar^2\psi_q^{+''}(0) = \hbar(q_- - iq)\psi_q^{+'}(0) + iqq_-\psi_q^+(0) - 2iq(q_- - iq),\\ &\hbar^3\psi_q^{+'''}(0) = \hbar(q_-^2 - iq(q_- - iq))\psi_q^{+'}(0) + iqq_-(q_- - iq)\psi_q^+(0) - 2iqq_-(q_- - iq),\\ &\hbar^2\psi_q^{+''}(1) = -\hbar(p_- - ip_+)\psi_q^{+'}(1) + ip_+p_-\psi_q^+(1),\\ &\hbar^3\psi_q^{+'''}(1) = \hbar(p_-^2 - ip_+(p_- - ip_+))\psi_q^{+'}(1) - ip_+p_-(p_- - ip_+)\psi_q^+(1).\end{aligned}$$

When $V_2 < V_1$ and q is small such that (ie $q^2 \leq A$), we get

$$\begin{aligned}&\mathbb{K}\psi_q^+ - eV(x)\psi_q^+ = (E(q) - eV_1)\psi_q^+,\\ &\hbar^2\psi_q^{+''}(0) = \hbar(q_- - iq)\psi_q^{+'}(0) + iqq_-\psi_q^+(0) - 2iq(q_- - iq),\\ &\hbar^3\psi_q^{+'''}(0) = \hbar(q_-^2 - iq(q_- - iq))\psi_q^{+'}(0) + iqq_-(q_- - iq)\psi_q^+(0) - 2iqq_-(q_- - iq),\\ &\hbar^2\psi^{+''}(1) = -i\hbar(p_-^c - p_+^c)\psi^{+'}(1) - p_+^c p_-^c\psi^+(1),\\ &\hbar^3\psi^{+'''}(1) = \hbar(-p_-^{c\,2} + p_+^c(p_-^c - p_+^c))\psi^{+'}(1) - ip_+^c p_-^c(p_-^c - p_+^c)\psi^+(1),\end{aligned}$$

where q, q_-, p_+, p_-, p_+^c and p_-^c given by (2.28), (2.33), (2.34) and (2.36).

2.2 The right injection

In this case, the electron is coming from the right at $x = 1$ with a negative momentum $-q$. Its energy is equal to $E = E(q) - eV_2$. We denote by ψ_q^- the wave function corresponding to this electron. It verifies the following Kohn-Luttinger equation

$$\mathbb{K}\psi_q^- - eV(x)\psi_q^- = (E(q) - eV_2)\psi_q^-. \tag{2.37}$$

By symmetry to the left case, we obtain the same results replacing $x = 0$ by $x = 1$, V_1 by V_2, ψ_q^+ by ψ_q^- and A in (2.35) by

$$A' = 2\frac{\sqrt{\alpha}}{\alpha}\sqrt{m^2 e(V_2 - V_1)}) - \frac{m}{\alpha}. \tag{2.38}$$

Consequently, we get the following table.

$x=1$	$x=0$			
	$V_2 < V_1$	$V_2 > V_1$		
		$A^{'} > 0$		$A^{'} < 0$
		$q^2 < A^{'}$	$q^2 > A^{'}$	
	$\Delta^{'} > 0$	$\Delta^{'} < 0$	$\Delta^{'} > 0$	$\Delta^{'} > 0$
q_+, q_-	$p^{'}_+, p^{'}_-$	$p^{'\,c}_+, p^{'\,c}_-$	$p^{'}_+, p^{'}_-$	$p^{'}_+, p^{'}_-$

FIG. 2.3: Computing the momentum vectors according to the discriminant in the case of the right injection.

Summary

When $V_2 < V_1$ and $V_2 > V_1$ with q such that (ie $q^2 \geq A^{'}$) , we get the following system

$$
\begin{aligned}
&\mathbb{K}\psi^-_q - eV(x)\psi^-_q = (E(q) - eV_2)\psi^-_q,\\
&\hbar^2\psi^{-\,''}_q(0) = \hbar(p^{'}_- - ip^{'}_+)\psi^{-\,'}_q(0) + ip^{'}_+p^{'}_-\psi^-_q(0),\\
&\hbar^3\psi^{-\,'''}_q(0) = \hbar(p^{'\,2}_- - ip^{'}_+(p^{'}_- - ip^{'}_+))\psi^{-\,'}_q(0) + ip^{'}_+p^{'}_-(p^{'}_- - ip^{'}_+)\psi^-_q(0),\\
&\hbar^2\psi^{-\,''}_q(1) = -\hbar(q_- - iq)\psi^{-\,'}_q(1) + iqq_-\psi^-_q(1) - 2iq(q_- - iq),\\
&\hbar^3\psi^{-\,'''}_q(1) = \hbar(q^2_- - iq(q_- - iq))\psi^{-\,'}_q(1) - iqq_-(q_- - iq)\psi^-_q(1) + 2iqq_-(q_- - iq),
\end{aligned}
$$

with

$$
p^{'}_{\pm} = \sqrt{\frac{\mp m + \sqrt{(m+\alpha q^2)^2 + 4\alpha m^2 e(V_1 - V_2)}}{\alpha}}.
$$

When $V_2 > V_1$ and q is small such that (ie $q^2 \leq A^{'}$), we find

$$
\begin{aligned}
&\mathbb{K}\psi^-_q - eV(x)\psi^-_q = (E(q) - eV_2)\psi^-_q,\\
&\hbar^2\psi^{-\,''}(0) = i\hbar(p^{'\,c}_+ - p^{'\,c}_-)\psi^{-\prime}(0) - p^{'\,c}_+p^{'\,c}_-\psi^-(0),\\
&\hbar^3\psi^{-\,'''}(0) = -\hbar(p^{'\,c2}_- - p^{'\,c}_+(p^{'\,c}_- - p^{'\,c}_+))\psi^{-\,'}(0) - ip^{'\,c}_+p^{'\,c}_-(p^{'\,c}_+ - p^{'\,c}_-)\psi^-(0),\\
&\hbar^2\psi^{-\,''}_q(1) = -\hbar(q_- - iq)\psi^{-\,'}_q(1) + iqq_-\psi^-_q(1) - 2iq(q_- - iq)\\
&\hbar^3\psi^{-\,'''}_q(1) = \hbar(q^2_- - iq(q_- - iq))\psi^{-\,'}_q(1) - iqq_-(q_- - iq)\psi^-_q(1) + 2iqq_-(q_- - iq),
\end{aligned}
$$

where

$$
p^{'\,c}_{\pm} = \sqrt{\frac{-m \pm \sqrt{-(m+\alpha q^2)^2 - 4\alpha m^2 e(V_1 - V_2)}}{\alpha}}.
$$

2.3 The macroscopic quantities

The probability current is given by

$$
J(x) = -\frac{\alpha\hbar^3}{2m^2}\Im m(\overline{\psi}\frac{d^3\psi}{dx^3} - \frac{d\overline{\psi}}{dx}\frac{d^2\psi}{dx^2}) + \frac{\hbar}{m}\Im m(\overline{\psi}\frac{d\psi}{dx}). \tag{2.39}
$$

The interest is based on the following standard conservation relation

Proposition 2.1 *We have the continuity equation*

$$\frac{dJ}{dx} = 0. \tag{2.40}$$

Proof : Computing the derivative of J according to x, we obtain

$$\begin{aligned}\frac{dJ}{dx} &= \frac{\alpha\hbar^3}{2m^2}\frac{d}{dx}\left[\Im m(\overline{\psi}\frac{d^3\psi}{dx^3} - \frac{d\overline{\psi}}{dx}\frac{d^2\psi}{dx^2})\right] - \frac{\hbar}{m}\frac{d}{dx}\left[\Im m(\overline{\psi}\frac{d\psi}{dx})\right] \\ &= \frac{2}{\hbar}\Im m\left((\frac{\alpha\hbar^4}{4m^2}\frac{d^4\psi}{dx^4} - \frac{\hbar^2}{2m}\frac{d^2\psi}{dx^2})\overline{\psi}\right).\end{aligned}$$

From the following Khon-Luttinger equation

$$\mathbb{K}\psi_q = -\frac{\hbar^2}{2m}\frac{d^2\psi}{dx^2} + \frac{\alpha\hbar^4}{4m^2}\frac{d^4\psi}{dx^4} = E\psi.$$

with E real, we deduce the result. ■

Remark 2.2 *If $\psi = e^{ikx}$ is a plane wave, then J, given by (2.39), is nothing but*

$$J(x) = \frac{1}{\hbar}\frac{dE(k)}{dk} = \mathcal{V}_g(k)$$

where $\mathcal{V}_g(k)$ is the group velocity.

3 The linear problem

Before analyzing the coupled problem, we first study the existence and uniqueness of the linear Kohn-Luttinger problem(1.14)-(1.18), denoted by (KL).

3.1 Existence and uniqueness of solution

Theorem 3.1 *Let V in $L^\infty(0,1)$, then there exists an increasing sequence $E_j = E(q_j), j \geq 0$ of positive real numbers going to infinity, such that the linear problem (KL) admits a unique solution $\psi_q \in H^2(0,1)$, $\forall E(q) \neq E(q_j)$, $j \geq 0$.*

3.1.1 Proof of Theorem 3.1

Some details in the proof of this Theorem, based on the Fredholm alternative ([27]), are similar to those of the proof of Theorem 3.1 in [12].

Solving the problem (1.14)-(1.18) is equivalent to searching ψ_q on $H^2(0,1)$, such that for all test function φ on $H^2(0,1)$, we have

$$\begin{aligned}
&\alpha\frac{\hbar^4}{4m^2}\int_0^1 \psi_q{}''\overline{\varphi}''dx+\frac{\hbar^2}{2m}\int_0^1 \psi_q{}'\overline{\varphi}'dx-\int_0^1(E(q)+e(V(x)-V_1))\psi_q\overline{\varphi}dx\\
&+\frac{\alpha\hbar}{4m^2}\Big[q_-\left(\hbar^2\psi_q{}'(0)\overline{\varphi}'(0)-q^2\psi_q(0)\overline{\varphi}(0)\right)+p_-\left(\hbar^2\psi_q{}'(1)\overline{\varphi}'(1)-p_+^2\psi_q(1)\overline{\varphi}(1)\right)\\
&-ip_+\left(\hbar\psi_q{}'(1)+p_-\psi_q(1)\right)\left(\hbar\overline{\varphi}'(1)+p_-\overline{\varphi}(1)\right)-iq\left(\hbar\psi_q{}'(0)-q_-\psi_q(0)\right)\left(\hbar\overline{\varphi}'(0)-q_-\overline{\varphi}(0)\right)\Big]\\
&=i\frac{\alpha\hbar}{2m^2}q(q_--iq)\left(\hbar\overline{\varphi}'(0)-q_-\overline{\varphi}(0)\right). \qquad (3.41)
\end{aligned}$$

First of all, let us introduce the following sesquilinear and anti-linear forms

$$\begin{aligned}
Q(\psi_q,\varphi) &= \alpha\frac{\hbar^4}{4m^2}\int_0^1 \psi_q{}''\overline{\varphi}''dx+\frac{\hbar^2}{2m}\int_0^1 \psi_q{}'\overline{\varphi}'dx+\frac{\alpha\hbar^4}{4m}\int_0^1\psi_q\overline{\varphi}dx, \qquad (3.42)\\
C(\psi_q,\varphi) &= -\int_0^1(E(q)+e(V(x)-V_1)+\frac{\alpha\hbar^4}{4m})\psi_q\overline{\varphi}dx+\frac{\alpha\hbar}{4m^2}\Big[q_-\left(\hbar^2\psi_q{}'(0)\overline{\varphi}'(0)-q^2\psi_q(0)\overline{\varphi}(0)\right)\\
&\quad+p_-\left(\hbar^2\psi_q{}'(1)\overline{\varphi}'(1)-p_+^2\psi_q(1)\overline{\varphi}(1)\right)-ip_+\left(\hbar\psi_q{}'(1)+p_-\psi_q(1)\right)\left(\hbar\overline{\varphi}'(1)+p_-\overline{\varphi}(1)\right)\\
&\quad-iq\left(\hbar\psi_q{}'(0)-q_-\psi_q(0)\right)\left(\hbar\overline{\varphi}'(0)-q_-\overline{\varphi}(0)\right)\Big], \qquad (3.43)\\
L(\varphi) &= i\frac{\alpha\hbar}{2m^2}q(q_--iq)\left(\hbar\overline{\varphi}'(0)-q_-\overline{\varphi}(0)\right). \qquad (3.44)
\end{aligned}$$

The weak formulation (3.41) can be written in the following way

$$(FV)\begin{cases}\text{search } \psi_q\in H^2(0,1),\text{such that}\\ \forall\varphi\in H^2(0,1),\quad Q(\psi_q,\varphi)+C(\psi_q,\varphi)=L(\varphi).\end{cases}$$

We prove easily the following inequalities

$$\begin{aligned}
Q(\psi_q,\psi_q) &\geq C||\psi_q||^2_{H^2(0,1)},\\
C(\psi_q,\varphi) &\leq C||\psi_q||_{C^1(0,1)}||\varphi||_{C^1(0,1)},\quad \forall\varphi\in H^2(0,1).
\end{aligned}$$

Q, C and L are sesquilinear continuous forms respect to φ. From the Riesz representation Theorem [98], there exist a unique $A_Q\psi_q$, $A_C\psi_q$ and f_L in $H^2(0,1)$ such that $\forall\varphi\in H^2(0,1)$

$Q(\psi_q,\varphi)=(A_Q\psi_q,\varphi)_{H^2(0,1)}$, $C(\psi_q,\varphi)=(A_C\psi_q,\varphi)_{H^2(0,1)}$ and $L(\varphi)=(f_L,\varphi)_{H^2(0,1)}$.

The weak formulation can be written

$$A_Q\psi_q+A_C\psi_q=(A_Q+A_C)\psi_q=f_L.$$

The operator A_Q is inversible and A_C is compact ($H^2(0,1)\hookrightarrow C^1(0,1)$ compact (see Sobolev's injections in [1] and [27]). The Fredholm alternative ensures the uniqueness of the solution of the Kohn-Luttinger problem, only if A_Q+A_C is injective. But this is equivalent to prove that the weak formulation (FV), with zero at the right-hand

side, has zero as a solution. We take $L(\varphi) = 0$. Then, we choose $\varphi = \psi_q$ and look for the imaginary part of the weak formulation (FV). We get

$$p_+|\hbar\psi_q{}'(1) + p_-\psi_q(1)|^2 + q|\hbar\psi_q{}'(0) - q_-\psi_q(0)|^2 = 0.$$

Both p_+ and q are positive. Hence, we obtain

$$\hbar\psi_q{}'(1) \;=\; -p_-\psi_q(1), \quad \hbar\psi_q{}'(0) = q_-\psi_q(0).$$

Using the previous results, the weak formulation (FV) becomes

$$\alpha\frac{\hbar^4}{4m^2}\int_0^1 \psi_q{}''\overline{\varphi}{}''\,dx + \frac{\hbar^2}{2m}\int_0^1 \psi_q{}'\overline{\varphi}{}'\,dx - \int_0^1 (E(q) + e(V(x) - V_1))\psi_q\overline{\varphi}dx + \frac{\alpha\hbar}{4m^2}\left[q_-\left(\hbar^2\psi_q{}'(0)\overline{\varphi}{}'(0) - q^2\psi_q(0)\overline{\varphi}(0)\right) + p_-\left(\hbar^2\psi_q{}'(1)\overline{\varphi}{}'(1) - p_+^2\psi_q(1)\overline{\varphi}(1)\right)\right] = 0. \quad (3.45)$$

Moreover, the problem associated to the previous formulation is the following

$$\mathbb{K}\psi_q - eV(x)\psi_q = (E(q) - eV_1)\psi_q, \quad (3.46)$$
$$\hbar^2\psi_q{}''(0) = q_-^2\psi_q(0), \quad (3.47)$$
$$\hbar^3\psi_q{}'''(0) = -q_-^3\psi_q(0), \quad (3.48)$$
$$\hbar^2\psi_q{}''(1) = p_-^2\psi_q(1), \quad (3.49)$$
$$\hbar^3\psi_q{}'''(1) = -p_-^3\psi_q(1). \quad (3.50)$$

Consequently, the solution ψ_q appears as an eigenfunction of the unbounded operator A_E on $L^2(0,1)$ given by

$$A_E\psi_q = \mathbb{K}\psi_q - e(V(x) - V_1)\psi_q. \quad (3.51)$$

Moreover, we define the associated domain

$$\mathcal{D}(A_E) = \{\psi_q \in H^4(0,1), \text{ such that conditions ((3.47)-(3.50)) hold }\}. \quad (3.52)$$

We are interested on the spectral structure of the operator A_E. We search for a non-vanishing solution ψ_q satisfying

$$(A_E - E(q))\psi_q = 0, \qquad \text{on } \mathcal{D}(A_E).$$

This is equivalent to

$$E(q) \in sp(A_E),$$

where $sp(A_E)$ is the spectrum of A_E and $E(q)$ is an eigenvalue.

The operator A_E is a densely defined self-adjoint operator bounded from below and with compact resolvent (see the proof of Lemma 3.2). We apply a classical result satisfied by this type of operator. The spectrum of such an operator A_E is an increasing sequence of eigenvalues $(\lambda_j(A_E))$ tending to infinity, with $(\psi_{q_j})_j$ as the associated eigenvector sequence.

In addition, the eigenvalues $(\lambda_j(A_E))$ are obtained by the min-max principle (see [98] and [88])

$$\lambda_j(A_E) = \max_{\psi_{q_1},\cdots\psi_{q_{j-1}}} \left\{ \min_{\substack{\psi \in \mathcal{D}(A_E),\quad ||\psi||_{L^2(0,1)}=1 \\ \int \psi_{q_i}\overline{\psi}=0,\ i=1\cdots j-1}} G(V,p,\psi) \right\}$$

where

$$\begin{aligned} G(V,p,\psi) &= (\psi, A_E\psi)_{L^2(0,1)} \\ &= \alpha\frac{\hbar^4}{4m^2}\|\psi^{''}\|^2_{L^2(0,1)} + \frac{\hbar^2}{2m}\|\psi^{'}\|^2_{L^2(0,1)} - e\int_0^1 V(x)|\psi|^2dx \\ &\quad + \frac{\alpha\hbar}{4m^2}\left[q_-(q_-^2-q_+^2)|\psi(0)|^2 + p_-(p_-^2-p_+^2)|\psi(1)|^2\right]. \end{aligned}$$

For each j, $\lambda_j(A_E)$ are continuous decreasing functions of q. This implies that for each j, the equation $E(q) = \lambda_j(A_E)$ admits a unique fixed point solution $E_j = E(q_j)$. Moreover, the sequence $E(q_j)$ is a positive increasing sequence going to infinity.

Then, we can conclude that the (KL) problem admits a unique solution $\forall E(q) \neq E(q_j),\ j \geq 0$. ■

Lemma 3.2 *A_E is a densely defined, self-adjoint operator, bounded from below and with compact resolvent.*

3.1.2 Proof of Lemma 3.2

The space C^∞ of compactly supported functions is dense in $L^2(0,1)$. It is contained in $\mathcal{D}(A_E)$. Then, we can deduce, that the domain $\mathcal{D}(A_E)$ is dense in $L^2(0,1)$.

In order to check that the operator A_E is self-adjoint we only need to prove that A_E is symmetric and maximal. Indeed, let ψ and φ in $\mathcal{D}(A_E)$. From the weak formulation (3.45), we have

$$(A_E\psi,\varphi)_{L^2(0,1)} = (\psi, A_E\varphi)_{L^2(0,1)}.$$

This proves that A_E is symmetric. In addition, there exists a positive constant C_2 such that $A_E + C_2 I$ is monotonous. Moreover, if $\psi \in \mathcal{D}(A_E)$, we get from the weak formulation (3.45) the subsequent inequality

$$(A_E\psi,\psi)_{L^2(0,1)} \geq C_1||\psi||^2_{H^2(0,1)} - C_2||\psi||^2_{L^2(0,1)}, \qquad \text{where } C_2 = e||V||_{L^\infty(0,1)}.$$

Then, from this we can have the following inequality for each $\gamma > 0$

$$((A_E(C_2+\gamma)Id)\psi,\psi)_{L^2(0,1)} \geq \gamma||\psi||^2_{L^2(0,1)}.$$

Consequently, for each function f in $L^2(0,1)$, the following equation

$$(A_E + (C_2+\gamma)Id)\psi = f$$

admits a unique solution in $H^2(0,1)$ for each $\gamma > 0$. Moreover, the Lax Milgram Theorem (see [98]) implies

$$||\psi||_{H^2(0,1)} \leq C_\gamma ||f||_{L^2(0,1)}.$$

This solution ψ also satisfies in $\mathcal{D}'$

$$\mathbb{K}\psi - eV(x)\psi + (C_2 + \gamma))\psi = (E(q) - eV_1)\psi + f.$$

This implies that $\psi \in H^4(0,1)$ and

$$||\psi||_{H^4(0,1)} \leq C_\gamma ||f||_{L^2(0,1)}$$

where C_γ is a new constant depending on γ. It follows that

$$(A_E + (C_2 + \gamma)Id)\psi = f$$

admits a unique solution in $\mathcal{D}(A_E)$.

It remains only to show that the operator A_E is bounded from below. Indeed,

$$(A_E\psi, \psi)_{L^2(0,1)} \geq -C_2 ||\psi||^2_{L^2(0,1)}, \ \forall \psi \in L^2(0,1).$$

Finally, the embedding of $\mathcal{D}(A_E)$ in $L^2(0,1)$ is compact which implies the compactness of the resolvent of A_E. ■

3.2 The modified Kohn-Luttinger problem

The modified Kohn-Luttinger model is solved exactly like the Kohn-Luttinger model (see paragraph 3.1). We just have to add the absorption term $i\frac{\hbar\nu}{4}$ to the energy in (1.14). We denote by (KLM),

$$\mathbb{K}\psi_q - eV(x)\psi_q = (E(q) - eV_1 + i\frac{\hbar\nu}{4})\psi_q, \tag{3.53}$$

$$\hbar^2 \psi_q{}''(0) = \hbar(q_- - iq)\psi_q{}'(0) + iqq_-\psi_q(0) - 2iq(q_- - iq), \tag{3.54}$$

$$\hbar^3 \psi_q{}'''(0) = \hbar(q_-^2 - iq(q_- - iq))\psi_q{}'(0) + iqq_-(q_- - iq)\psi_q(0) - 2iqq_-(q_- - iq), \tag{3.55}$$

$$\hbar^2 \psi_q{}''(1) = -\hbar(p_- - ip_+)\psi_q{}'(1) + ip_+p_-\psi_q(1), \tag{3.56}$$

$$\hbar^3 \psi_q{}'''(1) = \hbar(p_-^2 - ip_+(p_- - ip_+))\psi_q{}'(1) - ip_+p_-(p_- - ip_+)\psi_q(1). \tag{3.57}$$

Theorem 3.3 *:*
The (KLM) problem (3.53)-(3.57) admits a unique solution $\psi_q \in H^2(0,1)$.

Proof : It is based on the Fredholm alternative (see [27]). The (KLM) problem (3.53)-(3.57) has the following weak formulation

$$\begin{cases} \text{search } \psi_q \in H^2(0,1) \text{ such that} \\ \forall \varphi \in H^2(0,1), \quad Q(\psi_q, \varphi) + C^\nu(\psi_q, \varphi) = L(\varphi). \end{cases} \tag{3.58}$$

The forms Q and L are already given by (3.42) respectively (3.44) and C^ν has the form

$$C^\nu(\psi_q,\varphi) \;=\; C(\psi_q,\varphi) - i\frac{\hbar\nu}{4}\int_0^1 \psi_q\overline{\varphi}dx$$

where C is defined in (3.43).

For the same reason as in the linear case, we are interested in searching a solution of the weak formulation (3.58) with vanishing right-hand side. We choose ψ_q as a test function. Then, the imaginary part of the weak formulation (3.58) becomes

$$p_+|\hbar{\psi_q}'(1)+p_-\psi_q(1)|^2+q|\hbar{\psi_q}'(0)-q_-\psi_q(0)|^2+\frac{\nu m^2}{\alpha}\int_0^1|\psi_q(x)|^2dx=0.$$

The constants ν and α are strictly positive. This leads to

$$\psi_q=0,$$

which proves the uniqueness of the solution of the (KLM) problem. In the sequel, we will denote by ψ_q^ν this solution.

4 The modified coupled (Kohn-Luttinger)-Poisson model

In this section, we study the existence of a solution of the modified coupled (Kohn-Luttinger)-Poisson model. It is composed of the (KLM) problem (3.53)-(3.57) given in section 3.2 coupled to the following Poisson problem

$$\frac{d^2V^\nu}{d^2x} \;=\; n^\nu(x)\,,\quad n^\nu(x)=\int_0^{+\infty}G(q)|\psi_q^\nu(x)|^2dx \tag{4.59}$$

$$V^\nu(0) \;=\; V_1,\quad V^\nu(1)=V_2. \tag{4.60}$$

Theorem 4.1 *Let G be a positive compactly supported function. We assume that $V\in L^\infty(0,1)$ and $\nu>0$. Then, the modified coupled Kohn Luttinger-Poisson model (3.53)-(4.60) admits a solution (V^ν,ψ_q^ν) such that $V^\nu\in W^{2,3}(0,1)$ and $\psi_q^\nu\in H^2(0,1)$.*

The steps of the proof are similar to those of Theorem 5.1 in [12]. Indeed, the proof relies on a Leray-Schauder fixed point Theorem (see [54]). Starting from a potential V^ν in $L^\infty(0,1)$, we solve the (KLM) problem. We get the solution ψ_q^ν. Then, we construct the charge density $n^\nu(V^\nu)$ according to (4.59) and a new potential $(V^\nu)^*$ via the Poisson equation. To prove the existence of a fixed point of this map which we denote by $\mathcal{T}$, we need to prove that this map is compact. For this purpose, let us consider the following Lemma where the details of the proof are also similar to those of the proof of Theorem 5.1 in [12].

Lemma 4.2 *There exists a positive constant C_ν depending on ν such that*

$$||V^\nu||_{L^\infty(0,1)} \leq C_\nu.$$

Proof : To obtain this estimate, we need to get bounds on boundary terms of the weak formulation (3.58) of the (KLM) problem. Choosing ψ_q^ν as a test function in (3.58) and taking the imaginary part, we get

$$R + T + \frac{\nu m^2}{\alpha q(q_-^2 + q^2)} \int_0^1 |\psi_q^\nu(x)|^2 dx = 1 \tag{4.61}$$

where

$$T = \frac{p_+}{q(q_-^2 + q^2)} |\hbar(\psi_q^\nu)'(1) + p_- \psi_q^\nu(1)|^2 \tag{4.62}$$

and

$$\begin{aligned} R &= \frac{1}{(q_-^2 + q^2)}(|\hbar \Re e(\psi_q^\nu)'(0) - q_- \Re e(\psi_q^\nu(0)) + q_-|^2 + \\ &\qquad |\hbar \Im m(\psi_q^\nu)'(0) - q_- \Im m(\psi_q^\nu(0)) + q|^2). \end{aligned} \tag{4.63}$$

The real part is given by

$$\begin{aligned} &\alpha \frac{h^4}{4m^2} \int_0^1 |(\psi_q^\nu)''(x)|^2 dx + \frac{\hbar^2}{2m} \int_0^1 |(\psi_q^\nu)'(x)|^2 - \int_0^1 (E(q) + e(V^\nu - V_1))|(\psi_q^\nu)|^2 dx \\ &+ \frac{\alpha h}{4m^2} \left[q_- \left(\hbar^2 |(\psi_q^\nu)'(0)|^2 - q^2 |\psi_q^\nu(0)|^2 \right) + p_- \left(\hbar^2 |\psi_q^{\nu\prime}(1)|^2 - p_+^2 |\psi_q^\nu(1)|^2 \right) \right] \\ &= \frac{\alpha \hbar}{2m^2} q \left[q_- \left(\hbar \Im m((\psi_q^\nu)'(0)) - q_- \Im m(\psi_q^\nu(0)) \right) + q \left(\hbar \Re e((\psi_q^\nu)')(0) - q_- \Re e(\psi_q^\nu(0)) \right) \right]. \end{aligned} \tag{4.64}$$

Equation (4.61) implies that

$$|\hbar(\psi_q^\nu)'(0) - q_- \psi_q^\nu(0)| \leq 2(q_- + q) \tag{4.65}$$

and leads to

$$\begin{aligned} p_+ |\hbar(\psi_q^\nu)'(1) + p_- \psi_q^\nu(1)|^2 &+ q|\hbar(\psi_q^\nu)'(0) - q_-(\psi_q^\nu)(0)|^2 \\ + \frac{\nu m^2}{\alpha} \int_0^1 |(\psi_q^\nu)(x)|^2 dx &\leq 4q(q_- + q)^2. \end{aligned} \tag{4.66}$$

Applying the maximum principle ([27]) to system (4.59)-(4.60), with n^ν nonnegative, we also have V^ν is nonnegative. Using equation (4.64) and inequality (4.66), we get the following estimation

$$||\psi_q^\nu||_{H^2(0,1)}^2 \leq C(E(q) + 1)q^3, \tag{4.67}$$

where C depends on ν. Then, due to the fact that $H^2(0,1)$ is imbedded in $L^\infty(0,1)$ (from [91]), we have

$$||\psi_q^\nu||_{L^\infty(0,1)}^2 \leq C'||\psi_q^\nu||_{H^2(0,1)}^2 \leq C(E(q) + 1)q^3, \tag{4.68}$$

where C' a positive constante and C is a new constant depending on ν. Let us now recall the expression of the density $n^\nu(x) = \int_0^{+\infty} G(q)|\psi_q^\nu(x)|^2 dq$. We obtain

$$||n^\nu||_{L^\infty(0,1)} \leq \int_0^{+\infty} G(q)||\psi_q^\nu||^2_{L^\infty(0,1)} dq. \tag{4.69}$$

Then, from the Poisson problem, V^ν is bounded in $W^{2,\infty}(0,1)$. As $W^{2,\infty}(0,1)$ is compactly imbedded in $L^\infty(0,1)$, we deduce that there exists a constant C_ν such that

$$||V^\nu||_{L^\infty(0,1)} \leq C_\nu. \tag{4.70}$$

■

Now, let us introduce the following Proposition.

Proposition 4.3 *The map $\mathcal{T}$ is compact and continuous over $L^\infty(0,1)$.*

In the sequel, we set by

$$\psi_j^\nu = \psi_q(V_j^\nu), \quad N_j^\nu = N(\psi_j^\nu) \text{ and } (V_j^\nu)^* = \mathcal{T}V_j^\nu.$$

Proof : We split the proof into two steps. The first step is to show the compactness. Then, the second one is to show the continuity of $\mathcal{T}$.

Compactness : Let V_j^ν be a bounded sequence in $L^\infty(0,1)$. Then, using estimation (4.67), we show that the sequence ψ_j^ν, solution of the Kohn-Luttinger equation, is also bounded in $L^\infty(0,1)$. In addition, from estimation (4.69), N_j^ν is bounded in $L^\infty(0,1)$. It follows that the sequence $(V_j^\nu)^*$, solution of the Poisson equation, is bounded in $W^{2,\infty}(0,1)$. Underling that $W^{2,\infty}(0,1) \hookrightarrow L^\infty(0,1)$ is compact, we get after a possible extraction that the sequence $(V_j^\nu)^*$ converges strongly in $L^\infty(0,1)$. Thus, $\mathcal{T}$ is compact.

Continuity : It is sufficient to show

$$\text{If } (\ V_j^\nu \longrightarrow V^\nu \quad L^\infty \text{ strong }) \text{ then } \quad (\mathcal{T}V_j^\nu \longrightarrow \mathcal{T}V^\nu \quad L^\infty \text{ strong}).$$

The sequence V_j^ν in $L^\infty(0,1)$ converges strongly in $L^\infty(0,1)$ towards V^ν. Thanks to the compactness of $\mathcal{T}$ we have that for each subsequence of j there exists a subsequence of the further one, denoted again by j, such that $(V_j^\nu)^*$ converges strongly in $L^\infty(0,1)$. Let us denote this limit by $(V^\nu)^*$.
To prove continuity of $\mathcal{T}$, we verify that the limit $(V^\nu)^*$ is nothing but $\mathcal{T}V^\nu$ the image of V^ν over the map $\mathcal{T}$.
Since, the sequence V_j^ν is bounded in $L^\infty(0,1)$, we infer that the sequence ψ_j^ν, solution of the Kohn-Luttinger equation, is bounded in $W^{4,\infty}(0,1)$. The embedding of $W^{4,\infty}(0,1)$ in $C^2(0,1)$ is compact. After a possible extraction the sequence ψ_j^ν converges strongly in $C^2(0,1)$. Moreover, passing to the limit in the Kohn-Luttinger equation (3.53) the sequence $\psi_q(V_j^\nu)$ converges strongly in $C^2(0,1)$ towards $\psi_q^\nu = \psi_q(V^\nu)$ solution of the (KLM) problem. The limit is unique and all the

sequences converge towards ψ_q^ν.
We have also that the density sequence N_j^ν is bounded in $L^\infty(0,1)$. Hence after possible extraction, we get

$$N_j^\nu \rightharpoonup \tilde{N} \qquad L^\infty \text{ weak}^*.$$

Once again, it is sufficient to check that the limit density $\tilde{N}$ is nothing but the density $N(\psi_q^\nu)$ associated to $\psi_q(V^\nu)$ (i.e $\tilde{N}(x) = \int_0^{+\infty} G(q)|\psi_q(x)|^2 dq$). From Lemma 4.4, we conclude from the uniqueness of the limit that $\tilde{N} = N(\psi_q^\nu)$.

Now, it remains to pass to the limit in the Poisson problem

$$\begin{cases} -\dfrac{d^2(V_j^\nu)^*}{d^2x} = N(\psi_q(V_j^\nu)) \\ (V_j^\nu)^*(0) = V_1, \qquad (V_j^\nu)^*(1) = V_2. \end{cases}$$

As $N(\psi_q(V_j^\nu))$ is bounded in $L^\infty(0,1)$, $(V_j^\nu)^*$is bounded in $W^{2,\infty}(0,1)$. Recalling that the embedding of $W^{2,\infty}(0,1)$ in $L^\infty(0,1)$ is compact, we have after a possible extraction, that $(V_j^\nu)^*$ converges strongly in L^∞ towards $\mathcal{T}V^\nu$, solution of the Poisson problem. By the uniqueness of the limit $(V^\nu)^*$ is equal to $\mathcal{T}V^\nu$. Thus, the continuity of $\mathcal{T}$ is justified. ■

Lemma 4.4

$$N(\psi_j^\nu) \longrightarrow N(\psi_q^\nu) \qquad C^0(0,1) \ \textit{strong.}$$

Proof of Lemma 4.4 : Consider the following difference

$$N(\psi_j^\nu) - N(\psi_q^\nu) = \int_0^{+\infty} G(q)(|\psi_j^\nu(x)|^2 - |\psi_q^\nu(x)|^2)dq,$$

such that, we get

$$|N(\psi_j^\nu) - N(\psi_q)| \leq \int_0^{+\infty} G(q)||\psi_j^\nu - \psi_q^\nu||_{L^\infty(0,1)}(||\psi_j^\nu||_{L^\infty(0,1)} + ||\psi_q^\nu||_{L^\infty(0,1)})dq.$$

ψ_j^ν converges strongly in $C^2(0,1)$ towards ψ_q^ν and then we have

$$\psi_j^\nu \longrightarrow \psi_q^\nu \quad C^0(0,1) \quad \text{strong.} \tag{4.71}$$

From (4.71) and that ψ_j^ν is bounded in $L^\infty(0,1)$, we deduce that there exists $C > 0$ such that

$$||\psi_q^\nu||_{L^\infty(0,1)} \leq C.$$

After that, we denote by

$$f_j(q) = G(q)||\psi_j^\nu - \psi_q^\nu||_{L^\infty(0,1)}(||\psi_j^\nu||_{L^\infty(0,1)} + ||\psi_q^\nu||_{L^\infty(0,1)}).$$

There exists a constant C independent of j such that f_j satisfy

$$|f_j(q)| \leq C|G(q)|.$$

Moreover, the function G is a compactly supported function integrable over $[0,+\infty[$ and we have

$$f_j \underset{j\longrightarrow\infty}{\longrightarrow} 0 \quad p.p.$$

Applying the Lebesgue Theorem, we obtain

$$\int_0^{+\infty} |f_j(q)|dq \underset{j\longrightarrow\infty}{\longrightarrow} 0.$$

Consequently, $N(\psi_j^\nu)$ converges L^∞ strong towards $N(\psi_q^\nu)$. ■

Proof of Theorem 4.1 : (Conclusion)
From Lemma 4.2 and Proposition 4.3, we see that the conditions of the Leray Schauder Theorem hold. Thus, the modified coupled (Kohn-Luttinger)-Poisson problem admits a solution (V^ν, ψ_q^ν). ■

4.1 Estimates independent of ν

In order to pass to the limit, ν going to zero, we need a ν-independent estimate.

Proposition 4.5 *The density n^ν is bounded in $L^\infty(0,1)$ independently of ν.*

The proof of this Proposition is similar to Proposition 5.2 in [12].

Proof : We deduce from imaginary part (4.61) and real part (4.64) the following estimate

$$\alpha\frac{\hbar^4}{4m^2}||(\psi_q^\nu)''||^2_{L^2(0,1)} + \frac{\hbar^2}{2m}||(\psi_q^\nu)'||^2_{L^2(0,1)} - \int_0^1 (E(q)+e(V^\nu - V_1)|(\psi_q^\nu)(x)|^2dx \leq 2\alpha\frac{\hbar}{4m^2}q(q+q_-)^2. \tag{4.72}$$

We begin by multiplying (4.72) by $G(q)$ and integrating over the interval $[0,+\infty[$. We introduce then the kinetic energy density

$$K^\nu(x) = \alpha\frac{\hbar^4}{4m^2}\int_0^{+\infty} G(q)|(\psi_q^\nu)''(x)|^2dq + \frac{\hbar^2}{2m}\int_0^{+\infty} G(q)|(\psi_q^\nu)'(x)|^2dq. \tag{4.73}$$

As G is a compactly supported function, estimate (4.72) becomes

$$\int_0^1 K^\nu(x)dx + \int_0^1 (-eV^\nu)(x)n^\nu(x)dx \leq C(1+||n^\nu||_{L^1(0,1)}). \tag{4.74}$$

Let us now use the equations (4.59)-(4.60) and integrate by parts the previous inequality. Thus, we get

$$\int_0^1 K^\nu(x)dx + e\int_0^1 |(V^\nu)'(x)|^2dx \leq C(1+||(V^\nu)'||_{L^\infty(0,1)}). \tag{4.75}$$

Moreover, as α is positive, the expression of K^ν in (4.73) implies the following inequality

$$\int_0^1 K^\nu(x)dx \geq C\int_0^{+\infty} G(q)|(\psi_q^\nu)'(x)|^2 dq.$$

Then, given that

$$\psi_q{}^2(x) = \psi_q{}^2(0) + 2\int_0^x \psi_q{}'(u)\psi_q(u)du,$$

we obtain

$$||\psi_q'||^2_{L^2(0,1)} \geq C||\psi_q'||^2_{L^\infty(0,1)} - C.$$

The integral $K^\nu(x)$ can be estimated by

$$\int_0^1 K^\nu(x)dx \;\; \geq \;\; C\int_0^{+\infty} G(q)||(\psi_q^\nu)||^2_{L^\infty(0,1)}dq - C. \tag{4.76}$$

The charge density satisfy also

$$||n^\nu||_{L^\infty(0,1)} \leq \int_0^{+\infty} G(q)||(\psi_q^\nu)||^2_{L^\infty(0,1)}dq.$$

Since V^ν is a solution of the Poisson equation (4.59)-(4.60), we get the following estimate

$$||V^{\nu'}||_{W^{1,\infty}(0,1)} \leq C||V^\nu||_{W^{2,\infty}(0,1)} \leq C||n^\nu||_{L^\infty(0,1)}.$$

Estimate (4.76) becomes

$$\int_0^1 K^\nu(x)dx \;\; \geq \;\; C||V^{\nu'}||_{W^{1,\infty}(0,1)} - C.$$

Coming back to estimate (4.75), we have

$$C_1||(V^\nu)'||_{W^{1,\infty}(0,1)} + e||(V^\nu)'||^2_{L^2(0,1)} \;\; \leq \;\; C_2 + C_3||(V^\nu)'||_{L^\infty(0,1)}). \tag{4.77}$$

We notice, that there is a non homogeneity between the left-hand side and the right one of the above estimate (4.77). For this aim, we apply a Gagliardo-Nirenberg interpolation result (see [27]) to to $(V^\nu)'$ wihch leads to

$$||(V^\nu)'||_{L^\infty(0,1)} \;\; \leq \;\; C_4||(V^\nu)'||^{\frac{2}{3}}_{L^2(0,1)}||(V^\nu)'||^{\frac{1}{3}}_{W^{1,\infty}(0,1)}.$$

Then, applying Young inequality (see [27]), we get

$$C_4||(V^\nu)'||^{\frac{2}{3}}_{L^2(0,1)}||(V^\nu)'||^{\frac{1}{3}}_{W^{1,\infty}(0,1)} \leq \frac{C_4}{2}(||(V^\nu)'||^{\frac{4}{3}}_{L^2(0,1)} + ||(V^\nu)'||^{\frac{2}{3}}_{W^{1,\infty}(0,1)}).$$

Hence, under these previous manipulations, estimate (4.77) becomes

$$C_1||(V^\nu)'||_{W^{1,\infty}(0,1)} + e||(V^\nu)'||^2_{L^2(0,1)} \leq C_2 + C_5(||(V^\nu)'||^{4/3}_{L^2(0,1)} + ||(V^\nu)'||^{2/3}_{W^{1,\infty}(0,1)}), \quad (C_5 = C_4C_3).$$

Then, this estimate implies the bound of V in $L^\infty(0,1)$ by a constant C depending on C_1, e, C_2 and C_5. Therefore, in inequality (4.75) K^ν is bounded in $L^1(0,1)$. It follows from

$$||n^\nu||_{L^\infty(0,1)} \leq \int_0^1 K^\nu(x)dx + C,$$

that also the density n^ν is bounded in $L^\infty(0,1)$ regardless of ν. ■

4.1.1 Conclusion

It results from the bound of V^ν and n^ν respectively in $W^{2,\infty}(0,1)$ and in $L^\infty(0,1)$ that after possible extraction there exist V and n such that

$$V^\nu \underset{\nu\to 0}{\to} V \quad C^0(0,1) \quad \text{strong}, \tag{4.78}$$

$$n^\nu \underset{\nu\to 0}{\rightharpoonup} n \quad L^\infty(0,1) \quad \text{weak} * . \tag{4.79}$$

4.2 The limit problem

Let ψ_q be a solution of the weak formulation with $\nu = 0$. It is defined for all $E(q)$ except for $E(q_j)_{j\geq 0}$. We denote then by n_0 the density corresponding to these scattering states

$$n_0(x) = \int_0^{+\infty} G(q)|\psi_q(x)|^2 dq. \tag{4.80}$$

In the sequel, we propose to study the limit, when ν goes to zero, of the (KLPM) problem towards the (KLP) problem. Here, we refer to the paper of N.B Abdallah [12], where he studied this limit in the multidimensional case.

Theorem 4.6 *The density n_0 belongs to $L^\infty(0,1)$. Moreover, there exist a positive sequence $(\lambda_j^l)_{j\in\mathbb{N},l\in[1,d_j]}$ and an orthonormal basis $(\varphi_j^l)_{j\in\mathbb{N},l\in[1,d_j]}$ of the space $\oplus S_j$, where d_j and S_j are given in (1.23) and (1.22), such that*

$$n(x) = n_0(x) + \sum_{j=1}^{\infty}\sum_{l=1}^{d_j} \lambda_j^l |\varphi_j^l(x)|^2. \tag{4.81}$$

We first introduce some notations. Let $\mathcal{I}_\epsilon$ be the set of energies close to the eigenenergies defined by

$$\mathcal{I}_\epsilon = \cup_{i=1}^{\infty} I_{E_i,\epsilon} \tag{4.82}$$

where

$$I_{E_i,\epsilon} = [E_i - \epsilon, E_i + \epsilon].$$

The $\mathcal{J}_\epsilon$ is the complementary set to $\mathcal{I}_\epsilon$, given by

$$\mathcal{J}_\epsilon = \{E(q) \text{ such that } E(q) \notin \mathcal{I}_\epsilon\}. \tag{4.83}$$

Let us denote by $\mathcal{P}_i$ the L^2 orthogonal projection on S_i and

$$\mathcal{Q}_i = Id - \mathcal{P}_i. \tag{4.84}$$

The proof of Theorem 4.6 follows the steps of the proof of Theorem 6.3 in [12]. In the previous section 4.1, we have obtained the results of the bound on the density n^ν and not on ψ_q^ν. The following Lemmas will enable us to show this.

Lemma 4.7 *Let q_ν be a convergent sequence when ν goes to zero towards q_0 and we assume that*

$$\lim_{\nu\to 0} ||\psi_{q_\nu}^\nu||_{L^2(0,1)} = +\infty.$$

Then, there exists $j \in \mathbb{N}^*$ such that $q_0 = q_j$ and

$$||\mathcal{Q}_j(\psi_{q_\nu}^\nu)||_{L^2(0,1)} = o(||\psi_{q_\nu}^\nu||_{L^2(0,1)}).$$

Proof : The proof of this Lemma is similar to the proof of Lemma 6.5 in [12]. In our case, we obtain

$$C||\psi_q^\nu||_{L^2(0,1)} \leq ||\psi_q^\nu||_{H^2(0,1)} \leq C||\psi_q^\nu||_{L^2(0,1)} + C. \tag{4.85}$$

The first inequality follows from the Poincaré inequality([27]) whereas the second one comes from the inequalities (4.64), (4.66) and the boundness of V in $L^\infty(0,1)$. From (4.85),

$$\theta_\nu = \frac{\psi_{q_\nu}^\nu}{||\psi_{q_\nu}^\nu||_{L^2(0,1)}}$$

is bounded in $H^2(0,1)$, converges strongly in $L^2(0,1)$ and weakly in $H^2(0,1)$ towards a limit θ_0 which L^2 norm is equal to 1.

Multiplying the weak formulation (3.58) by $\frac{1}{||\psi_{q_\nu}^\nu||_{L^2}^2}$, we can pass to the weak limit in $H^2(0,1)$. We find that θ_0 is a solution of the problem (3.46)-(3.50) and have as energy $E(q_0)$. This is equivalent to write that θ_0 is an eigenvector and $E(q_0)$ is the associated eigenvalue. As a consequence, there exists $j \geq 0$ such that $E(q_0) = E(q_j)$ and θ_0 belongs to the subspace S_j.

Now, we prove the second part of the Lemma. To this aim, we recall that $\mathcal{Q}_j(\theta_0) = 0$ because $\theta_0 \in S_j$. Moreover, θ_ν converges strongly in $L^2(0,1)$ towards θ_0 then

$$\mathcal{Q}_j(\theta_\nu) = o(1).$$

Thus, this ends the proof. ■

Corollary 4.8 *For all $\epsilon > 0$, we set by*

$$n_\epsilon^\nu = \int_{q\in\mathcal{J}_\epsilon} G(q)|\psi_q^\nu(x)|^2 dq$$

and

$$n_\epsilon = \int_{q\in\mathcal{J}_\epsilon} G(q)|\psi_q(x)|^2 dq,$$

where $\mathcal{J}_\epsilon$ was defined in (4.83). Then, n_ϵ^ν converges strongly towards n_ϵ in $L^2(0,1)$.

Proof : We take as a starting point the proof of corollary 6.7 in [12]. We notice that Proposition 4.5 still holds when we replace n^ν by n_ϵ^ν. Therefore, there exists the density n_ϵ^0 such that n_ϵ^ν converges strongly towards n_ϵ^0 in $L^2(0,1)$. Thus, it remains to prove that n_ϵ^0 is nothing but n_ϵ.
From Lemma 4.7, we deduce that

$$||\psi_q^\nu||_{H^2(0,1)} \leq C_\epsilon, \qquad \forall q \in \mathcal{J}_\epsilon.$$

This infers that after possible extraction ψ_q^ν converges weakly in $H^2(0,1)$ and strongly in $L^\infty(0,1)$ for each $E(q)$ in $\mathcal{J}_\epsilon$ towards the solution of the weak formulation (3.58) with $\nu = 0$ and replacing V^ν by V. Then, the limit of ${\psi_q}^\nu$ is nothing but ψ_q and according to the uniqueness of the limit the whole sequence converges.
In addition, for all $f \in L^2(0,1)$ we can pass to the limit in the following expression,

$$\begin{aligned}\lim_{\nu\to 0}\int_0^1 f(x)n_\epsilon^\nu(x)dx &= \lim_{\nu\to 0}\int_0^1\int_{\mathcal{J}_\epsilon} f(x)G(q)|{\psi_q}^\nu(x)|^2 dqdx \\ &= \int_0^1\int_{\mathcal{J}_\epsilon} f(x)G(q)|\psi_q(x)|^2 dqdx = \int_0^1 f(x)n_\epsilon(x)dx.\end{aligned}$$

We conclude that $n_\epsilon^0 = n_\epsilon$. ■

Corollary 4.9 *The density n_0 is in $L^\infty(0,1)$.*

Proof : We deduce from the inequality $n_\epsilon^\nu \leq n^\nu$ that $n_\epsilon \leq n$. Then, when ϵ goes to zero we find

$$0 \leq n_0 \leq n.$$

As $n \in L^\infty(0,1)$ then n_0 is too. ■

Now, we return to $E(q) \in I_{E_j,\epsilon}$. Let us give the following Proposition.

Proposition 4.10 *For every $j \in \mathbb{N}^*$, we have (i)*

$$\lim_{\epsilon\to 0}\lim_{\nu\to 0}\int_{I_{E_j,\epsilon}} G(q)||\mathcal{Q}_j(\psi_q^\nu)||^2_{L^2(0,1)}dq = 0.$$

(ii) There exist a sequence of positives reals $(\lambda_j^l)_{l\in[1,d_j]}$ and an orthonormal basis $(\varphi_j^l)_{l\in[1,d_j]}$ of S_j such that

$$\lim_{\epsilon\to 0}\lim_{\nu\to 0}\int_{I_{E_j,\epsilon}} G(q)|\mathcal{P}_j{\psi_q}^\nu(x)|^2 dq = \sum_{l=1}^{d_j}\lambda_j^l|\varphi_j^l(x)|^2, \quad L^1(0,1) \text{ strong.}$$

To prove this Proposition, we use Lemma 6.10 given and proven in [12].

Lemme 4.1 *Let $f_j \geq 0$ and $0 \leq g_j \leq 1$ two sequences of continuous functions in $\mathbb{R}$, μ is a positive measure such that $\mu \leq A\mathcal{L}$ where $\mathcal{L}$ is the Lebesgue measure and A is a positive constant. We assume that there exists $C_0 \geq 0$ such that*

$$\int f_j d\mu \leq C_0.$$

Moreover, we suppose that the following propriety holds : For each subsequence of reals x_{n_k} converging to x_0 such that $f_{n_k}(x_{n_k})$ goes to $+\infty$, we have also $g_{n_k}(x_{n_k})$ going to 0.
Thus

$$\lim_{\epsilon \to 0^+} \limsup_{n \to +\infty} \int_{x_0-\epsilon}^{x_0+\epsilon} f_j(x) g_j(x) d\mu = 0.$$

Proof of Proposition 4.10 : In order to prove (i), we set like in the proof of Proposition 6.9 in [12] by

$$g_\nu(q) = \frac{||\mathcal{Q}_l(\psi_q^\nu)||^2_{L^2(0,1)}}{||\psi_q^\nu||^2_{L^2(0,1)}}, \ f_\nu(q) = ||\psi_q^\nu||^2_{L^2(0,1)}$$

and

$$d\mu = G(q)dq.$$

Due to the fact that n^ν is bounded in $L^1(0,1)$, we obtain

$$\int f_\nu d\mu \leq C.$$

Lemma 4.7 infers that the second hypothesis of Lemma 4.1 holds when $x_0 = q_0$. Consequently, (i) of Lemma 4.1 is verified.

To prove (ii), we choose an orthonormal basis $(f_j^1, .., f_j^{d_j})$ of the subspace S_j. Then, for every $E(q) \in I_{E_j,\epsilon}$ we write $\mathcal{P}_j(\psi_q^\nu)$ in the following way

$$\mathcal{P}_j(\psi_q^\nu) = (\sum_{l=1}^{d_j} \alpha_{\nu,l}(q) f_j^l(x)) ||\psi_q^\nu||_{L^2(0,1)}.$$

The coefficients $\alpha_{\nu,l}$ satisfy

$$\sum_{l=1}^{d_j} |\alpha_{\nu,l}|^2 \leq 1. \tag{4.86}$$

We get the following equality

$$\int_{I_{E_j,\epsilon}} G(q) |\mathcal{P}_j \psi_q^\nu(x)|^2 dq = \sum_{l,l'=1}^{d_j} A_\epsilon^\nu(l,l') f_j^l(x) \overline{f_j^{l'}}(x)$$

with

$$A_\epsilon^\nu(l,l') = \int_{I_{E_j,\epsilon}} \alpha_{\nu,l}(q)\overline{\alpha}_{\nu,l'}(q)||\psi_q^\nu||^2_{L^2(0,1)}G(q)dq. \tag{4.87}$$

We deduce from estimate (4.86) and the bound of n^ν in $L^1(0,1)$ that

$$[A_\epsilon^\nu(l,l')]_{l,l'=1,..d_j}$$

is a bounded sequence of a non-negative Hermitian matrix. Passing to the limits ϵ and ν to zero, we get in $L^1(0,1)$ the following limit

$$\lim_{\epsilon\to 0}\lim_{\nu\to 0}\int_{I_{E_j,\epsilon}} G(q)|\mathcal{P}_j\psi_q^\nu(x)|^2dq = \sum_{l,l'=1}^{d_j} A_j(l,l')f_j^l(x)\overline{f_j^{l'}}(x) \tag{4.88}$$

with A_j the limit of the sequence A_ϵ^ν is also a non-negative Hermitian matrix. This matrix can be diagonalized. Indeed, there exists a unitary matrix U and D a diagonal one composed of a non-negative real numbers $(\lambda^j)_{j=1,...,d_j}$ such that

$$D = diag(\lambda^1, ...\lambda^{d_j})$$

and

$$A_j = U^tDU.$$

Let us set $F_j = (f_j^1, ..., f_j^{d_j})^t$ and $UF_j = (\varphi_j^1, ..., \varphi_j^{d_j})^t$. As U is unitary and that $(f_j^1, ..., f_j^{d_j})$ is an orthonormal basis then $(\varphi_j^1, ..., \varphi_j^{d_j})$ forms too an orthonormal basis of S_j. Consequently, the limit of expression (4.88) is the following

$$\sum_{l,l'=1}^{d_j} A_j(l,l')f_j^l(x)\overline{f_j^{l'}}(x) = \sum_{l=1}^{d_j}\lambda_j^l|\varphi_j^l(x)|^2.$$

■

Proof of Theorem 4.6 : We set by

$$\Delta_\epsilon^\nu = n^\nu - n_\epsilon^\nu - \sum_{j=1}^{+\infty}\int_{I_{E_j,\epsilon}} G(q)|\mathcal{P}_j\psi_q^\nu|^2dq.$$

It is sufficient to prove that Δ_ϵ^ν goes to 0 when ν and ϵ tend respectively to 0. To do so, we notice that immediately from expressions of n^ν, n_ϵ^ν and $\mathcal{Q}_j$ given respectively in (4.59), corollary 4.8 and (4.84), Δ_ϵ^ν becomes

$$\Delta_\epsilon^\nu = \sum_{j=1}^{+\infty}\int_{\mathcal{I}_\epsilon} G(q)|\mathcal{Q}_j\psi_q^\nu|^2dq + 2\Re e(\sum_{j=1}^{+\infty}\int_{\mathcal{I}_\epsilon} G(q)((\mathcal{Q}_j\psi_q^\nu)(\mathcal{P}_j\overline{\psi_q^\nu}))dq.$$

Applying the Cauchy Schwartz inequality ([27]), we obtain the following estimate

$$||\Delta_\epsilon^\nu||_{L^1(0,1)} \leq \sum_{j=1}^{+\infty} \int_{\mathcal{I}_\epsilon} G(q)||\mathcal{Q}_j\psi_q^\nu||^2_{L^2(0,1)}dq + \sum_{j=1}^{+\infty} ||n^\nu||^{1/2}_{L^1(0,1)}(\int_{\mathcal{I}_\epsilon} G(q)||\mathcal{Q}_j\psi_q^\nu)||^2_{L^2(0,1)}dq)^{1/2}.$$

From Proposition 4.10(i), we deduce that

$$\Delta_\epsilon^\nu \underset{\epsilon,\nu\to 0}{\longrightarrow} 0 \qquad L^1(0,1).$$

In the sequel, using the results of corollary 4.8 and those of Proposition 4.10 (ii), we get

$$n(x) = n_0(x) + \sum_{j=1}^{\infty}\sum_{l=1}^{d_j} \lambda_j^l|\varphi_j^l(x)|^2.$$

■

Chapitre 3

Numerical analysis of the KL model : Application to the intraband device

Sommaire

1 Introduction

In this chapter, we give a numerical analysis of the coupled (Kohn-Luttinger)-Poisson problem. Our disctretization is based on a finite element method. In the following, we recall briefly the principle of this method, for details one can see [35], [37], [72], [98], [45] and [103]). The finite element method is based on determining the solution of the weak problem in a finite space. This space must approach the space of the continuous problem. The construction of the discrete space is based on the networking of the domain. It consists on dividing the domain in a finite disjointed subdomains on which we choose a finite numbers of nodes. The function of the discrete space are defined by piece in each interior node of the domain and verify the boundary conditions in the edges of the domain. They make a linear combination of simple finite elements (in general 1, 2 or 3th degree polynomial). Then, the weak formulation is expressed in function of the finite elements. We obtain in the sequel a matrix system where the unknowns are the value of the solution in each node. The matrix treatment can be done on a reference element. For this aim, we derive different elementary matrix associated to one element. Then, we assemble them in order to compose the global matrix along the domain. The obtained matrix system is band which is useful for storage.

2 The different equations to solve

Now, we draw up an inventory of the equations that we will use in the numerical study. For this, we separate them in two categories : the Kohn-Luttinger open equation and the elliptic equation on the potential.

2.1 The Kohn-Luttinger open equation

We solve the one-dimensional Kohn-Luttinger equation with the open boundary conditions in the case of two-sided injections under a variation of potential. For the sake of simplicity, we focus in the case where $V_2 > V_1$.

In the case of the left injection, the system is the following

$$\mathbb{K}\psi_q^+ - eV(x)\psi_q^+ = (E(q) - eV_1)\psi_q^+ \tag{2.1}$$

$$\hbar^2\psi_q^{+''}(0) = \hbar(q_- - iq)\psi_q^{+'}(0) + iqq_-\psi_q^+(0) - 2iq(q_- - iq) \tag{2.2}$$

$$\hbar^3\psi_q^{+'''}(0) = \hbar(q_-^2 - iq(q_- - iq))\psi_q^{+'}(0) + iqq_-(q_- - iq)\psi_q^+(0) - 2iqq_-(q_- - iq) \tag{2.3}$$

$$\hbar^2\psi_q^{+''}(1) = -\hbar(p_- - ip_+)\psi_q^{+'}(1) + ip_+p_-\psi_q^+(1) \tag{2.4}$$

$$\hbar^3\psi_q^{+'''}(1) = \hbar(p_-^2 - ip_+(p_- - ip_+))\psi_q^{+'}(1) - ip_+p_-(p_- - ip_+)\psi_q^+(1). \tag{2.5}$$

However, in the case of the right injection, two cases are possible. The first is when q is such that $q^2 \geq A'$ (see (2.38) in chapter 2), then we obtain the next system

$$\mathbb{K}\psi_q^- - eV(x)\psi_q^- = (E(q) - eV_2)\psi_q^- \tag{2.6}$$

$$\hbar^2\psi_q^{-''}(0) = \hbar(p_-^{'} - ip_+^{'})\psi_q^{-'}(0) + ip_+^{'}p_-^{'}\psi_q^{-}(0) \tag{2.7}$$
$$\hbar^3\psi_q^{-'''}(0) = \hbar(p_-^{'\,2} - ip_+^{'}(p_-^{'} - ip_+^{'}))\psi_q^{-'}(0) + ip_+^{'}p_-^{'}(p_-^{'} - ip_+^{'})\psi_q^{-}(0) \tag{2.8}$$
$$\hbar^2\psi_q^{-''}(1) = -\hbar(q_- - iq)\psi_q^{-'}(1) + iqq_-\psi_q^{-}(1) - 2iq(q_- - iq) \tag{2.9}$$
$$\hbar^3\psi_q^{-'''}(1) = \hbar(q_-^2 - iq(q_- - iq))\psi_q^{-'}(1) - iqq_-(q_- - iq)\psi_q^{-}(1) + 2iqq_-(q_- - iq). \tag{2.10}$$

where

$$p_{\pm}^{'} = \sqrt{\frac{\mp m + \sqrt{(m+\alpha q^2)^2 + 4\alpha m^2 e(V_1 - V_2)}}{\alpha}}.$$

The second case is when q is very small, such that ($ie\ q^2 \leq A^{'}$). We get so

$$\mathbb{K}\psi_q^{-} - eV(x)\psi_q^{-} = (E(q) - eV_2)\psi_q^{-} \tag{2.11}$$
$$\hbar^2\psi_q^{-''}(0) = i\hbar(p_+^{'\,c} - p_-^{'\,c})\psi_q^{-\prime}(0) - p_+^{'\,c}p_-^{'\,c}\psi_q^{-}(0) \tag{2.12}$$
$$\hbar^3\psi_q^{-'''}(0) = -\hbar(p_-^{'\,c2} - p_+^{'\,c}(p_-^{'\,c} - p_+^{'\,c}))\psi_q^{-'}(0) - ip_+^{'\,c}p_-^{'\,c}(p_+^{'\,c} - p_-^{'\,c})\psi_q^{-}(0) \tag{2.13}$$
$$\hbar^2\psi_q^{-''}(1) = -\hbar(q_- - iq)\psi_q^{-'}(1) + iqq_-\psi_q^{-}(1) - 2iq(q_- - iq) \tag{2.14}$$
$$\hbar^3\psi_q^{-'''}(1) = \hbar(q_-^2 - iq(q_- - iq))\psi_q^{-'}(1) - iqq_-(q_- - iq)\psi_q^{-}(1) + 2iqq_-(q_- - iq), \tag{2.15}$$

where

$$p_{\pm}^{'\,c} = \sqrt{\frac{-m \pm i\sqrt{-(m+\alpha q^2)^2 - 4\alpha m^2 e(V_1 - V_2)}}{\alpha}}.$$

It is necessary to solve the Kohn-Luttinger equation several times according to the energy for each iteration of the complete (Kohn-Luttinger)-Poisson for a fixed potential. Existence and uniqueness of solution is given by theorem 3.1 in chapter 2.

2.2 The elliptic equation on the potential

The electrons are charged particles which contribute on the electrostatic potential V via the Poisson equation. Hence, the potential V can be decomposed as :

$$V = V_e + V_s$$

where V_e a given external potential including the double-barriers and the applied voltage and V_s a self-consistent potential solution of

$$-\frac{\partial}{\partial x}(\epsilon_r(x)\frac{\partial V}{\partial x}) = e(N_D - n(x)) \tag{2.16}$$

with the boundary conditions

$$V(0) = 0, \quad V(1) = 0. \tag{2.17}$$

where ϵ_r is the relative dielectric constant of the material, N_D is the doping density and n is given by

$$n(x) = \int_0^{+\infty} \left(G(q)|\psi_q^+(x)|^2 + G(q)|\psi_q^-(x)|^2 \right) dq. \tag{2.18}$$

In the sequel, we solve this equation by an iterative method such that the Gummel method ([56]).

3 The discretization by Hermitian finite elements

The domain of the device is one dimension, it occupies an interval $\Omega =]0,1[$. Then, we subdivide the interval on $N+1$ sub-intervals $T_l = [x_{l-1}, x_l]$ (which are the finite elements) such that $\overline{\Omega} = \cup_{l=1}^{N} T_l$, corresponding to the subdivision $0 = x_0 < x_1 < .. < x_{N-1} < x_N = 1$ (see figure 3.1)

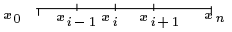

FIG. 3.1: Schematic of uniform mesh.

As we need to approach the Kohn-Luttinger model, in point of view functional analysis we use a finite elements in $H^2(0,1)$. This implies that these finite elements are $C^1(0,1)$. In the one dimensional case, the degree of these finite elements is at least equal to 3 and where we recall the space of polynomials with degree smaller than or equals to 3 is given by

$$P = P_3, \quad dim P_3 = 4 \quad (dim P_k = C_k^{n+k} \text{ with n=dimension of the space}).$$

These elements are called the Hermitian finite elements (see ref [35], [37], [72], [98], [45] and [103]). These elements and derivatives are continuous over all the interval.

For this, we can express the solution ψ of the Kohn-Luttinger problem in terms of elements of the basis associated to the set P_3. It is constituted by four functions with degree smaller than or equals to 3, noted by

$$\phi_k(\xi), \quad k = 1, .., 4.$$

Then, the function ψ can be written on the interval $[x_l, x_{l+1}]$ in a unique manner such that

$$\psi(\xi) = \lambda_l \phi_1(\xi) + \beta_l \phi_2(\xi) + \lambda_{l+1} \phi_3(\xi) + \beta_{l+1} \phi_4(\xi)$$

where

$$\lambda_l = \psi(x_l) = \psi_R(x_l) + i\psi_I(x_l), \quad \beta_l = \psi'(x_l) = \psi_R'(x_l) + i\psi_I'(x_l).$$

Each components $\phi_k(\xi), (k = 1, 2, 3, 4)$ can be chosen such that the new variables $\psi^{'}(x_l)$ and $\psi^{'}(x_{l+1})$ are respectively equal to $\dfrac{d\psi}{dx}$ in $\xi = -1$ and $\xi = 1$. Then, in the interval $[-1, 1]$, ϕ_k,(k=1,..,4) verify the following relations

$$\begin{array}{llll} \phi_1(x_l) = 1 & \phi_2(x_l) = 0 & \phi_3(x_l) = 0 & \phi_4(x_l) = 0 \\ \phi_1^{'}(x_l) = 0 & \phi_2^{'}(x_l) = 1 & \phi_3^{'}(x_l) = 0 & \phi_4^{'}(x_l) = 0 \\ \phi_1(x_{l+1}) = 0 & \phi_2(x_{l+1}) = 0 & \phi_3(x_{l+1}) = 1 & \phi_4(x_{l+1}) = 0 \\ \phi_1^{'}(x_{l+1}) = 0 & \phi_2^{'}(x_{l+1}) = 0 & \phi_3^{'}(x_{l+1}) = 0 & \phi_4^{'}(x_{l+1}) = 1. \end{array}$$

The functions of minimum degree satisfying the previous conditions are given by

$$\phi_1(x) = H_1(\xi), \quad \phi_2(x) = H_2(\xi)(\tfrac{d\xi}{dx})^{-1}, \tag{3.19}$$

$$\phi_3(x) = H_3(\xi), \quad \phi_4(x) = H_4(\xi)(\tfrac{d\xi}{dx})^{-1}, \tag{3.20}$$

where $(H_k)_{k=1,..,4}$ are the Hermite interpolation polynomials (see figure 3.2)

$$\begin{aligned} H_1(\xi) &= \frac{1}{4}(\xi^3 - 3\xi + 2),\ H_2(\xi) = \frac{1}{4}(\xi^3 - \xi^2 - \xi + 1) \\ H_3(\xi) &= \frac{1}{4}(-\xi^3 + 3\xi + 2),\ H_4(\xi) = \frac{1}{4}(\xi^3 + \xi^2 - \xi - 1). \end{aligned}$$

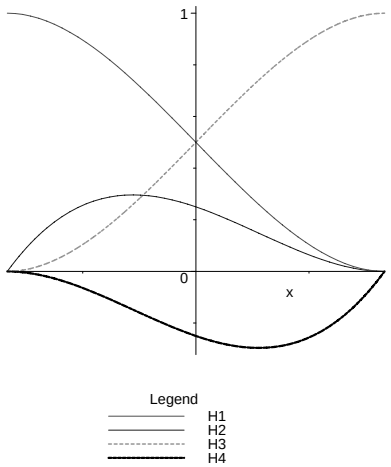

FIG. 3.2: The Hermitian finite elements .

Let $\xi \in [-1, 1]$, then $x \in [x_l, x_{l+1}]$ such that $x_l = lh_x$ with $h_x = \frac{x_N - x_0}{N+1}$ is the mesh step. In addition, ξ can be written as

$$\xi = \frac{2}{h_x}(x - x_{l+\frac{1}{2}}) \text{ where } x_{l+1/2} = \frac{x_{l+1} + x_l}{2}$$

and

$$\frac{d\xi}{dx} = \frac{2}{h_x}.$$

In the sequel, we need the following integrals

$$\begin{aligned}
\frac{h_x}{2}\int_{-1}^{1}\phi_1(\xi)\phi_1(\xi)d\xi &= \frac{13}{35}h_x, \quad \frac{h_x}{2}\int_{-1}^{1}\phi_1(\xi)\phi_2(\xi)d\xi = \frac{11}{210}h_x^2,\\
\frac{h_x}{2}\int_{-1}^{1}\phi_1(\xi)\phi_3(\xi)d\xi &= \frac{9}{70}h_x, \quad \frac{h_x}{2}\int_{-1}^{1}\phi_1(\xi)\phi_4(\xi)d\xi = -\frac{13}{420}h_x^2,\\
\frac{h_x}{2}\int_{-1}^{1}\phi_2(\xi)\phi_2(\xi)d\xi &= \frac{1}{105}h_x^3, \quad \frac{h_x}{2}\int_{-1}^{1}\phi_2(\xi)\phi_4(\xi)d\xi = -\frac{1}{140}h_x^3.
\end{aligned}$$

Consequently, on the reference interval $[x_l, x_{l+1}]$, we obtain the elementary symmetric matrix mass M associated to the two nodes cubic Hermite elements

$$M = \frac{h_x}{420}\begin{pmatrix} 156 & 22h_x & 54 & -13h_x \\ & 4h_x^2 & 13h_x & -3h_x^2 \\ & & 156 & -22h_x \\ & & & 4h_x^2 \end{pmatrix}. \tag{3.21}$$

Now, we look for the elementary matrix corresponding to the first derivative of functions $\phi_k, (k = 1, 2, 3, 4)$. Let

$$\phi^T = (\phi_1, \phi_2, \phi_3, \phi_4)$$

where the first derivative is

$$\frac{d\phi}{dx} = \frac{d\phi}{d\xi}\frac{d\xi}{dx} = \frac{1}{4}\begin{pmatrix} \frac{2}{h_x}(3\xi^2 - 3) \\ 3\xi^2 - 2\xi - 1 \\ \frac{2}{h_x}(-3\xi^2 + 3) \\ 3\xi^2 + 2\xi - 1 \end{pmatrix}.$$

In the sequel, we have

$$\begin{aligned}
\int_{-1}^{1}\phi_1^{'}(\xi)\phi_1^{'}(\xi)\frac{h_x}{2}d\xi &= \frac{6}{5h_x}, \quad \int_{-1}^{1}\phi_1^{'}(\xi)\phi_2^{'}(\xi)\frac{h_x}{2}d\xi = \frac{1}{10},\\
\int_{-1}^{1}\phi_2^{'}(\xi)\phi_2^{'}(\xi)\frac{h_x}{2}d\xi &= \frac{2}{15}h_x, \quad \int_{-1}^{1}\phi_2^{'}(\xi)\phi_4^{'}(\xi)\frac{h_x}{2}d\xi = -\frac{1}{30}h_x.
\end{aligned}$$

Then, we obtain the elementary symmetric matrix K_m

$$K_m = \frac{1}{30h_x}\begin{pmatrix} 36 & 3h_x & -36 & 3h_x \\ & 4h_x^2 & -3h_x & -h_x^2 \\ & & 36 & -3h_x \\ & & & 4h_x^2 \end{pmatrix}. \tag{3.22}$$

Now, we will calculate the integrals of the second derivative of $\phi_k, (k = 1, .., 4)$. Using the fact that

$$\frac{d^2\phi}{dx^2} = \frac{d}{dx}(\frac{d\phi}{d\xi}\frac{d\xi}{dx}) = \frac{d}{d\xi}(\frac{d\phi}{d\xi})(\frac{d\xi}{dx})^2 + \frac{d\phi}{d\xi}(\frac{d^2\xi}{dx^2}) = \frac{1}{4} * \frac{2}{h_x}\begin{pmatrix} \frac{12}{h_x}\xi \\ 6\xi - 2 \\ -\frac{12}{h_x}\xi \\ 6\xi + 2 \end{pmatrix},$$

we get

$$\begin{aligned}\int_{-1}^{1}\phi_1^{''}(\xi)\phi_1^{''}(\xi)\frac{h_x}{2}d\xi &= \frac{12}{h_x^3}, \quad \int_{-1}^{1}\phi_1^{''}(\xi)\phi_2^{''}(\xi)\frac{h_x}{2}d\xi = \frac{6}{h_x^2},\\ \int_{-1}^{1}\phi_2^{''}(\xi)\phi_2^{''}(\xi)\frac{h_x}{2}d\xi &= \frac{4}{h_x}, \quad \int_{-1}^{1}\phi_2^{''}(\xi)\phi_4^{''}(\xi)\frac{h_x}{2}d\xi = \frac{2}{h_x}.\end{aligned}$$

Finally, we obtain the last elementary symmetric matrix K_f

$$K_f = \frac{1}{h_x^3}\begin{pmatrix} 12 & 6h_x & -12 & 6h_x \\ & 4h_x^2 & -6h_x & 2h_x^2 \\ & & 12 & -6h_x \\ & & & 4h_x^2 \end{pmatrix}. \tag{3.23}$$

4 The discrete spaces

In this study, $\mathsf{V} = H^2(0,1)$ is the functional space associated to the Kohn-Luttinger model and $\mathsf{W} = H_0^1(0,1)$ is for the Poisson model. Consequently, the approximated spaces are respectively noted by V_{h_x} and W_{h_x}. They satisfy

$$\mathsf{V}_{h_x} = \{\phi/\phi \in C^1 \text{ and } \phi_{|[x_l,x_{l+1}]} \in P_3, \text{ for } l = 0,..,N\}, \tag{4.24}$$
$$\mathsf{W}_{h_x} = \{\omega/\omega \in C^1 \text{ and } \omega_{|[x_l,x_{l+1}]} \in P_3, \text{ for } l = 0,..,N \text{ and } \omega(0) = \omega(1) = 0\}. \tag{4.25}$$

Proposition 4.1 *The spaces V_{h_x} and W_{h_x} defined respectively in (4.24) and (4.25), are finite-dimensional spaces with respective dimensions $2N+2$ and $2N$.*

In addition, they are included respectively in $H^2(0,1)$ and $H_0^1(0,1)$. Consequently, we are in an internal approximation.

Now, we choose as a test function for V_{h_x} and W_{h_x}, the function f_k satisfying

$$\begin{aligned} f_k(x_l) &= \begin{cases} 1 & \text{if} \quad k = l \\ 0 & \text{if} \quad k \neq l \end{cases} \\ f_k^{'}(x_l) &= 0 \qquad \text{for } k,l = 0,..,N \end{aligned}$$

and the function g_k such that

$$\begin{aligned} g_k(x_l) &= 0 \\ g_k^{'}(x_l) &= \begin{cases} 1 & \text{if} \quad k = l \\ 0 & \text{if} \quad k \neq l \end{cases} \qquad \text{for } k,l = 0,..,N. \end{aligned}$$

More precisely, the function f_k can be written in term of ϕ_1 and ϕ_3 (given by (3.19)-(3.20)) such that

$$f_k(x) = \begin{cases} \phi_3 & \text{on } [x_{k-1}, x_k] \\ \phi_1 & \text{on } [x_k, x_{k+1}] \\ 0 & \text{else} \end{cases}, \qquad \text{for } k = 1,..,N-1$$

and

$$f_0(x) = \begin{cases} \phi_1 & \text{on } [0, x_1] \\ 0 & \text{else} \end{cases} \quad , \quad f_N(x) = \begin{cases} \phi_3 & \text{on } [x_{N-1}, x_N] \\ 0 & \text{else} \end{cases} \quad .$$

The function g_k can also be written in term of ϕ_2 and ϕ_4 (given by (3.19)-(3.20))

$$g_k(x) = \begin{cases} \phi_4 & \text{on } [x_{k-1}, x_k] \\ \phi_2 & \text{on } [x_k, x_{k+1}] \\ 0 & \text{else} \end{cases} \quad , \quad \text{for } k = 1, .., N-1$$

and

$$g_0(x) = \begin{cases} \phi_2 & \text{on } [0, x_1] \\ 0 & \text{else} \end{cases} \quad , \quad g_N(x) = \begin{cases} \phi_4 & \text{on } [x_{N-1}, x_N] \\ 0 & \text{else} \end{cases} \quad .$$

The set of each function defined below compose the basis of V_{h_x} and W_{h_x}. Then, the approximate solution $\psi_{h_x} \in \mathsf{V}_{h_x}$ is written as

$$\psi_{h_x}(x) = \sum_{k=0}^{N} \lambda_k f_k(x) + \sum_{k=0}^{N} \beta_k g_k(x) \tag{4.26}$$

where the coefficients λ_k and β_k are given by

$$\lambda_k = \psi_{h_x}(x_k) = \Re e(\psi_{h_x}(x_k)) + i\Im m(\psi_{h_x}(x_k)), \tag{4.27}$$
$$\beta_k = \psi'_{h_x}(x_k) = \Re e(\psi'_{h_x}(x_k)) + i\Im m(\psi'_{h_x}(x_k)). \tag{4.28}$$

For the approximate solution in W_{h_x}, we only make a summation from 1 to $N-1$.

Remark 4.2 *In the sequel , we will note by*

$$F = (F_1, F_2, .., F_j, F_{j+1}, .., F_{2N+1}, F_{2N+2}) \tag{4.29}$$

the basis of V_{h_x} *with dimension* $2N+2$ *corresponding to the basis* $(f_0, g_0, .., f_j, g_j, .., f_N, g_N)$.

We have treated the choice of the discretization according to x. Now, we need to treat the choice of the discretization according to k. We will note by k_{max} the real such that the support of the distribution G is included in $[0, k_{max}]$. We denote by P_0 the discretization on k. Then, the wave functions ψ_q^+ and ψ_q^- are constants for each k in $[k_j, k_{j+1}]$, with

$$k_j = jh_k, \text{ for } j = 0, .., m \text{ and } h_k = \frac{k_{max}}{m+1}.$$

Then, the associated discrete space is given by

$$\mathsf{V}_{h_x}^{h_k} = \{g = (g_y)_{y \in [0, k_{max}]} / g_y \in \mathsf{V}_{h_x} \text{ and } g_y \in P_0(]k_j, k_{j+1}]), \text{ for } y \in]k_j, k_{j+1}]\}. \tag{4.30}$$

4.1 The assembling of the elementary matrix

4.1.1 Assembling of the mass matrix M

In order to calculate the global mass matrix M, we begin by give the following relation

$$\int_0^1 F_i(x)F_j(x)dx = \sum_{k=1}^{N_x+1} \int_{x_k}^{x_{k+1}} F_i(x)F_j(x)dx.$$

Then, we define an expansion of the elementary mass matrix $M^{(k)}$ replacing in the zero matrix the coefficients of $(2k-1)$-th, $2k$-th, $(2k+1)$-th and , $(2k+2)$-th rows and columns with the components of the elementary matrix M (3.21)

$$M^{(k)} = \frac{h_x}{420}\begin{pmatrix} 0 & \dots & \dots & \dots & \dots & \dots & \dots & 0 \\ \dots & \dots & \dots & \dots & \dots & \dots & \dots & \dots \\ 0 & \dots & 156 & 22h_x & 54 & -13h_x & \dots & 0 \\ 0 & \dots & 22h_x & 4h_x^2 & 13h_x & -3h_x^2 & \dots & 0 \\ 0 & \dots & 54 & 13h_x & 156 & -22h_x & \dots & 0 \\ 0 & \dots & -13h_x & -3h_x^2 & -22h_x & 4h_x^2 & \dots & 0 \\ \dots & \dots & \dots & \dots & \dots & \dots & \dots & \dots \\ 0 & \dots & \dots & \dots & \dots & \dots & \dots & 0 \end{pmatrix}. \tag{4.31}$$

Then, the global matrix $\mathcal{A}_M$ is obtained by assembling the elementary matrix $M^{(k)}$. It is a $(2N+2)\times(2N+2)$ symmetric band matrix.

$$\mathcal{A}_M = \sum_{k=1}^{N+1} M^{(k)} = \frac{h_x}{420}\begin{pmatrix} 156 & 22h_x & 54 & -13h_x & & & & & & & & \\ & 4h_x^2 & 13h_x & -3h_x^2 & & & & & & & & \\ & & 312 & 0 & 54 & -13h_x & & & & & & \\ & & & 8h_x^2 & 13h_x & -3h_x^2 & & & & & & \\ & & & & . & . & & & & & & \\ & & & & & . & . & & & & & \\ & & & & & & . & . & & & & \\ & & & & & & & 312 & 0 & 54 & -13h_x \\ & & & & & & & & 8h_x^2 & 13h_x & -3h_x^2 \\ & & & & & & & & & 156 & -22h_x \\ & & & & & & & & & & 4h_x^2 \end{pmatrix}. \tag{4.32}$$

4.1.2 Assembling of the stiffness matrix K_m

Using the same manner, the global matrix $\mathcal{A}_{K_m}$ is obtained by an expansion of the elementary stiffness matrix K_m. Let

$$K_m^{(k)} = \frac{1}{30h_x}\begin{pmatrix} 0 & \dots & \dots & \dots & \dots & \dots & \dots & 0 \\ \dots & \dots & \dots & \dots & \dots & \dots & \dots & \dots \\ 0 & \dots & 36 & 3h_x & -36 & 3h_x & \dots & 0 \\ 0 & \dots & 3h_x & 4h_x^2 & -3h_x & -h_x^2 & \dots & 0 \\ 0 & \dots & -36 & -3h_x & 36 & -3h_x & \dots & 0 \\ 0 & \dots & 3h_x & -h_x^2 & -3h_x & 4h_x^2 & \dots & 0 \\ \dots & \dots & \dots & \dots & \dots & \dots & \dots & \dots \\ 0 & \dots & \dots & \dots & \dots & \dots & \dots & 0 \end{pmatrix}. \tag{4.33}$$

Then, the global matrix is

$$\mathcal{A}_{K_m} = \sum_{k=1}^{N+1} K_m^{(k)} = \frac{1}{30h_x} \begin{pmatrix} 36 & 3h_x & -36 & 3h_x & & & & & & & & \\ & 4h_x^2 & -3h_x & -h_x^2 & & & & & & & & \\ & & 72 & 0 & -36 & 3h_x & & & & & & \\ & & & 8h_x^2 & -3h_x & -h_x^2 & & & & & & \\ & & & & . & . & & & & & & \\ & & & & & . & . & & & & & \\ & & & & & & . & . & & & & \\ & & & & & & . & . & . & & & \\ & & & & & & & 72 & 0 & -36 & 3h_x & \\ & & & & & & & & 8h_x^2 & -3h_x & -h_x^2 & \\ & & & & & & & & & 36 & -3h_x & \\ & & & & & & & & & & 4h_x^2 & \end{pmatrix}. \quad (4.34)$$

4.1.3 Assembling of the matrix K_f

Similarly to the case of the mass matrix and stiffness matrix, we set by

$$K_f^{(k)} = \frac{1}{h_x^3} \begin{pmatrix} 0 & ... & ... & ... & ... & ... & ... & 0 \\ ... & ... & ... & ... & ... & ... & ... & ... \\ 0 & ... & 12 & 6h_x & -12 & 6h_x & ... & 0 \\ 0 & ... & 6h_x & 4h_x^2 & -6h_x & 2h_x^2 & ... & 0 \\ 0 & ... & -12 & -6h_x & 12 & -6h_x & ... & 0 \\ 0 & ... & 6h_x & 2h_x^2 & -6h_x & 4h_x^2 & ... & 0 \\ ... & ... & ... & ... & ... & ... & ... & ... \\ 0 & ... & ... & ... & ... & ... & ... & 0 \end{pmatrix}. \quad (4.35)$$

Then, we get the next global $(2N+2) \times (2N+2)$ symmetric band matrix

$$\mathcal{A}_{K_f} = \sum_{k=1}^{N+1} K_f^{(k)} = \frac{1}{h_x^3} \begin{pmatrix} 12 & 6h_x & -12 & 6h_x & & & & & & & & \\ & 4h_x^2 & -6h_x & 2h_x^2 & & & & & & & & \\ & & 24 & 0 & -12 & 6h_x & & & & & & \\ & & & 8 & -6h_x & 2h_x^2 & & & & & & \\ & & & & . & . & & & & & & \\ & & & & & . & . & & & & & \\ & & & & & & . & . & & & & \\ & & & & & & . & . & . & & & \\ & & & & & & & 24 & 0 & -12 & 6h_x & \\ & & & & & & & & 8 & -6h_x & 2h_x^2 & \\ & & & & & & & & & 12 & -6h_x & \\ & & & & & & & & & & 4h_x^2 & \end{pmatrix}. \quad (4.36)$$

5 The approached problem

The weak formulation of the discrete problem associated to the continue problem (2.1)-(2.17) consists on searching $((\psi_{h_x}^{h_k})_q^{\pm}, V_{h_x}) \in \mathsf{V}_{h_x}^{h_k} \times \mathsf{W}_{h_x}$, such that

$$Q((\psi_{h_x}^l)^+, \phi_{h_x}) + C^+((\psi_{h_x}^l)^+, \phi_{h_x}) = L^+(\phi_{h_x}), \quad (5.37)$$

$$Q((\psi_{h_x}^l)^-, \phi_{h_x}) + C^-((\psi_{h_x}^l)^-, \phi_{h_x}) = L^-(\phi_{h_x}), \quad \text{for } q^2 \geq A' \quad (5.38)$$

$$Q((\psi_{h_x}^l)^-, \phi_{h_x}) + C_c^-((\psi_{h_x}^l)^-, \phi_{h_x}) = L^-(\phi_{h_x}), \quad \text{for } q^2 \leq A' \quad (5.39)$$

and

$$P(V_{h_x},\omega_{h_x}) = (n,\omega_{h_x})_{L^2(0,1)}, \tag{5.40}$$

$\forall(\phi_{h_x},\omega_{h_x}) \in \mathsf{V}_{h_x}\times\mathsf{W}_{h_x}$ with $(\psi_{h_x}^{h_k})^{\pm} = (\psi_{h_x}^{l})_{l=0,m}^{\pm}$, $\phi_{h_x}^{h_k} = (\phi_{h_x}^{l})_{l=0,m}$ and $(\psi_{h_x}^{l})^{\pm}$, $\phi_{h_x}^{l} \in V_{h_x}$.

The form Q is given by

$$Q(\psi_q,\varphi) = \alpha\frac{\hbar^4}{4m^2}\int_0^1 \psi_q{}''\overline{\varphi}''dx + \frac{\hbar^2}{2m}\int_0^1 \psi_q{}'\overline{\varphi}'dx + \frac{\alpha\hbar^4}{4m}\int_0^1 \psi_q\overline{\varphi}dx, \tag{5.41}$$

and the forms C^+,C^- and C_c^- are written as

$$\begin{aligned}
C^+(\psi_q,\varphi) &= -\int_0^1 (E(q)+em(V(x)-V_1)+\frac{\alpha\hbar^4}{4m})\psi_q\overline{\varphi}dx + \frac{\alpha\hbar}{4m^2}\Big[q_-\Big(\hbar^2\psi_q{}'(0)\overline{\varphi}'(0)-q^2\psi_q(0)\overline{\varphi}(0)\Big)\\
&+ p_-\Big(\hbar^2\psi_q{}'(1)\overline{\varphi}'(1)-p_+^2\psi_q(1)\overline{\varphi}(1)\Big) - ip_+\Big(\hbar\psi_q{}'(1)+p_-\psi_q(1)\Big)\Big(\hbar\overline{\varphi}'(1)+p_-\overline{\varphi}(1)\Big)\\
&- iq\Big(\hbar\psi_q{}'(0)-q_-\psi_q(0)\Big)\Big(\hbar\overline{\varphi}'(0)-q_-\overline{\varphi}(0)\Big)\Big],
\end{aligned} \tag{5.42}$$

$$\begin{aligned}
C^-(\psi_q,\varphi) &= -\int_0^1 (E(q)+e(V(x)-V_2)+\frac{\alpha\hbar^4}{4m})\psi_q\overline{\varphi}dx + \frac{\alpha\hbar}{4m^2}\Big[q_-\Big(\hbar^2\psi_q{}'(1)\overline{\varphi}'(1)-q^2\psi_q(1)\overline{\varphi}(1)\Big)\\
&+ p_-'\Big(\hbar^2\psi_q{}'(0)\overline{\varphi}'(0)-(p_+')^2\psi_q(0)\overline{\varphi}(0)\Big) - iq\Big(\hbar\psi_q{}'(1)+q_-\psi_q(1)\Big)\Big(\hbar\overline{\varphi}'(1)+q_-\overline{\varphi}(1)\Big)\\
&- ip_+'\Big(\hbar\psi_q{}'(0)-p_-'\psi_q(0)\Big)\Big(\hbar\overline{\varphi}'(0)-p_-'\overline{\varphi}(0)\Big)\Big],
\end{aligned} \tag{5.43}$$

$$\begin{aligned}
C_c^-(\psi_q,\varphi) &= -\int_0^1 (E(q)+em(V(x)-V_2)+\frac{\alpha\hbar^4}{4m})\psi_q\overline{\varphi}dx + \frac{\alpha\hbar}{4m^2}\Big[q_-\Big(\hbar^2\psi_q{}'(1)\overline{\varphi}'(1)-q^2\psi_q(1)\overline{\varphi}(1)\Big)\\
&- p_-'{}^c p_+'{}^c\Big(\hbar\psi_q{}'(0)\overline{\varphi}(0)+\psi_q(0)\hbar\overline{\varphi}'(0)\Big) - iq\Big(\hbar\psi_q{}'(1)+q_-\psi_q(1)\Big)\Big(\hbar\overline{\varphi}'(1)+q_-\overline{\varphi}(1)\Big)\\
&+ i(p_+'{}^c - p_-'{}^c)\Big(\hbar^2\psi_q{}'(0)\overline{\varphi}'(0)-p_+'{}^c p_-'{}^c\psi_q(0)\overline{\varphi}(0)\Big)\Big].
\end{aligned} \tag{5.44}$$

Finally for the forms L^+ and L^-, we have

$$L^+(\varphi) = i\frac{\alpha\hbar}{2m^2}q(q_- - iq)\Big(\hbar\overline{\varphi}'(0)-q_-\overline{\varphi}(0)\Big), \tag{5.45}$$

$$L^-(\varphi) = -i\frac{\alpha\hbar}{2m^2}q(q_- - iq)\Big(\hbar\overline{\varphi}'(1)+q_-\overline{\varphi}(1)\Big). \tag{5.46}$$

Further, we have

$$P(V,\omega) = \int_0^1 V'\omega'dx, \quad \forall\,(V,\omega)\in\mathsf{W}_{h_x}\times\mathsf{W}_{h_x}, \tag{5.47}$$

$$n(x) = \int_0^{q_{max}} G(q)|\psi_q^+(x)|^2 + G(q)|\psi_q^-(x)|^2dq. \tag{5.48}$$

First, we study the equations (5.37)-(5.39). We take as a test function ϕ_{h_x} the basis functions $(F_i)_{i=1,2N+2}$ in (4.29) of V_{h_x} . Then, we obtain

$$Q(\psi_{h_x}^l,F_i)+C^+(\psi_{h_x}^l,F_i) = L^+(F_i), \tag{5.49}$$

$$Q(\psi_{h_x}^l,F_i)+C^-(\psi_{h_x}^l,F_i) = L^-(F_i), \tag{5.50}$$

$$Q(\psi_{h_x}^l,F_i)+C_c^-(\psi_{h_x}^l,F_i) = L^-(F_i), \quad \forall\, i=1,..,2N+2. \tag{5.51}$$

Replacing $\psi_{h_x}^l$ by (4.26), we have

$$Q(\psi_h, F_i) = \sum_{k=0}^{N} \lambda_k Q(f_k, F_i) + \sum_{k=0}^{N} \beta_k Q(g_k, F_i),$$
$$C_c^{\pm}(\psi_h, F_i) = \sum_{k=0}^{N} \lambda_k C_c^{\pm}(f_k, F_i) + \sum_{k=0}^{N} \beta_k C_c^{\pm}(g_k, F_i), \quad \text{for i=1,..,2N+2}$$

where λ_k and β_k are defined respectively by (4.27) and (4.28).

In formulation (5.49)-(5.51) the $\mathcal{A}_Q$ is the matrix corresponding to the sesquilinear form Q which is defined by

$$(\mathcal{A}_Q)_{ij} = Q(F_j, F_i), \quad \text{for i,j=1,..2N+2.}$$

It is a symmetric matrix and can be written as

$$\mathcal{A}_Q = \alpha \frac{\hbar^4}{4m^2} \mathcal{A}_{K_f} + \frac{\hbar^2}{2m} \mathcal{A}_{K_m} + \alpha \frac{\hbar^4}{4m} \mathcal{A}_M \tag{5.52}$$

where $\mathcal{A}_M$, $\mathcal{A}_{K_m}$ and $\mathcal{A}_{K_m}$ are given in (4.32), (4.34) and (4.36).

The $\mathcal{A}_{C_c^{\pm}}$ matrix corresponding to the sesquilinear form $C_c^{\pm}$ has the following general term

$$(A_{C_c^{\pm}})_{ij} = C_c^{\pm}(F_j, F_i), \quad \text{for i,j=1,..2N+2.}$$

It can be written as

$$\mathcal{A}_{C_c^{\pm}} = -(E(q) + \frac{\alpha\hbar^4}{4m})\mathcal{A}_M - e\mathcal{A}_V + \mathcal{A}_{TDB_c^{\pm}}, \tag{5.53}$$

where the matrix $\mathcal{A}_V$ is defined by

$$(\mathcal{A}_V)_{ij} \quad = \quad (\int_0^1 V(x) F_j(x) F_i(x) dx), \quad \text{for i,j=1,..2N+2,} \tag{5.54}$$

and the matrix $\mathcal{A}_{TDB_c^{\pm}}$ corresponds to the boundary terms.

The compute and details for determining the matrix $\mathcal{A}_V$ and $\mathcal{A}_{TDB_c^{\pm}}$ are found in appendix A.

In the following, we study the right-hand side of equation (5.49)-(5.51).

5.1 The vector $L^{\pm}$

From (5.45) and (5.46), for each $i = 1, .., 2N + 2$, we obtain

$$\begin{aligned} L^+(F_i) &= i\frac{\alpha\hbar}{2m}q(q_- - iq)\left(\hbar\overline{F_i}^{'}(0) - q_-\overline{F_i}(0)\right), \\ L^-(F_i) &= -i\frac{\alpha\hbar}{2m}q(q_- - iq)\left(\hbar\overline{F_i}^{'}(1) + q_-\overline{F_i}(1)\right). \end{aligned}$$

Then after simplification we get

$$L^+ = i\frac{\alpha\hbar}{2m}q(q_- - iq)\begin{pmatrix} -q_- \\ \hbar \\ 0 \\ . \\ . \\ . \\ 0 \\ 0 \end{pmatrix} \quad \text{and } L^- = i\frac{\alpha\hbar}{2m}q(q_- - iq)\begin{pmatrix} 0 \\ 0 \\ 0 \\ . \\ . \\ . \\ -q_- \\ -\hbar \end{pmatrix}.$$

Now, it remains to make calculations on the Poisson equation (5.40).

$$P(V_{h_x}, F_i) = (n, F_i)_{L^2(0,1)}, \qquad \text{for } i = 1, 2N + 2. \tag{5.55}$$

Replacing V_{h_x} and $n(x)$ by their expression in the basis $(F_j)_{j=1,2N+2}$, we obtain

$$\mathcal{A}_P\mathcal{V} = L_P.$$

The matrix $\mathcal{A}_P$ is nothing but the stiffness matrix $\mathcal{A}_{K_m}$ (4.34). The vector $\mathcal{V}$ corresponds to the potential V in the basis $(F_j)_{j=1,2N+2}$ and the right-hand side vector L_P is the result of the product between the mass matrix $\mathcal{A}_m$ and the density vector $\mathcal{N}$.

$$L_P = \mathcal{A}_M\mathcal{N}, \qquad \text{with } \mathcal{N} = \begin{pmatrix} n(x_0) \\ n^{'}(x_0) \\ . \\ . \\ . \\ n(x_N) \\ n^{'}(x_N) \end{pmatrix}.$$

The weak formulation (5.37)-(5.40) becomes an algebraic system

$$\mathcal{A}^+\Psi^+ = (\mathcal{A}_Q + \mathcal{A}_{C^+})\Psi^+ = L^+ \tag{5.56}$$

$$\mathcal{A}^-\Psi^- = (\mathcal{A}_Q + \mathcal{A}_{C^-})\Psi^- = L^-, \qquad \text{for } q^2 \geq A^{'} \tag{5.57}$$

$$\mathcal{A}_c^-\Psi^- = (\mathcal{A}_Q + \mathcal{A}_{C_c^-})\Psi^- = L^-, \qquad \text{for } q^2 \leq A^{'} \tag{5.58}$$

$$\mathcal{A}_P\mathcal{V} = L_P \tag{5.59}$$

where the vector $\Psi^{\pm}$ represent the wave vector $\psi_q^{\pm}$ in the basis $(F_j)_{j=1,2N+2}$.

Proposition 5.1 *The matrix $\mathcal{A}^{\pm}$ are complex and $\mathcal{A}_P$ is real. They are symmetric, inversible and heptadiagonal.*

6 Numerical implementation

We will present the flow chart which we will use for the resolution of the system (Kohn-Luttinger)-Poisson. We will also make an inventory of all the numerical methods of resolution necessary to these calculations.

6.1 The flow chart

The computation of the electrostatic potential and electronic density is represented in figure 3.3. We assume that for iteration i, the potential is known and we need to compare it with the potential obtained at iteration $i+1$

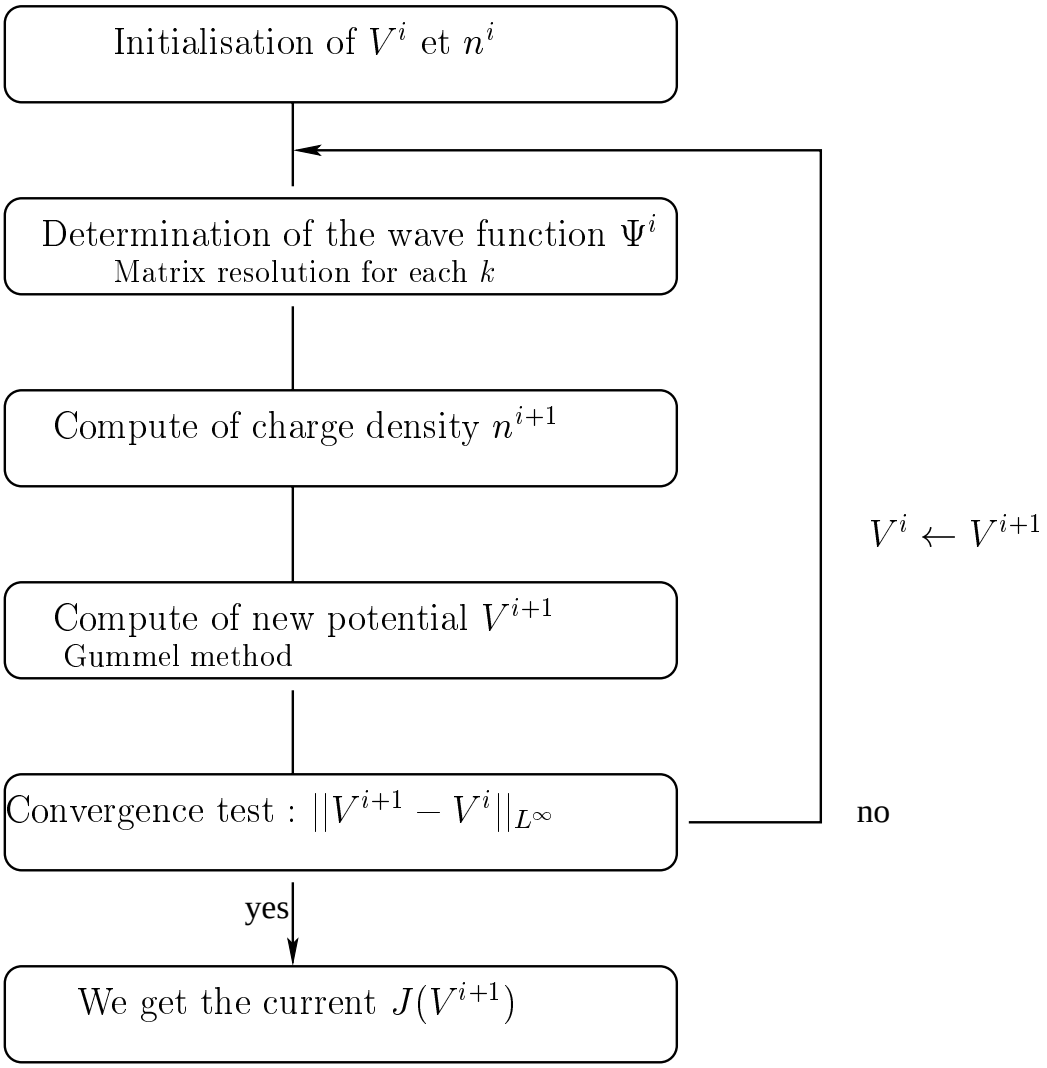

FIG. 3.3: The flow chart present the general procedure to compute the potential, density and current at iteration i.

6.1.1 Initialization

We seek to determine the potential at iteration $i = 0$. The choice of a potential V^0 not too different from the final solution, is essential to ensure convergence of the method of the iterations of Gummel. We thus leave a potential fixed V_s (2.16) equals to zero.

6.1.2 Determination of the charge density

The calculation of the density requires the resolution of a great number of matrix system (5.56)-(5.58) for each wave vector k. We recall that in proposition 5.1 the matrix $\mathcal{A}^{\pm}$ is a symmetric complex matrix and heptadiagonal. Then, we carry out the resolution of this linear system by the direct and iterative methods [72]. For the direct method, due to the fact of the hollow character of the matrix, it is not question of storing all the matrix. If not, it would be too expensive from point of view places memory and time computing. For this, we use a storage type skyline introduced by Jennings [58] and [59]. Then, the direct subroutine ZGBSV used, is a subroutine from the mathematical package LAPACK [2]. Once, the matrix is stored, the subroutine ZGBSV consists on reversing the complex symmetric band matrix by LU decomposition [72]. For the iterative method, we store the matrix in a "condensed" form [59] usually used for the implementation of the iterative method in order to solve linear system. Then, we use the iterative method QMR (Quasi Minimal Residual) suggested by Freund ([49] and [50]) with a preconditionnor (SSOR or ILUT). This method QMR is well adapted to the symmetric problem and much more effective for our calculations.
We obtain a whole of wave functions $\Psi_c^{\pm}$ using a loop on the wave vectors $k = q/\hbar$. Further, we recall that the electronic density (5.48) can be written in term of k,

$$n(x) = 2\left(\int_0^{k_{max}} G(k)|\Psi^+(x)|^2 \frac{dk}{2\pi} + \int_0^{k_{max}} G(k)|\Psi^-(x)|^2 \frac{dk}{2\pi}\right). \tag{6.60}$$

where $|\Psi^{\pm}(x)|^2$ is the probability density of presence of the electron in x, $1/2\pi$ represents the state density in k space and the factor 2 intervenes like factor of spin of the electron. The one-dimensional distribution $G(k)$ of Fermi-Dirac is given by

$$G(k) = \frac{mk_bT}{\pi\hbar^2} log(1 + exp(\frac{-E(k) - e\mu}{k_bT})) \tag{6.61}$$

where $E(k) = \alpha\frac{(\hbar k)^4}{4m^2} + \frac{(\hbar k)^2}{2m}$ and μ the chemical potential given at equilibrium.

Afterthat, the computation of the electronic density requires the calculation of the integral over the wave vector k. In practice, the maximum wave vector $k_{max}(= q_{max}/\hbar)$ of the integration is not infinite, it depends on Fermi level. We set by

$$\frac{\hbar^2 k_{max}^2}{2m} = \frac{\hbar^2 k_{fermi}^2}{2m} + 5k_BT$$

and assume that for $k > k_{max}$, the Fermi-Dirac integral is null. It is not necessary to store in memory all the wave functions because we use a Simpson method

$$\int_0^{k_{max}} f(k)dk = \sum_{i=0}^{k_{max}-1} \frac{k_{i+1}-k_i}{6}(f(k_i) + 4f(\frac{k_i+k_{i+1}}{2}) + f(k_{i+1}))$$

inside the loop on the wave vectors. Moreover, we use a one step of a uniform discretization in k for the obtained results.

6.1.3 Determination of the potential

We calculate the self-consistent potential from the Poisson equation. The problem is not linear, so there is a little chance that the algorithm converges. One solution is to use an implicit iterative method such that the Gummel method ([18], [56], [95] and [93]). Then, the Poisson equation (2.16) can still be written under the following iterative diagram where V^{i+1} is given according to V^i

$$-\frac{\partial}{\partial x}(\epsilon_r(x)\frac{\partial V^{i+1}}{\partial x}) = e\left(N_D - n(x)exp(\frac{e(V^{i+1}-V^i)}{k_BT})\right). \quad (6.62)$$

Thus, we obtain a nonlinear system on V^{i+1}. To raise this non-linearity, we linearize the exponential and we get

$$-\frac{\partial}{\partial x}(\epsilon_r(x)\frac{\partial V^{i+1}}{\partial x}) - \frac{e^2}{k_BT}n(x)V^{i+1} = e\left(N_D - n(x)(1-\frac{eV^i}{k_BT})\right). \quad (6.63)$$

The procedure of the determination of the potential at iteration $i+1$ using $n(x)$ at the same iteration, requires the resolution of the linear system (5.59) where we recall that the matrix $\mathcal{A}_P$ is real symmetric and heptadiagonal. Thus, we use another subroutine DGBSV from the package LAPACK. It is the real version of the subroutine ZGBSV already quote previously.

6.1.4 Test on the potential

We compare the potential at iteration i with that at iteration $i+1$ with respect to norm L^∞. When the norm is less than a certain threshold ϵ, then convergence holds.

Finally, knowing that our goal is to compute the characteristic of the current-voltage, then we repeat the general procedure presented on the flow chart 3.3 for small increasing or decreasing variations of the potential of the polarization. Thus, each obtained potential after convergence of computing procedure could be used as initialization for the new procedure to solve.

7 Numerical results

The reason for which we choose to simulate the resonant intraband tunneling diode RTD, is that it has intriguing properties which make it the primary nanoelectronic device. Nanoelectronics offers the promise of an ultra-low power and ultra-high integration density. Among the different nanoelectronic devices discovered and studied so far, the RTD ([18], [40], [4], [47], [48], [66], [70], [93], [95], [109] and [113]) occupies a prominent position. Its intriguing property is its non-monotonic voltage-current characteristic. Indeed, the negative differential resistance between the peak and the valley is shown in figure 3.4.

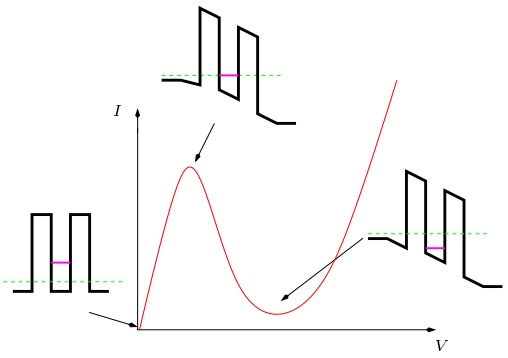

FIG. 3.4: I(V) characteristic and energy band diagram of the resonant intraband tunneling diode.

Initially in figure 3.4, with a low voltage across the device (the first structure), the electrons are below the resonant level (the solid line in the well) and no current can flow through the device. As a bias voltage is applied (the second structure), the resonant level is pulled down in energy so that it lines up with the occupied electron states, permitting resonant tunneling. As the voltage is increased (the third structure), the resonant level eventually passes below the lowest occupied state (the dashed line) and the resonant tunneling current ceases. The current subsequently increases as conduction through higher energy states becomes possible.

7.1 Resonant intraband tunneling diode RTD

The resonant intraband tunneling diode RTD consists of a set of three ultra-thin layers. Those layers, a "well" of GaAs sandwiched between two barrier layers of GaAlAs which are thin enough to permit tunneling. Outside the barriers layers are thick layers of lower effective potential which are doped so as to have a significant density and to which electrical contact is made.

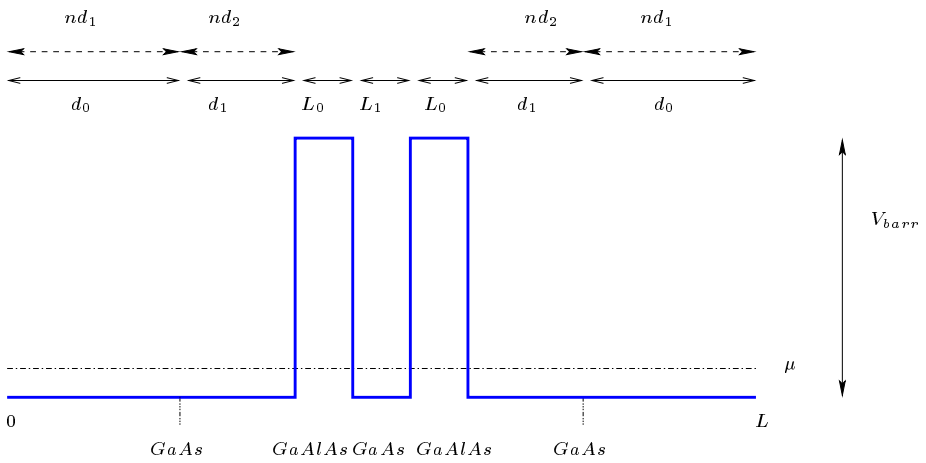

FIG. 3.5: Potential associated to the resonant intraband tunneling diode .

7.2 Numerical data

All our computations are carried out in a double precision, because the data and the constants of the problem are very small. We present in the following tables the numerical values which we took in the case of the resonant intraband tunneling diode GaAs-GaAlAs-GaAs-GaAlAs-GaAs (see figure 3.5) :

d_0	d_1	L_0	L_1	L	nd_1	nd_2	V_{barr}	$m^*ofGaAs$
$50nm$	$10nm$	$5nm$	$5nm$	$135nm$	$1e+24m^{-3}$	$5e+21m^{-3}$	$0.28eV$	$0.067m_e$

7.3 Current density

7.3.1 The current in term of the transmission

In the preceding chapter 2, we have already give the particle probability current along the x direction in (2.39). But, as we inject particles according to the Fermi distribution in (6.61), the current density is obtained by a vector wave average

$$J(x) = \frac{e\hbar}{2m}\left(\int_0^{+\infty} G(k)\left(-\frac{\alpha\hbar^2}{m}\Im m(\overline{\psi}.\frac{\partial^3\psi}{\partial x^3} - \frac{\partial\overline{\psi}}{\partial x}.\frac{\partial^2\psi}{\partial x^2}) + 2\Im m(\overline{\psi}.\frac{\partial\psi}{\partial x})\right)dk. \quad (7.64)$$

However, according to the continuity equation (2.40) and that the model is independent of time, then the current density is independent of position. Thus, current density can be calculated from the wave function at any point in the device. Since the wave function in $x = 1$ is simpler than $x = 0$, it is invariably used in the current calculation. From another standpoint, it is more intuitive to calculate the current flow from the transmission amplitudes. Then, using the expression of transmission $T(k)$ in (4.62), we get

$$J(V) = \frac{e\hbar}{m}\int_0^{+\infty} G(k)\left(\frac{\alpha}{m}\hbar^2k^2 + 1\right)kT(k)dk, \quad (7.65)$$

For this in the sequel, we begin by presenting the transmission simulations for both parabolic approximation and non-parabolic one. Then, we show the current simulation.

7.3.2 The transmission

The resonance effect appears clearly in figure 3.6, where the graph of the logarithm of the transmission probability T (4.62) through the resonant tunneling diode is plotted in term of the energy in eV. We compare the logarithm transmission for the parabolic and non-parabolic approximation. We notice that the effect is more pronounced for non-parabolic approximation when $\alpha > 0$ (solid curve).

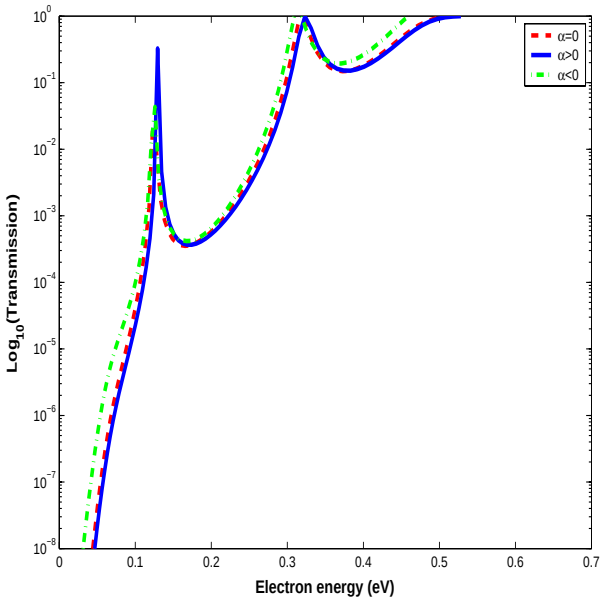

FIG. 3.6: The transmission coefficient corresponding to the parabolic (dashed curve) and non-parabolic (solid curve and dash-dot curve) energies at $T = 300K$.

The main result is that the difference in the transmission are quite small throughout the energy range considered. In the critical first peak transmission (through which most of the current flows), the shape and size of the peak are indistinguishable for the two approximations, and the location of the peak varies only by 0.007 eV. Another conclusion is that the non-parabolic approach is as expected preferable than the parabolic approach.

7.3.3 Computing the current density

In figure 3.7, the peak current for the KL simulation with $\alpha > 0$ occurs at a voltage equals to 0.24 Volts whereas when $\alpha = 0$ and $\alpha < 0$, it occurs respectively at 0.17 and 0.18 Volts . Similarly, the valley current is reached first at 0.23 Volts when $\alpha < 0$, at 0.25 Volts when $\alpha = 0$ and 0.33 Volts when $\alpha > 0$. The ratio peak current

to valley current is higher when $\alpha = 0$. It is about 18%. Contrarily, when $\alpha < 0$ is about 10% and when $\alpha > 0$ is about 7%.

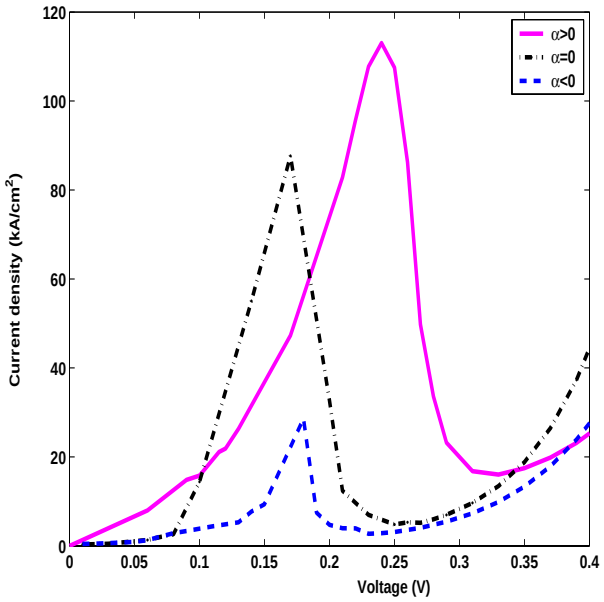

FIG. 3.7: The current density in kiloamps/cm^2 versus the voltage corresponding to the parabolic (dashed curve) and non-parabolic (solid curve for $\alpha > 0$ and dashed-dot curve for $\alpha < 0$) energies at $T = 300K$.

The three-calculations agree on the qualitative shape of the current-voltage characteristic curve [18], [30], [67], [93] and [94]. First, when $\alpha = 0$ which corresponds to the parabolic case we can compare our result to those obtained by O. Pinaud in refs [93] and [94], we notice that the position of the peak is roughly the same. Further, physically the case of $\alpha < 0$ is the more accurate to describe non parabolicity. The non-parabolic model predicts as a whole smaller current densities than the parabolic model (see refs [30] and [69]). Indeed, we obtain a small current density for nonparabolic case when $\alpha < 0$. In the case of $\alpha > 0$ which is not physical case the current is larger than the one obtained from the parabolic model, the first maximum is displaced to the right and is high.

7.3.4 Computing the charge density

As mentioned in section 6, we need to initialize the Gummel algorithm when the applied bias is not zero. In the absence of polarization (ie $V = 0$), the initial self-consistent potential V_s is set equal to zero. Then, after convergence of the Gummel algorithm in this case, the obtained potential will be used like an initialisator. For this, in figure 3.8, we plot the obtained potential and density in the different parabolic and non-parabolic cases.

In figure 3.9, we plot the carrier density versus the voltage for each parabolicity and nonparabolicity cases. The behavior of the carrier density is in conformity with

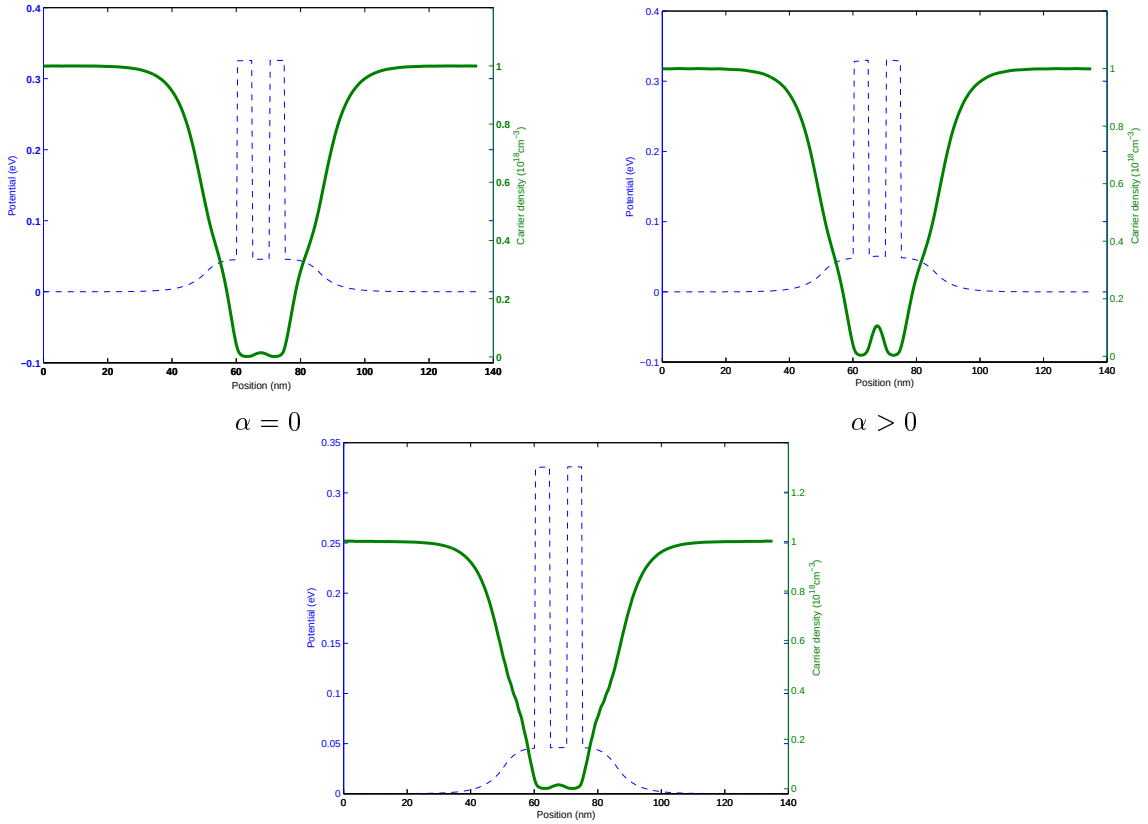

FIG. 3.8: The charge density in $10^{18}cm^{-3}$ and the potential at a bias of $V = 0$ Volt for both parabolic ($\alpha = 0$) and non-parabolic ($\alpha > 0$ and $\alpha < 0$) energies.

what occurs in the device such as the resonant tunneling diode. Indeed, from the low to high voltage, we notice that the density increases until a maximum in the well reached when the voltage corresponds to the peak value of the current (see figure 3.7) and decreases to a bias of the voltage corresponding to the valley current.

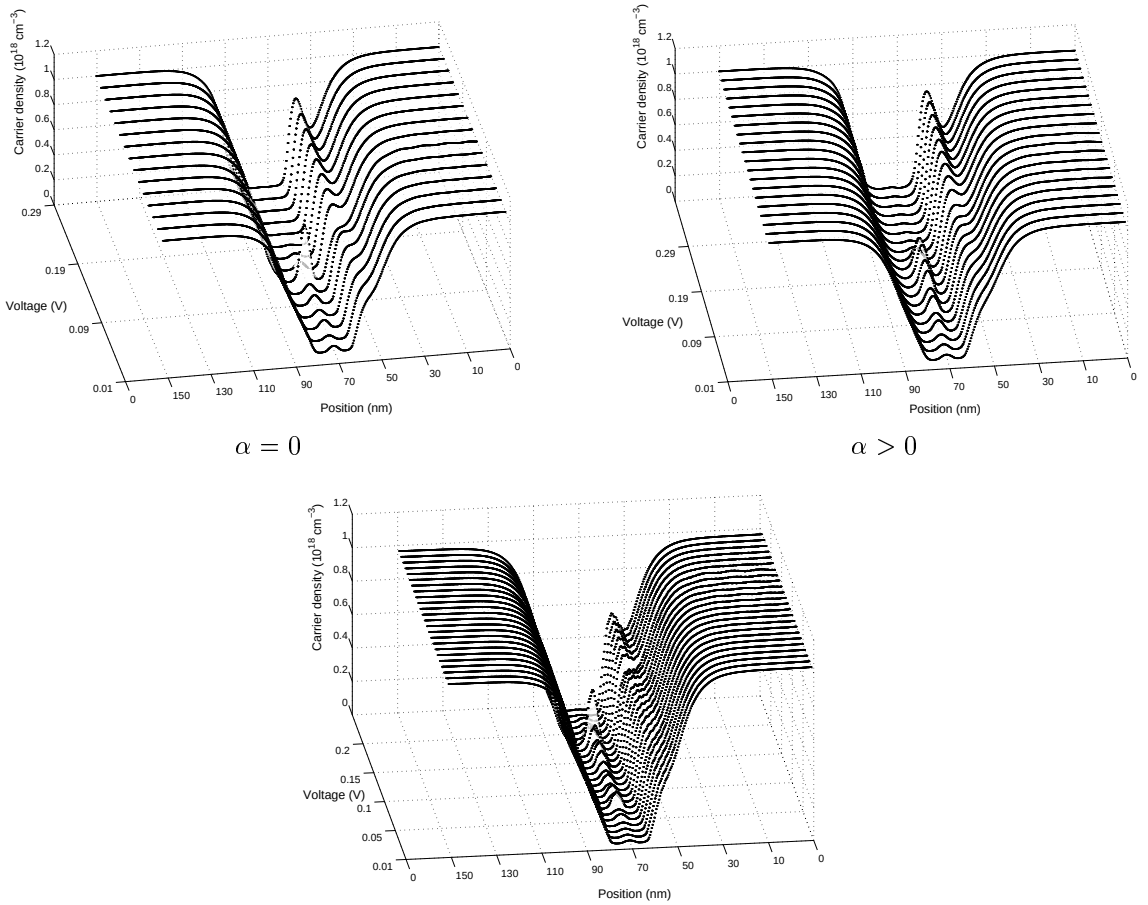

FIG. 3.9: The charge density in $10^{18}cm^{-3}$ versus the voltage corresponding to the parabolic ($\alpha = 0$) and non-parabolic ($\alpha > 0$ and $\alpha < 0$) energies at $T = 300K$.

Then, in the following figure 3.10, the self-consistent electron density and potential profiles were shown when the current reaches the peak for the parabolic and non-parabolic models. As is apparent the effects of nonparabolicity of energy band give a damping effect which reduces also the behavior of the electron densities inside the well. This is shown when $\alpha = 0$ et $\alpha < 0$. Contrarily, when $\alpha > 0$ the electron density rises inside the well.

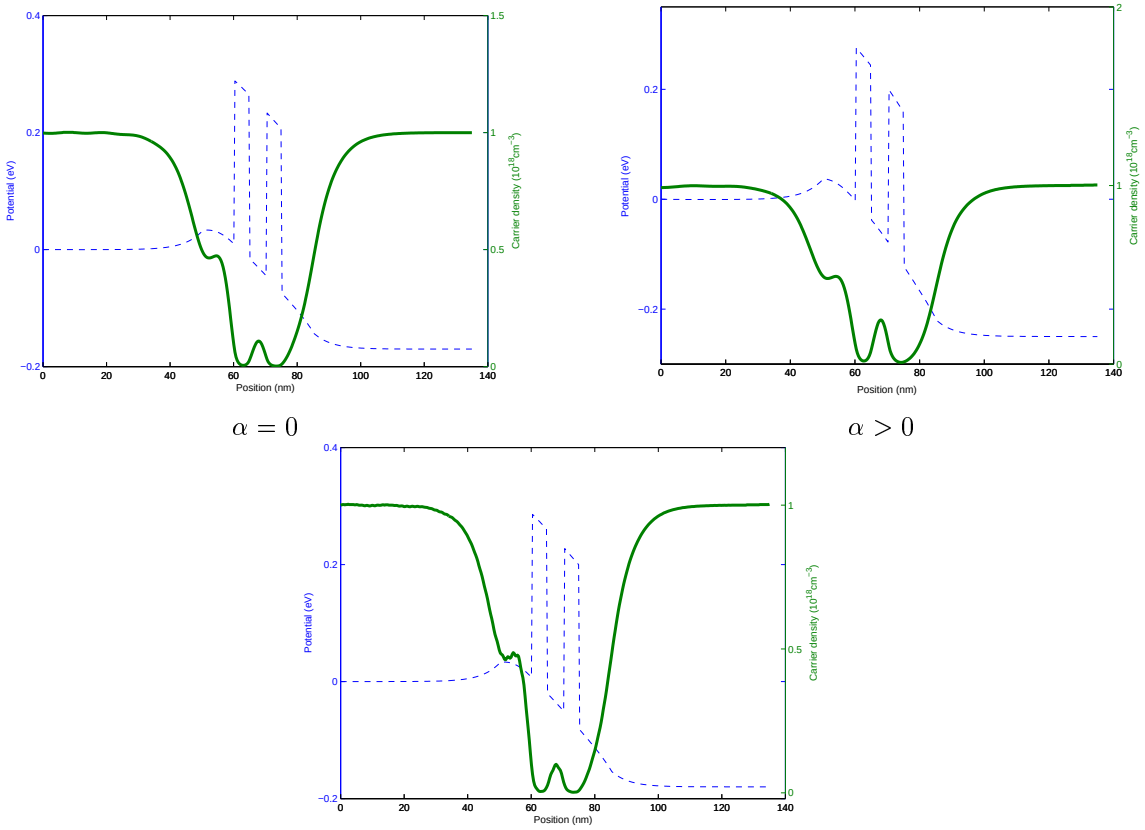

FIG. 3.10: The charge density in $10^{18}cm^{-3}$ and the potential at a bias corresponding to the peak of the I-V curve in fig 3.7 for each parabolic ($\alpha = 0$) and non-parabolic ($\alpha > 0$ and $\alpha < 0$) energies.

8 Appendix A

8.1 The matrix $\mathcal{A}_V$ corresponding to the potential

On $[x_l, x_{l+1}]$, for the potential V we have the following decomposition

$$V(x) = V(x_l)f_l(x) + V^{'}(x_l)g_l(x) + V(x_{l+1})f_{l+1}(x) + V^{'}(x_{l+1})g_{l+1},$$

which can be written as

$$V(x) = V(x_l)\phi_1(x) + V^{'}(x_l)\phi_2(x) + V(x_{l+1})\phi_3(x) + V^{'}(x_{l+1})\phi_4(x).$$

Then, on the elementary element $[-1, 1]$ associated to $[x_l, x_{l+1}]$, we obtain the following symmetric elementary matrix

$$Ve = \begin{pmatrix} V_{11}(x_l, x_{l+1}) & V_{12}(x_l, x_{l+1}) & V_{13}(x_l, x_{l+1}) & V_{14}(x_l, x_{l+1}) \\ & V_{22}(x_l, x_{l+1}) & V_{23}(x_l, x_{l+1}) & V_{24}(x_l, x_{l+1}) \\ & & V_{33}(x_l, x_{l+1}) & V_{34}(x_l, x_{l+1}) \\ & & & V_{44}(x_l, x_{l+1}) \end{pmatrix}$$

with for the first row, we have

$$\begin{aligned}
V_{11}(x_l, x_{l+1}) &= \frac{43}{140}\,h_x\,V(x_l) + \frac{97}{2520}\,h_x^2\,V^{'}(x_l) + \frac{9}{140}\,h_x\,V(x_{l+1}) - \frac{43}{2520}\,h_x^2\,V^{'}(x_{l+1}) \\
V_{12}(x_l, x_{l+1}) &= \frac{97}{2520}\,h_x^2\,V(x_l) + \frac{2}{315}\,h_x^3\,V^{'}(x_l) + \frac{1}{72}\,h_x^2\,V(x_{l+1}) - \frac{1}{280}\,h_x^3\,V^{'}(x_{l+1}) \\
V_{13}(x_l, x_{l+1}) &= \frac{9}{140}\,h_x\,V(x_l) + \frac{1}{72}\,h_x^2\,V^{'}(x_l) + \frac{9}{140}\,h_x\,V(x_{l+1}) - \frac{1}{72}\,h_x^2\,V^{'}(x_{l+1}) \\
V_{14}(x_l, x_{l+1}) &= -\frac{43}{2520}\,h_x^2\,V(x_l) - \frac{1}{280}\,h_x^3\,V^{'}(x_l) - \frac{1}{72}\,h_x^2\,V(x_{l+1}) + \frac{1}{315}\,h_x^3\,V^{'}(x_{l+1}).
\end{aligned}$$

Then, for the second row, we get

$$\begin{aligned}
V_{22}(x_l, x_{l+1}) &= \frac{2}{315}\,h_x^3\,V(x_l) + \frac{1}{840}\,h_x^4\,V^{'}(x_l) + \frac{1}{315}\,h_x^3\,V(x_{l+1}) - \frac{1}{1260}\,h_x^4\,V^{'}(x_{l+1}) \\
V_{23}(x_l, x_{l+1}) &= \frac{1}{72}\,h_x^2\,V(x_l) + \frac{1}{315}\,h_x^3\,V^{'}(x_l) + \frac{43}{2520}\,h_x^2\,V(x_{l+1}) - \frac{1}{280}\,h_x^3\,V^{'}(x_{l+1}) \\
V_{24}(x_l, x_{l+1}) &= -\frac{1}{280}\,h_x^3\,V(x_l) - \frac{1}{1260}\,h_x^4\,V^{'}(x_l) - \frac{1}{280}\,h_x^3\,V(x_{l+1}) + \frac{1}{1260}\,h_x^4\,V^{'}(x_{l+1}).
\end{aligned}$$

In the end, for the third and fourth row, we obtain

$$\begin{aligned}
V_{33}(x_l, x_{l+1}) &= \frac{9}{140}\,h_x\,V(x_l) + \frac{43}{2520}\,h_x^2\,V^{'}(x_l) + \frac{43}{140}\,h_x\,V(x_{l+1}) - \frac{97}{2520}\,h_x^2\,V^{'}(x_{l+1}) \\
V_{34}(x_l, x_{l+1}) &= -\frac{1}{72}\,h_x^2\,V(x_l) - \frac{1}{280}\,h_x^3\,V^{'}(x_l) - \frac{97}{2520}\,h_x^2\,V(x_{l+1}) + \frac{2}{315}\,h_x^3\,V^{'}(x_{l+1}) \\
V_{44}(x_l, x_{l+1}) &= \frac{1}{315}\,h_x^3\,V(x_l) + \frac{1}{1260}\,h_x^4\,V^{'}(x_l) + \frac{2}{315}\,h_x^3\,V(x_{l+1}) - \frac{1}{840}\,h_x^4\,V^{'}(x_{l+1}).
\end{aligned}$$

To determine all the terms of the matrix $\mathcal{A}_V$, it requires a discussion according the even or odd numbered of the rows of the matrix. The first and the last rows are simple to determine. For this, we consider $l = 3, 2N$

First case : if l is even then it can be written as $l = 2p$ with p takes the value from $p = 2$ to N. Thus, we obtain

$$\begin{array}{lcllcl}
(\mathcal{A}_V)_{l,k} & = & 0, \quad \text{for } k < l-3 \text{ and } k > l+2 & & & \\
(\mathcal{A}_V)_{l,l-3} & = & V_{14}(x_{p-2}, x_{p-1}), & (\mathcal{A}_V)_{l,l-2} & = & V_{24}(x_{p-2}, x_{p-1}) \\
(\mathcal{A}_V)_{l,l-1} & = & V_{34}(x_{p-2}, x_{p-1}) + V_{12}(x_{p-1}, x_p), & (\mathcal{A}_V)_{l,l} & = & V_{44}(x_{p-2}, x_{p-1}) + V_{22}(x_{p-1}, x_p) \\
(\mathcal{A}_V)_{l,l+1} & = & V_{32}(x_{p-1}, x_p), & (\mathcal{A}_V)_{l,l+2} & = & V_{42}(x_{p-1}, x_p).
\end{array}$$

Second case : if l is odd then it write $l = 2p+1$ with $p = 1, N-1$. In this case, we have

$$\begin{array}{lcllcl}
(\mathcal{A}_V)_{l,k} & = & 0, \quad \text{for } k < l-2 \text{ and } k > l+3 & & & \\
(\mathcal{A}_V)_{l,l-2} & = & V_{13}(x_{p-1}, x_p), & (\mathcal{A}_V)_{l,l-1} & = & V_{23}(x_{p-1}, x_p) \\
(\mathcal{A}_V)_{l,l} & = & V_{33}(x_{p-1}, x_p) + V_{11}(x_p, x_{p+1}), & (\mathcal{A}_V)_{l,l+1} & = & V_{43}(x_{p-1}, x_p) + V_{21}(x_p, x_{p+1}) \\
(\mathcal{A}_V)_{l,l+2} & = & V_{31}(x_p, x_{p+1}), & (\mathcal{A}_V)_{l,l+3} & = & V_{41}(x_p, x_{p+1}).
\end{array}$$

8.2 The matrix $\mathcal{A}_{TDB_c^{\pm}}$ corresponding to the boundary terms

8.2.1 The matrix $\mathcal{A}_{TDB^+}$

For this matrix, we need also to determine the two first and the two last rows . From C^+ in (5.42), we get

$$\begin{aligned}
(\mathcal{A}_{TDB^+})_{ij} = \frac{\alpha\hbar}{4m^2}\Big[& q_-\left(\hbar^2 F_j^{'}(0)\overline{F_i}^{'}(0) - q^2 F_j(0)\overline{F_i}(0)\right) + p_-\left(\hbar^2 F_j^{'}(1)\overline{F_i}^{'}(1) - p_+^2 F_j(1)\overline{F_i}(1)\right) \\
& -ip_+\left(\hbar F_j^{'}(1) + p_- F_j(1)\right)\left(\hbar\overline{F_i}^{'}(1) + p_-\overline{F_i}(1)\right) \\
& -iq\left(\hbar F_j^{'}(0) - q_- F_j(0)\right)\left(\hbar\overline{F_i}^{'}(0) - q_-\overline{F_i}(0)\right)\Big]. \qquad (8.66)
\end{aligned}$$

For $i = 1$, we have the next coefficients

$$\begin{array}{lcl}
(\mathcal{A}_{TDB^+})_{11} & = & -q_- q(q + iq_-)\dfrac{\alpha\hbar}{4m^2}, \quad (\mathcal{A}_{TDB^+})_{12} = +iqq_-\dfrac{\alpha\hbar^2}{4m^2} \\
(\mathcal{A}_{TDB^+})_{1j} & = & 0, \quad \text{for j=3,2N+2.}
\end{array}$$

For $i = 2$, we find

$$\begin{array}{lcl}
(\mathcal{A}_{TDB^+})_{21} & = & +iqq_-\dfrac{\alpha\hbar^2}{4m^2}, \quad (\mathcal{A}_{TDB^+})_{22} = (q_- - iq)\dfrac{\alpha\hbar^3}{4m^2} \\
(\mathcal{A}_{TDB^+})_{2j} & = & 0, \quad \text{for j=3,2N+2.}
\end{array}$$

For the rows $i = 2N+1$ and $i = 2N+2$, we get

$$\begin{array}{lcl}
(\mathcal{A}_{TDB^+})_{2N+1,j} & = & 0, \quad \text{for j=1,2N} \\
(\mathcal{A}_{TDB^+})_{2N+1,2N+1} & = & -p_- p_+(p_+ + ip_-)\dfrac{\alpha\hbar}{4m^2}, \quad (\mathcal{A}_{TDB^+})_{2N+1,2N+2} = -ip_- p_+\dfrac{\alpha\hbar^2}{4m^2},
\end{array}$$

and

$$
\begin{aligned}
(\mathcal{A}_{TDB^+})_{2N+2,j} &= 0, \quad \text{for j=1,2N} \\
(\mathcal{A}_{TDB^+})_{2N+2,2N+1} &= -ip_+p_-\frac{\alpha\hbar^2}{4m^2}, \quad (\mathcal{A}_{TDB^+})_{2N+2,2N+2} = (p_- - ip_+)\frac{\alpha\hbar^3}{4m^2}.
\end{aligned}
$$

Consequently, the matrix $\mathcal{A}_{TDB^+}$ is the following

$$
\mathcal{A}_{TDB^+} = \frac{\alpha\hbar}{4m}\begin{pmatrix}
-q_-q(q+iq_-) & i\hbar q_-q & 0 & 0 & 0 & 0 & 0 & 0 & 0 & 0 & 0 & 0 & 0 & 0 \\
i\hbar qq_- & \hbar^2(q_- - iq) & 0 & 0 & 0 & 0 & 0 & 0 & 0 & 0 & 0 & 0 & 0 & 0 \\
0 & 0 & 0 & . & . & . & . & . & . & . & . & 0 & 0 & 0 \\
0 & 0 & 0 & . & . & . & . & . & . & . & . & 0 & 0 & 0 \\
0 & 0 & 0 & . & . & . & . & . & . & . & . & 0 & 0 & 0 \\
0 & 0 & 0 & . & . & . & . & . & . & . & . & 0 & 0 & 0 \\
0 & 0 & 0 & . & . & . & . & . & . & . & . & 0 & 0 & 0 \\
0 & 0 & 0 & . & . & . & . & . & . & . & . & 0 & 0 & 0 \\
0 & 0 & 0 & . & . & . & . & . & . & . & . & 0 & 0 & 0 \\
0 & 0 & 0 & . & . & . & . & . & . & . & . & 0 & 0 & 0 \\
0 & 0 & 0 & . & . & . & . & . & . & . & . & 0 & 0 & 0 \\
0 & 0 & 0 & . & . & . & . & . & . & . & . & 0 & 0 & 0 \\
0 & 0 & 0 & 0 & 0 & 0 & 0 & 0 & 0 & 0 & 0 & 0 & -p_-p_+(p_+ + ip_-) & -i\hbar p_+p_- \\
0 & 0 & 0 & 0 & 0 & 0 & 0 & 0 & 0 & 0 & 0 & 0 & -i\hbar p_+p_- & \hbar^2(p_- - ip_+)
\end{pmatrix}.
$$

8.2.2 The matrix $\mathcal{A}_{TDB^-}$

As it was shown in the previous paragraph, to determine the matrix $\mathcal{A}_{TDB^+}$ we need to determine the two first and the two last rows. For this, from C^- in (5.43), we get

$$
\begin{aligned}
(\mathcal{A}_{TDB^-})_{ij} = \frac{\alpha\hbar}{4m^2}\Big[& q_-\left(\hbar^2 F_j^{'}(1)\overline{F_i}^{'}(1) - q^2 F_j(1)\overline{F_i}(1)\right) + p_-^{'}\left(\hbar^2 F_j^{'}(0)\overline{F_i}^{'}(0) - {p_+^{'}}^2 F_j(0)\overline{F_i}(0)\right) \\
& -ip_+^{'}\left(\hbar F_j^{'}(0) + p_-^{'} F_j(0)\right)\left(\hbar\overline{F_i}^{'}(0) + p_-^{'}\overline{F_i}(0)\right) \\
& -iq\left(\hbar F_j^{'}(1) + q_- F_j(1)\right)\left(\hbar\overline{F_i}^{'}(1) + q_-\overline{F_i}(1)\right)\Big]. \qquad (8.67)
\end{aligned}
$$

For $i = 1$ and $i = 2$, we have

$$
\begin{aligned}
(\mathcal{A}_{TDB^-})_{11} &= -p_-^{'}p_+^{'}(p_+^{'} + ip_-^{'})\frac{\alpha\hbar}{4m^2}, \quad (\mathcal{A}_{TDB^-})_{12} = -ip_-^{'}p_+^{'}\frac{\alpha\hbar^2}{4m^2} \\
(\mathcal{A}_{TDB^-})_{22} &= (p_-^{'} - ip_+^{'})\frac{\alpha\hbar^3}{4m^2}
\end{aligned}
$$

and

$$
(\mathcal{A}_{TDB^-})_{1j} = 0, \quad (\mathcal{A}_{TDB^-})_{2j} = 0 \quad \text{for j=3, 2N+2.}
$$

For the rows $i = 2N + 1$ and $i = 2N + 2$, we find

$$
\begin{aligned}
(\mathcal{A}_{TDB^-})_{2N+1,j} &= 0, \quad (\mathcal{A}_{TDB^-})_{2N+2,j} = 0 \quad \text{for j=1, 2N} \\
(\mathcal{A}_{TDB^-})_{2N+1,2N+1} &= -q_-q_+(q_+ + iq_-)\frac{\alpha\hbar}{4m^2}, \quad (\mathcal{A}_{TDB^-})_{2N+1,2N+2} = -iq_-q_+\frac{\alpha\hbar^2}{4m^2},
\end{aligned}
$$

and

$$(\mathcal{A}_{TDB^-})_{2N+2,2N+1} = -iq_+q_-\frac{\alpha\hbar^2}{4m^2}, \quad (\mathcal{A}_{TDB^-})_{2N+2,2N+2} = (q_- - iq_+)\frac{\alpha\hbar^3}{4m^2}.$$

Next, the matrix $\mathcal{A}_{TDB^-}$ is

$$\mathcal{A}_{TDB^-} = \frac{\alpha\hbar}{4m^2}\begin{pmatrix}
-p_-^{'}p_+^{'}(p_+^{'}+ip_-^{'}) & -i\hbar p_-^{'}p_+^{'} & 0 & 0 & 0 & 0 & 0 & 0 & 0 & 0 & 0 & 0 & 0 & 0 \\
-i\hbar p_-^{'}p_+^{'} & \hbar^2(p_-^{'}-ip_+^{'}) & 0 & 0 & 0 & 0 & 0 & 0 & 0 & 0 & 0 & 0 & 0 & 0 \\
0 & 0 & 0 & . & . & . & . & . & . & . & . & 0 & 0 & 0 \\
0 & 0 & 0 & . & . & . & . & . & . & . & . & 0 & 0 & 0 \\
0 & 0 & 0 & . & . & . & . & . & . & . & . & 0 & 0 & 0 \\
0 & 0 & 0 & . & . & . & . & . & . & . & . & 0 & 0 & 0 \\
0 & 0 & 0 & . & . & . & . & . & . & . & . & 0 & 0 & 0 \\
0 & 0 & 0 & . & . & . & . & . & . & . & . & 0 & 0 & 0 \\
0 & 0 & 0 & . & . & . & . & . & . & . & . & 0 & 0 & 0 \\
0 & 0 & 0 & . & . & . & . & . & . & . & . & 0 & 0 & 0 \\
0 & 0 & 0 & . & . & . & . & . & . & . & . & 0 & 0 & 0 \\
0 & 0 & 0 & . & . & . & . & . & . & . & . & 0 & 0 & 0 \\
0 & 0 & 0 & 0 & 0 & 0 & 0 & 0 & 0 & 0 & 0 & 0 & -q_-q_+(q_++iq_-) & -i\hbar q_+q_- \\
0 & 0 & 0 & 0 & 0 & 0 & 0 & 0 & 0 & 0 & 0 & 0 & -i\hbar q_+q_- & \hbar^2(q_--iq_+)
\end{pmatrix}.$$

8.2.3 The matrix $\mathcal{A}_{TDB_c^-}$

From expression C_c^- in (5.44), we have

$$\begin{aligned}
(\mathcal{A}_{TDB_c^-})_{ij} = {} & +\frac{\alpha\hbar}{4m^2}\Big[q_-\left(\hbar^2F_j^{'}(1)\overline{F_j}^{'}(1) - q^2F_j(1)\overline{F_i}(1)\right) \\
& -p_-^{'c}p_+^{'c}\left(\hbar F_j^{'}(0)\overline{F_i}(0) + F_j(0)\hbar\overline{F_i}^{'}(0)\right) - iq\left(\hbar F_j^{'}(1) + q_-F_j(1)\right)\left(\hbar\overline{F_i}^{'}(1) + q_-\overline{F_i}(1)\right) \\
& +i(p_+^{'c} - p_-^{'c})\left(\hbar^2F_j^{'}(0)\overline{F_i}^{'}(0) - p_+^{'c}p_-^{'c}F_j(0)\overline{F_i}(0)\right)\Big].
\end{aligned} \tag{8.68}$$

For $i = 1$ and $i = 2$, we obtain

$$\begin{aligned}
(\mathcal{A}_{TDB_c^-})_{11} &= -ip_+^{'c}p_-^{'c}(p_+^{'c} - p_-^{'c})\frac{\alpha\hbar}{4m^2}, \quad (\mathcal{A}_{TDB_c^-})_{12} = -p_+^{'c}p_-^{'c}\frac{\alpha\hbar^2}{4m^2} \\
(\mathcal{A}_{TDB^+})_{22} &= i(p_+^{'c} - p_-^{'c})\frac{\alpha\hbar^3}{4m^2}
\end{aligned}$$

and

$$(\mathcal{A}_{TDB_c^-})_{1j} = 0, \quad (\mathcal{A}_{TDB^+})_{2j} = 0 \quad \text{for j=3,2N+2.}$$

For the rows $i = 2N+1$ and $i = 2N+2$, we obtain the same coefficients as for the matrix $\mathcal{A}_{TDB_c^-}$.

Deuxième partie

Multiband transport

Chapitre 4

The two-band Schrödinger model

Sommaire

Abstract. A mathematical model for quantum transport in an interband resonant tunneling diode is studied. The wave function of electrons has two components and is a solution of a 2×2 matrix Schrödinger equation derived from $k.P$ theory. The first component representing that part of electrons living in the conduction band while the second part is for the valence band. Transparent boundary conditions are derived and the Schrödinger equation is coupled to the Poisson equation for the electrostatic potential. Using the repulsivity of the electrostatic interaction an a priori estimate is derived and used to construct a solution of the overall problem.

Keywords. Two-band Schrödinger model ; Kane model ; conduction band ; valence band ; gap energy.

1 Introduction

Since the emergence of new devices such that resonant interband tunneling diodes ([84], [104], [110], [119], [76], [121], [75] and [79]), a single band effective mass model becomes insufficient to simulate the quantum transport in such structures. This has prompted a growing effort on the part of theorists to include realistic band structures in the transport models. For this, the multiple band model has been developed to describe such phenomena ([33], [46], [107], [51] and [70]). It has been already proposed by E.O. Kane in [60] and [61], by using the $k.P$ approach (see [77], [86], [7]) and used in electronics simulation (see [8], [117], [57], [112], [70], [63], [115] and [43]). The classical approach is that the excited electron can pass from the valence band to the conduction band letting the place to a quasi-particle which is called the hole in the valence band. Here, another approach consists on considering that electron can be both in the conduction and in the valence band. This implies the coupling between the two-band. Indeed, the aim of this paper is the study of a one dimensional Kane's two-band system for the modeling of an open structure : Boundary conditions and self-consistent effects are particularly considered.

2 The setting of the problem and the main results

We consider a one dimensional resonant tunneling interband device (see fig.4.1). It is based upon a broken band gap material, such that the band-gap of the quantum well does not overlap with the barrier and contact material. This means that electrons will tunnel from the conduction band through the valence band of the quantum well. The source S is placed at $x = 0$. The drain D at $x = 1$. We apply a positive voltage between $S - D$. We shall suppose $V(0) = 0$ and $V(1) = V_1 > 0$ in order to create electron flow from source to drain.

The plotted energy E_0 in fig 4.1 corresponds to a conduction band state at the device edges while it falls into the valence band in the middle of the device.

Denoting by $\mathbf{\Psi}$ the wave function along the growth x direction in the conduction and the valence bands as ψ^1 and ψ^2 respectively. We write

$$\mathbf{\Psi} = \begin{pmatrix} \psi^1 \\ \psi^2 \end{pmatrix}. \tag{2.1}$$

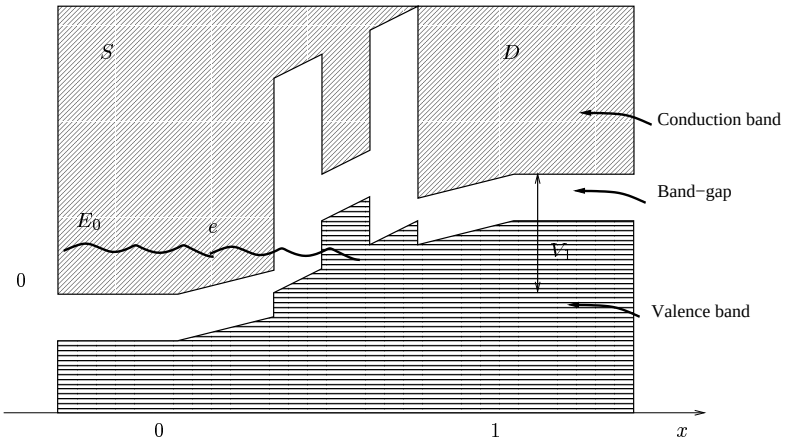

FIG. 4.1: Schematic energy-band diagrams for a one dimension interband tunnel device under a potential V.

It verifies the two-band Schrödinger equation

$$\mathbb{H}\mathbf{\Psi}(x) = E\mathbf{\Psi}(x). \tag{2.2}$$

where E is the conduction energy and

$$\mathbb{H} = \begin{pmatrix} -\dfrac{d^2}{dx^2} + V(x) & iP\dfrac{d}{dx} \\ iP\dfrac{d}{dx} & -\dfrac{d^2}{dx^2} - 2\delta + V(x) \end{pmatrix},$$

with P is the coupling coefficient between the conduction band and the light-hole valence bands and δ is the half of the gap energy. We assume that

$$P^2 > \delta.$$

This is nothing but a condition of a non-parabolicity of the valence band. Then, the corresponding transparent boundary conditions are

$$\frac{d\mathbf{\Psi}}{dx}(0) - i\mathbb{K}_-(E)\mathbf{\Psi}(0) = i(k_c(E)\mathbb{I}_2 - \mathbb{K}_-(E))\mathbf{e}_c^+(E), \tag{2.3}$$

$$\frac{d\mathbf{\Psi}}{dx}(1) - i\mathbb{K}_+(E - V_1)\mathbf{\Psi}(1) = 0. \tag{2.4}$$

The computed self consistently potential V is the solution of the next Poisson problem

$$\frac{d^2V}{dx^2} = n(x), \tag{2.5}$$

$$V(0) = 0, \qquad V(1) = V_1 > 0. \tag{2.6}$$

The macroscopic quantities such that the density charge and the current density are given by

$$n(x) = \int_0^{+\infty} f_0(E)|\mathbf{\Psi}(x)|^2 \frac{dE}{V_c(E)}, \tag{2.7}$$

$$J(x) = \int_0^{+\infty} f_0(E)\left(\Im m(\mathbb{D}\ \mathbf{\Psi} \bullet \mathbf{\Psi})\right)\frac{dE}{V_c(E)}. \tag{2.8}$$

where f_0 is the distribution profile according to which injection occurs, $V_c(E)$ is the group velocity defined in (3.19) (and which will be discussed further) and

$$\mathbb{D} = \begin{pmatrix} \frac{d}{dx} & -iP \\ -iP & \frac{d}{dx} \end{pmatrix}. \tag{2.9}$$

In addition, $''\bullet''$ is the standard Hermitian scalar product on $\mathbb{C}$

$$\mathbf{\Psi}(x) \bullet \mathbf{\Phi}(x) = \psi_1(x)\overline{\varphi_1(x)} + \psi_2(x)\overline{\varphi_2(x)}. \tag{2.10}$$

The first result is concerning the linear model. It is shown in the following Proposition.

Proposition 2.1 *The linear two-band Schrödinger model (2.2)-(2.4) admits a unique solution* $\mathbf{\Psi}$ *in* $H^1(0,1) \times H^1(0,1)$, *for* $E > 0$.

The main result of this paper is

Theorem 2.2 *Let assume that* $f_0(E)$ *is compactly supported function such that* $suppf_0 \subset [0, E_0]$ *with* $E_0 > 0$ *and verify*

$$f_0(E) \geq 0 \text{ and } \int_0^{+\infty} f_0(E)dE < \infty. \tag{2.11}$$

Then, the system (2.2)-(2.6) admits a solution $(\mathbf{\Psi}, V)$ *such that*

$$\mathbf{\Psi} \in H^1(0,1) \times H^1(0,1), \quad V \in W^{2,+\infty}(0,1).$$

The outline of the paper is as follows. In section 2, we set the problem and then in section 3 we justify boundary conditions (2.3)-(2.4). After that, in section 4, we analyze the linear problem. We prove the existence and uniqueness of solution. Finally, in section 5 we give the a priori estimates needed to prove the nonlinear problem and in section 6 we end with some concluding remarks concerning the four band model.

3 The derivation of the boundary conditions

As mentioned above, the device occupies the interval $[0,1]$. The electrostatic potential varies self-consistently. Outside the interval $[0,1]$, the potential is constant equals to the value at $x = 0$ (for $x < 0$) and at $x = 1$ (for $x > 1$). We shall denote by $V_0 = 0$, and $V_1 > 0$ these values.
Like in the single band Schrödinger equation ([48], [11], [12], [15], [16] and [62])), two populations of electrons are to be modeled; those injected at the source $x = 0$ and those injected at the drain $x = 1$. However to simplify the representation we shall only consider electrons injected from the source ($x = 0$).

The derivation of the boundary conditions is based on solving explicitly the Schrödinger equation with $V = 0$. Which leads to the dispersion relation. We define it in the next subsection.

3.1 The dispersion relation

The dispersion relation is obtained by looking for plane wave solutions of (2.2) when $V(x)$ is a constant taken equal to zero for simplicity (otherwise, the energy is to be shifted accordingly). The "Ansatz"

$$\mathbf{\Psi}(x) = e^{ik(E)x}\mathbf{e}$$

is a solution of (2.2) if and only if

$$\mathbb{M}(k)\mathbf{e} = E\mathbf{e}, \quad \mathbb{M}(k) = \begin{pmatrix} k^2 & -Pk \\ -Pk & k^2 - 2\delta \end{pmatrix}.$$

Where $\mathbf{e}$ is a unitary vector. This means that E has to be an eigenvalue of $\mathbb{M}$ and leads to the dispersion relation

$$(k^2 - E)(k^2 - 2\delta - E) - P^2k^2 = 0. \tag{3.12}$$

This equation can be solved by expression E in terms of k. Leading to the solutions

$$E_c(k) = k^2 - \delta + \sqrt{\delta^2 + P^2k^2}, \quad E_v(k) = k^2 - \delta - \sqrt{\delta^2 + P^2k^2}. \tag{3.13}$$

We identify them as energy distributions in the conduction and in the valence bands. The corresponding normalized eigenvectors are

$$\mathbf{e}_c(k) = \sqrt{\frac{(\sqrt{\delta^2 + P^2k^2} + \delta)}{2\sqrt{\delta^2 + P^2k^2}}} \begin{pmatrix} 1 \\ \frac{-Pk}{\delta + \sqrt{\delta^2 + P^2k^2}} \end{pmatrix}, \tag{3.14}$$

$$\mathbf{e}_v(k) = \sqrt{\frac{(\sqrt{\delta^2 + P^2k^2} + \delta)}{2\sqrt{\delta^2 + P^2k^2}}} \begin{pmatrix} \frac{Pk}{\delta + \sqrt{\delta^2 + P^2k^2}} \\ 1 \end{pmatrix}. \tag{3.15}$$

They reduce to $\begin{pmatrix} 1 \\ 0 \end{pmatrix}$ and $\begin{pmatrix} 0 \\ 1 \end{pmatrix}$ respectively when the wave vector k is equal to zero. In the sequel, we also note by

$$\mathbf{e}_c^{\pm}(E) = \mathbf{e}_c(\pm k_c(E)), \quad \mathbf{e}_v^{\pm}(E) = \mathbf{e}_v(\pm k_v(E)). \tag{3.16}$$

Another way to invert the dispersion relation (3.12) is to express k in terms of E which gives,

$$k_c(E) = \sqrt[+]{(\delta + E + \frac{P^2}{2}) - \sqrt{(\delta + \frac{P^2}{2})^2 + EP^2}}, \tag{3.17}$$

$$k_v(E) = \sqrt[+]{(\delta + E + \frac{P^2}{2}) + \sqrt{(\delta + \frac{P^2}{2})^2 + EP^2}}. \tag{3.18}$$

k_c and k_v are the wave vectors of respectively the conduction band and valence band waves, with energy E. In addition, $\sqrt[+]{a}(a \in \mathbb{R})$ is the complex square root with non-negative real and imaginary parts. In particular, we have

$$\begin{aligned} \forall k \in \mathbb{C}, \qquad & k_c(E_c(k)) = k, \quad k_v(E_v(k)) = k, \\ & E_c(k_c(E)) = E, \quad E_v(k_v(E)) = E. \end{aligned}$$

The group velocities are then given by the usual formulae

$$V_c(E) = \mathcal{V}_c(k_c(E)) = \frac{dE_c(k)}{dk}_{|k=k_c(E)} = k_c(E)(2 + \frac{P^2}{\sqrt{\delta^2 + k_c(E)^2 P^2}}), \quad (3.19)$$

$$V_v(E) = \mathcal{V}_v(k_v(E)) = \frac{dE_v(k)}{dk}_{|k=k_v(E)} = k_v(E)(2 - \frac{P^2}{\sqrt{\delta^2 + k_v(E)^2 P^2}}). \quad (3.20)$$

We notice that the group velocity in the valence band is not monotonous (see fig.4.2). In particular, it has the unlike sign of the wave vector k (which has the like sign as the phase velocity) for k^2 less than $\frac{P^2}{4} - \frac{\delta^2}{P^2}$.

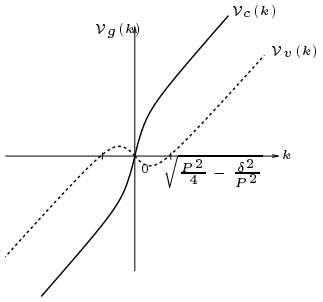

FIG. 4.2: Group velocity

Let us remark that for k small, $E_c(k)$ in (3.13) can be written in the following way

$$E_c(k) = (1 + \frac{P^2}{2\delta})k^2 + O(k^4).$$

In physical variables, from the non-scaled Hamiltonian

$$\mathbb{H} = \begin{pmatrix} -\frac{\hbar^2}{2m}\frac{d^2}{dx^2} + V(x) & i\hbar P\frac{d}{dx} \\ i\hbar P\frac{d}{dx} & -\frac{\hbar^2}{2m}\frac{d^2}{dx^2} - \mathcal{E}_g + V(x) \end{pmatrix}, \quad (3.21)$$

we have the conduction energy equals to

$$E_c(k) = \frac{\hbar^2 k^2}{2m^*}$$

with m^* the effective mass in the conduction band. It is given by

$$m^* = \frac{m}{1 + \frac{2P^2 m}{\mathcal{E}_g}},$$

where $\mathcal{E}_g$ is the x-dependent gap energy ([24]). We assume that

$$mP^2 \geq \mathcal{E}_g,$$

and which is valid in usual semiconductor crystals (N. V. : $mP^2 \equiv 20eV$)

3.2 The different modes and boundary conditions

Equation (2.2) can be solved explicitly in the source region $x < 0$ and we have

$$\mathbf{\Psi}(x) = a_0 e^{ik_c(E)x}\mathbf{e}_c^+(E) + b_0 e^{-ik_c(E)x}\mathbf{e}_c^-(E) + c_0 e^{ik_v(E)x}\mathbf{e}_v^+(E) + d_0 e^{-ik_v(E)x}\mathbf{e}_v^-(E) \quad (3.22)$$

where k_c and k_v are given respectively by (3.17) and (3.18).
The first term (resp. second) corresponds to the wave of the conduction band traveling to the right (resp. to the left), while the third and the fourth term stand for the wave of the valence band.

Remark 3.1 *We notice that for $E \geq 0$, $k_c(E)$ and $k_v(E)$ have respectively the same sign as the group velocity $\mathcal{V}_c(k_c(E))$ in the conduction band and $\mathcal{V}_v(k_v(E))$ in the valence band. This is called a direct mode.*

We shall suppose that electrons are injected on the conduction band modes only with amplitude 1. Therefore $a_0 = 1$, $c_0 = 0$ while b_0 and d_0 are the left reflection coefficients that we shall denote from now by r_c and r_v respectively. Then, we read

$$\mathbf{\Psi}(x) \quad = \quad e^{ik_c(E)x}\mathbf{e}_c^+(E) + r_c e^{-ik_c(E)x}\mathbf{e}_c^-(E) + r_v e^{-ik_v(E)x}\mathbf{e}_v^-(E).$$

In the drain region $x > 1$, we have

$$\begin{aligned}\mathbf{\Psi}(x) \quad = \quad & a_1 e^{ik_c(E-V_1)(x-1)}\mathbf{e}_c^+(E-V_1) + b_1 e^{-ik_c(E-V_1)(x-1)}\mathbf{e}_c^-(E-V_1) \\ & + c_1 e^{ik_v(E-V_1)(x-1)}\mathbf{e}_v^+(E-V_1) + d_1 e^{-ik_v(E-V_1)(x-1)}\mathbf{e}_v^-(E-V_1). \quad (3.23)\end{aligned}$$

But according to the sign of $E - V_1$ four cases have to be distinguished according to the four regions (see figure 4.3)

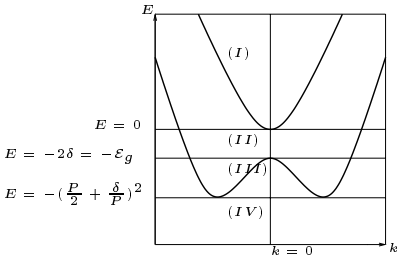

FIG. 4.3: Energy Bands

The upper curve is the conduction energy band while the lower one is the valence energy band.

Formula (3.23) contains the contribution of four waves. Two of them are outgoing (or vanishing) and the two other are in-going (or exponentially increasing). The assumption we make is that the last have zero amplitude. Now, the outgoing waves correspond to a positive group velocity when we are in regions I, II and IV (see figure 4.3). In this case, we are in a direct mode. At variance, when $E - V_1$ is in region III the outgoing wave of the valence band corresponds to a negative group velocity. This is well shown in figure 4.2 and 4.3. This is a reverse mode. As a consequence, the outgoing wave for $x > 1$ is

$$\mathbf{\Psi}(x) \quad = \quad t_c e^{\pm ik_c(E-V_1)(x-1)}\mathbf{e}_c^+(E-V_1) + t_v e^{ik_v(E-V_1)(x-1)}\mathbf{e}_v^+(E-V_1),$$

where t_c and t_v are the transmission coefficients.
The boundary condition on $\mathbf{\Psi}$ is obtained like in the single band model by eliminating the coefficients r_c,r_v, t_c and t_v. Indeed, this can be done through an algebraic manipulation which gives

$$\frac{d\mathbf{\Psi}}{dx}(0) - i\mathbb{K}_-(E)\mathbf{\Psi}(0) = i(k_c(E)\mathbb{I}_2 - \mathbb{K}_-(E))\mathbf{e}_c^+(E),$$
$$\frac{d\mathbf{\Psi}}{dx}(1) - i\mathbb{K}_+(E - V_1)\mathbf{\Psi}(1) = 0,$$

with $\mathbb{I}_2$ is the 2×2 identity matrix and $\mathbb{K}_\mp(.)$ represent also a 2×2 matrix wave with $''-''$ for waves at $x<0$ and $''+''$ for waves at $x>1$. It is defined by the following expression

$$\mathbb{K}_\mp(E) \quad = \quad \mathbb{B}_\mp(E)\mathbb{D}_\mp(E)\mathbb{B}_\mp^{-1}(E), \tag{3.24}$$

where $\mathbb{B}_\mp(E)$ is the 2×2 matrix transforming the canonical basis on to the basis vectors $(\mathbf{e}_c^\mp(E), \mathbf{e}_v^\mp(E))$ and $\mathbb{B}_\mp^{-1}(E)$ its inverse matrix. Indeed, $\mathbb{D}_\mp(E)$ is a diagonal matrix. It is equal to

$$\mathbb{D}_\mp(E) = \begin{pmatrix} \mp k_c(E) & 0 \\ 0 & \mp k_v(E) \end{pmatrix}. \tag{3.25}$$

Then, the first question we answer is whether the above problem with the following boundary conditions has a solution for a fixed V and a fixed value of E. This will be proved in the following section.

4 The linear problem

Before we prove Proposition 2.1, we recall that we work in the space $L^2(0,1)\times L^2(0,1)$. Then, we will use the scalar product

$$(\mathbf{\Psi},\mathbf{\Phi}) = \int_0^1 \mathbf{\Psi}(x)\bullet\mathbf{\Phi}(x)dx; \quad \mathbf{\Psi},\mathbf{\Phi}\in L^2(0,1)\times L^2(0,1).$$

with $''\bullet''$ is defined in (2.10). The induced norm is

$$\|\mathbf{\Psi}(x)\|_{L^2(0,1)\times L^2(0,1)} = \sqrt{(\mathbf{\Psi},\mathbf{\Psi})}.$$

4.1 The proof of Proposition 2.1

Let us first take the weak formulation of the problem (2.2)-(2.4) which is obtained by multiplying (2.2) with an arbitrary test function $\mathbf{\Phi} = \begin{pmatrix} \varphi^1 \\ \varphi^2 \end{pmatrix} \in H^1(0,1)\times H^1(0,1)$ and integrating by parts :

$$\mathcal{Q}(\mathbf{\Psi},\mathbf{\Phi}) + \mathcal{C}(\mathbf{\Psi},\mathbf{\Phi}) = \mathcal{L}(\mathbf{\Phi}). \tag{4.26}$$

Here, $\mathcal{Q}(.,.)$ denotes the coercive, bounded and sesquilinear form on $(H^1(0,1)\times H^1(0,1))^2$:

$$\mathcal{Q}(\mathbf{\Psi},\mathbf{\Phi}) = \int_0^1 \frac{d\mathbf{\Psi}}{dx}(x)\bullet\frac{d\mathbf{\Phi}}{dx}(x)dx + \int_0^1 \mathbf{\Psi}(x)\bullet\mathbf{\Phi}(x)dx.$$

$\mathcal{C}(.,.)$ denotes the bounded and sesquilinear form on $(H^1(0,1)\times H^1(0,1))^2$:

$$\begin{aligned}\mathcal{C}(\mathbf{\Psi},\mathbf{\Phi}) &= \int_0^1 (V(x)-E_c-1)\mathbf{\Psi}(x)\bullet\mathbf{\Phi}(x)dx - \int_0^1 \mathcal{E}_g\psi^2(x)\overline{\varphi^2}(x)dx\\ &\quad -i[\mathbb{K}_+(E-V_1)\mathbf{\Psi}(1)\bullet\mathbf{\Phi}(1)-\mathbb{K}_-(E)\mathbf{\Psi}(0)\bullet\mathbf{\Phi}(0)]\\ &\quad +iP(\int_0^1\left(\frac{d\psi^2}{dx}(x)\overline{\varphi^1}(x)-\psi^1(x)\frac{d\overline{\varphi^2}}{dx}(x)\right)dx+[\psi^1(1)\overline{\varphi^2}(1)-\psi^1(0)\overline{\varphi^2}(0)])\end{aligned}$$

and $\mathcal{L}(.)$ denotes the anti-linear form on $H^1(0,1)\times H^1(0,1)$:

$$\mathcal{L}(\mathbf{\Phi}) = -i((k_c(E)\mathbb{I}_2-\mathbb{K}_-(E))\mathbf{e}_c^+(E))\bullet\mathbf{\Phi}(0).$$

According to the Riesz representation Theorem ([27]), there exist $A_Q\mathbf{\Psi}$, $A_C\mathbf{\Psi}$ and f_L in $H^1(0,1)\times H^1(0,1)$ such that

$$\begin{aligned}\mathcal{Q}(\mathbf{\Psi},\Phi) &= <A_Q\mathbf{\Psi},\Phi>_{H^1(0,1)\times H^1(0,1)},\ \mathcal{C}(\mathbf{\Psi},\Phi)=<A_C\mathbf{\Psi},\Phi>_{H^1(0,1)\times H^1(0,1)},\\ \mathcal{L}(\Phi) &= <f_L,\Phi>_{H^1(0,1)\times H^1(0,1)}.\end{aligned}$$

The weak formulation (4.26) reads

$$(A_Q+A_C)\mathbf{\Psi} = f_L.$$

We notice that $A_Q = Id$ whereas A_C satisfies

$$||A_C\mathbf{\Psi}||_{H^1(0,1)\times H^1(0,1)} \le C||\mathbf{\Psi}||_{H^1(0,1)\times H^1(0,1)},$$

and is a compact operator from $H^1(0,1)\times H^1(0,1)$ into $H^1(0,1)\times H^1(0,1)$. Therefore, the Fredholm alternative ([27]) insures that the weak formulation (4.26) is uniquely solvable if A_Q+A_C is injective. But this is equivalent to prove that the weak formulation (4.26) with vanishing right hand side has no solution but the identically vanishing one. Let now $\mathbf{\Psi}$ be a solution of the weak formulation (4.26) where $L\equiv 0$. Choosing $\mathbf{\Psi}$ as a test function $\mathbf{\Psi}=\mathbf{\Phi}$, we first notice that

$$iP(\int_0^1\left(\frac{d\psi^2}{dx}(x)\overline{\psi}^1(x)-\psi^1(x)\frac{d\overline{\psi}^2}{dx}(x)\right)dx = -2P\int_0^1 \Im m(\frac{d\psi^2}{dx}(x)\overline{\psi}^1(x))dx.$$

Then, taking the imaginary part of (4.26), we obtain

$$-\Re e\left((\mathbb{K}_+(E-V_1)\mathbf{\Psi}(1))\bullet\mathbf{\Psi}(1)+(\mathbb{K}_-(E)\mathbf{\Psi}(0))\bullet\mathbf{\Psi}(0)\right)+P\Re e([\psi^1(x)\overline{\psi}^2(x)]_0^1)=0. \quad (4.27)$$

Replacing $\mathbb{K}_\pm$ by its expression (3.24) and making algebraic manipulation, (4.27) becomes

$$\begin{aligned}\Re e\,\big[\big(\mathbb{T}_+(E-V_1)\,\mathbb{B}_+^{-1}(E-V_1)\,\mathbf{\Psi}(1)\,\big)\bullet\mathbb{B}_+^{-1}(E-V_1)\,\mathbf{\Psi}(1)\\ -\big(\,\mathbb{T}_-(E)\,\mathbb{B}_-^{-1}(E)\,\mathbf{\Psi}(0)\,\big)\,\bullet\mathbb{B}_-^{-1}(E)\,\mathbf{\Psi}(0)\,\big]=0,\end{aligned} \quad (4.28)$$

where

$$\mathbb{T}_\mp(E) = (\mathbb{B}_\mp)^T(E)\mathbb{B}_\mp(E)\mathbb{D}_\mp(E) - P(\mathbb{B}_\mp)^T(E)\mathbb{A}\mathbb{B}_\mp(E) \quad (4.29)$$

and $(\mathbb{B}_{\mp})^T$ is the transpose matrix of $(\mathbb{B}_{\mp})$ and the matrix

$$\mathbb{A} = \begin{pmatrix} 0 & 0 \\ 1 & 0 \end{pmatrix}. \tag{4.30}$$

After some computations, we prove in Appendix A that equation (4.28) can be written as

$$\begin{aligned} \big(\mathbb{S}_+(E-V_1)\, \mathbb{B}_+^{-1}(E-V_1) \quad \mathbf{\Psi}(1) \big) \bullet \mathbb{B}_+^{-1}(E-V_1)\, \mathbf{\Psi}(1) \\ - \big(\mathbb{S}_-(E)\, \mathbb{B}_-^{-1}(E)\, \mathbf{\Psi}(0) \big) \bullet \mathbb{B}_-^{-1}(E)\, \mathbf{\Psi}(0) \ = 0, \end{aligned} \tag{4.31}$$

where $\mathbb{S}_{\pm}$ is given by (7.64),

$$\mathbb{B}_+^{-1}(E-V_1)\mathbf{\Psi}(1) = \begin{pmatrix} t_c \\ t_v \end{pmatrix} \quad \text{and} \quad \mathbb{B}_-^{-1}(E)\mathbf{\Psi}(0) = \begin{pmatrix} r_c \\ r_v \end{pmatrix}. \tag{4.32}$$

Due to the fact that $\mathbb{S}_{\pm}$ is positive definite then solving equation (4.31) implies that

$$\mathbb{B}_-^{-1}\mathbf{\Psi}(0) = 0.$$

As a consequence $\mathbf{\Psi}(0) = 0$. Using the homogeneous boundary conditions

$$\begin{aligned} &\frac{d\mathbf{\Psi}}{dx}(0) - i\mathbb{K}_-(E)\mathbf{\Psi}(0) = 0, \\ &\frac{d\mathbf{\Psi}}{dx}(1) - i\mathbb{K}_+(E-V_1)\mathbf{\Psi}(1) = 0, \end{aligned}$$

we deduce that the derivative function $\frac{d\mathbf{\Psi}}{dx}(0) = 0$. The Cauchy Lipschitz Theorem ([27]) implies that $\mathbf{\Psi}$ vanishes every where and then uniqueness is proved.

4.2 The macroscopic quantities

The probability density is given by

$$\rho = \mathbf{\Psi}\overline{\mathbf{\Psi}} = |\mathbf{\Psi}|^2 = |\psi^1|^2 + |\psi^2|^2,$$

and the particle probability current along the x direction is

$$J = \Im m(\mathbb{D}\mathbf{\Psi} \bullet \mathbf{\Psi}),$$

with $\mathbb{D}$ given in (2.9).

Coming back to our problem, we set by $f_0(E)$ be the statistics of injected particles at $x = 0$ with energy $E = E_c(k) > 0$. Then, the charge and the current density associated to electrons injected at the source is obtained by energy average

$$n(x) = \int_0^{+\infty} f_0(E)|\mathbf{\Psi}(x)|^2 \frac{dE}{V_c(E)}, \tag{4.33}$$

$$J(x) = \int_0^{+\infty} f_0(E)\, (\Im m(\mathbb{D}\ \mathbf{\Psi} \bullet \mathbf{\Psi}))\, \frac{dE}{V_c(E)}. \tag{4.34}$$

Remark 4.1 *The density n can be written as the sum of both density n_1 and n_2 corresponding to the two compounds of $\mathbf{\Psi}$ given in (2.1). We write*

$$n_{1,2}(x) = \int_0^{+\infty} f_0(E)|\psi^{1,2}(x)|^2 \frac{dE}{V_c(E)}. \tag{4.35}$$

The previous notation of the charge density and the current density are expressed in terms of E. When, we use the expression of the group velocity given by (3.19) and set

$$\mathbf{\Phi}_k = \mathbf{\Psi} \text{ and } g_0(k) = f_0(E(k)) \text{ for } k > 0.$$

The charge density and the current density are given by

$$n(x) = \int_0^{+\infty} g_0(k)|\mathbf{\Phi}_k(x)|^2 dk, \tag{4.36}$$

$$J(x) = \int_0^{+\infty} g_0(k)\,(\Im m(\mathbb{D}\ \mathbf{\Phi}_k(x) \bullet \mathbf{\Phi}_k(x))\,dk. \tag{4.37}$$

5 The coupling with the Poisson equation

In this section, we study the two-band Schrödinger problem coupled with the Poisson problem given by (2.2)-(2.6). The proof of the existence of solution of Theorem 2.2 is based on decoupling the two-band Schrödinger problem and the Poisson problem. We use a fixed point argument (The Leray Schauder's Theorem [54]) thereafter.
The fixed point operator is constructed as follows, for given $V \in L^\infty(0,1)$, we solve the two-band Schrödinger problem, we obtain a solution $\mathbf{\Psi}(V)$. Then, we define the charge density $n(V)$ associated to $\mathbf{\Psi}(V)$ to which we will calculate a new potential V^* solution of the Poisson problem. For this, we define the map T by

$$\begin{array}{ccc} T : L^\infty(0,1) & \longrightarrow & L^\infty(0,1) \\ V & \longmapsto & V^*. \end{array} \tag{5.38}$$

At first, we have shown in section 4 that the problem (2.2)-(2.4) is uniquely soluble for a appropriately given V. Then, in the below section we shall give some a priori estimates

5.1 A priori estimates

First, let us give some bounds on $\mathbf{\Psi}$. For this, choosing $\mathbf{\Psi}$ as a test function in formulation of problem (2.2)-(2.4). Then, taking the real part, this yields to

$$\begin{aligned} &\|\frac{d\mathbf{\Psi}}{dx}(x)\|^2_{L^2(0,1)\times L^2(0,1)} + \int_0^1 (V(x)-E)|\mathbf{\Psi}(x)|^2 dx - \int_0^1 \mathcal{E}_g|\psi^2(x)|^2 dx \\ &-2P\int_0^1 \Im m\left(\frac{d\psi^2}{dx}(x)\overline{\psi^1}(x)\right) dx = \Im m\left(((k_c(E)\mathbb{I}_2 - \mathbb{K}_-(E))\mathbf{e}_c^+(E)) \bullet \mathbf{\Psi}(0)\right), \end{aligned} \tag{5.39}$$

whereas the imaginary part is the following identity

$$\begin{aligned} &\left(\mathbb{S}_+(E-V_1)\mathbb{B}_+^{-1}(E-V_1)\mathbf{\Psi}(1)\right) \bullet \mathbb{B}_+^{-1}(E-V_1)\mathbf{\Psi}(1) - \left(\mathbb{S}_-(E)\mathbb{B}_-^{-1}(E)\mathbf{\Psi}(0)\right) \bullet \mathbb{B}_-^{-1}(E)\mathbf{\Psi}(0) \\ &= \Re e\left(((k_c(E)\mathbb{I}_2 - \mathbb{K}_-(E))\mathbf{e}_c^+(E)) \bullet \mathbf{\Psi}(0)\right). \end{aligned} \tag{5.40}$$

Using the expression of $\mathbb{S}_{\mp}$ in (7.64) (see Appendix A) and that

$$\begin{pmatrix} t_c \\ t_v \end{pmatrix} = \mathbb{B}_{+}^{-1}(E - V_1)\mathbf{\Psi}(1) \quad \text{and} \quad \begin{pmatrix} r_c \\ r_v \end{pmatrix} = \mathbb{B}_{-}^{-1}(E)\left(\mathbf{\Psi}(0) - \mathbf{e}_c^{+}(E)\right), \tag{5.41}$$

the imaginary part (5.40) (see details in Appendix A) becomes

$$\mathcal{R} + \mathcal{T} = 1. \tag{5.42}$$

This ensures the particle conservation in the two-band picture and where

$$\mathcal{R} = \mathcal{R}_c + \mathcal{R}_v, \quad \mathcal{T} = \mathcal{T}_c + \mathcal{T}_v,$$

with

$$\mathcal{R}_c = |r_c|^2, \quad \mathcal{R}_v = \frac{\mathcal{V}_v(k_v(E))}{\mathcal{V}_c(k_c(E))}|r_v|^2,$$

and

$$\mathcal{T}_v = \frac{\Re e(k_v(E - V_1))}{k_v(E - V_1)} \frac{\mathcal{V}_v(k_v(E - V_1))}{\mathcal{V}_c(k_c(E))}|t_v|^2.$$

For the conduction transmission $\mathcal{T}_c$, it depends on $E - V_1$ (see figure 4.1). Indeed, we have for $E - V_1 \geq -2\delta$ and $E - V_1 \leq -(\frac{P}{2} - \frac{\delta}{P})^2$ which correspond to regions I, II and IV (see figure 4.3)

$$\mathcal{T}_c = \frac{\Re e(k_c(E - V_1))}{k_c(E - V_1)} \frac{\mathcal{V}_c(k_c(E - V_1))}{\mathcal{V}_c(k_c(E))}|t_c|^2.$$

Then, when $-(\frac{P}{2} - \frac{\delta}{P})^2 \leq E - V_1 \leq -2\delta$, we are in region III and we have

$$\mathcal{T}_c = -\frac{\Re e(k_c(E - V_1))}{k_c(E - V_1)} \mathcal{V}_v(k_c(E - V_1))|t_c|^2.$$

As a consequence, after some algebraic manipulations we obtain from (5.41) and (5.42) that

$$|\mathbf{\Psi}(0)| \leq 2. \tag{5.43}$$

Using the boundary conditions (2.3)-(2.4), this implies that there exists a constant C depending on E, such that

$$|\mathbf{\Psi}'(0)| \leq C. \tag{5.44}$$

Now, let us give the bound of $\mathbf{\Psi}$ in $L^\infty(0,1) \times L^\infty(0,1)$.

Lemma 5.1 *Let $V \in L^\infty(0,1)$, $\mathbf{\Psi}$ solution of ((2.2)-(2.4)) and let $E_0 > 0$ be given. Then, there exists $C > 0$ dependent on E_0 such that $\forall E \in [0, E_0]$, that*

$$||\mathbf{\Psi}||_{L^\infty(0,1)\times L^\infty(0,1)} \leq Ce^{C\sqrt{(1+||V||_{L^\infty(0,1)})}}. \tag{5.45}$$

For the proof we need the subsequent Lemma.

Lemma 5.2 *Let f be a function satisfying*

$$|f^{''}| \leq a|f| + b|f^{'}| \tag{5.46}$$

on the interval $[0,1]$, where a and b are constants. Then f satisfies the following bound

$$|f(t)| \leq C(|f(0)| + \frac{|f^{'}(0)|}{\sqrt{a+\frac{b^2}{2}}})e^{C\sqrt{a}t}.$$

Proof Lemma 5.2 . Let set by

$$X(t) = |f(0)| + |f^{'}(0)|t + \int_0^t \int_0^s |f^{''}(u)|duds.$$

It satisfies

$$|f(t)| \leq X(t), \quad |f^{'}(t)| \leq X^{'}(t). \tag{5.47}$$

Moreover, using inequality (5.46), $X(t)$ verifies

$$\begin{aligned} X^{''}(t) &\leq aX(t) + bX^{'}(t) \\ X(0) &= |f(0)| \\ X^{'}(0) &= |f^{'}(0)|. \end{aligned}$$

If we make a variable change such that

$$Y(t) = X(t)e^{-\frac{b}{2}t} \tag{5.48}$$

then, Y satisfies

$$\begin{aligned} Y^{''}(t) &\leq (a + \frac{b^2}{2})Y(t) \\ Y(0) &= |f(0)| \\ Y^{'}(0) &= |f^{'}(0)| - \frac{b}{2}|f(0)| \leq |f^{'}(0)|. \end{aligned}$$

Solving this system, we obtain a solution such that

$$Y(t) \leq |f(0)|ch(\sqrt{a+\frac{b^2}{2}}t) + \frac{|f^{'}(0)|}{\sqrt{a+\frac{b^2}{2}}}sh(\sqrt{a+\frac{b^2}{2}}t).$$

This leads to

$$Y(t) \leq (|f(0)| + \frac{|f^{'}(0)|}{\sqrt{a+\frac{b^2}{2}}})e^{\sqrt{a+\frac{b^2}{4}}t} \Rightarrow X(t) \leq Ce^{C^{'}\sqrt{a}t}.$$

Then, from (5.47) and (5.48), we have

$$f(t) \leq C(|f(0)| + \frac{|f^{'}(0)|}{\sqrt{a+\frac{b^2}{2}}})e^{C\sqrt{a}t}.$$

Consequently, this ends the proof.

Proof Lemma 5.1. Using estimates (5.43)-(5.44) and making some algebraic manipulation to equation (2.2), we obtain the following inequality

$$|\frac{d^2\mathbf{\Psi}}{dx^2}| \leq C(1+||V||_{L^\infty})|\mathbf{\Psi}| + C|\frac{d\mathbf{\Psi}}{dx}|. \tag{5.49}$$

Applying Lemma 5.2 to equation (5.49) and using estimates (5.43)-(5.44) leads to the bound

$$||\mathbf{\Psi}||_{L^\infty(0,1)\times L^\infty(0,1)} \leq Ce^{C\sqrt{(1+||V||_{L^\infty})}}$$

where C is a constant which depends on E. Given that, there exists E_0, such that $\forall E \in [0, E_0]$, we find a constant $C > 0$ independent of E, such that

$$||\mathbf{\Psi}||_{L^\infty(0,1)\times L^\infty(0,1)} \leq Ce^{C\sqrt{(1+||V||_{L^\infty})}}.$$

In order to apply the Leray-Schauder fixed point Theorem (see ref.[54]), we need to prove that T, defined by (5.38), is compact, continuous and to have a uniform bound on fixed points of σT for $\sigma \in [0,1]$. Let us begin by the last step.

As a consequence of the previous Lemma 5.1, we obtain the following bound on V.

Lemma 5.3 *For all $\sigma \in [0,1]$ and for all $V \in L^\infty(0,1)$ such that $V = \sigma TV$, we have V is bounded in $W^{2,\infty}(0,1)$ independently of σ.*

Proof. Let's again take the real part of the formulation (4.26) given by (5.39). Then, using estimate (5.43), this yields to

$$\begin{aligned}&\|\frac{d\mathbf{\Psi}}{dx}(x)\|^2_{L^2(0,1)\times L^2(0,1)} + \int_0^1 (V(x)-E)|\mathbf{\Psi}(x)|^2dx - \int_0^1 \mathcal{E}_g|\psi^2(x)|^2dx \\ &-2P\int_0^1 Im\left(\frac{d\psi^2}{dx}(x)\overline{\psi^1}(x)\right)dx \leq C.\end{aligned}$$

First of all, we multiply this inequality by $f_0(E)$ and we integrate with respect to E. After some algebraic manipulations, the assumption that $f_0(E)$ is a compactly supported function and the Hölder's inequality ([27]) imply

$$\begin{aligned}&\int_0^{+\infty} f_0(E)\|\frac{d\psi^1}{dx}(x)\|^2_{L^2(0,1)}\frac{dE}{V_c(E)} + (1-2P)\int_0^{+\infty} f_0(E)\|\frac{d\psi^2}{dx}(x)\|^2_{L^2(0,1)}\frac{dE}{V_c(E)} \\ &+\int_0^1 V(x).n(x)dx \leq C_1 + C_2\int_0^1 n(x)dx + \mathcal{E}_g\int_0^1 n_2(x)dx + 2P\int_0^1 n_1(x)dx \quad (5.50)\end{aligned}$$

where $n(x)$, $n_1(x)$ and $n_2(x)$ are given by (4.33) and (4.35) and $C_1 = C\int_0^{+\infty} f_0(E)dE$.

In order to simplify expression of inequality (5.50), we set by

$$K(x) = \int_0^{+\infty} f_0(E)|\frac{d\psi^1}{dx}(x)|^2\frac{dE}{V_c(E)} + (1-2P)\int_0^{+\infty} f_0(E)|\frac{d\psi^2}{dx}(x)|^2\frac{dE}{V_c(E)}.$$

Then, we write

$$\int_0^1 K(x)dx + \int_0^1 V(x).n(x)dx \leq C_1 + C_2 \int_0^1 n(x)dx + \mathcal{E}_g \int_0^1 n_2(x)dx + 2P \int_0^1 n_1(x)dx. \quad (5.51)$$

Using the identities

$$\frac{d^2V_\sigma}{dx^2} = \sigma n(x), \quad V_\sigma(0) = 0, \quad V_\sigma(1) = \sigma V_1, \quad (5.52)$$

and integrating by parts the expression (5.51), we obtain

$$\int_0^1 K(x)dx - \int_0^1 \frac{1}{\sigma}|V_\sigma^{'}|^2 dx \leq C_1 + \frac{C_2}{\sigma}|V_\sigma^{'}(1) - V_\sigma^{'}(0)| \leq C_1 + \frac{2C_2}{\sigma}||V_\sigma^{'}||_{L^\infty(0,1)}. \quad (5.53)$$

Using the relation between ψ and $\dfrac{d\psi}{dx}$

$$\psi^2(x) = \psi^2(0) + 2\int_0^x \frac{d\psi}{dt}(t)\psi(t)dt,$$

we deduce the following estimate

$$||\frac{d\psi}{dx}(x)||^2_{L^2(0,1)} \geq C_3||\psi||^2_{L^\infty(0,1)} - C_4.$$

As a consequence, taking into account the compactness of the support of $f_0(k)$, we get

$$\begin{aligned}
\int_0^1 K(x)dx &\geq C_3\Big(\int_0^{+\infty} f_0(E)\|\psi^1(x)\|^2_{L^\infty(0,1)}\frac{dE}{V_c(E)} + (1-2P)\int_0^{+\infty} f_0(E)\|\psi^2(x)\|^2_{L^\infty(0,1)}\frac{dE}{V_c(E)}\Big) - 2C_4, \\
&\geq Inf(C_3, (1-2P)C_3)\int_0^{+\infty} f_0(E)(\|\psi^1(x)\|^2_{L^\infty(0,1)} + \|\psi^2(x)\|^2_{L^\infty(0,1)})\frac{dE}{V_c(E)} - 2C_4 \\
&\geq C_5\int_0^{+\infty} f_0(E)(\|\psi^1(x)\|^2_{L^\infty(0,1)} + \|\psi^2(x)\|^2_{L^\infty(0,1)})\frac{dE}{V_c(E)} - 2C_4, \qquad (5.54)
\end{aligned}$$

with $C_5 = Inf(C_3, (1-2P)C_3)$. Moreover, as the charge density $n_{1,2}$ according to ψ^1 and ψ^2 verify

$$||n_{1,2}||_{L^\infty(0,1)} \leq \int_0^{+\infty} f_0(E)||\psi^{1,2}||^2_{L^\infty(0,1)}\frac{dE}{V_c(E)},$$

inequality (5.54) gives

$$\begin{aligned}
\int_0^1 K(x)dx &\geq C_5(||n_1||_{L^\infty(0,1)} + ||n_2||_{L^\infty(0,1)}) - 2C_4 \\
&\geq C_5||n||_{L^\infty(0,1)} - 2C_4. \qquad (5.55)
\end{aligned}$$

Since V_σ is a solution of the Poisson problem, we have the following estimate

$$\frac{1}{\sigma}||V_\sigma^{'}||_{W^{1,\infty}(0,1)} \leq \frac{C_6}{\sigma}||V_\sigma||_{W^{2,\infty}(0,1)} \leq C_7||n||_{L^\infty(0,1)}.$$

Hence, inequality (5.55) becomes

$$\int_0^1 K(x)dx \geq \frac{C_8}{\sigma}||V_\sigma^{'}||_{W^{1,\infty}(0,1)} - 2C_4, \quad C_8 = \frac{C_5}{C_7}.$$

In view of (5.53), this leads to

$$\frac{C_8}{\sigma}||V_\sigma^{'}||_{W^{1,\infty}(0,1)} \leq C_9 + \frac{1}{\sigma}||V_\sigma^{'}||^2_{L^2(0,1)} + \frac{2C_2}{\sigma}||V_\sigma^{'}||_{L^\infty(0,1)}, \quad C_9 = C_1 + 2C_4. \tag{5.56}$$

In the above estimate, we notice non-homogeneity between the left and the right hand side. This is due to the nonlinear character of the system. Our purpose is to obtain a σ-independent bound. Indeed, a Gagliardo-Nirenberg interpolation result (see [27]) leads to

$$||f||_{L^\infty(0,1)} \leq C||f||^{\frac{2}{3}}_{L^2(0,1)}||f||^{\frac{1}{3}}_{W^{1,\infty}(0,1)}.$$

Applying this inequality to $V_\sigma^{'}$, we get

$$||V_\sigma^{'}||_{L^\infty(0,1)} \leq C||V_\sigma^{'}||^{\frac{2}{3}}_{L^2(0,1)}||V_\sigma^{'}||^{\frac{1}{3}}_{W^{1,\infty}(0,1)}.$$

Then, applying Young inequality (see [27]), we have

$$C||V_\sigma^{'}||^{\frac{2}{3}}_{L^2(0,1)}||V_\sigma^{'}||^{\frac{1}{3}}_{W^{1,\infty}(0,1)} \leq \frac{C}{2}(||V_\sigma^{'}||^{\frac{4}{3}}_{L^2(0,1)} + ||V_\sigma^{'}||^{\frac{2}{3}}_{W^{1,\infty}(0,1)}).$$

Hence, under these previous manipulations, estimate (5.56) becomes

$$\frac{C_8}{\sigma}||V_\sigma^{'}||_{W^{1,\infty}(0,1)} \leq C_9 + \frac{1}{\sigma}||V_\sigma^{'}||^2_{L^2(0,1)} + \frac{C_{10}}{\sigma}(||V_\sigma^{'}||^{\frac{4}{3}}_{L^2(0,1)} + ||V_\sigma^{'}||^{\frac{2}{3}}_{W^{1,\infty}(0,1)}), \quad C_{10} = C_2 C.$$

Since the parameter σ is in $[0,1]$, we obtain a σ-independent bound

$$C_8||V^{'}||_{W^{1,\infty}(0,1)} - ||V^{'}||^2_{L^2(0,1)} - C_{10}(||V^{'}||^{\frac{4}{3}}_{L^2(0,1)} + ||V^{'}||^{\frac{2}{3}}_{W^{1,\infty}(0,1)}) \leq C_9.$$

Therefore, this estimate implies the bound of V in $W^{2,\infty}(0,1)$ by a constant C depending on C_8, C_9 and C_{10}. This ends the proof of Lemma 5.3.

As a consequence of this result, $V^*(= TV)$ solution of the Poisson problem satisfy a standard regularity result

$$\|V^*\|_{W^{2,\infty}(0,1)} \leq C\|n\|_{L^\infty(0,1)}.$$

Then according to estimates (5.45) and the fact that f_0 is compactly supported, V^* is bounded in $W^{2,\infty}(0,1)$.

5.2 Compactness and continuity

Lemma 5.4 *The operator T defined by (5.38), is a continuous and compact operator on $L^\infty(0,1)$.*

Proof. At first, we show that the operator T is compact. It follows from Lemma 5.1, regularities and proprieties of the Poisson equation. In fact, the image of a bounded set of $L^\infty(0,1)$ is a bounded set of $W^{2,\infty}(0,1)$.

To prove continuity, let V_j be a converging sequence in $L^\infty(0,1)$. Let V be its limit. Then, we set by

$$(\mathbf{\Psi})_j = \mathbf{\Psi}(V_j) = (\psi^1(V_j), \psi^2(V_j)), \quad n_j = n((\mathbf{\Psi})_j) = n_1((\mathbf{\Psi})_j) + n_2((\mathbf{\Psi})_j).$$

Since T is compact, we deduce after a possible extraction of a sequence that

$$V_j^*(=TV_j) \to V^* \quad L^\infty(0,1) \text{ strong.}$$

It remains to show that $V^* = TV$. This incidentally will prove that there is no need to extract a sub-sequence.
Since for any given E, $(\mathbf{\Psi})_j$ and n_j are respectively bounded in $(H^1(0,1))^2$ and $L^\infty(0,1)$, we have after a possible extraction that

$$(\mathbf{\Psi})_j \quad \to \quad \mathbf{\Psi} \quad (H^1(0,1))^2 \text{ strong}, \quad n_j \rightharpoonup n \quad L^\infty(0,1) \text{ weak } *\,.$$

We pass to the limit in system (2.2)-(2.4) in sense of distribution. We easily deduce that the limit $\mathbf{\Psi}$ of $(\mathbf{\Psi})_j$ is nothing but $\mathbf{\Psi}(V)$. The uniqueness of the limit implies that all the sequence converges. Now, using the Lebesgue dominated convergence Theorem ([27]), we deduce the uniform convergence respect to x

$$\lim_{n\to+\infty} \int_0^{+\infty} f_0(E)||(\mathbf{\Psi})_j(x)|^2 - |\mathbf{\Psi}(x)|^2| \frac{dE}{V_c(E)} = 0.$$

Passing to the limit in Poisson equation

$$-\frac{d^2V_j^*}{dx^2}(x) = n_j, \qquad \text{with } V_j(0) = 0 \quad \text{and } V_j(1) = V_1,$$

we obtain

$$-\frac{d^2V^*}{dx^2}(x) = n, \qquad \text{with } V(0) = 0 \quad \text{and } V(1) = V_1.$$

This leads to the end of the proof.

Finally, using Lemma 5.3 and Lemma 5.4, the Leray-Schauder Theorem proves the existence of a fixed point V of T. This ends the proof of Theorem 2.2.

6 Some remarks and comments

The introduction of more than one band in a study of the quantum model, has been necessarily since we want to describe more and more realistic quantum devices. Here, we have dealt with the two-band in description of the Schrödinger model. We have derived the associated boundary conditions and we have studied mathematically this model coupled with the Poisson model. Note that the proof of the existence of solution is not without difficulty. It has been done thanks to algebraic manipulations (see appendix A). Then, as we have mentioned in the beginning of this work, we have made several simplifications to illustrate the Kane model. In fact, we have decoupled the heavy holes of the valence band and we have neglected the spin-orbit coupling.

A suitable model describing the coupling between the four band (see figure.4.4) is given

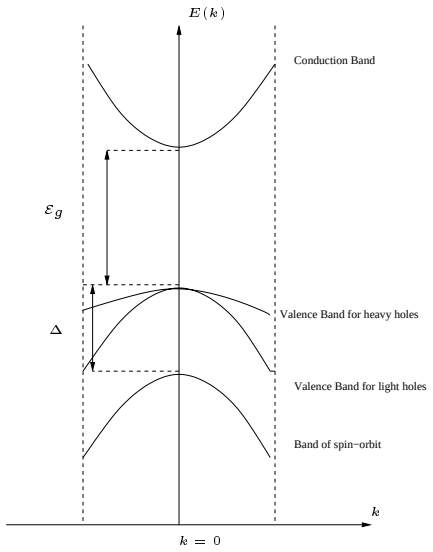

FIG. 4.4: Schematic band structure .

by Kane ([60]) and its Hamiltonian ([7]) reads

$$\begin{pmatrix} -\frac{\hbar^2}{2m}\frac{d^2}{dx^2}+V(x) & i\sqrt{\frac{2}{3}}\hbar P\frac{d}{dx} & -i\sqrt{\frac{1}{3}}\hbar P\frac{d}{dx} & 0 \\ i\sqrt{\frac{2}{3}}\hbar P\frac{d}{dx} & -\frac{\hbar^2}{2m}\frac{d^2}{dx^2}-\mathcal{E}_g+V(x) & 0 & 0 \\ -i\sqrt{\frac{1}{3}}\hbar P\frac{d}{dx} & 0 & -\frac{\hbar^2}{2m}\frac{d^2}{dx^2}-\mathcal{E}_g-\Delta+V(x) & 0 \\ 0 & 0 & 0 & -\frac{\hbar^2}{2m}\frac{d^2}{dx^2}-\mathcal{E}_g+V(x) \end{pmatrix}$$

The extension of the derivation of the boundary conditions to more than two-bands presents no difficulty in principle once the basic concepts are understood for the two-bands. In fact, this can be dealt to the previous four-bands. Where, the associated dispersion relation is

$$(k^2-\mathcal{E}_g-E)\left[(k^2-E)(k^2-\mathcal{E}_g-E)(k^2-\mathcal{E}_g-\Delta-E)-P^2k^2(k^2-\mathcal{E}_g-\frac{2}{3}\Delta-E)\right]=0.$$

Solving this relation according to E, we obtain four values of energy which are nothing but the energy corresponding to the energy of the each four bands. We denote them by $E_i(k),(i=1,..,4)$. We notice that these values have been given approximately by Kane ([60]) using the perturbation theory, once parabolic and once non-parabolic. Then, the corresponding normalized eigenvectors are denoted by $\mathbf{e_i}(k),(i=1,..,4)$. They reduce to the canonical bases of $\mathbb{R}^4$ when the coupling parameter $P=0$.
In addition solving the dispersion relation according to k, we obtain eight values $\pm k_i(E),(i=1,..,4)$. In particular, we have

$$\forall k\in\mathbb{C},\qquad k_i(E_i(k))=k,\quad E_i(k_i(E))=E,\ \forall i=1,..,4.$$

The group velocity in the E_i band is given by

$$V_i(E) \quad = \quad \mathcal{V}_i(k_i(E))=\frac{dE_i}{dk}(k),\ \forall i=1,..,4. \tag{6.57}$$

Then by analogy with the two-bands, we derive the boundary conditions for which in a future work, we will treat the model numerically.

7 Appendix A : Calculation of the matrix $\mathbb{S}_{\mp}$

The imaginary part of the weak formulation of problem (2.2)-(2.4) is the following

$$\begin{aligned}&\Re e\left[\left(\mathbb{T}_+(E-V_1)(\mathbb{B}_+(E-V_1))^{-1}\mathbf{\Psi}(1)\right)\bullet(\mathbb{B}_+(E-V_1))^{-1}\mathbf{\Psi}(1)\right.\\&\left.-\left(T_-(E)(\mathbb{B}_-(E))^{-1}\mathbf{\Psi}(0)\right)\bullet(\mathbb{B}_-(E))^{-1}\mathbf{\Psi}(0)\right]=\Re e((k_c(E)\mathbb{I}_2-\mathbb{K}_-(E))\mathbf{e}_c^+(E))\bullet\mathbf{\Psi}(0)).\end{aligned}\quad(7.58)$$

where $(\mathbb{B}_{\mp})$, $\mathbb{D}_{\mp}(E)$, $\mathbb{T}_{\pm}(E)$ and $\mathbb{A}$ are given respectively in (3.25), (4.29) and (4.30).
We start computing the right hand side of (7.58). For this, we use

$$\mathbb{B}_-^{-1}(E)\mathbf{\Psi}(0)=\mathbb{B}_-^{-1}(E)\mathbf{e}^+(E)+\begin{pmatrix}r_c\\r_v\end{pmatrix}.$$

In sense of duality, we obtain

$$\begin{aligned}&Re((k_c(E)\mathbb{I}_2-\mathbb{K}_-(E))\mathbf{e}_c^+(E))\bullet\mathbf{\Psi}(0))=\\&\frac{V_c(k_c(E))}{2}-\Re e(\mathbb{T}_-(E)\mathbb{B}_-(E)^{-1})\mathbf{\Psi}(0)\bullet(\mathbb{B}_-(E)^{-1})\mathbf{\Psi}(0)-\Re e(T_-(E)\begin{pmatrix}r_c\\r_v\end{pmatrix})\bullet\begin{pmatrix}r_c\\r_v\end{pmatrix})\\&+\Re e((k_c(E)\mathbb{I}_2-PA)\mathbf{e}_c^+(E)\bullet\mathbb{B}_-(E)\begin{pmatrix}r_c\\r_v\end{pmatrix})+\Re e(\mathbb{T}_-(E)\begin{pmatrix}r_c\\r_v\end{pmatrix})\bullet(\mathbb{B}_-(E)^{-1})\mathbf{e}_c^+(E)).\end{aligned}$$

Moreover, we have that the sum of the two last terms in the right hand side of the above equation is equal to zero. This will reduces and leads to

$$\begin{aligned}&Re((k_c(E)\mathbb{I}_2-\mathbb{K}_-(E))\mathbf{e}_c^+(E))\bullet\mathbf{\Psi}(0))=\\&\frac{V_c(k_c(E))}{2}-\Re e(\mathbb{T}_-(E)\mathbb{B}_-(E)^{-1})\mathbf{\Psi}(0)\bullet(\mathbb{B}_-(E)^{-1})\mathbf{\Psi}(0)-\Re e(\mathbb{T}_-(E)\begin{pmatrix}r_c\\r_v\end{pmatrix})\bullet\begin{pmatrix}r_c\\r_v\end{pmatrix}).\end{aligned}$$

Now, we substitute the previous expression in (7.58). We get

$$\Re e\left[\left(\mathbb{T}_+(E-V_1)\mathbb{B}_+^{-1}(E-V_1)\mathbf{\Psi}(1)\right)\bullet\mathbb{B}_+^{-1}(E-V_1)\mathbf{\Psi}(1)+(\mathbb{T}_-(E)\begin{pmatrix}r_c\\r_v\end{pmatrix})\bullet\begin{pmatrix}r_c\\r_v\end{pmatrix}\right]=\frac{V_c(k_c(E))}{2}.\quad(7.59)$$

For clarity, we compute only the term on $\mathbb{T}_-$. This is not with no difficulty. For this, in order to reduce the heavy calculus, the unitary vectors $\mathbf{e}_c^-(E)$, $\mathbf{e}_v^-(E)$ defined by (3.14) and (3.15), can be written as

$$\mathbf{e}_c^-(E)=\begin{pmatrix}a\\b\end{pmatrix}=\sqrt{\frac{(\sqrt{\delta^2+P^2(k_c(E))^2}+\delta)}{2\sqrt{\delta^2+P^2(k_c(E))^2}}}\begin{pmatrix}1\\\frac{Pk_c(E)}{\delta+\sqrt{\delta^2+P^2(k_c(E))^2}}\end{pmatrix},\quad(7.60)$$

$$\mathbf{e}_v^-(E)=\begin{pmatrix}a'\\b'\end{pmatrix}=\sqrt{\frac{(\sqrt{\delta^2+P^2(k_v(E))^2}+\delta)}{2\sqrt{\delta^2+P^2(k_v(E))^2}}}\begin{pmatrix}-\frac{P(k_v(E))}{\delta+\sqrt{\delta^2+P^2(k_v(E))^2}}\\1\end{pmatrix}.\quad(7.61)$$

After that, expressing (7.60) and (7.61) in terms of a, b, a' and b'. Then, using the expression of the group velocity given by (3.19)-(3.20), $\mathbb{T}_-$ defined by (4.29) becomes

$$\mathbb{T}_-(E)=\begin{pmatrix}-\frac{\mathcal{V}c(k_c(E))}{2}&-k_v(E)(aa'+bb')-Pa'b\\-k_c(E)(aa'+bb')-Pab'&-\frac{\mathcal{V}_v(k_v(E))}{2}\end{pmatrix}.$$

As E is positive, we notice that each $k_c(E)$ and $k_v(E)$ is real. Consequently, for the second term of the left hand side of (7.59), we get

$$\begin{aligned}\Re e\left[\left(\mathbb{T}_-(E)\begin{pmatrix} r_c \\ r_v\end{pmatrix}\right)\bullet\begin{pmatrix} r_c \\ r_v\end{pmatrix}\right] &= -\frac{\mathcal{V}_c(k_c(E))}{2}|r_c|^2 - \frac{\mathcal{V}_v(k_v(E))}{2}|r_v|^2 \\ &+ (-(k_v(E)+k_c(E))(aa^{'}+bb^{'}) - P(a^{'}b+ab^{'}))\Re e(r_v.\overline{r_c}). \quad (7.62)\end{aligned}$$

But, from (3.17)-(3.18), when we express k_v in term of $k_c(E)$ and replace a, $a^{'}$, b and $b^{'}$ by their expression from (7.60) and (7.61), we have

$$(-(k_v(E)+k_c(E))(aa^{'}+bb^{'}) - P(a^{'}b+ab^{'}) = 0.$$

This leads to that (7.62) becomes

$$\Re e\left[\left(\mathbb{T}_-(E)\begin{pmatrix} r_c \\ r_v\end{pmatrix}\right)\bullet\begin{pmatrix} r_c \\ r_v\end{pmatrix}\right] = \mathbb{S}_-(E)\begin{pmatrix} r_c \\ r_v\end{pmatrix}\bullet\begin{pmatrix} r_c \\ r_v\end{pmatrix}, \quad (7.63)$$

with in all cases of the value of E, we have

$$\mathbb{S}_\pm(E) = \begin{pmatrix} \pm\frac{\Re e(k_c(E))}{2k_c(E)}\mathcal{V}_c(k_c(E)) & 0 \\ 0 & \pm\frac{\Re e(k_v(E))}{2k_v(E)}\mathcal{V}_v(k_v(E))\end{pmatrix}. \quad (7.64)$$

Finally, the expression (7.59) is simplified. In direct mode, it is equivalent to the following particle conservation

$$\frac{Re(k_c(E-V_1))}{k_c(E-V_1)}\frac{\mathcal{V}_c(k_c(E-V_1))}{\mathcal{V}_c(k_c(E))}|t_c|^2 + \frac{Re(k_v(E-V_1))}{k_v(E-V_1)}\frac{\mathcal{V}_v(k_v(E-V_1))}{\mathcal{V}_c(k_c(E))}|t_v|^2 + |r_c|^2 + \frac{\mathcal{V}_v(k_v(E))}{\mathcal{V}_c(k_c(E))}|r_v|^2 = 1.$$

However, in reverse mode we obtain

$$\frac{-Re(k_c(E-V_1))}{k_c(E-V_1)}\frac{\mathcal{V}_v(k_c(E-V_1))}{\mathcal{V}_c(k_c(E))}|t_c|^2 + \frac{Re(k_v(E-V_1))}{k_v(E-V_1)}\frac{\mathcal{V}_v(k_v(E-V_1))}{\mathcal{V}_c(k_c(E))}|t_v|^2 + |r_c|^2 + \frac{\mathcal{V}_v(k_v(E))}{\mathcal{V}_c(k_c(E))}|r_v|^2 = 1.$$

Acknowledgments. This work has been supported by the European IHP network. Ref. HPRN-CT-2002-00282 entitled HYKE (HYperbolic and Kinetic Equations : Asymptotics, Numerics, Analysis).

Chapitre 5

Numerical analysis : Application to InAs/AlSb/GaSb/AlSb/InAs Interband device

Sommaire

1 Introduction

The tunneling phenomena in semiconductor heterostructure has been the focus of intensive research since the pioneering work of Tsu and Esaki [113]. They discovered a region of negative differential resistance (NDR) in the current voltage characteristics of electron tunneling through a one-barrier heterostructure. Much experimental and theoretical work has been done to study their applications and to describe the transport process in these types of structures. Indeed, the resonant tunneling devices have been attracting much attention recently because they exhibit high peak current densities which is desirable for ultra-high-speed application. For instance, the double-barrier resonant tunneling diode (RTD) has been a subject of great interest over the past several years. It displays multiple NDR regions in their current-voltage characteristics than the Esaki diodes. However, recent progress in the growth of materials with different band gaps has stimulated the development of novel tunnel structures. Recently, a resonant interband tunneling diodes (RITD) was proposed [110] as away to combine the features of both interband tunneling in the Esaki diode and resonant tunneling in quantum wells. Contrarily to the conventional RTD with one alignment band, the RITD has two band alignment. The tunneling in such structures takes place through resonant valence-band levels. Such devices were predicted to have a very low valley current as in tunnel diodes owing to the band-gap blocking of the non-resonant components and a high peak current as in RTD due to the sharp resonance on a quasi-bound state.

In this chapter, the quantum-well double-barrier resonant interband tunneling diode RITD has been taken to be the prototype interband quantum semiconductor device ([110]). This device consists of two band alignment with a single quantum well bounded by tunneling barriers, as shown in the following figure 5.1.

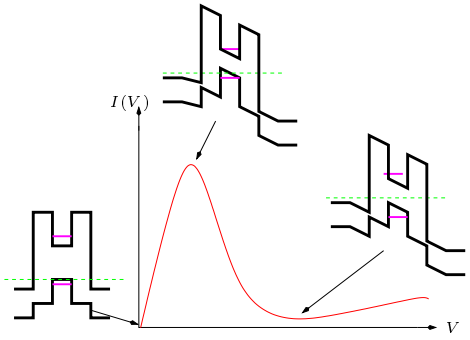

FIG. 5.1: Qualitative $I(V)$ for the resonant interband tunneling diode.

The first structure shows the equilibrium. As a bias voltage is applied to the device, the resonant states in the well are pulled down in energy. More particularly, in the second structure, electrons can resonantly tunnel from the conduction band through the barrier to the valence band with energy equals to the resonant confined state. As the voltage is increased in the last structure the resonant state in the valence band is pulled below the occupied levels and the tunneling current decreases, leading to a negative-resistance characteristic, as the current decreases with increasing voltage.
As mentioned in the previous chapter 4, this type of structure can be described by the two-band Schrödinger equation. More precisely, the transport properties of these structure requires the self-consistent solution of both Poisson and two-band Schrödinger equations.

The outline of this chapter is as follows : section 2 is devoted to the introduction of the different equations to solve and the description of the iterative procedure for obtaining the self-consistent two-band Schrödinger and the Poisson solution. In section 3, the numerical methods are presented. They deal with an explicit Runge Kutta of order 4 with adaptatif mesh applied to the two-band Schrödinger equation and the Gummel method to solve the Poisson equation. In section 4, the numerical results for an InAs/AlSb/GaSb/AlSb/InAs type structure in the stationary case is presented.

2 The different equations to solve

In this section, we use two types of equations in order to solve the coupled two-band Schrödinger-Poisson model. The first one is a one-dimensional non-scaled two-band Schrödinger equation.

$$\begin{pmatrix} -\frac{\hbar^2}{2m}\frac{d^2}{dx^2} - eV_c(x) & i\hbar P\frac{d}{dx} \\ i\hbar P\frac{d}{dx} & -\frac{\hbar^2}{2m}\frac{d^2}{dx^2} - \mathcal{E}_g - eV_c(x) \end{pmatrix} \begin{pmatrix} \psi^1 \\ \psi^2 \end{pmatrix} = E \begin{pmatrix} \psi^1 \\ \psi^2 \end{pmatrix}. \quad (2.1)$$

The associated Fourier boundary conditions are given by

$$\frac{d\mathbf{\Psi}}{dx}(0) - iK_-(E)\mathbf{\Psi}(0) = i(k_c(E)I_2 - K_-(E))\vec{e_c}^+(E), \quad (2.2)$$

$$\frac{d\mathbf{\Psi}}{dx}(1) - iK_+(E + eV_1)\mathbf{\Psi}(1) = 0, \quad (2.3)$$

where $\psi^{1,2}$ the components of the wave function $\mathbf{\Psi}$ according to the two bands, E is the energy, V is the potential energy, $\hbar$ the reduced Planck constant and m is the electron mass. The terms $\vec{e_c}^+(E)$, $k_c(E)$ and $K_\pm(E)$ are given respectively by (3.14), (3.17) and (3.24). The one dimensional Poisson equation is

$$-\frac{d^2V}{dx^2}(x) = \frac{e}{\epsilon_r}(n_D - n), \qquad \text{with } V(0) = 0 \quad \text{and } V(1) = V_1 \quad (2.4)$$

where ϵ_r is the relative dielectric constant and n_D is the ionized donor concentration and n is the electron density distribution. The wave function $\mathbf{\Psi}$ and electron density n are related by

$$n(x) \quad = \quad \int_0^{+\infty} g_0(k)|\mathbf{\Psi}(x)|^2 dk \quad (2.5)$$

where $g_0(k)$ the one dimensional full Fermi-Dirac statistic

$$g_0(k) = \frac{m^* k_b T}{\pi\hbar^2} log(1 + exp(\frac{-Ec(k) + e\mu}{k_b T})). \quad (2.6)$$

$Ec(k)$ is the conduction energy band, T is the temperature, m^* is the effective mass and μ is the Fermi potential related to the Fermi energy E_F by $E_F = -e\mu$.

Once again and in the same spirit as in the numerical study of the KL model, we use an iteration procedure to obtain a self-consistent solution for equations (2.1)-(2.3) and (2.4).

Starting with a trial potential $V(x)$, the wave function corresponding to each wave vector k can be used to calculate the electron density distribution $n(x)$ using (2.5). The computed $n(x)$ and a given donor concentration $n_D(x)$ can be used to calculate the Poisson potential via equation (2.4). The new potential V is then obtained. The subsequent iteration will yield the final self-consistent solution for V and n which satisfy a certain error criteria. This result has been predict from Theorem 2.2 in chapter 4 which ensures the existence of solution.

3 Numerical methods

3.1 Runge Kutta method

The simple way to solve the linear system (2.1)-(2.3) is to set

$$\Psi(1) := 1 = Y_1(1) + Y_2(1) \quad \text{such that} \quad Y_1(1) = \begin{pmatrix} 1 \\ 0 \end{pmatrix} \text{ and } Y_2(1) = \begin{pmatrix} 0 \\ 1 \end{pmatrix}.$$

Thus, we get two problems on Y_1 and Y_2

$$\begin{pmatrix} -\frac{\hbar^2}{2m}\frac{d^2}{dx^2} - eV_c(x) & iP\hbar\frac{d}{dx} \\ i\hbar P\frac{d}{dx} & -\frac{\hbar^2}{2m}\frac{d^2}{dx^2} - \mathcal{E}_g - eV_c(x) \end{pmatrix} Y_{1,2}(x) = EY_{1,2}(x) \tag{3.7}$$

with the following boundary conditions

$$\frac{dY_1}{dx}(1) = iK_+(E + eV_1), Y_1(1) = \begin{pmatrix} 1 \\ 0 \end{pmatrix} \tag{3.8}$$

$$\frac{dY_2}{dx}(1) = iK_+(E + eV_1), Y_2(1) = \begin{pmatrix} 0 \\ 1 \end{pmatrix}. \tag{3.9}$$

Like an ordinary differential equation, the previous problem can be solved using for example fourth order Runge-Kutta method ([97]). For this aim, we make the following variable change setting by T the vector with four components

$$T = \begin{pmatrix} Y_{1,2}(x) \\ \frac{dY_{1,2}}{dx}(x) \end{pmatrix}.$$

Then, (3.7) becomes

$$\frac{dT}{dx} = f(x,T) \quad \text{with} \quad f(x,T) = M(x).T$$

and

$$M(x) = \begin{pmatrix} 0 & 0 & 1 & 0 \\ 0 & 0 & 0 & 1 \\ -\frac{2m}{\hbar^2}(E + eV_c(x)) & 0 & 0 & \frac{2miP}{\hbar} \\ 0 & -\frac{2m}{\hbar^2}(E + eV_v(x)) & \frac{2miP}{\hbar} & 0 \end{pmatrix},$$

with $V_v(x) = \frac{\mathcal{E}_g}{e} + V_c(x)$.

Let us now approach the numerical discretization. For this, we introduce a partition $0 = x_1 < x_2 < .. < x_n = L$, where L is the length of the device. Moreover, due to the fact that the device is composed of thin barrier we use a non-regular mesh of step $x_i = ih_i$ and $h_i = x_{i+1} - x_i$.

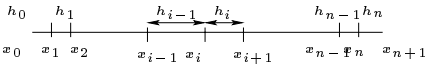

FIG. 5.2: Schematic of non uniform mesh.

Then, we write the associated Runge Kutta algorithm

$$\begin{aligned} K_1 &= f(x_i, T_i) \\ K_2 &= f(x_i + \frac{h_i}{2}, T_i + \frac{h_i}{2}.K_1) \\ K_3 &= f(x_i + \frac{h_i}{2}, T_i + \frac{h_i}{2}.K_2) \\ K_4 &= f(x_i + h_i, T_i + h_i.K_3) \\ T_{i+1} &= T_i + \frac{h_i}{6}(K_1 + 2.K_2 + 2.K_3 + K_4). \end{aligned}$$

The result of this case gives T_i in the node x_i such that $T_i = \begin{pmatrix} Y_{1,2}(x_i) \\ \frac{dY_{1,2}}{dx}(x_i) \end{pmatrix}$ for all $i = 1, .., n$. Furthermore, the problem is linear, then we can normalize the obtained solution. Indeed, Ψ is related to Y_1 and Y_2 by

$$\Psi = \gamma_1 Y_1 + \gamma_2 Y_2,$$

where

$$\gamma_1 = \frac{B_1 * A_{22} - B_2 * A_{12}}{detA}, \quad \gamma_2 = \frac{B_2 * A_{11} - B_1 * A_{21}}{detA}$$

and

$$B_l = (i(k_c(E)I_2 - K_-(E))\vec{e_c}^+(E)).\vec{e}_l, \quad A_{lj} = (\frac{dYj}{dx}(0) - iK_-(E)Yj(0)).\vec{e}_l, \quad l, j \in \{1, 2\}$$

where $(\vec{e}_1, \vec{e}_2)$ is the canonical basis.

3.2 Discretization of the Poisson equation

In the same spirit as treated in the case of the KL model in chapter 3 and for one band Schrödinger equation in [93] and [95], we use the linear Gummel method [56]. Once again, equation (2.4) becomes

$$-\frac{d^2 V_{new}}{dx^2}(x) + \frac{e^2}{\epsilon_r k_B T}|n(x)|V_{new} = \frac{e}{\epsilon_r}(n_D - n + \frac{e}{k_B T}|n(x)|V_{old})), \tag{3.10}$$

$$V_{new}(0) = 0 \quad \text{and } V_{new}(1) = V_1. \tag{3.11}$$

Using the non uniform step (see figure 5.2), we first have

$$V_{i+\frac{1}{2}} = V_i + \frac{h_i}{2}V_i^{'} + \frac{h_i^2}{4}V_i^{''}, \quad V_{i-\frac{1}{2}} = V_i - \frac{h_{i-1}}{2}V_i^{'} + \frac{h_{i-1}^2}{4}V_i^{''}$$

and

$$\frac{(h_{i-1}+h_i)}{2}V_i^{'} = V_{i+\frac{1}{2}} - V_{i-\frac{1}{2}}.$$

By analogy

$$\frac{(h_{i-1}+h_i)}{2}V_i^{''} = V_{i+\frac{1}{2}}^{'} - V_{i-\frac{1}{2}}^{'}. \tag{3.12}$$

Then, using a centered approximation

$$V_{i+\frac{1}{2}}^{'} = \frac{(V_{i+1}-V_i)}{h_i}, \quad V_{i-\frac{1}{2}}^{'} = \frac{(V_i - V_{i-1})}{h_{i-1}} \tag{3.13}$$

and substituting (3.13) in (3.12), we get

$$V_i^{''} = \frac{2}{h_{i-1}(h_{i-1}+h_i)}V_{i-1} - \frac{2}{h_{i-1}h_i}V_i + \frac{2}{h_i(h_{i-1}+h_i)}V_{i+1}.$$

Now, solving (3.11), we obtain a band matrix with three diagonal (A, B, C) and a second member such that a vector F

$$\begin{pmatrix} B_1 & C_1 & .. & .. & .. \\ .. & .. & .. & .. & .. \\ .. & A_i & B_i & C_i & .. \\ .. & .. & .. & .. & .. \\ .. & .. & .. & A_n & B_n \end{pmatrix} = \begin{pmatrix} F_1 \\ .. \\ F_i \\ .. \\ F_n \end{pmatrix},$$

where

$$\begin{aligned} A_i &= -\frac{2h_i}{(h_{i-1}+h_i)}, \quad B_i = 2 + \frac{eh_{i-1}h_i}{\epsilon_r Uth}|n_i|, \quad Uth = \frac{1}{k_B T} \\ C_i &= -\frac{2h_{i-1}}{(h_{i-1}+h_i)}, \quad F_i = \frac{eh_{i-1}h_i}{\epsilon_r}(n_D - n_i + \frac{1}{Uth}|n_i|V_i)), \quad for\ i = 2, n-1, \end{aligned}$$

and

$$\begin{aligned} B_1 &= 2 + \frac{eh_0h_1}{\epsilon_r Uth}|n_1|, \quad C_1 = -\frac{2h_0}{(h_0+h_1)} \\ F_1 &= \frac{eh_0h_1}{\epsilon_r}(n_D - n_1 + \frac{1}{Uth}|n_1|V_1)) + \frac{2h_1}{(h_0+h_1)}V_0 \\ A_n &= -\frac{2h_n}{(h_{n-1}+h_n)}, \quad B_n = 2 + \frac{eh_{n-1}h_n}{\epsilon_r Uth}|n_n| \\ F_n &= \frac{eh_{n-1}h_n}{\epsilon_r}(n_D - n_n + \frac{1}{Uth}|n_n|V_n)) + \frac{2h_{n-1}}{(h_{n-1}+h_n)}V_{n+1}. \end{aligned}$$

To maximize the computing efficiency and to save the memory space, we use a Cholesky decomposition [108]. We notice that this is not the unique method. Other methods have been proposed such that in thesis of E. Polizzi [95]. He used an iterative method which is a conjugate gradient with incomplete Cholesky preconditionor. Moreover, in the team of O. Vanbésien, they developed a direct resolution of the Poisson equation [43] and [115].

4 Numerical results

We refer here to [43], [63], [79] and [115]. Indeed, the device simulated is a one dimensional RITD (see figure 5.3) which consists of L_b barrier width (see table 5.1) and 1.97 eV height (see table 5.2). The quantum well is of L_w width. Then, the double barrier quantum well region of the resonant interband consists of undoped GaSb well sandwiched between AlSb barriers. This region is separated from InAs electrode layers by 4.5 nm wide unintentionally doped InAs space layers (see table 5.1). Moreover, the conduction of InAs is chosen as the energy reference (zero) point.

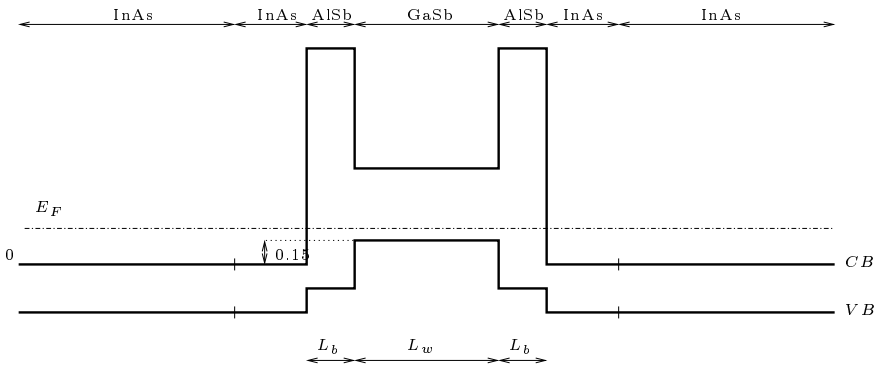

FIG. 5.3: Schematic energy-band diagrams for a one dimension interband tunnel device.

Material	Width(A)	N_D (cm^{-3})
InAs	600	1 10^8
InAs	45	und (undoped)
AlSb	L_b	und
GaSb	L_w	und
AlSb	L_B	und
InAs	45	und
InAs	600	1 10^8

TAB. 5.1:

At $T = 300K$

Material	Gap(eV)	$\Delta E_c(eV)$	$\Delta E_v(eV)$
InAs	0.36	Ref	Ref
AlSb	2.22	1.97	0.11
GaSb	0.67	0.82	0.51

TAB. 5.2:

Moreover, for InAs we have

ϵ_r	P	m^*	E_F
$12.5\epsilon_0$	1.4*1e+6 eV.m	$0.023m$	0.161 eV

TAB. 5.3:

4.1 Current voltage curve simulation

4.1.1 The expression of the current

For this we recall its expression given by

$$J(x) = e(\int_0^{+\infty} g_0(k)\,(\Im m(\mathbb{D}\Psi(x) \bullet \Psi(x)))\,dk. \tag{4.14}$$

4.1.2 Determining the transmission amplitude

Consider a quantum wave with energy E, which is incident from the left, is partially reflected back into the left, and partially transmitted through the device into the right. The obvious point at which to determine the wave function coefficients is one of the device contacts. As we assume that the potential is constant in each contact of the device, we get

$$\begin{aligned}\Psi(x) &= e^{ik_c(E)x}\mathbf{e}_c{}^+(E) + r_c e^{-ik_c(E)x}\mathbf{e}_c{}^-(E) + r_v e^{-ik_v(E)x}\mathbf{e}_v^-(E),\ x<0,\\ \Psi(x) &= t_c e^{ik_c(E-V_1)(x-1)}\mathbf{e}_c{}^+(E-V_1) + t_v e^{ik_v(E-V_1)(x-1)}\mathbf{e}_v{}^+(E-V_1),\ x>1.\end{aligned}$$

Then the transmission and the reflection amplitudes are given by

$$\begin{pmatrix} t_c \\ t_v \end{pmatrix} = \mathbb{B}_+^{-1}(E-V_1)\Psi(1) \quad \text{and} \quad \begin{pmatrix} r_c \\ r_v \end{pmatrix} = \mathbb{B}_-^{-1}(E)(\Psi(0) - \mathbf{e}_c{}^+(E)). \tag{4.15}$$

Since the wave function in $x=1$ is simpler than $x=0$, it is invariably used in the current calculation. From another standpoint, it is more intuitive to calculate current flow from transmission amplitudes.

The quantities related to the amplitudes t_c and t_v are respectively the transmission coefficients

$$\mathcal{T}_v = \frac{\Re e(k_v(E-V_1))}{k_v(E-V_1)}\frac{\mathcal{V}_v(k_v(E-V_1))}{\mathcal{V}_c(k_c(E))}|t_v|^2, \quad \mathcal{T}_c = \frac{\Re e(k_c(E-V_1))}{k_c(E-V_1)}\frac{\mathcal{V}_c(k_c(E-V_1))}{\mathcal{V}_c(k_c(E))}|t_c|^2$$

where the sum is the total transmission coefficient

$$\mathcal{T} = \mathcal{T}_c + \mathcal{T}_v. \tag{4.16}$$

Upon determining $\mathcal{T}$, the current flow can be calculated through

$$J(V) = \frac{e}{m}\int_0^{+\infty} g_0(k)\frac{\mathcal{V}_c(k_c(E))}{2}\mathcal{T}dk \tag{4.17}$$

4.1.3 I-V curve simulation overview

The complete procedure for calculating the current-voltage of a RITD is as follows

1. At a given incident wave energy E and applied bias V, compute the Two-band Schrödinger equation.
2. Determine the transmission coefficient of the system $\mathcal{T}$ from (4.16)
3. Repeat step (1)-(2) to determine $\mathcal{T}(E)$ over the range of energies at which there are significant incident carriers from either contact.
4. Use (4.17) to calculate the current density at that applied bias.
5. Finally, repeat steps (1)-(4) over a desired range of applied biases, yielding the current-voltage curve.

The first simulation results are shown in figure 5.4 and 5.5. Indeed, the more indicator of electronic device operation is the current voltage (I-V) curve. Therefore, figure 5.4 shows I-V curve for the RITD in figure 5.3

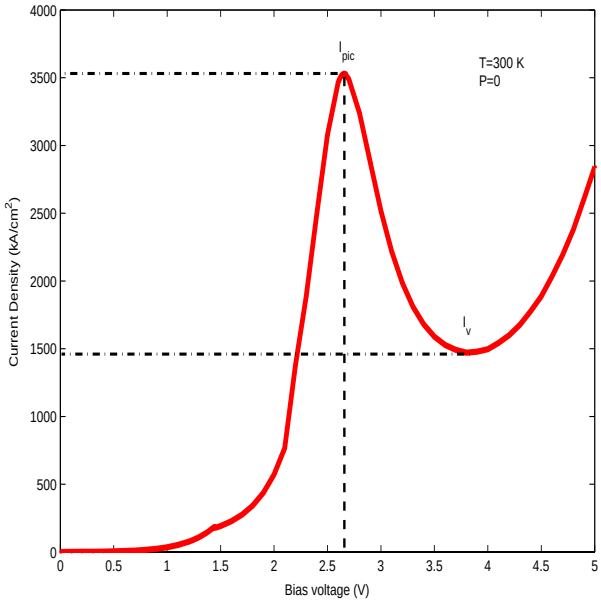

FIG. 5.4: The current-voltage for an InAs/AlSb/GaSb/AlSb/InAs resonant interband tunneling with $10Ang$ AlSb barriers and $30Ang$ GaSb well when $P = 0$.

In figure 5.4, we have taken $P = 0$ in our simulation. This case corresponds to decoupling between the two bands : the conduction and valence band. More precisely, the conduction band is treated as a monoband case. The device is run from 0 to 5 $Volts$ in 0.1 increments. The peak current I_{pic} on the order of 3500 kA/cm^2 is reached at a voltage 2.65 $Volts$. It corresponds to tunneling through the conduction band. The peak-to-valley current (I_{pic}/I_{valley}) ratio is 2.33 at room temperature. Due to the fact that the barrier height is about 1.97 eV, the current curve corresponds well to a curve of an intraband structure.

In figure 5.5, we treat the case where the two-band are coupled through the parameter P. Its value is $P = 1.4 * 1e + 6\ eV.m$. Then, the device is run from 0 to 0.3 $Volts$ in 0.01

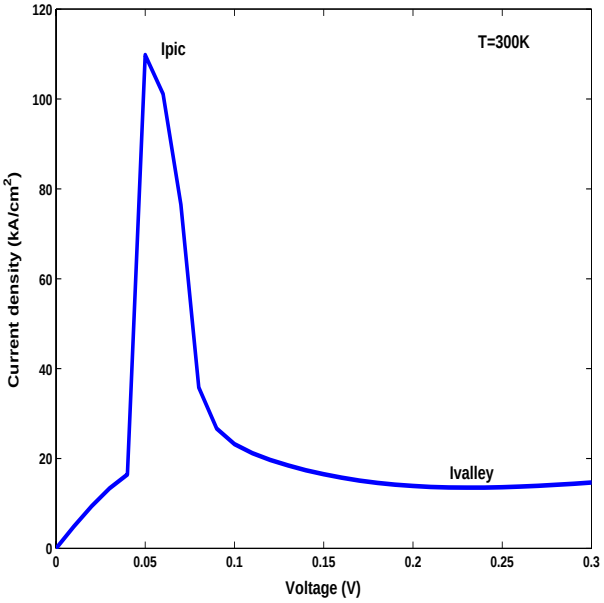

FIG. 5.5: The current-voltage for an InAs/AlSb/GaSb/AlSb/InAs resonant interband tunneling with $10Ang$ AlSb barriers and $30Ang$ GaSb well when $P = 1.4 * 1e + 6\ eV.m$.

increments. The peak current I_{pic} on the order of $110\ kA/cm^2$ is reached at a voltage 0.05 $Volts$. It corresponds to tunneling through the valence band. The peak-to-valley current (I_{pic}/I_{valley}) ratio is 8.3 at room temperature.

Consequently, the fact that we take into account the coupling between the conduction band and valence band is well seen in the curve of the current-voltage in figure 5.5. Indeed, we notice a reduction on the peak current for a low voltage then in the case where we look for the conduction band alone (see figure 5.4).

More interesting, we can show in figure 5.6 that the value of the peak current is obtained due to the coupling between the two bands. From the expression of the current in (4.14), we can write it as the sum of the current due to the conduction band, the valence band and the interference between the two bands noted respectively by J_c, J_v and J_{inter}. Thus, we have

$$J(V) = J_c(V) + J_v(V) + J_{inter}(V) \tag{4.18}$$

where

$$J_c(V) = e(\int_0^{+\infty} g_0(k) \left(\frac{\hbar}{m} \Im m(\frac{d\psi^1}{dx}(x) \bullet \psi^1(x)) \right) dk \ , \tag{4.19}$$

$$J_v(V) = e(\int_0^{+\infty} g_0(k) \left(\frac{\hbar}{m} \Im m(\frac{d\psi^2}{dx}(x) \bullet \psi^2(x)) \right) dk \tag{4.20}$$

and

$$J_{inter}(V) = -2eP(\int_0^{+\infty} g_0(k) \left(\Re e(\psi^1(x).\overline{\psi^2(x)}) \right) dk. \tag{4.21}$$

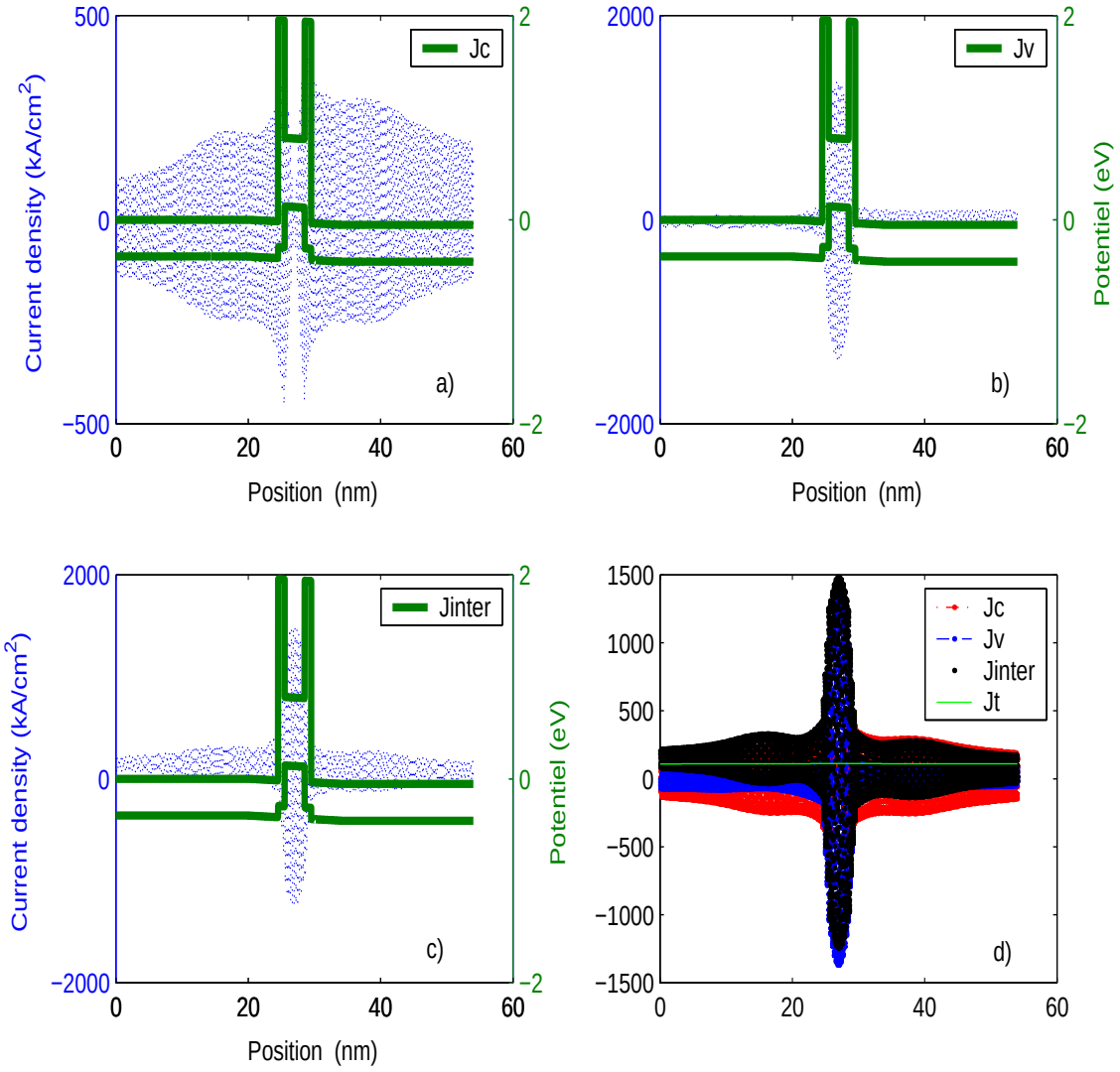

FIG. 5.6: Behavior of the current in the interband resonant tunneling diode at $V_{pic} = 0.05\,Volts$.

In this global figure 5.6, we plot in figure 5.6a the current associated to the conduction band. In figure 5.6b, we plot the current associated to the valence band and in figure 5.6c, we plot the current associated to the interference between the two bands. In the last figure 5.6d, we plot the sum of this three current which implies the value of the total current at $V = 0.05\ Volts$ where it is constant. We see in the well of the RITD where the coupling occurs that the current due to the conduction band in figure 5.6a is lower than those due to the valence band and the interference between the two bands in figure 5.6b and 5.6c. This implies that the peak current in such structure is due to the influence of the valence band and the interference between the two bands.

In these heterostructure RITD, the device operation depends entirely on the unique feature that the valence band edge of GaSb is higher than the conduction band edge of InAs by $0.15eV$. This gives rise to a tunneling window for the transmission of electrons between the valence band edge and the conduction band edge. This is shown in the following figure.

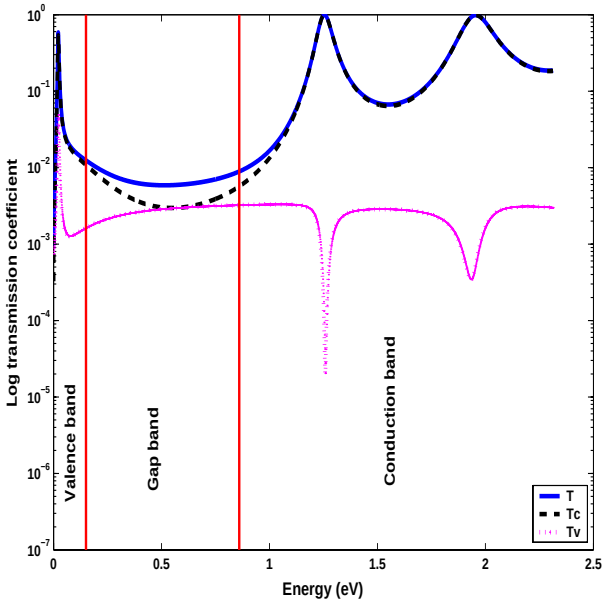

FIG. 5.7: Calculated transmission coefficients of the interband resonant tunneling diode according to the two bands.

In figure 5.7, the transmission coefficients of electrons according to the valence band (dotted) and the conduction band (dashed) are calculated. The sum of both transmission coefficients gives the total transmission coefficient (solid). The resonant peaks are seen clearly in the figure. The first peak is reached for a low energy $0.02eV$ in the energetic region of 0.15 eV corresponding to the valence band. The two peaks after are reached for a higher energies corresponding to resonance energies in the conduction band. These two peaks will not take part in the conduction taking into account that the distribution of carriers holds with a $0.161eV$ Fermi level in InAs. Moreover, the high contrast between transmission in the valence and the gap band was already found in the current curve (see figure 5.5) with a lower potential corresponding to a high peak current. We also note the existence of energies having a transmission probability according to the valence band going to zero (-∞ on a logarithmic scale). The second set simulation results shown in figure 5.8 compares the transmission coefficient versus energy for the two potential obtained when the

current reached the peak and the valley in figure 5.5. The resonance effect appears clearly

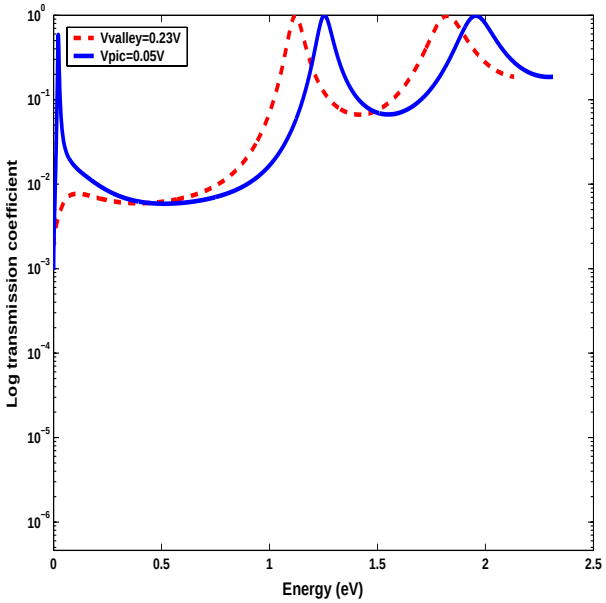

FIG. 5.8: Calculated transmission coefficients of the interband resonant tunneling diode according to the two potentials.

in figure 5.8, where the graph of the transmission coefficient (4.16) is plotted in function of energy in eV. Notice that the effect is more pronounced for applied voltage corresponding to the peak current (solid curve) rather than corresponding to the valley current (dashed curve).

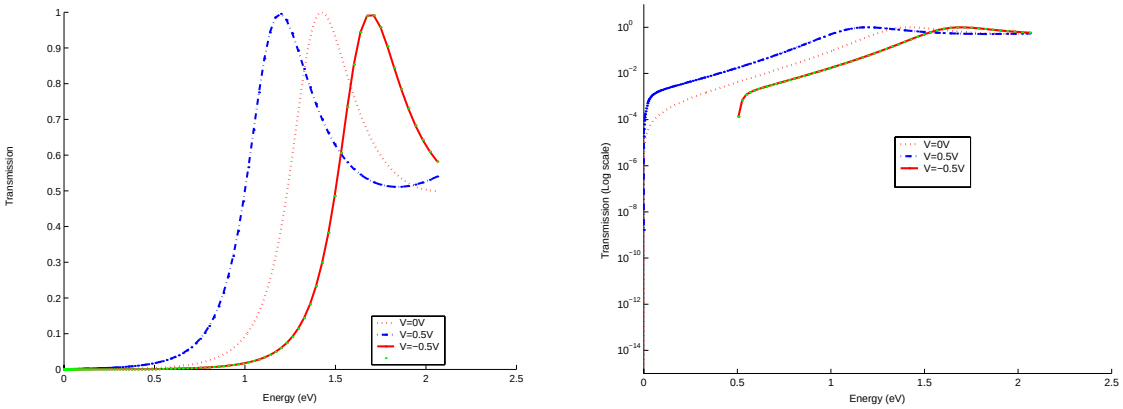

FIG. 5.9: Calculated transmission coefficients of the interband resonant tunneling diode when $P = 0$ with $V = 0$, $V > 0$ and $V < 0$.

In figure 5.9, we show the profile of the transmission coefficient obtained when $P = 0$. Here, we remark once again that the decoupling between the conduction band and the valence band induce that the resonance peak is reached for a resonance energy belonging to the conduction well. We compare also the transmission coefficient versus energy for three

potential $V = 0$, $V = 0.5$ and $V = -0.5\ Volts$. We notice that they have the same shape. For the opposite potential, the transmission curve is exactly the symmetric to the positive potential.

4.2 Carrier density profile

Another essential quantum device simulation result is the carrier density profile, which in the two-band simulation is calculated by integrating over all the wave functions over the wave vector k. As a typical example figure 5.10 shows the carrier density for the simulated RITD at a bias of $0\ Volts$.

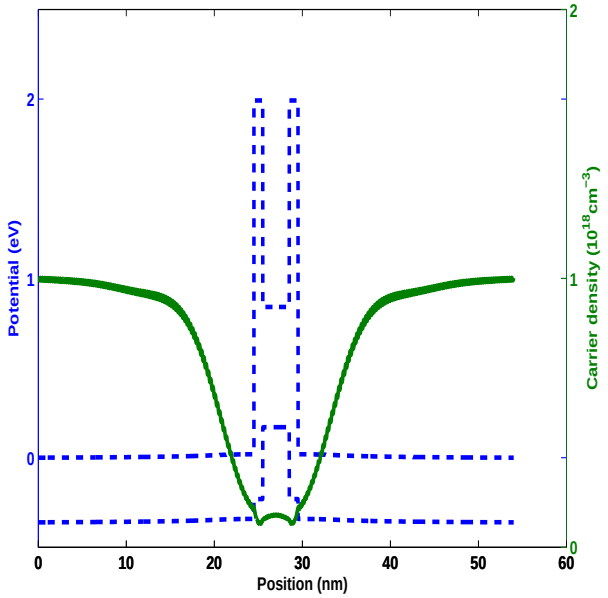

FIG. 5.10: Carrier density for $V = 0\ Volts$.

Then, we show in figure 5.11, the carrier density at a bias of $0.05\ Volts$, which is near resonance (peak current) for this RITD.

The dashed curves in figure 5.11 are the self-consistent potential and barrier potential at a bias of $0.05\ Volts$ corresponding to the peak of the I-V curve in figure 5.5. The solid curve is the associated density profile showing a large increase of density in the well due to the resonant tunneling.

The dashed curves in figure 5.12 are the self-consistent potential and barrier potential at a bias of $0.23\ Volts$ corresponding to the valley of the I-V curve in figure 5.5. The solid curve is the associated density profile showing a large decrease of the density in the well respect to what we obtain in the case where bias is associated to the peak current in figure 5.11.

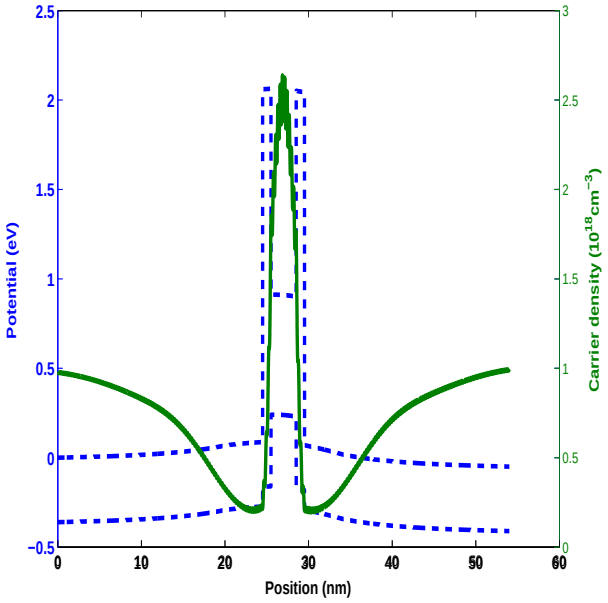

FIG. 5.11: Carrier density for 0.05 $Volts$, corresponding to the peak current.

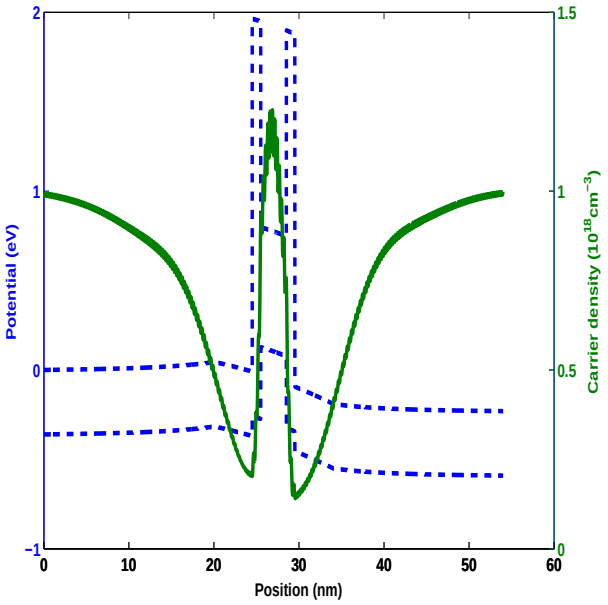

FIG. 5.12: Carrier density for 0.23 $Volts$, corresponding to the valley current.

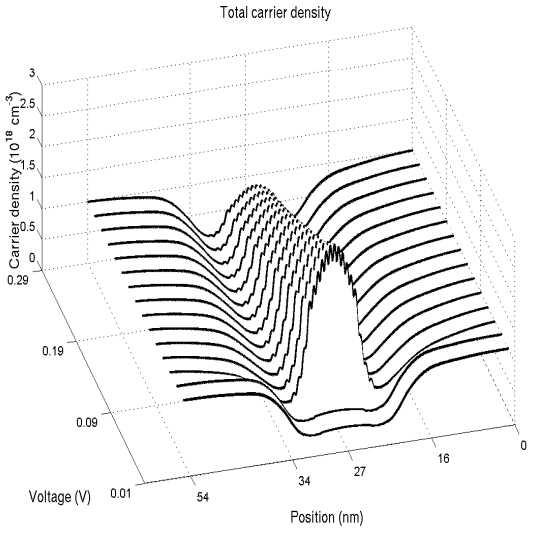

FIG. 5.13: The total carrier density versus the voltage.

In figure 5.13, we plot the total carrier density versus the voltage. The evolution of the carrier density is agree with what happens in device such that the resonant tunneling diode. Indeed from the low to the high voltage, we notice that the density increases until a maximum in the well reached when the voltage corresponds to the peak value of the current (see figure 5.5) and decreases to a bias of the voltage corresponding to the valley current. We can show the details of the behavior of the total carrier density. As, we know also the total density is nothing but the sum of the density according to the conduction, the valence band and the interference between the two bands.

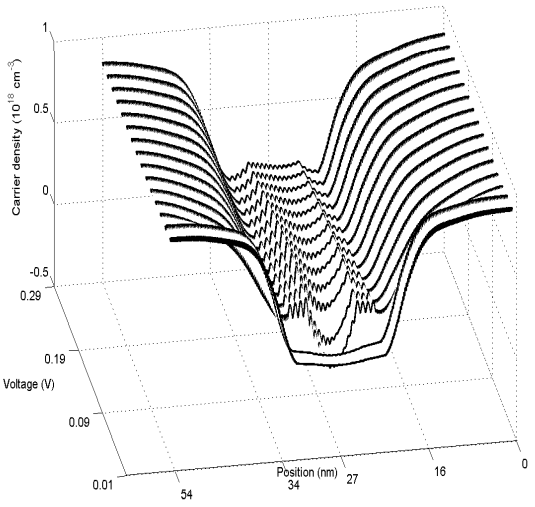

FIG. 5.14: Carrier density according to the interference and conduction terms.

In figure 5.14, we plot the density according to the conduction band. We can see clearly in this case that outside the quantum region, composed of the barriers and the well, the charge density is very larger than which is in the well.

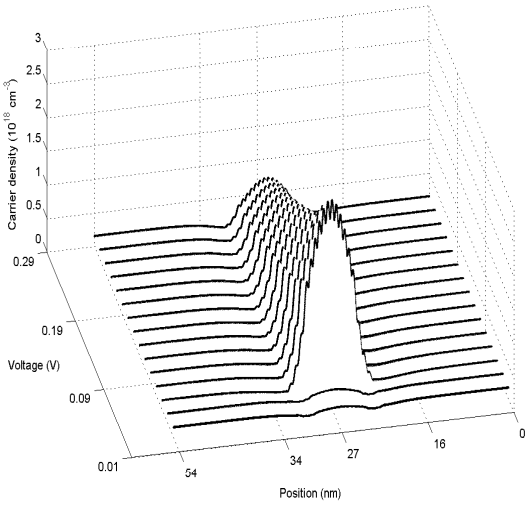

FIG. 5.15: Carrier density according to the valence terms.

In the same situation, in figure 5.15 the charge density is approximately null outside the quantum region and is high in the well. This confirms the fact that electrons, injected from the reservoirs, are in the conduction band and not in the valence band. Moreover, once electrons travel the barriers then they are confined in the well of the valence band.

Références

[1] **Adams R. A.**, *Sobolev spaces.* Academic press, 1975.

[2] **Anderson E. et al.**, *LAPACK user's guide.* Third edition, 1999. (http ://netlib.org/lapack/lug/)

[3] **Arnold A.**, *On absorbing boundary conditions for quantum transport equations.* Math. Modell. Num. Anal. 28, 7, 853-872, 1994.

[4] **Arnold A.**, *Numerical absorbing boundary conditions for quantum evolution equation.* VLSI Design 6, 1-4, 313, 1998.

[5] **Ashcroft N. W. and Mermin N. D.**, *Solid state physics.* Saunders, 1976.

[6] **Barletti L.**, *Wigner envelope functions for electron transport in semiconductor devices.* Trans. Theo. Stat. Phys., 32 (3/4), 2003.

[7] **Bastard G.**, *Wave mechanics applied to semiconductor heterostructures.* Monographies de Physique. les éditions de physique, 1996.

[8] **Bastard G.**, *Super-lattice Band structure in the envelope-function approximation.* Phys. rev B, 24, 5693, 1981.

[9] **Bechouche P., Mauser N. J. and Poupaud F.**, *Semi-classical limit for the Schrödinger-Poisson equation in a crystal.* Comm. Pure Appl. Math, 54 (7), 851-890, 2001.

[10] **Ben Abdallah N.**, *Modèles classiques et quantiques de transport de particules chargées : Analyse asymptotique, Modèle hybride, Application aux semi-conducteurs.* Habilitation à diriger Les recherches en sciences, Université Paul Sabatier, Toulouse. 1997.

[11] **Ben Abdallah N.**, *A Hybrid kinetic-Quantum model for stationary electron transport in a Resonant Tunneling Diode.* J. Statis. Phys 90, n : 3-4, pp 627-662, 1998.

[12] **Ben Abdallah N.**, *On multi-dimensional Schrödinger-Poisson Scattering model for semiconductors.* J. Math. Phys, 41, n : 7, pp 4241-4261, 2000.

[13] **Ben Abdallah N., Degond P. and Gamba I.**, *Inflow boundary conditions for the time dependent one-dimensional Schrödinger equation.* C. R. Acad. Sci. Paris t. 331, Série I, (12), pp 1023-1028, 2000.

[14] **Ben Abdallah N., Degond P. and Gamba I.**, *Coupling one-dimensional time-dependent classical and quantum transport models.* J. Math. Phys. 43, (1), 1-24, 2002.

[15] **Ben Abdallah N., Degond P. and Markowich P. A.**, *On a one-dimensional Schrödinger-Poisson Scattering model.* ZAMP. 48, pp 135-155, 1997.

[16] **Ben Abdallah N. and Kefi J.**, *Limite semi-classique du problème de Schrödinger avec masse variable.* C. R. Acad. Sci. Paris t. 331, Série I, pp 165-170, 2000.

[17] **Ben Abdallah N. and Negulescu C.**, *A one dimensional quantum transport model with small coherence lengths.* Transport Theory Statist. Phys. 31, n : 4-6, 559-578, 2002.

[18] **Ben Abdallah N. and Pinaud O.**, *A mathematical model for the transient evolution of a resonant tunneling diode.* C. R. Math. Acad. Sci. Paris. 334, n.4, 283-288, 2002.

[19] **Ben Abdallah N., Pinaud O., Gardner L. and Ringhofer C.**, *A comparison of resonant tunneling based on Schrödinger's equation and quantum hydrodynamics.* VLSI design 15, 695-700, 2002.

[20] **Ben Daniel D. J. and Duke C.B.**, *Space-Charge Effects on Electron Tunneling.* Phys. Rev.,152, pp 683-693, 1966.

[21] **Biegel B. A.**, *Quantum Electronic Device Simulation.* PhD Thesis, Stanford University, Mar. 1997.

[22] **Bohm D.**, *Quantum theory.*, dover, New-york, 1989.

[23] **Borgioli G., Frosali G. and Zweifel P.**, *Wigner approach to the two-band Kane model for a tunneling diode.*(submitted to Transp. Theor. Stat. Phys.)

[24] **Bournel A.**, *Magnéto-électronique dans des dispositifs à semi-conducteurs.* Ann. Phys. Fr., Vol 25 n :1, 1-167, 2000.

[25] **Bowen R. C. et al**, *Transmission resonances and zero in multi-band models.* Phys. Rev. B., Vol 52, 2754, 1995.

[26] **Bowen R. C. et al**, *Quantitative simulation of a resonant tunneling diode.* J. Appl. Phys 81, 7, 3207-3213, 1997.

[27] **Brézis H.**, *Analyse Fonctionnelle,Théorie et Applications.* Masson,Paris., 1983

[28] **Brezzi H. and Markowich P. A.**, *The Three Dimensional Wigner-Poisson Model : Existence Uniqueness and Approximation.* Math. Meth. Appl. Sci., 14, pp 35-61, 1991.

[29] **Brezzi H. and Markowich P. A.**, *A mathematical analysis of quantum transport in three dimensional crystals.* Anna. di Mathematica Pura Apllicata, 160, pp 171-191, 1991.

[30] **Boykin T. B. et al.**, *Tight-binding model for GaAs/AlAs resonant-tunneling diodes.* Phys. Rev. B, 43, 4777-4784, 1991.

[31] **Carrillo J. A., Gamba I. and Shu C. W.**, *Computational macroscopic approximation of the 1-D relaxation-time kinetic system for semi-conductors.* Physica D., 146, pp 289-306, 2000.

[32] **Carrillo J. A., Gamba I., Majorana A. and Shu C. W.**, *A WENO-solver for 1D non-stationary Boltzmann-Poisson system for semi-conductor devices.* Journal of Computational Electronics 1, pp 365-370, 2002.

[33] **Chao C. Y. and Chuang S. L.**, *Resonant tunneling of holes in the multi-band effective-mass approximation.* Phys. Rev. B, 43 (9), 7027-7039, 1991.

[34] **Chen B., Lazzouni M. and Ram-Mohan**, *Diagonal representation for the transfer-matrix method for obtaining electronic energy levels in layered semiconductor heterostructures.* Phys. Rev. B, 45 (3), 1204-1212, 1992.

[35] **Ciarlet P. G.**, *The finite element method for elliptic problems.* North Holand, Amsterdam, 1978.

[36] **Cohen-Tannoudji C.**, *Mécanique quantique.* Volumes 1 et 2. Hermann, 1996.

[37] **Dautray R. and Lions J.L.**, *Analyse Mathématique et Calcul Numérique pour les Sciences et les Techniques.* Tome 3, Masson, Paris, 1985.

[38] **Degond P.**, *Introduction à la théorie quantique.*

[39] **Degond P.**, *Mathematical modeling of microelectronics semiconductor devices : some current topics on nonlinear conservation laws.* AMS/IP Stud. Adv. Math. Amer. Math. Soc. Providence RI, 15 :77, 2000.

[40] **Degond P. and Elayyadi A.**, *A coupled Schrödinger Drift-Diffusion model for quantum semiconductor device simulations.* J. Comp. Phys 181, p 222-259, 2002.

[41] **Degond P., Jüngel A. and Pietra P.**, *Numerical discretization of energy transport models for semiconductors with non-parabolic band structure.* SIAM on Scientific Computing, 22, 986-1007, 2000.

[42] **Degond P. and Markowich P. A.** , *A Quantum Transport Model for Semiconductors : The Wigner-Poisson Problem on a bounded Brillouin zone.* M2AN, 24, n : 6, pp 697-710, 1990.

[43] **Duez V.**, *Hétérostructures semiconductrices uni- et bi-polaires : de la physique au composant.* Thèse de doctorat, Université de Lille. Juillet 2000.

[44] **Elayyadi A.**, Thèse de doctorat, Institut National des Sciences appliquées, Toulouse, 2003.

[45] **Ern A. and Guermond J.L**, *Eléments finis : théorie, applications, mise en oeuvre.* Mathématiques et Applications 36. SMAI. Springer, 2001.

[46] **Fobelets K., Vounckx R. and Borghs G.**, *Matrix formalism for the triple-band effective-mass equation.* Semicond. Sci. Technol. 8, 1815-1821, 1993.

[47] **Frensley W. R.**, *Wigner-function model of a resonant-tunneling semiconductor device.* Appl. Phys. Lett., 36 (3), :1570, 1987.

[48] **Frensley W. R.**, *Boundary Conditions for open Quantum Systems driven far from Equilibrium.* Reviews of Modern Physics, Vol.62, n.3, 745-791, 1990.

[49] **Freund R. W.**, *Conjugate gradient-type methods for linear systems with complex symmetric coefficient matrices.* SIAM J. Sci. Stat. Comput., 12 (1) :425, 1992.

[50] **Freund R. W.**, *A transpose-free quasi-minimal residual algorithm for non-hermitian linear systems.* SIAM J. Sci. Stat. Comput., 14 (2) :470, 1993.

[51] **Genoe J., Fobelets K., Van Hoof C. and Borghs G.**, *In-plane dispersion relations of InAs/AlSb/ GaSb/AlSb/InAs interband resonant-tunneling diodes.* Phys. Rev. B. 52 (19), 14 025-14 034, 1995.

[52] **Gérard P.**, *Mesures semiclassiques et ondes de bloch.* Sém. Ecole Polytechnique XVI, pp 1-19, 1990-1991.

[53] **Gérard P., Markowich P. A., Mauser N. and Poupaud F.**, *Homogenization Limits and Wigner Transforms.* Comm. Pure Appl. Math. 50, n : 4, pp 323-379, 1997.

[54] **Gilbarg D. and Trudinger N. S.**, *Elliptic Partial Differential Equations of second Order.* Springer, New-york, 1977.

[55] **Goudon Thierry**, *Analysis of a semi-discrete version of the wigner equation.* SIAM. J. Num. anal., 40, 6, pp 2007-2025, 2002.

[56] **Gummel H. K.**, *A self-consistent iterative scheme for one-dimensional steady state transistor calculations.* IEEE Trans. on Elec. dev., 11 (10) : 455-465, 1964.

[57] **Heremans J., Partin D. L. and Dresselhaus P. D.** , *Tunneling through narrow-gap semiconductor barriers.* Appl. Phys. Lett. 48 (10) 644-646, 1986.

[58] **Jennings A.**, *A compact storage scheme for the solution of symmetric linear simultaneous equations.* Computing Journal, Vol 9, 1966.

[59] **Joly P.**, *Mise en oeuvre de la méthode des éléments finis.* n :2 SMAI, 1990.

[60] **Kane E.O.**, *Energy band structure in p-type Germanium and Silicon.* J. Phys. Chem. Solids. Vol.1, 82-99, 1956.

[61] **Kane E.O.**, *Band structure of indium antimonide.* J. Phys. Chem. Solids. Vol.1, 249-261, 1957.

[62] **Kefi J.**,*The Schrödinger with variable mass model : mathematical analysis and semi-classical limit.* Quart. Appl. Math . (à paraître)

[63] **Kitabayashi H., Waho T. and Yamamoto M.**, *Dependence of resonant interband tunneling current on barrier and well width in InAs/AlSb/GaSb/ AlSb/InAs double barrier structures.* Jpn. J. App. Phys. Vol.36, 1807-1810, 1997.

[64] **Kitabayashi H., Waho T. and Yamamoto M.**, *Resonant interband tunneling current in InAs/AlSb/GaSb/AlSb/InAs double barrier diodes.* J. App. Phys. 84, 1460-1466, 1998.

[65] **Kittel C.**, *Introduction to solid state physics.* Wiley, 1996.

[66] **Klimeck G. et al.**, *Quantum device simulation with a generalized tunneling formula.* Appl. Phys. Lett Vol 67, 2539, 1995.

[67] **Klimeck G.**, *Quantum and semi-classical transport in Nemo* $1D$. Accepted for publication in J. Comp. Elec, 2003.

[68] **Kluksdahl N. C., Kriman A. M., Ferry D. K. and Ringhofer C.**, *Self-consistent study of the resonant-tunneling diode.* Phys. rev. B Vol (39), 11,7720-7735, 1989.

[69] **Kyoung-Youm K. and Byoungho L.**, *Wigner function formulation in non-parabolic semiconductors using power series dispersion relation.* J. Appl. Phys. Vol 86, 9, 5085-5093, 1999.

[70] **Lake R., Kilmek G., Bowen R.C. and Jovanovic D.C**, *Single and multi-band modeling of quantum electron transport through layered semiconductor devices.* J. Appl. Phys. 81, 7845-7869, 1997.

[71] **Landau L. and Lifshitz**, *Mécanique quantique.* Mir 1967.

[72] **Lascaux P. and Théodor R.**, *Analyse numérique matricielle appliquée à l'art de l'ingénieur.* Masson, Paris, 1987.

[73] **Lent C. S. and Kirkner D. J.**, *The quantum transmitting boundary method.* J. Appl. Phys., 67 (10) :6353 , 1990.

[74] **Lions P. L. and Paul T.**, *Sur les mesures de Wigner.* Revista Mathematica Iberoamericana, 9, pp 553-618, 1993.

[75] **Liu M. H., Wang Y. H. and Houng M.P.**, *Carrier transport in InAs/AlSb/GaSb interband tunneling structures.* J. Appl. Phys. 74 (10), 6222-6226, 1993.

[76] **Longenbach K. F., Luo L. F. and Wang W. I.**, *Resonant interband tunneling in InAs/GaSb/ AlSb/InAs and GaSb/InAs/ AlSb/ GaSb heterostructures.* Appl. Phys. Lett 57 (15), 1554-1556, 1990.

[77] **Luttinger J.M. and Kohn W.**, *Motion of electrons and holes in perturbed periodic fields.* Phys. Rev. Vol.94, n.4, 869-883, 1955.

[78] **Lyford W. C. D.**, *Spectral analysis of the Laplacian in domains with cylinders.* Math. Ann. 218, pp 229-251, 1975.

[79] **Magno R., Bracker A. S., Bennett B. R., Nosho B.Z. and Whitman L. J.**, *Barrier roughness effects in resonant interband tunnel diodes.* J. App. Phys. 90 (12), 6177-6181, 2001.

[80] **Markowich P. A.**, *The stationary semiconductor device equations.* Springer-Verlag, Wien, 1985.

[81] **Markowich P. A. and Mauser N. J.**, *The classical limit of a self-consistent quantum-Vlasov equation in 3-D.* Math. Meth. Mod. 16, n : 6, pp 409-442, 1993.

[82] **Markowich P. A., Mauser N. J. and Poupaud F.**, *A Wigner function approach to semi-classical limits : electrons in a periodic potential.* J. Math. Phys. 35, n : 3, pp 1066-1094, 1994.

[83] **Markowich P. A., Ringhofer C. and Schmeiser C.**, *Semiconductor Equations.* Springer-Verlag, Wien, 1990.

[84] **Mathieu H.**, *Physique des semiconducteurs et des composants électroniques.* Edition Dunod, 2001.

[85] **Messiah A.**, *Mécanique quantique I.* Dunod, Paris, 1958.

[86] **Ming-Fu Li**, *Modern semiconductor quantum physics.* 1994.

[87] **Mounaix P., Vanbésien O. and Lippens D.**, *Effect of cathode spacer layer on the current voltage characteristics of resonant tunneling diodes.* Appl. Phys. Lett. 57, 1517, 1990.

[88] **Nedelec J.C. and Starling F.**, *Integral equation method in a quasi-periodic diffraction problem for the time harmonic Maxwell equation.* SIAM J. of Math Anal Vol 22, n :6, 1679-1702, 1991.

[89] **Nier F.**, *A stationary Schrödinger-Poisson system arising from the modeling of electronic devices.* Forum Mathematicum 2, 5, pp 489-551, 1990.

[90] **Nier F.**, *A variational formulation of Schrödinger-Poisson systems in dimension* $d \leq 3$. Comm. Part. Diff. Equations, 18, pp 1125-1147, 1993.

[91] **Pazy A.**, *Semigroups of linear operators and applications to partial differential equations.* Springer ; NewYork, 1983.

[92] **Persson A. and Cohen R. M.**, *Reformulated Hamiltonian for non-parabolic bans in semiconductor quantum wells.* Phys. Rev B, Vol 38, 8, 5568-5575, 1988.

[93] **Pinaud O.**, Thèse de doctorat, Université Paul Sabatier, Toulouse, 2003.

[94] **Pinaud O.**, Transient simulations of a resonant tunneling diode. J. Appl. Phys., 92 4, 1987-1994, 2002.

[95] **Polizzi E.** *Modélisation et simulations numériques du transport quantique balistique dans les nanostructures semi-conductrices.* Thèse de doctorat, Institut National des Sciences appliquées, Toulouse, 2001.

[96] **Poupaud F. and Ringhofer C.**, *Semi-classical limits in a crystal with exterior potentials and effective mass theorems.* Comm. Partial Differential Equations. 21, n : 11-12, pp 1897-1918, 1996.

[97] **Quarteroni A., Sacco A. and Saleri F.**, *Méthodes numériques pour le calcul scientifique : programmes en matlab.* Springer 2000.

[98] **Raviart P.A. and Thomas J.M.**, *Introduction à l'analyse numérique des équations aux dérivées partielles.* Masson, Paris, 1988.

[99] **Reed M. and Simon B.**, *Methods of Modern Mathematical Physics IV.* Academic Press, New York-San Francisco-London, 4th edition, 1987.

[100] **Reggiani L.**, *Hot-electron transport in semiconductors.* Springer-Verlag, Berlin, 1985.

[101] **Register L. F., Ravaioli U. and Hess K.**, *Numerical simulation of mesoscopic systems with open boundaries using the multidimensional time-dependent Schrödinger equation.* J. Appl. Phys. 69 (10), 7153-7158, 1991.

[102] **Ringhofer C., Ferry D. K. and Kluksdahl N. C.**, *Absorbing boundary conditions for the simulation of quantum transport phenomena.* trans. Theo. stat. Phys 18, pp 331-346, 1989.

[103] **Sainsaulieu L.**, *Calcul scientifique.* Dunod 2 edition Paris, 2000.

[104] **Sapoval B. and Hermann C.**, *Physique des semiconducteurs.* Edition ellipses, 1990.

[105] **Selberherr S.**, *Analysis and simulation of semiconductor devices.* Springer, Verlag Wien, 1984.

[106] **Söderström J. R., Chow D. H. and McGill T. C.**, *New negative differential resistance device based on resonant interband tunneling.* Appl. Phys. Lett. 55 (11), 1094-1096, 1989.

[107] **Söderström J. R., Yu E. T., Jackson M. K., Rajakarunanayake Y. and McGill T. C.**, *Two-band modeling of narrow band gap and interband tunneling devices.* J. Appl. Phys 68 (3), 1372-1375, 1990.

[108] **Stewart G. W.**, *Matrix algorithms : Volume I Basic decomposition.* SIAM,. 1998.

[109] **Sze S. M.**, *Physics of Semiconductor Devices.* Wiley-Interscience, 1981.

[110] **Sweeny M. and Xu J.**, *Resonant interband tunnel diodes.* Appl. Phys. Lett. 54 (6) 546-548, 1989.

[111] **Tan I. H., Snider L., Chang L.D. and Hu E. L.**, *A self-consistent solution of Schrödinger-Poisson equations using a non uniform mesh.* J. Appl. Phys 68, 4071-4076, 1990.

[112] **Ting D. Z. Y., Yu E. T. and McGill T. C.**, *Multiband treatment of quantum transport in interband tunnel devices.* Phys. Rev. B, 3583-3592, 1992.

[113] **Tsu R. and Esaki L.**, *Tunneling in a finite superlattice.* Appl. Phys. Lett. 22 (11), 562-564, 1973.

[114] **Vanbésien O.**, *Simulation et caractérisation électronique des diodes double barrière à effet tunnel résonnant.* Thèse de doctorat, Université de Lille. 1991.

[115] **Vanbésien O.**, *Aspects ondulatoires du transport dans les structures artificielles : applications aux dispositifs électroniques quantiques et cristaux photoniques*, Habilitation à diriger des recherches en sciences, Université de Lille. Février 1999.

[116] **Vasileska D. and Goodnick S. M.**, *Computational electronics.* Materials Science and Engineering. R 38, 181-236, 2002.

[117] **White S.R. and Sham L.J.**, *Electronic properties of flat-band semiconductor heterostructures.* Phys. Rev. Letters , 47 (12) 879-882, 1981.

[118] **Wigner E. P.**, *On the quantum correction for the thermodynamic equilibrium.* Phys. Rev. 40, pp 749-759, 1932.

[119] **Yang L., Chen J. F. and Cho A. Y.**, *A new GaSb/ AlSb/GaSb/InAs double-barrier interband tunneling diode and its tunneling mechanism.* J. Appl. Phys. 68 (6), 2997-3000, 1990.

[120] **Yang R. Q., Sweeny M., Day D. and Xu J. M.**, *interband tunneling in heterostructure tunnel diodes.* IEEE Transactions on Electron Devices, 38 (3), 442-446, 1991.

[121] **Yang R. Q. and Xu J. M.**, *Analysis of transmission in polytype interband tunneling heterostructures.* J. Appl. Phys. 72 (10), 4714-4726, 1992.

[122] **Zweifel P.**, *The Wigner transform and the Wigner-Poisson system.* Trans. Theo. Stat. Phys., 22, 459-484, 1993.

tures semi-conductrices. Le modèle quantique que nous utilisons est celui de Schrödinger. On a pris en considération deux approches. Une première approche monobande où deux modèles unidimensionnels stationnaires sont étudiés. Le premier que nous abordons prend en compte la variation de la masse effective en fonction du matériau semi-conducteur. C'est le modèle Schrödinger avec masse variable. Le second est un modèle où les effets non paraboliques dans la relation de dispersion vecteur d'onde-énergie sont pris en compte. C'est le modèle Kohn-Luttinger. La deuxième approche est de type bibande obtenue à partir du modèle de Kane qui lui aussi découle de la méthode $k.P$. On note par le modèle Schrödinger à deux bandes. La partie théorique renferme des résultats d'existence de solutions (à l'aide du théorème de point fixe de Leray Schauder) et de comportement asymptotique. Dans les différents cas, nous avons dérivé des conditions aux bords transparentes. Nous avons établi un résultat concernant la limite semi-classique lorsque $\hbar$ tend vers zéro du modèle Schrödinger avec masse variable. Nous avons montré l'existence et l'unicité de solutions sauf peut-être pour une suite de valeurs d'énergie correspondant à des valeurs propres du spectre discret de l'opérateur de Kohn-Luttinger. Nous montrons l'existence de solutions du modèle Schrödinger à deux bandes dans le cas non-linéaire (le champ électrostatique est calculé auto-consistant). Finalement, dans la partie numérique, nous avons utilisé des éléments finis Hermitiens pour Kohn-Luttinger et une méthode de différences finies pour le modèle Schrödinger à deux bandes. Dans les deux cas, pour le système couplé nous avons utilisé un schéma itératif type Gummel. Nous avons pu réaliser des simulations numériques de dispositifs type diode à effet tunnel résonnant intrabande RTD (resp. inter-bande RITD) pour décrire l'approche monobande (resp. bibande). Nous avons obtenu les caractéristiques courant-tension, les coefficients de transmission et le profil des densités de charge électronique.
Mots clés : Modèle Schrödinger, équation de Poisson, limite-semiclassique, transformée de Wigner, diode à effet tunnel résonnant intrabande et interbande.

Abstract : This thesis is concerned with the mathematical study and the numerical resolution of quantum models of electronic transport in the nanostructures. The model that we use is that of Schrödinger. We took in consideration two approaches. The first is monoband where two stationary models are studied. The first that we approach takes into account the variation of the effective mass according to semiconductor material. It is the Schrödinger with variable mass model. The second is a model where the non-parabolic effects in the dispersion relation are taken into account. It is the Kohn-Luttinger model. The second approach is a bibande one obtained starting from the Kane model which also rises from the $k.P$ method. The model is the two bands Schrödinger. The theoretical part contains the results of the existence of the solutions (using the fixed point Leray Schauder theorem) and of asymptotic behavior. In the various cases, we derived the transparent boundary conditions. We established a result concerning the semi-classical limit when $\hbar$ tends toward zero of the one dimensional Schrödinger with variable mass model. We showed the existence and uniqueness of solutions only for the energies different of the energies corresponding to eigenvalues of the discrete spectrum of the Kohn-Luttinger operator. We show the existence of solutions of the two bands Schrödinger model in the non-linear case (the electrostatic field is calculated self-consistent). Finally, in the numerical part, we used a Hermitian finite elements for the Kohn-Luttinger model and a finite difference method for the two bands Schrödinger model. For the coupled system, we used an iterative diagram based on Gummel method. We could carry out numerical simulations of devices type intraband (resp. interband) resonant tunneling diode RTD (resp. RITD) to describe the mono-band (resp. multiband) approach. We obtain the characteristics current-voltage, the coefficients of transmission and the profile of the charge density.
Keywords : Schrödinger model, Poisson equation, semiclassical limit, Wigner transform, resonant intraband and interband tunneling diode.